Charles University

Faculty of Science

Study programme: Organic chemistry

Ing. Ivana Gergelitsová

Design, Synthesis, and Application of Novel Bifunctional (Thio)urea Organocatalysts Derived from Saccharides & Catalytic Asymmetric C−H Arylation of (η^6-Arene)Chromium Complexes

Návrh, syntéza a využití nových bifunkčních katalyzátorů odvozených od sacharidů & Katalytická asymetrická C−H arylace komplexů (η^6-aren)chromu

Doctoral thesis

Supervisor: Doc. RNDr. Jan Veselý, PhD.

Prague, 2021

Prohlášení:

Prohlašuji, že jsem závěrečnou práci zpracovala samostatně a že jsem uvedla všechny použité informační zdroje a literaturu. Tato práce ani její podstatná část nebyla předložena k získání jiného nebo stejného akademického titulu.

V Praze, 25.02.2021

Podpis

The work was supported by the Ministry of Education, Youth and Sport of the Czech Republic (No. MSM0021620857), by the Grant Agency of the Czech Republic (No. P207/10/0428) and by the Charles University in Prague, project GA UK (No. 704213).

Acknowledgements

First and foremost, I would like to thank my supervisor Jan Veselý for his ideas, advice and for his patience, especially when I was completing the thesis. He always supported my involvement in Chemistry Olympiad and my teaching activities. I really appreciate his help in finding financial support for my internship in Larrosa's group at the University of Manchester.

I like to remember small discussions with my lab mates Marek, Martin, Jiří, Bedřich, and Michal which were both very helpful and enjoyable.

Aleš Machara deserves my thanks for his advice on Eschweiler-Clark methylation and for great tips for interesting chemical books.

My thanks belong to Bohunka Šperlichová for the measurement of optical rotations, to Simona Hybelbauerová for taking the measurement on NMR spectrometer Bruker AVANCE III (600 MHz), to Martin Popr and Adam Málek for IR spectroscopy, to Martin Štícha for recording the mass spectra, to group of mass spectrometry of IOCB Prague for HRMS analysis and to Ivana Císařová for crystal X-ray analyses. I would like to thank School of Chemistry at the University of Manchester for providing analytical services.

I am very grateful for the opportunity to work in the Larrosa's group on School of Chemistry at the University of Manchester. During the internship I learned a different approach to organic synthesis and it helped me to become a more independent chemist. I would like to thank my internship supervisor Igor Larrosa for his very caring leading. I am grateful to my lab mates for the very positive and inspiring working atmosphere and the feeling of home. I will always remember our "competing" lunch time breaks. Daniel deserves big thanks for his kind advice and help with synthetic troubles. I am grateful to Maria who finished C−H arylation project so that it was published. My special thanks go to Chiara and Greg who were always positive and showed me the world outside of the lab as well.

My special thanks goes to my friend Oldřích Hudeček, who read my thesis and gave me valuable comments and recommendations.

Gratitude to my devoted family is infinite and endless. Their compassion, understanding and thoughtful suggestions in hard times mean more to me than I can ever express. My beloved Tomáš has kept me going when I felt like giving up. He was extraordinarily patient and supportive. He, Františka and Marianna tried to give me as much time as possible for writing and they always managed to cheer me up and remind me what is really essential in my life.

I would like to thank Faculty of Science of Charles University for providing me STARS-scholarship. Internship at the University of Manchester was greatly facilitated by granting the ERASMUS+ scholarship and the scholarship of Jiří Kroutil and financial support from the Mobility Fund of Charles University.

Abstrakt

Tato disertační práce se v první části zabývá návrhem, přípravou, evaluací a využitím nových bifunkčních (thio)močovinových organokatalyzátorů odvozených od sacharidů. Kombinace (thio)močoviny (donoru vodíkové vazby) a Lewisovy báze na chirálním nosiči (např. 1,2-*trans*-cyclohexanu, chininových alkaloidech, 1,1'-binaftalenu) se v návrhu bifunkčních organokatalyzátorů stala oblíbeným motivem. Dosud byla syntéze organokatalyzátorů, používajících jako chirální nosič sacharidy, věnována pouze omezená pozornost. Sacharidy jsou snadno dostupné v několika diastereomerních formách, a navíc nabízejí možnost změny sterických a elektronických vlastností a rozpustnosti skrze změnu *O*-substituentů. Byly navrženy tři typy nových organokatalyzátorů odvozených od sacharidů: C2-symetrické thiomočoviny/terciární aminy odvozené pouze od 2-amino-2-deoxy sacharidů, thiomočoviny/primární aminy tvořené pentopyranosovým a cyclohexanovým skeletem a (thio)močoviny/terciární fosfiny obsahující sacharidovou a α-aminokyselinovou jednotku.

Sacharidová jednotka katalyzátorů prvního typu nese obě funkční skupiny a je tak jediným prvkem, který plně určuje stereoselektivitu. Takový přístup je v organokatalýze ojedinělý, jelikož naprostá většina organokatalyzátorů odvozených od sacharidů využívá sacharidovou jednotku pouze jako objemný elektron-odtahující substituent. Syntetická cesta, vedoucí k těmto katalyzátorům, byla komplikována neslučitelností *O*- a/nebo *N*-chránících skupin s podmínkami jednotlivých reakcí. Následně byla úspěšně dokončena syntéza katalyzátoru druhého typu, který je odvozený od D-xylopyranosy (strukturního analogu osvědčené D-glukopyranosové jednotky). Bifunkční organokatalyzátory třetího typu jsou dobře dostupné z přírodních látek: sacharidů a α-aminokyselin. Dostupnost různých přírodních a syntetických α-aminokyselin umožňuje další modifikaci katalyzátoru, což vede k vylepšení stereokontroly. Účinnost katalyzátorů třetího typu byla demonstrována pomocí Morita-Baylis-Hillmanovy (MBH) reakce aromatických aldehydů s akryláty. Odpovídající MBH produkty byly získány v dobrých výtěžcích (až 85 %) a s vysokou enantioselektivitou (až 87 % ee).

Komplexy chromu s planární chiralitou jsou v asymetrické syntéze využívány jako užitečné pomocné skupiny a ligandy. Avšak syntéza planárně chirálních komplexů chromu, podle našeho nejlepšího vědomí, doposud vyžadovala přítomnost stechiometrického množství chirálních činidel a/nebo funkcionalizované výchozí látky. Druhá část dizertační práce je proto zaměřena na nalezení efektivní alternativy pro přípravu planárně chirálních komplexů, a to pomocí přímé katalytické asymetrické C−H arylace nefunkcionalizovaných komplexů (fluoraren)chromu. Planárně chirální ligandy z rodiny (*H*$_8$)-BINAP a Buchwaldovy katalyzátory byly připraveny a testovány v C−H arylaci komplexu (fluorbenzen)trikarbonylchromu. Kombinace (*H*$_8$)-BINAP(O) ligandu a Buchwaldova katalyzátoru založeném na XPhos ligandu vedla k nejlepším výsledkům a poskytla produkt monoarylace s vysokou enantioselektivitou (80 % ee) v dobrém výtěžku (45 %) společně s výrazně sníženým rozsahem vedlejší diarylace.

Klíčová slova

Organokatalyzátory, nekovalentní katalýza, donory vodíkové vazby, nukleofilní katalýza, bifunkční (thio)močoviny, sacharidy, aminofosfiny, MBH reakce, [4+1] cyklizace, asymetrická katalýza, C−H arylace, komplexy (η^6-aren)chromu, planární chiralita.

Abstract

The first part of the thesis is focused on the design, synthesis, evaluation, and application of novel bifunctional (thio)urea organocatalysts derived from saccharides. Combination of H-bonding donor (thio)urea moiety with Lewis base active site in a single chiral scaffold (e.g., 1,2-*trans*-cyclohexyl, cinchona alkaloids, 1,1'-binaphthyl) is a popular motif in catalyst design. Only limited attention has been paid to the synthesis of bifunctional (thio)ureas using saccharides as a chiral scaffold. Saccharides bring the advantage of the availability of various diastereomeric forms. Moreover, they offer modification of steric, electronic, and solubility properties *via O*-substitution. Three types of novel organocatalysts were designed: C2-symmetrical thiourea/tertiary amines entirely derived from 2-amino-2-deoxy saccharides, thiourea/primary amines based on pentopyranose and a cyclohexane skeleton, and (thio)urea/tertiary phosphines containing both saccharide and α-amino acid unit.

Both functional groups of organocatalysts of the first type are located on the saccharide unit, and it is the only element which fully determines stereoselectivity. This is an exceptional approach as the majority of saccharide-based organocatalysts use saccharide as a bulky electron-withdrawing substituent. However, the route to these catalysts was hindered by the interference of *O*- and/or *N*-protecting groups with the chosen synthetic steps. Organocatalyst of the second type derived from D-xylopyranose (a structural analogue of the proven glucopyranose unit) was successfully synthesized. Bifunctional organocatalysts of the third type are readily available from naturally occurring molecules: saccharides and amino acids. The availability of various natural and synthetic α-amino acids enables further modification of catalyst properties to tune the stereocontrol. The efficiency of organocatalysts of the third type was demonstrated in the asymmetric Morita-Baylis-Hillman (MBH) reaction of aromatic aldehydes with acrylates. The corresponding MBH products were obtained in good yields (up to 85%) with high enantioselectivities (up to 87% ee).

Planar chiral chromium complexes are useful chiral auxiliaries and ligands for asymmetric synthesis. To the best of our knowledge, their preparation required a stoichiometric amount of chiral reagents and/or functionalization of starting compounds. The second part of the thesis is focused on an efficient alternative to planar-chiral complexes using a direct catalytic asymmetric C−H arylation of non-functionalized (fluoroarene)chromium complexes. Planar-chiral ligands from a family of (*H*$_8$)-BINAP derivatives and Buchwald's catalysts were prepared and tested in the C−H arylation of (fluorobenzene)tricarbonylchromium complex. The combination of XPhos-based Buchwald's catalyst and (*H*$_8$)-BINAP(O) ligand led to the most promising results affording a monoarylated product with high enantioselectivity (80% ee) in moderate yield (43%) and with a significantly decreased extent of undesired bisarylation.

Keywords

Organocatalysis, non-covalent catalysis, H-bonding donors, nucleophilic catalysis, bifunctional (thio)ureas, saccharides, aminophosphines, MBH reaction, [4+1] cyclization, asymmetric catalysis, C−H arylation, (η^6-arene)chromium complexes, planar chirality.

1 List of abbreviations

*	chiral compound or stereocenter
α	optical rotation
[α]	specific rotation (expressed without units; the units, $10^{-1} \cdot \mathrm{deg} \cdot \mathrm{cm}^2 \cdot \mathrm{g}^{-1}$, are understood)
A	Lewis acid, deprotonated acid or an anion, more specified in concrete cases
AA	alkylating agent
Ac	acetyl
Ad	1-adamantyl
Ala	alanine
Alloc	allyloxycarbonyl
AMC	mixture of phosphomolybdenic acid (25 g), $Ce(SO_4)_2 \cdot H_2O$ (10 g), sulfuric acid (1.2 M aq sol, 1 L)
aq	aqueous
Ar	aryl
B	base
BH	Baylis-Hillman
BHT	butylated hydroxytoluene = 2,6-bis(1,1-dimethylethyl)-4-methylphenol
BINAP	2,2'-bis(diphenylphosphino)-1,1'-binaphthyl
BINAP(O)	[2'-(diphenylphosphino)-[1,1'-binaphthalen]-2-yl]diphenylphosphine oxide
BINOL	[1,1′-binaphthalene]-2,2′-diol
Bn	benzyl
Boc	*tert*-butoxycarbonyl
BQ	1,4-benzoquinone
br	broad (spectral)
Bu	butyl
calcd	calculated
cat	catalyst
CMD	concerted metalation-deprotonation
concd	concentrated
Cy	cyclohexyl
ΔH	enthalpy change
δ	chemical shift
d	day(s); doublet (spectral)
dd	doublet of doublet (spectral)
ddd	doublet of doublet of doublet (spectral)
DABCO	1,4-diazabicyclo[2.2.2]octane
DavePhos	2-dicyclohexylphosphino-2'-(*N*,*N*-dimethylamino)biphenyl
dba	dibenzylideneacetone
DCM	dichloromethane
de	diastereomeric excess

DFT	density functional theory
DG	directing group
DIPEA	*N*-ethyl-*N*-(propan-2-yl)propan-2-amine = Hünig's base
DKR	dynamic kinetic resolution
DMA	dimethylacetamide
DMAP	4-(*N*,*N*-dimethylamino)pyridine
DM-BINAP	2,2′-bis[bis(3,5-dimethylphenyl)phosphino]-1,1′-binaphthyl
DMF	dimethylformamide
DMSO	dimethyl sulfoxide
DOWEX®	cation exchange resin from The Dow Chemical Company
DPEDA	1,2-diphenylethane-1,2-diamine
dppb	1,4-bis(diphenylphosphino)butane
dppp	1,3-bis(diphenylphosphino)propane
dr	diastereomeric ratio
DRIFT	diffuse reflectance infrared Fourier transform spectroscopy
dt	doublet of triplet (spectral)
E	electrophile
EDC	1-ethyl-3-(3-dimethylaminopropyl)carbodiimide
ee	enantiomeric excess
EI	electron impact
ent	enantiomer
equiv	equivalent
ESI	electrospray ionization
Et	ethyl
FG	functional group
FTIR	Fourier-transform infrared spectroscopy
EWG(s)	electron withdrawing group(s)
GC	gas chromatography
η	hapticity
(*H*$_8$)-BINAP	2,2′-bis(diphenylphosphino)-5,5′,6,6′,7,7′,8,8′-octahydro-1,1′-binaphthyl
(*H*$_8$)-BINAP(O)	[2'-(diphenylphosphino)-5,5',6,6',7,7',8,8'-octahydro-[1,1'-binaphthalen]-2-yl] diphenylphosphine oxide
H-bond	hydrogen bond
Het	hetero
HIV	human immunodeficiency virus
HMPA	hexamethylphosphoramide
HMDS	hexamethyldisilazane
HOBt	1-hydroxybenzotriazole
HOMO	highest occupied molecular orbital
HPLC	high-performance liquid chromatography
HRMS	high-resolution mass spectrometry
i-Bu	isobutyl, 2-methylpropyl

ICD	isocupreidine
i.e.	id est, in other words
IR	infrared
IT	ion trap
IUPAC	The International Union of Pure and Applied Chemistry
J	coupling constant (in NMR spectrometry)
λ	wavelength
$L_{(n)}$	n ligand(s)
Leu	leucine
log	common logarithm, the logarithm with base 10
M	molar (moles per liter) or metal more specified in concrete cases
m	multiplet (spectral) or milli
M^+	parent molecular ion
$M^{+\cdot}$	parent radical cation
MBH	Morita-Baylis-Hillman
Me	methyl
mol%	mole percent
mp	melting point
MPAA	mono-*N*-protected amino acid
Ms	methylsulfonyl (mesyl)
MS	mass spectrometry
m/z	mass-to-charge ratio
n-Bu	normal (primary) butyl
NMM	*N*-methylmorpholine
NMP	*N*-methylpyrrolidone
NMR	nuclear magnetic resonance
Nu	nucleophile
P	product
PCC	pyridinium chlorochromate
PG	protecting group
Ph	phenyl
Phe	phenylalanine
Piv	pivaloyl
pK_a	negative log of the acid dissociation constant (K_a)
PMB	*p*-methoxybenzyl
ppm	parts per million
Pr	propyl
i-Pr	isopropyl
Py	pyridine
q	quartet (spectral)
R	general group attached to the rest of the molecule (usually via a carbon)
RA	reducing agent

rac	racemate
RDS	rate-determining step
rt	room temperature
S	substrate
s	singlet (spectral)
sat	saturated
SEGPHOS	[(4,4'-bi-1,3-benzodioxole)-5,5'diyl]bis(diphenylphosphine)
sol	solution
SOMO	single-occupied molecular orbital
sp^2	hybridisation the 2s orbital is mixed with two of the three available 2p orbitals
SPhos	2-dicyclohexylphosphino-2′,6′-dimethoxybiphenyl
t	triplet (spectral)
TADDOL	α,α,α',α'-tetraaryl-1,3-dioxolan-4,5-dimethanol
TBAB	tetrabutylammonium bromide
TBAF	tetrabutylammonium fluoride
TBHP	*tert*-butyl hydroperoxide
TBME	*tert*-butyl methyl ether
TBS	*tert*-butyldimethylsilyl
t-Bu	*tert*-butyl, 1,1-dimethylethyl
TES	triethylsilyl
Tf	trifluoromethanesulfonyl
TFA	trifluoroacetic acid
THF	tetrahydrofuran
TLC	thin-layer chromatography
TMDS	1,1,3,3-tetramethyldisilazane
TMP	2,2,6,6-tetramethylpiperidine
TMS	trimethylsilyl
TOF	time-of-flight
Tol	tolyl (-$C_6H_4CH_3$)
t_R	retention time
tRNA	transfer ribonucleic acid
Ts	*p*-toluenesulfonyl (tosyl)
TS	transition state
UV	ultraviolet
Val	valine
vs.	versus, in contrast to
wt%	weight percent
X	heteroatom, more specified in the concrete cases
Xanthpos	4,5-bis(diphenylphosphino)-9,9-dimethylxanthene
XPhos	2-dicyclohexylphosphino-2',4',6'-triisopropylbiphenyl
X-ray	energetic high-frequency electromagnetic radiation

2 Table of contents

3 Organocatalysis as a new synthetic field

As early as in 1932, Langenbeck introduced the term "Organische Catalyzatoren", while studying the similarities between enzymes and organic compounds.[1] However, it took almost a century until organocatalysis became a new synthetic field. Significant research results from the late 1990s proved that chiral small organic molecules are useful catalysts for important asymmetric transformations. Shi,[2] Denmark[3] and Yang[4] developed the enantioselective epoxidation of simple alkenes using chiral ketones as catalysts. Jacobsen[5] and Corey[6] described the first example of non-covalent hydrogen bonding (H-bonding) catalysts for the asymmetric Strecker reaction and Miller[7] introduced small molecular weight peptides as catalysts for the kinetic resolution of alcohols.

Finally, the simultaneous publishing of the paper by Barbas, Lerner and List on enamine catalysis (Scheme 1a)[8] and the paper by Ahrendt, Borths and MacMillan on iminium catalysis (Scheme 1b)[9] in 2000, led to the introduction of the term "organocatalysts" and the conceptualization of organocatalysis as a new synthetic field.

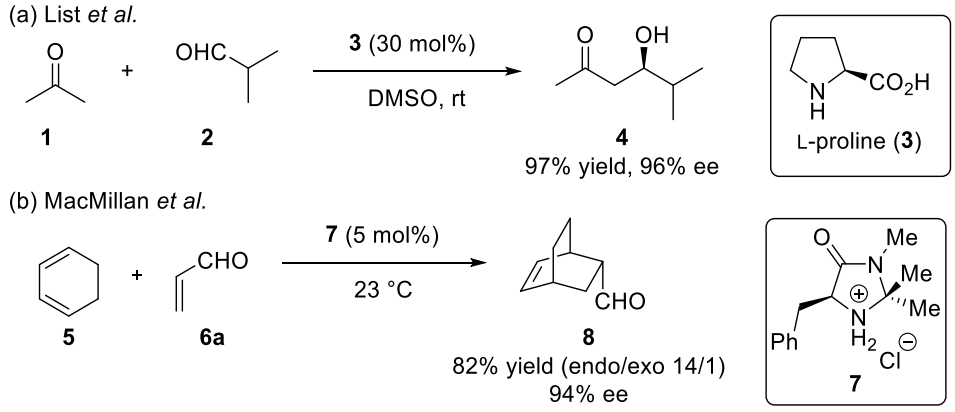

Scheme 1 (a) Enamine catalysis (List *et al.*) & (b) iminium catalysis (MacMillan *et al.*).

Organocatalysis has been defined as catalysis with low-molecular-weight organic compounds (i.e., compounds composed mainly of carbon, hydrogen, nitrogen, oxygen, sulphur, and phosphorus), in which a metal is not part of the active principle.[10,11]

Nowadays, asymmetric organocatalysis is considered as one of the main fields of enantioselective synthesis together with enzymatic catalysis and catalysis with transition metal complexes. Organocatalysts bring many benefits to asymmetric synthesis as they are mostly inexpensive, readily available, non-toxic, robust, and inert to moisture and oxygen. Moreover, they usually do not require special reaction conditions such as inert atmosphere and absolute solvents. They have great potential for fields where metal contamination is not tolerated such as pharmaceutical and food industry.[10]

4 Organocatalysts & modes of action

In the last two decades, plenty of new organocatalysts were designed and synthesized, therefore the need for organization and classification of organocatalysts arose. According to the nature of the catalyst-substrate interaction, two groups of organocatalysts are distinguished: covalent and non-covalent.[10,12] The first group of organocatalysts activates a substrate by the reversible formation of covalent intermediates. Typical examples of such intermediates are shown in Figure 1.[12]

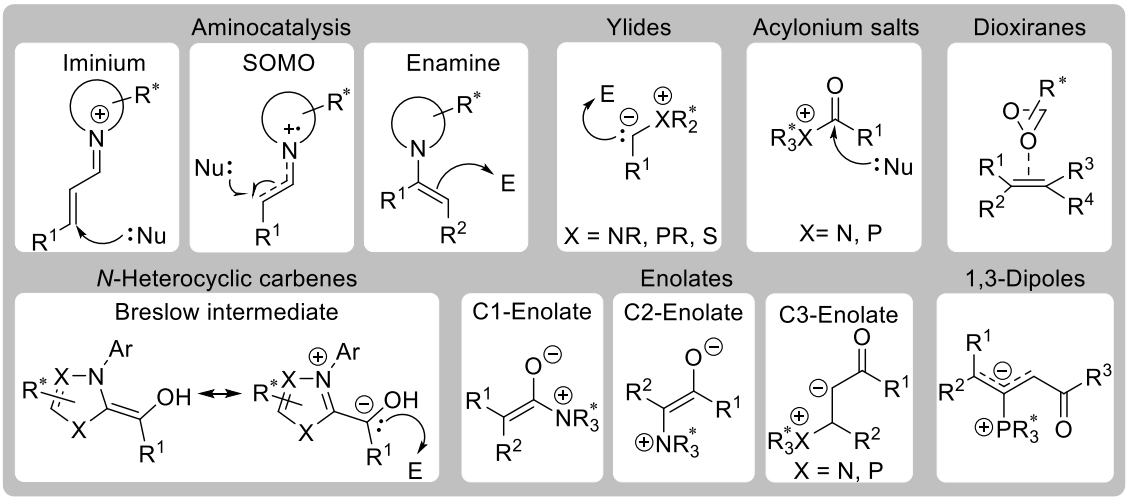

Figure 1 Covalent organocatalysis & classification of intermediates.

The second group of organocatalysts relies on non-covalent interactions (Figure 2),[12] e.g., H-bonding interactions, chiral ion pairs (counterion catalysis, including phase transfer catalysis)[13] and dynamic molecular recognition through multivalent interactions (shape and site selective catalysts based on host-guest interactions).[14]

The strength of the catalyst-substrate interaction decreases in the following order: covalent interactions, H-bonding, and chiral ion pairing. The stronger the interaction, the more directional it is. In covalent catalysis well-defined catalyst-substrate intermediates are usually formed and for that reason it can suffer from product inhibition. In contrast, catalyst turnover is not a problem in H-bonding catalysis and chiral ion pairing catalysis, but these usually need the incorporation of additional functional group(s). Further functional group induces a specific attractive or repulsive interaction and helps to form a structurally defined catalyst-substrate complex, which is required for high stereoinduction.

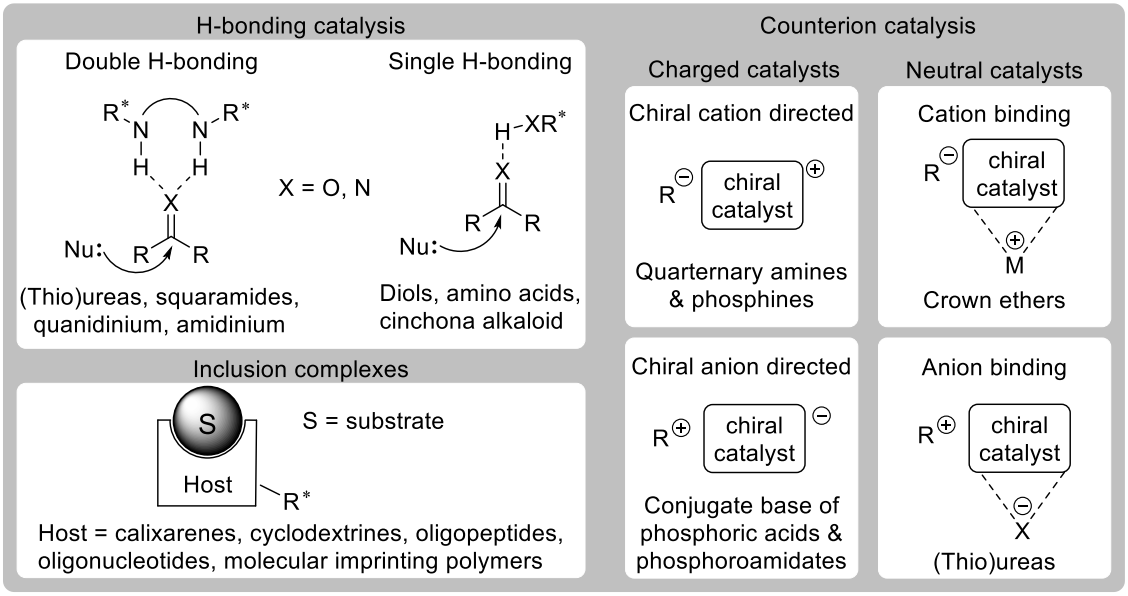

Figure 2 Non-covalent organocatalysis & classification of intermediates.

List suggested a classification of the organocatalysts into four groups: Lewis acids/basis and Brønsted acids/basis (Figure 3).[15] According to List, the majority of covalent catalysts are N, C, P, S based Lewis bases that operate through diverse mechanisms and

convert a substrate either to an activated nucleophile or electrophile.[15] Typical activated nucleophiles are enamines (enamine catalysis), ylides, Breslow intermediates (*N*-heterocyclic carbene catalysis), enolates, and 1,3-dipoles.[12,15,16] Typical activated electrophiles are iminium ions (iminium catalysis), iminium radical species (SOMO catalysis), and acyloniums.[12,15,16]

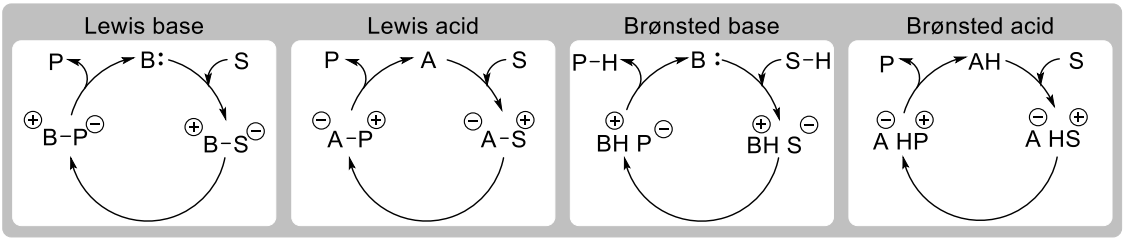

Figure 3 Classification of organocatalysts into Lewis/Brønsted acids/bases; S = substrate, P = product, B = base, A = Lewis acid or deprotonated Brønsted acid.

Chiral dioxiranes involved in the asymmetric epoxidation of olefins represents one of the examples of Lewis acid catalysis (see catalyst **108**, Figure 15, page 37).[2,15]

Brønsted bases activate substrates *via* the formation of a chiral ion pair between a protonated Brønsted base and a negatively charged nucleophile or a nucleophile-electrophile adduct. The most successful Brønsted base catalysts are based on tertiary amines, quanidines, amidines, and imidazoles.[17]

Chiral Brønsted acids act as H-bonding donors either to a substrate (activation of electrophiles) or to oxyanion intermediates (stabilization of reaction intermediates and transition states).[18–20] Typical Brønsted acid catalysts are (thio)ureas (see Chapter 5), squaramides,[21] phosphoric acids,[22] chiral diols (especially BINOL and TADDOL derivatives), amino acids, and cinchona alkaloids possessing a free hydroxy group.[18]

This thesis deals with bifunctional (thio)urea/amine or (thio)urea/tertiary phosphine organocatalysts based on a saccharide scaffold. Therefore, non-covalent organocatalysis aimed at hydrogen bonding (thio)ureas is discussed in Chapter 5. The most relevant facts of covalent nucleophilic organocatalysis using tertiary amines or phosphines are summarized in Chapter 6. The progress in the area of saccharide-based organocatalysis is described in Chapter 7.

5 Catalysis by H-bonding donors

Activation of electrophiles by chiral small molecule H-bonding donors is one of the most important paradigms for enantioselective organocatalysis.[18,23] Development in the understanding of enzyme functionalities, improvements in supramolecular chemistry, molecular recognition, co-crystallization and X-ray structural studies together with pioneering studies in achiral H-bonding donor catalysis bring important findings about behaviour of H-bonding donors and contributed to the successful utilization of H-bonding donors in asymmetric transformations in the late 1990s.[18,24]

At that time, Jacobsen and Corey developed the asymmetric Strecker reaction. Jacobsen used parallel synthetic libraries to identify and optimize the catalysts, which were originally designed as ligands for Lewis acidic metals.[5] The reaction of protected imines **9** with HCN in the presence of Schiff base **10** gave products **11** in high yields together with significant enantioselectivities (Scheme 2).[25] First mechanistic studies suggested activation of imine **9** toward nucleophilic attack through double H-bonding to the catalyst.[26] However, later

on, the mechanism was reviewed and the anion-binding mechanistic pathway was established instead.[27]

Corey applied C_2-symmetrical guanidine catalyst **13** in the asymmetric Strecker reaction to get products **14** with high yields and enantioselectivities (Scheme 3).[6] The catalytic cycle started with the generation of a guanidinium-cyanide ion pair, which serves as a hydrogen bonding donor to aldimine **12**. The formation of termolecular assembly **A1** was proposed to explain the high enantioselectivity.

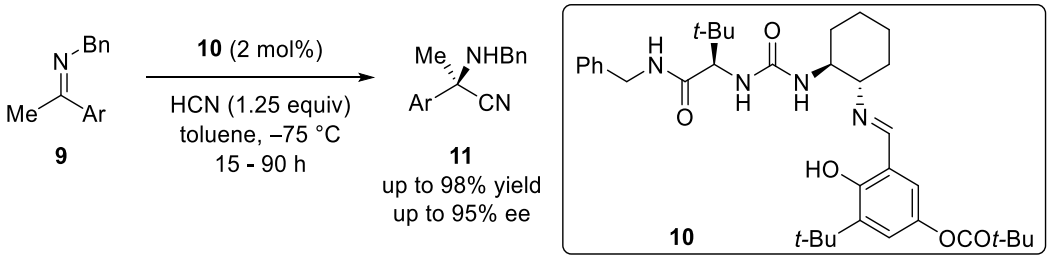

Scheme 2 Enantioselective Strecker reaction catalyzed by urea catalyst **10**.

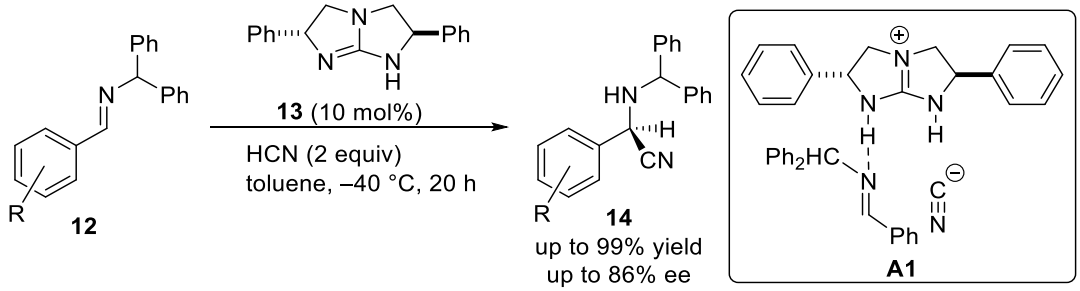

Scheme 3 Enantioselective Strecker reaction catalyzed by guanidine catalyst **13**.

5.1 Definition, properties, and the role of H-bonds

Steiner defined H-bonds as follows: *An X−H ··· A interaction is called a "hydrogen bond", if 1. it constitutes a local bond, and 2. X−H acts as a proton donor to A.*[28]

H-bonds can be further divided into strong, moderate, and weak (Table 1). In essence, the stronger the H-bond, the more covalent and the more directional it is. Organocatalytic transformation usually operates with moderate H-bonds.[18]

Table 1 Classification and properties of H-bonds.[18]

H-bond	Strong	Moderate	Weak
Type of bonding	Mostly covalent	Mostly electrostatic	Electrostatic
Length [Å]	1.2 – 1.5	1.5 – 2.2	2.2 – 3.2
Angle [°]	175 – 180	130 – 180	90 – 150
Energy [kcal/mol]	14 – 40	4 – 15	‹ 4
Typical example	Intramolecular NH---N bond in the conjugate acid of proton sponge	Bonds NH---O=C in peptide helices and sheets	Bonds involving CH donors to *N*- or *O*-acceptor

In organocatalytic transformations H-bonding activates substrates and/or stabilizes oxyanion intermediates and/or transition states.[18–20] H-bonding to an electrophile (e.g., carbonyl compounds, imine) leads to a decrease in electron density (of C=O and C=N bond, respectively) and activation toward an nucleophilic attack. Stabilization of oxyanions is governed either by pure H-bonding interactions, where the proton remains bonded in the

molecule of the catalyst or it is rather general acid catalysis, which starts with H-bonding interactions and moves further to the distinct proton transfer.[20]

5.2 Double vs. single H-bonding donors

Simultaneous donation of two hydrogen bonds proved to be a very general (double H-bonding donors activate, e.g., aldehydes, ketones, esters, imines, *N*-acyliminium ions, nitro compounds) and successful approach. Activation of substrates by typical double H-bonding donors, such as (thio)ureas **A2**,[29] guanidines **A3**,[30] amidinium ions **A4**,[31] and squaramides **A5**[32] is depicted in Figure 4.

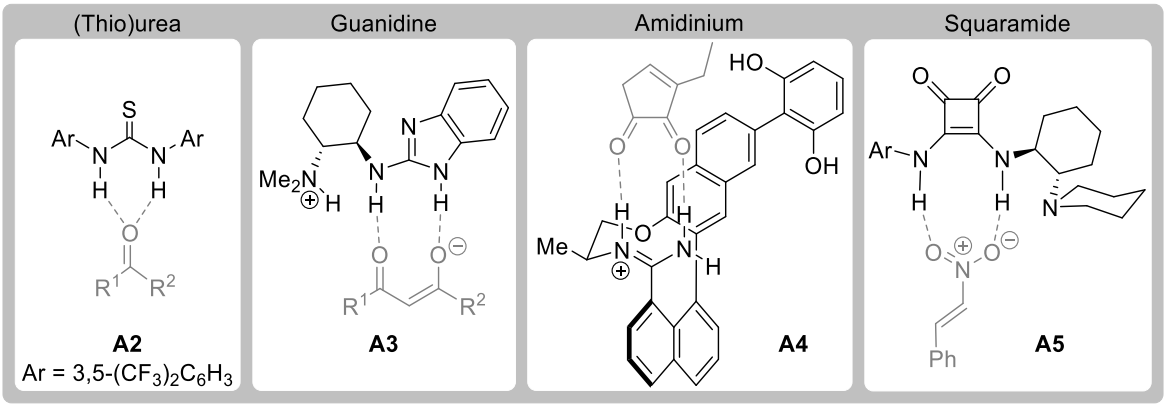

Figure 4 Activation of substrates using typical double H-bonding donors.

The advantage of double H-bonding lies in an increased strength and directionality relative to an isolated H-bond, leading to the formation of a more rigid catalyst-substrate complex. However, there are two structural motifs, which improve the properties of isolated H-bonds. The first possibility is the utilization of an intramolecular hydrogen bond, which tunes the properties of the intermolecular hydrogen bond and makes it more acidic and directional (assembly **A6**, Figure 5). This is typical for diols, such as TADDOL and BINOL derivatives.[18,20] The second option is the presence of another functional group, which directs the assembly of a well-defined catalyst-substrate complex *via* additional (non)covalent interactions,[18–20] for example activation of electrophiles using proline (**TS1**, Houk-List model, Figure 5)[19] and cinchona alkaloids (**TS2**, Figure 5).[33]

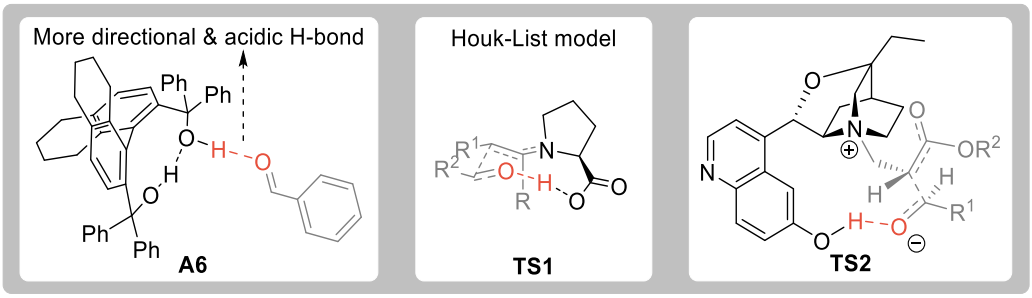

Figure 5 Intramolecular H-bond tunes properties of the intermolecular H-bond in assembly **A6**, simultaneous covalent and single H-bonding activation (**TS1** & **TS2**).

5.3 Typical structural patterns of successful (thio)urea catalysts

Key structural patterns that improve the catalytic activity of (thio)urea catalysts are discussed in this section. For a more detailed analysis, see Schreiner's publication and references therein.[24] Close correlation between acidity and double H-bonding ability was found for

(thio)ureas. Consequently, (thio)ureas with aryl *meta*- or *para*-EWG substituents proved to be better H-bonding donors compared to unsubstituted analogues. For the equilibrium acidities of (thio)urea organocatalysts in DMSO, see Schreiner's study.[34]

For (thio)urea catalysts, weak enthalpic binding (ΔH of thiourea group to carbonyl groups is ~ −7 kcal/mol at rt)[35] is characteristic, which results in very low product inhibition and makes the entropy term decisive in the formation of a catalyst-substrate complex. In relation to the catalyst structure, it means the more rigid the free (thio)urea is (the more conformationally stable), the more stable the catalyst-substrate complex is, and the entropy loss upon complexation is minimal and the rate enhancement is increased. (Thio)ureas with phenyl *meta*- and *para*-EWG substituents form stabilizing intramolecular H-bond(s) between acidic *ortho* hydrogen(s) and (thio)carbonyl group (Figure 6). This interaction blocks rotation within (thio)urea moiety and favours complexation entropically. Moreover, intramolecular interaction blocks self-association through intermolecular H-bonding. On the other hand, substituents at the *ortho* position decrease the rotational barrier due to repulsive interactions with the (thio)carbonyl group.

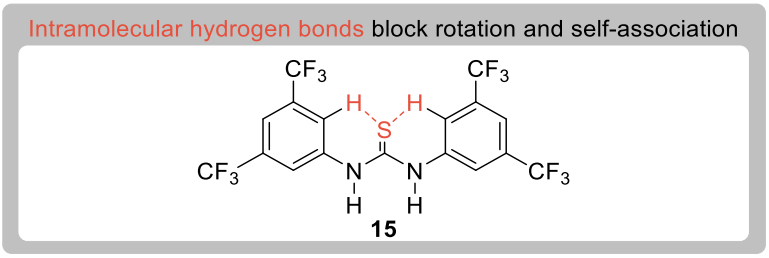

Figure 6 Stabilizing H-bonds between *ortho* hydrogens and the thiocarbonyl group.

3,5-Bis(trifluoromethyl)phenyl unit proved to be a privileged substituent. The presence of acidifying (EWG) and non-coordinating CF_3 groups enhances the H-bonding donor ability and suppresses self-association. Self-association is typical for catalysts substituted with other H-bonding acceptors, such as ester groups.[24]

Synthesis from the inexpensive starting material, easy modulation of electronic and steric properties, possible immobilization on solid support together with water compatibility, air stability, and low toxicity ensure that (thio)ureas dominate the H-bonding donor catalysis with the thioureas being much more represented. Thiocarbonyl group is a weaker H-bonding acceptor, which results in less catalyst self-association. Thioureas are more acidic than ureas (pK_a = 26.9 (urea), pK_a = 21 (thiourea) in DMSO at 25 °C)[36], which leads to a more stable catalyst-substrate complex. Thioureas are more soluble in organic solvents, and their preparation utilizes liquid thiophosgene, which is easier to handle than phosgene.

5.4 Stereoselective bifunctional (thio)urea catalysts

Bifunctional (thio)urea catalysts contain the (thio)urea group together with an additional functional group, mainly amines and tertiary phosphines. The presence of two functional groups enables concerted activation of both reaction partners *via* synergic interactions and thus, specifically controls the structure of a transition state leading to higher catalytic activity and better enantioselectivity (Figure 7).[24]

The combination of the privileged 3,5-bis(trifluoromethyl)phenyl unit (Section 5.3) with proven chiral scaffolds and chiral pool compounds, such as *trans*-cyclohexane-1,2-diamine, *trans*-1,2-diphenylethane-1,2-diamine (DPEDA), cinchona alkaloids, 2,2'-diamino-1,1'-binaphthyl, amino alcohols, and α-amino acids gave rise to powerful bifunctional (thio)urea catalysts (Figure **8**).[24]

Representative examples of stereoselective bifunctional (thio)urea organocatalysts are included in this section; for more details regarding (thio)urea organocatalysts, see, for example, selected reviews.[24,37–39]

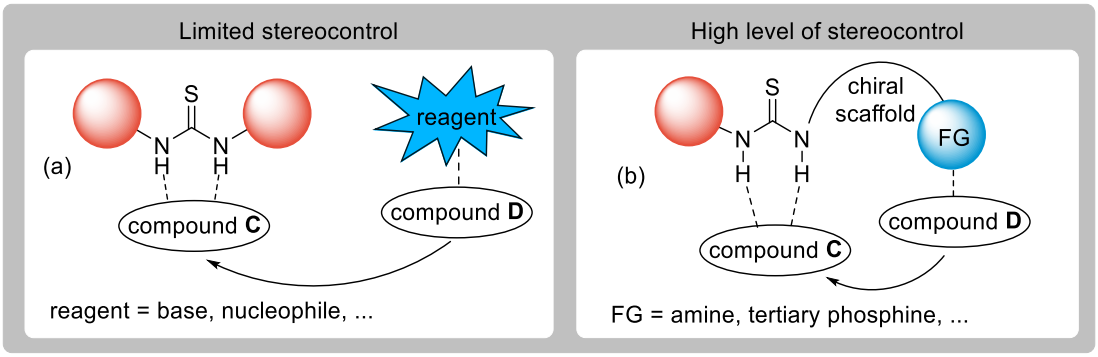

Figure 7 Activation of compounds **C**, **D**: (a) *via* a monofunctional thiourea catalyst and a distinct chiral additive; (b) simultaneous within a chiral catalyst.

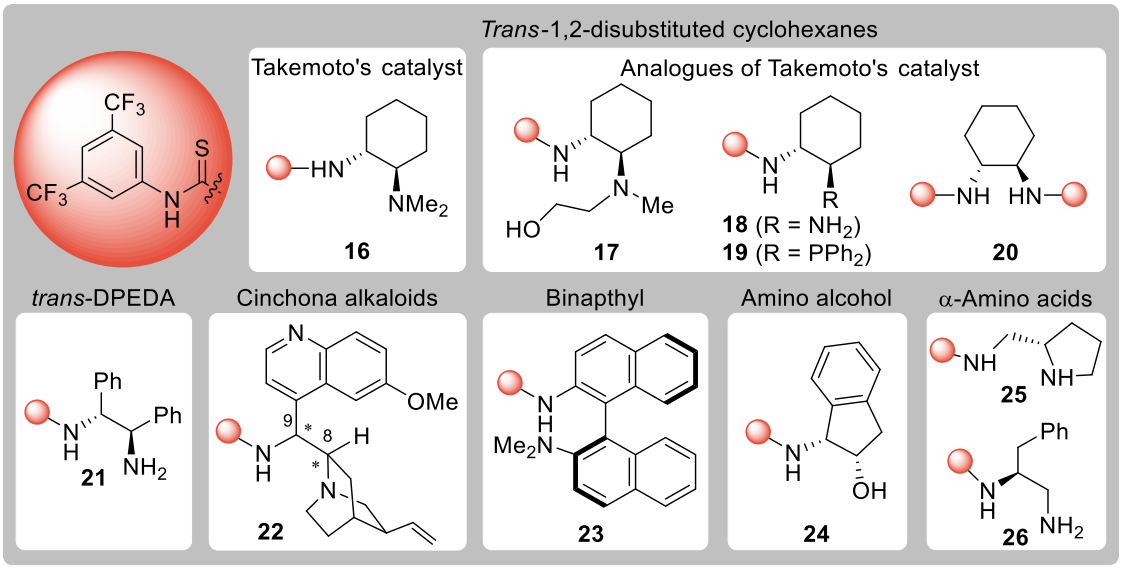

Figure 8 Selected examples of bifunctional thiourea organocatalysts with 3,5-bis(trifluoromethyl)phenyl unit.

5.4.1 Derivatives of *trans*-cyclohexane-1,2-diamine

Takemoto's catalyst **16** (Figure 8) is the first developed bifunctional catalyst based on (thio)urea and tertiary amine. It was tested in the Michael addition of malonates to *trans*-β-nitrostyrenes[40,41] and applied in the synthesis of (−)-epibatidine.[42,43] Takemoto's catalyst **16** proved to be successful in the reactions of CH- and SH-acidic nucleophiles, e.g., 1,3-dicarbonyl compounds, nitroalkanes, benzenethiol, and thioacetic acid, which can be deprotonated by tertiary amine moiety. Tertiary amine functional group acts as a base and activates a nucleophile *via* chiral ion pair formation,[17] while thiourea enables concerted double H-bonding activation of an electrophile. It was applied to asymmetric Michael,[44–48] domino Michael-aldol,[49] Mannich,[50,51] aza-Henry,[52,53] and Strecker reactions.[54]

The success of Takemoto's catalyst **16** led to the design of its analogues tailored precisely to the desired transformation. Catalyst **17** (Figure 8) represents an illustrative example. It was designed for the Petasis type 2-vinylation of *in situ* formed *N*-acylated

quinolinium ions. Chelating functionality activates boronic acid **28** and directs nucleophilic attack (Scheme 4).[55]

Catalyst **18** (Figure **8**) contains a primary amine functionality that enables either iminium activation of an electrophile (Figure **9**a)[56] or enamine activation of a nucleophile[57] (Figure 9b,c), while the second reactant is simultaneously activated by double H-bonding formation (Figure 9a,b) or by anion binding catalysis (Figure 9c).[58]

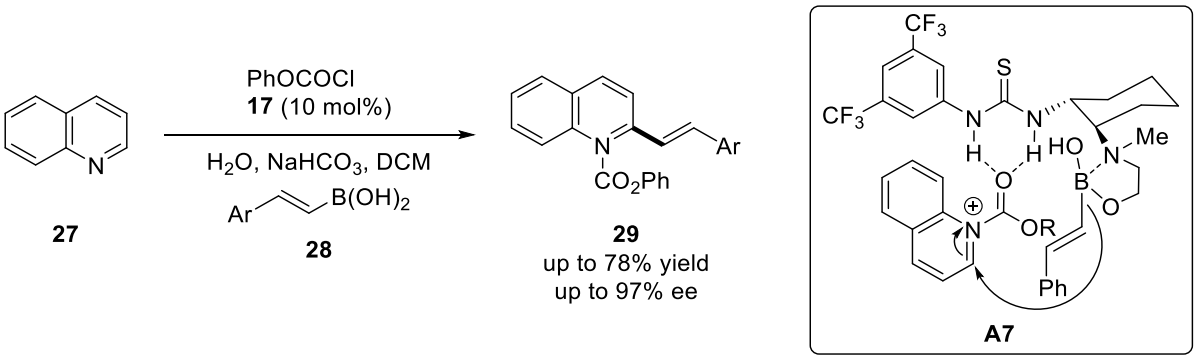

Scheme 4 The Petasis type 2-vinylation; reaction conditions & proposed mechanism **A7**.

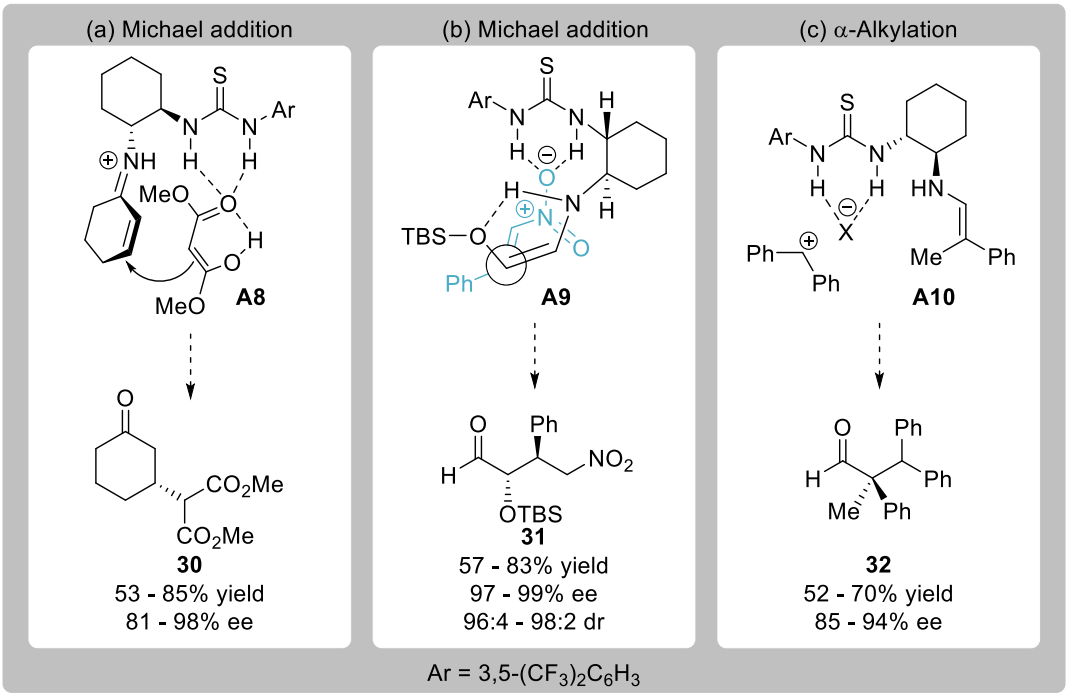

Figure 9 Activation modes of catalyst **18**: (a) iminium & double H-bonding; (b) enamine & double H-bonding; (c) enamine & anion binding.

Tertiary phosphine **19** (Figure 8)[59] and bis(thio)urea **20** (Figure 8)[60] were designed for the MBH reaction (for details, see Scheme 12, page 34 & Scheme 13, page 33). The effectivity of Takemoto's catalyst **16** inspired us to design a saccharide-based thiourea catalyst of type **I**, which will be discussed later (Section 9.2.1, page 53).

The exchange of the 3,5-bis(trifluoromethyl)phenyl unit for the amino acid moiety, well-known from the structure of Jacobsen Schiff bases (for a representative example, see catalyst **10**, Scheme 2, page 22), gave rise to catalysts such as **33** and **34** (Figure 10), which were applied in the enantioselective cyanosilylation of ketones [61,62] or in the asymmetric [3+2] cyclization, respectively.[63]

In 2008, Tsogoeva disclosed the first asymmetric Mannich reaction between unmodified ketones **36** and readily available and stable α-hydrazonoesters **35** catalyzed by thiourea/primary amine catalyst **37** (Scheme 5).[64]

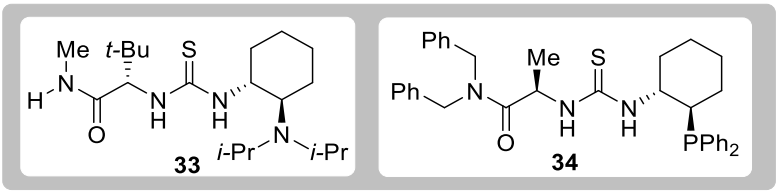

Figure 10 Structures of catalysts **33** & **34**.

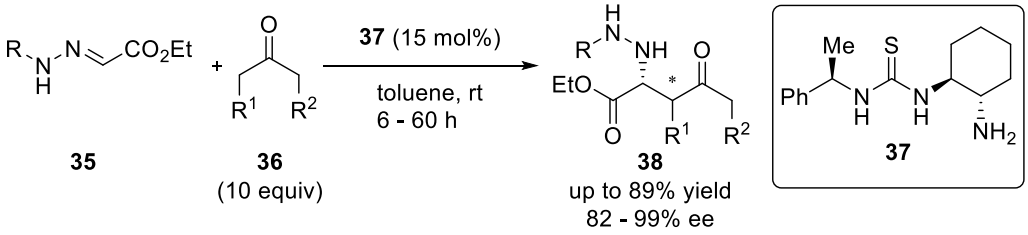

Scheme 5 First asymmetric Mannich reaction catalyzed by thiourea/primary amine **37**.

5.4.2 Derivatives of *trans*-1,2-diphenylethane-1,2-diamine

Thiourea/primary amine catalysts **21** (Figure 8) were tested in stereoselective Michael,[65,66] [3+3] cyclization,[67] Mannich,[68] and vinylogous aldol reactions.[69] Implementation of 1-naphthyl group(s) in chiral scaffold led to catalyst **40**, which showed excellent reactivity in the Nazarov cyclization (Scheme 6).[70]

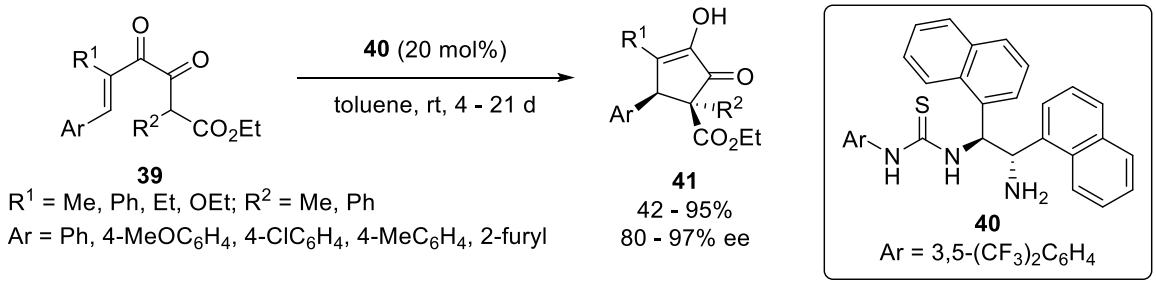

Scheme 6 Nazarov cyclization catalyzed by catalyst **40**.

5.4.3 Derivatives of cinchona alkaloids

Cinchona alkaloid backbone contains basic quinuclidine and secondary alcohol in a well-defined chiral environment and offers a simple modulation for the improvement of the bifunctional character. Introduction of aryl or alkyl (thio)urea groups in C9 position gave rise to powerful catalysts of general structure **22** (Figure 8). These catalysts are applicable to a broad spectrum of asymmetric transformations, including Mannich, Friedel-Crafts, Diels-Alder, aza-Henry, (hetero)-Michael reactions, the desymmetrization of *meso*-anhydrides and tandem Michael-aldol and Michael-Knoevenagel processes. The stereocontrol by these catalysts is strongly influenced by the configuration of key stereocenters at C8 and C9. Interestingly, derivatives with unnatural configurations were usually more effective in comparison to their natural analogues.[24,71,72]

The incorporation of well-known privileged chiral scaffolds, such as *trans*-cyclohexane-1,2-diamine or 1,1'-binaphthyl-2,2'-diamine, led to multifunctional catalysts **42** and **43**, respectively (Figure 11).

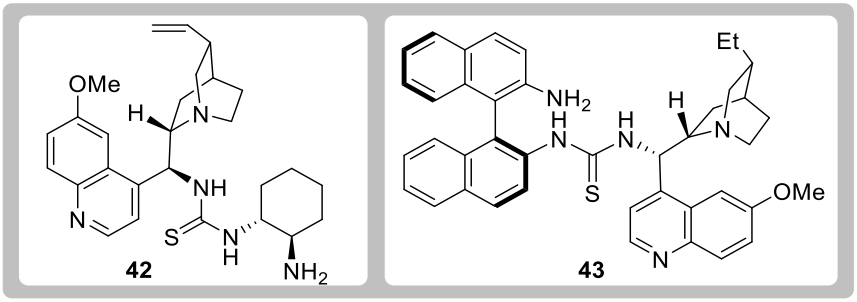

Figure 11 Structure of catalysts **42** & **43**.

Catalyst **42** activates substrates *via* simultaneous involvement of primary amine, thiourea, and quinuclidine functionalities, which lead to a well-defined assembly, resulting in excellent enantiocontrol (e.g., assembly **A11**, Scheme 7).[73]

In 2011, Barbas published the first asymmetric catalytic domino process between 3-substituted oxindoles **47** and methyleneindolinones **48** catalyzed by **43** to afford bispirooxindoles **49** with three quaternary stereocenters (Scheme 8).[74]

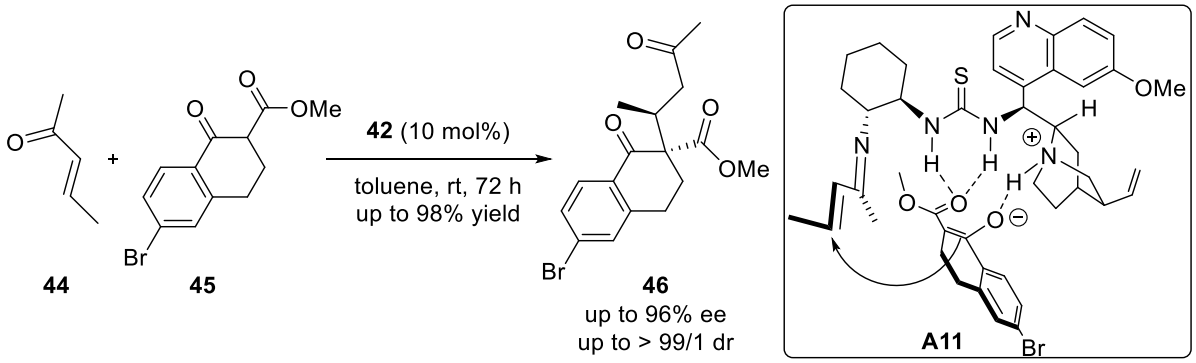

Scheme 7 Enantioselective Michael reaction under multifunctional catalysis.

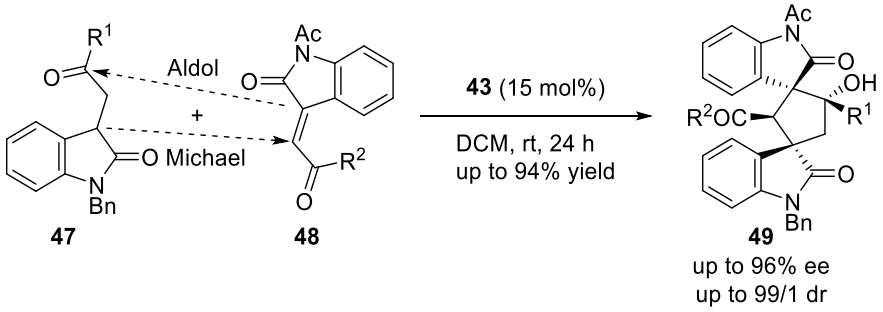

Scheme 8 Organocatalyzed domino process leading to bispirooxindoles **49**.

5.4.4 Derivatives with an axially chiral 1,1'-binaphthyl backbone

Thioureas based on an axially chiral 1,1'-binaphthyl scaffold can be tuned by a careful choice of steric and electronic properties of the achiral *N*-aryl or *N*-alkyl substituents, chiral backbone and by a precise choice of the second functional group, usually amines (e.g., catalyst **23**, Figure 8) or tertiary phosphines (e.g., catalyst **50**, Figure 12).

Thiourea/tertiary amine catalyst **23** was used as a powerful Brønsted base in the Michael addition,[75] and it was applied as a nucleophilic catalyst in the MBH reaction.[76] Binaphthyl-based phosphines proved to be an important part of nucleophilic phosphine

catalysis. For example, multifunctional catalyst **50** was successfully used in the [4+1] cyclization.[77]

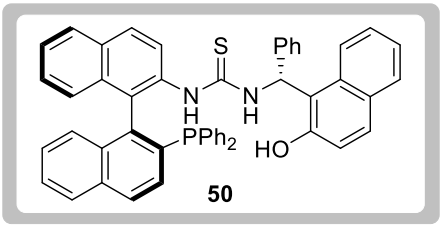

Figure 12 Structure of catalyst **50**.

5.4.5 Derivatives of amino alcohols

Amino alcohol-based (thio)ureas (e.g., **24**, Figure 8), enable simultaneous activation of both starting compounds *via* H-bonding interactions. The thiourea group acts as a double H-bonding donor, while the hydroxy group acts as an H-bonding acceptor (see assembly **A12**, Figure 13)[78] or an H-bonding donor (see assembly **A13**, Figure 13).[79]

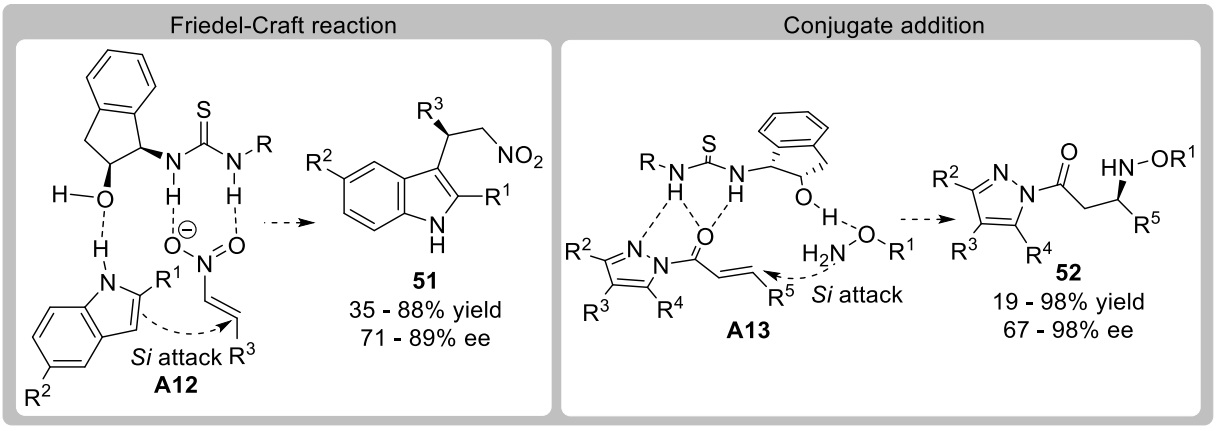

Figure 13 Hydroxy group of catalyst **24**: acts as an H-bonding acceptor in the Friedel-Crafts reaction & as an H-bonding donor in the conjugate addition.

5.4.6 Derivatives of α-amino acids and derivatives of saccharides

α-Amino acids and saccharides are an important part of chiral pool compounds. In recent years, they have come to the forefront of interest as easily available and variable chiral scaffolds for organocatalyst design.

The great success of bifunctional proline in asymmetric aminocatalysis[80] became an inspiration for the design of pyrrolidine-derived bifunctional thioureas, such as **25** (Figure 8), which were tested in the Michael addition.[81–83] Compound **26** (Figure 8), which was successfully used in the Michael addition, is an example of phenylalanine-derived catalyst.[84]

Bifunctional thioureas based on a saccharide scaffold are a central tenet of the first part of this thesis, thus a separate chapter is devoted to saccharide-based organocatalysts (see Chapter 7).

6 Tertiary amines & phosphines in nucleophilic catalysis

In IUPAC Gold Book, nucleophilic catalysis is described as catalysis by a Lewis base, involving the formation of a Lewis adduct as a reaction intermediate.[85] Nucleophilic catalysts

have to be very effective nucleophiles as well as leaving groups. Comparing tertiary amines and phosphines, the latter are more nucleophilic and less basic, which makes them compatible with base sensitive substrates, and it enables the involvement of Lewis or Brønsted acid co-catalysts.

During the catalytic cycle, tertiary amines can act as bases as well as nucleophiles. Nucleophilicity is highly sensitive to electronic and steric factors. Nucleophilic catalysis by tertiary amines can be further divided according to the nature of reactive species formed from the catalyst and substrate to acylammonium, C1-enolate, C2-enolate and C3-enolate catalysis (Figure 1, page 20). [15,86,87]

Trialkyl phosphines are more nucleophilic and therefore more catalytically active and consequently less air-stable than the aromatic ones. Careful choice of substituents with precise electronic and steric properties allows for synthesizing nucleophilic catalysts tailored to the desired transformation. Tertiary phosphines act as soft nucleophiles, which trigger a reaction by forming zwitterionic intermediates: C3-enolates, 1,3-dipoles, vinyl phosphonium ylides, or acylphosphonium salts (Figure 1, page 20).[88–90]

In the context of this thesis, asymmetric C3-enolate catalysis with chiral tertiary amines and phosphines and tertiary phosphine catalyzed [4+1] cyclization reactions are especially important. C3-enolate is a key intermediate of the (Morita)-Baylis-Hillman reaction and its aza-counterpart. The MBH reaction serves as a model transformation for the reactivity and stereoselectivity testing of organocatalysts of type **III** (Section 9.4, page 71). Therefore, separate Section 6.1 is devoted to this issue.

Construction of five-membered cycles *via* the tertiary phosphine catalyzed [4+1] cyclization represents a powerful alternative to the well-developed tertiary phosphine catalyzed [3+2] cyclization.[90–93] Only a limited number of asymmetric [4+1] cyclizations has been published to date.[94,95] We decided to address this issue and to develop the asymmetric [4+1] cyclization catalyzed by organocatalysts of type **III** (chapter 9.5.2, page 77). For that reason, the basic facts about [4+1] cyclization reactions will be listed in separate Section 6.2.

6.1 Morita-Baylis-Hillman (MBH) reaction

The Morita-Baylis-Hillman (MBH) reaction is an atom-economic formation of α-methylene-β-hydroxy compounds **55** by the creation of C–C bond between α-position of α,β-unsaturated carbonyls **53** (e.g., acrylonitriles, vinyl ketones, acrylates, α,β-unsaturated sulfones) and suitable electrophiles **54** (e.g., aldehydes, activated ketones) in the presence of a (chiral) nucleophilic catalyst (Scheme 9).[96] When imine serves as an electrophile, the reaction is referred to as the aza-MBH and the products are α-methylene-β-aminocarbonyls.

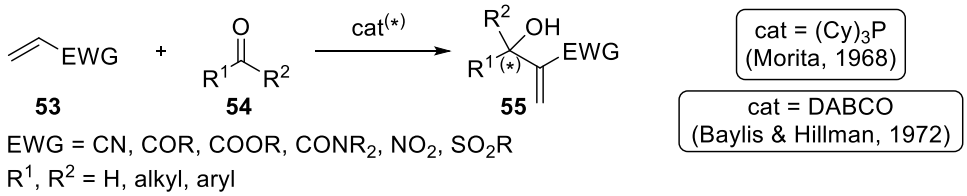

Scheme 9 (Morita)-Baylis-Hillman reaction.

In 1968, Morita was the first who reported the MBH reaction using trialkylphosphines as catalysts.[97] Four years later, Baylis and Hillman patented a similar reaction using a cheaper and less toxic tertiary amine DABCO as a catalyst.[98] The MBH reaction produces densely functionalized compounds, which are valuable building blocks for the synthesis of natural and

bioactive compounds,[99,100] such as pregabalin (**59**, Scheme 10), an approved drug used for example to treat epilepsy.[101]

In the following text, the mechanism of the MBH reaction together with representative examples of organocatalysts for the MBH reaction is reviewed. More details concerning the (aza)-MBH reaction can be found in selected reviews.[102–105]s

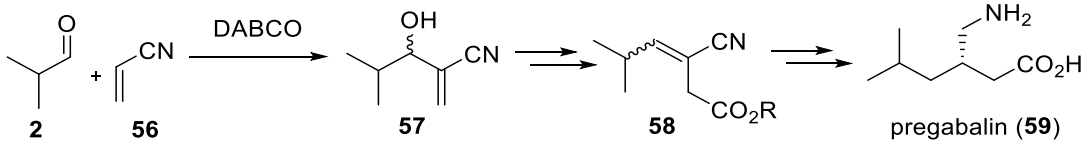

Scheme 10 Synthesis of pregabalin (**59**).

6.1.1 Mechanism of the MBH reaction

A nucleophilic catalyst triggers the MBH reaction by addition to Michael acceptor (e.g., compound **60**). Subsequent aldol reaction between C3-enolate **61** and electrophile **62** affords intermediate **63**, which undergoes α-proton transfer. The catalytic cycle is completed by the release of the catalyst from intermediates **64** or **66** (Scheme 11).[103,106,107]

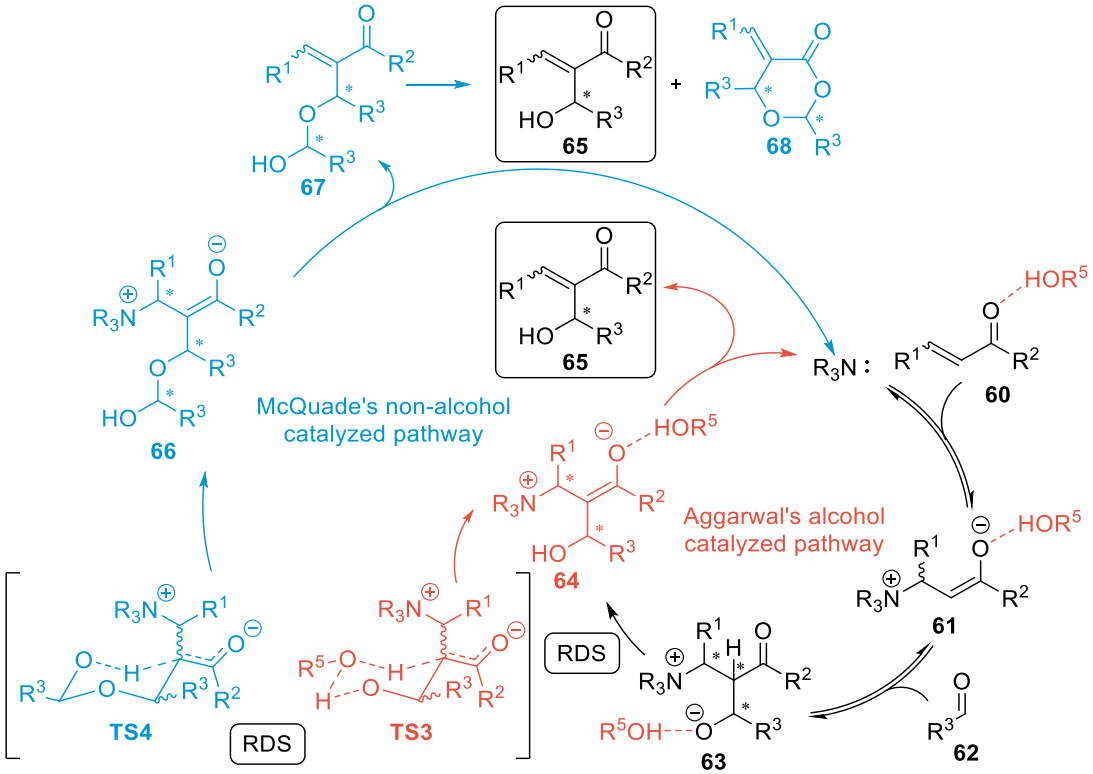

Scheme 11 Mechanism of the MBH reaction; RDS = rate-determining step.

The aldol reaction between **61** and **62** had been considered as a rate-determining step (RDS). However, the research groups of Aggarwal and Harvey[108,109] and McQuade[110,111] who studied the mechanism of the MBH reaction and the groups of Leitner,[112] Jacobsen and Raheem,[113] who themselves were interested in the mechanism of the aza-MBH reaction, claimed that the RDS is more likely proton transfer from α-position.

Two possible transition states **TS3** and **TS4** were suggested for α-proton transfer. Transition state **TS3** plays a role in the presence of protic species, and its existence is supported by the observations that the reaction is accelerated in the presence of protic solvents

and that it is autocatalytic. Autocatalysis is the reason this transition state has to be taken into account as well for reactions carried out in aprotic solvents at higher conversions (>20%) as there is an alcohol group present in the product.[109]

Transition state **TS4** plays a role in aprotic solvents and it is supported by the second-order relation of the reaction with respect to aldehyde. Transition state **TS4** explains the formation of dioxanones **68**, which are described by-products of the MBH reaction.[110,111]

The important conclusion resulting from mechanistic studies is that both pathways are competitive, and the reaction is going through one of them depending on the concrete reaction conditions. For example, reactive aldehydes (e.g., alkyl aldehydes and aromatic aldehydes with EWG groups) could lower the overall activation energy of the non-alcohol catalyzed pathway (due to the second-order relation), and thus it will be preferable even in the presence of protic species.[103]

6.1.2 Enantioselective MBH reaction

In the last two decades, organocatalysis has emerged as a powerful tool for the enantioselective MBH reaction, affording products with excellent selectivity.[102–104] However, enantioselectivity prediction and catalyst design are complicated for the reasons listed below.[103,109]

1. One stereocenter is present in a MBH product (e.g., compound **65**, Scheme 11). However, stereoisomers with two (intermediate **64**) or three (intermediates **63**, **66**) stereocenters are formed during the reaction course.
2. There are two competitive reaction pathways. The change of the reaction pathway during the reaction course (for example, due to autocatalysis) is reflected in the different nature of TS in which the enantioselectivity is determined.
3. The nature of the electrophile influences the degree of irreversibility of the aldol reaction and thus the nature of the RDS. For very reactive aldehydes or imines, the aldol reaction becomes less or non-reversible, and thus it can become a rate and stereoselectivity determining step.

It follows from the above-summarized statements that for designing a general stereoselective MBH reaction, one should consider the diastereoselectivity of the aldol reaction as well as the selectivity of α-proton transfer. High enantioselectivity would be achieved when a catalyst favours proton transfer from just one diastereomer while the other diastereomer undergoes a reverse reaction to the starting compounds.

6.1.3 Representative organocatalysts and their applications

A variety of organocatalysts have been already designed and synthesized for the asymmetric MBH reaction (for representative examples, see Figure 14). However, a universal catalyst for a broad spectrum of starting compounds is still missing.

In 1999, Hatakeyama reported the synthetic alkaloid β-ICD (**69**, Figure 14) as the first successful organocatalyst for the asymmetric MBH reaction of various aliphatic and aromatic aldehydes.[33,114,115] The success of the reaction was dependent on the usage of hexafluoroisopropyl acrylate (Entry 1, Table 2). In 2013, the synthesis of pseudo-enantiomeric α-ICD (**77**, Figure 14) was developed, and α-ICD showed comparable effectivities as β-ICD giving products with opposite enantioselectivity (Entry 2, Table 2, page 34).[116] Hatakeyama described dioxanes (e.g., compound **68**, Scheme 11) as the main by-products. The enantioselective MBH reaction catalyzed by β-ICD was applied, for example,

in the total synthesis of a potent immunosuppressant (−)-mycestericin E,[117] a plant cell-wall synthesis inhibitor epopromycin B,[118] and a potent and selective inhibitor of asparaginyl-tRNA synthase tirandamycin B.[119]

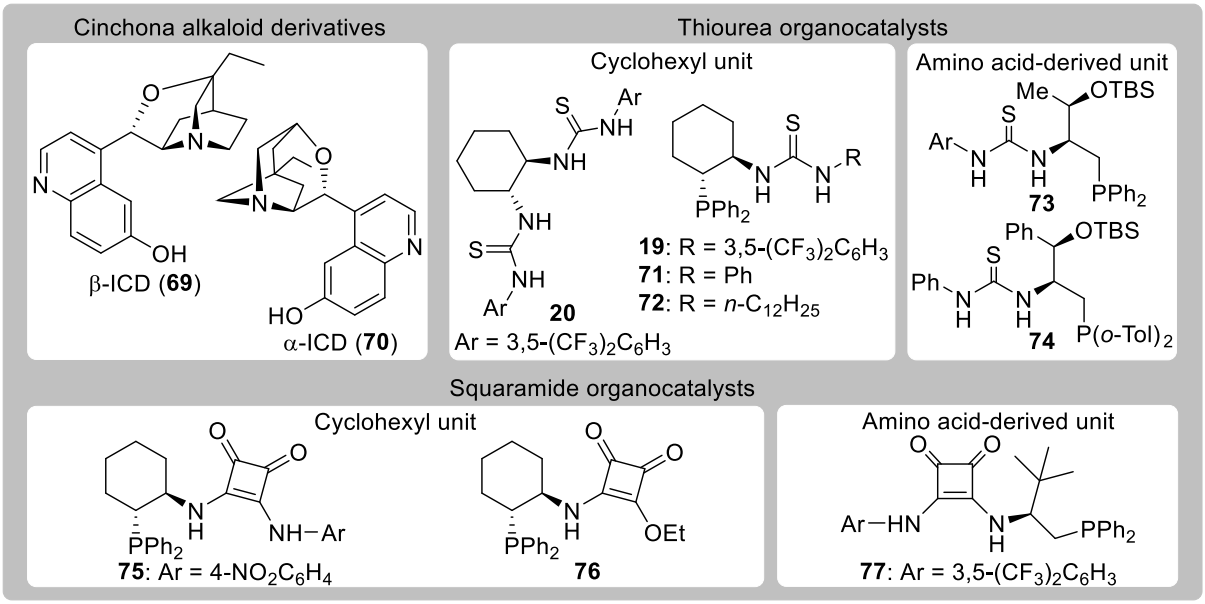

Figure 14 Representative catalysts for the MBH reaction.

In the following text, the most successful catalysts based on thiourea or squaramide functionalities are discussed. For H-bonding donor catalysts, there are two major approaches to the asymmetric organocatalytic MBH reaction, either the combination of a chiral Brønsted acid and an external achiral nucleophile or bifunctional organocatalysis.

The first approach can be demonstrated by the combination of bis(thiourea) **20** (Figure 8, page 25 & Figure 14) with DMAP or imidazole. Simultaneous activation of electrophile **62** and pronucleophile **81** through dual H-bonding was shown to be crucial for enantioinduction (Scheme 12).[60]

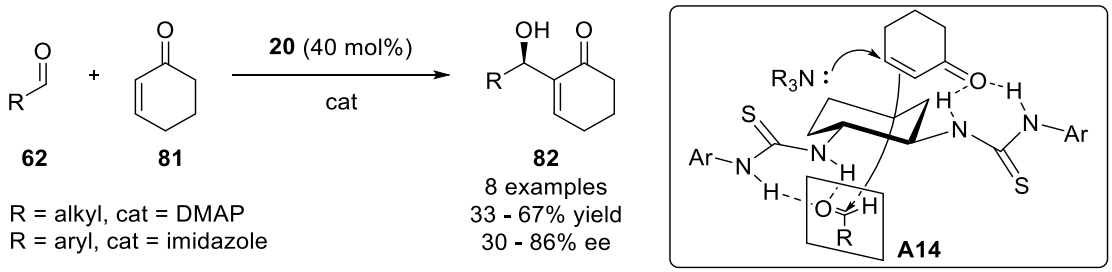

Scheme 12 BH reaction & proposed dual H-bonding activation **A14**.

So far, the most successful approach to the enantioselective MBH reaction has been the second one, which is based on the catalysts containing a nucleophilic active site (most often a tertiary phosphine) connected with a H-bonding donor (most often thiourea or squaramide) by a chiral backbone (most often *trans*-1,2-disubstituted cyclohexanes or derivatives of α-amino acids).

For the catalytic activity of thioureas **72** – **74** (Figure 14) in the asymmetric MBH reaction of aromatic aldehydes **78** with acrylates **79**, see entries 3 – 5, Table 2. The catalytic activity of thiourea **19** (Figure 14) and squaramide **76** (Figure 14) in the intramolecular MBH reaction is depicted in Scheme 13

Table 2 MBH reaction of aromatic aldehydes **78** with various acrylates **79**.

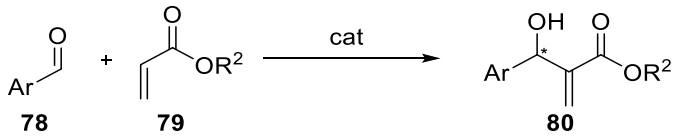

Entry	Ar	R^2	Cat	Yield (%)	Ee (%)
1[33]	7 examples	$CH(CF_3)_2$	**69**	31 – 58	91 – 99 (*R*)
2[116]	7 examples	$CH(CF_3)_2$	**70**	24 – 91	82 – 93 (*S*)
3[120]	6 examples	7 examples	**72**	24 – 96	33 – 80 (*S*)
4[121]	18 examples	4 examples	**73**	25 – 92	70 – 90 (*R*)
5[122]	11 examples	Me	**74**	42 – 98	80 – 94 (*S*)

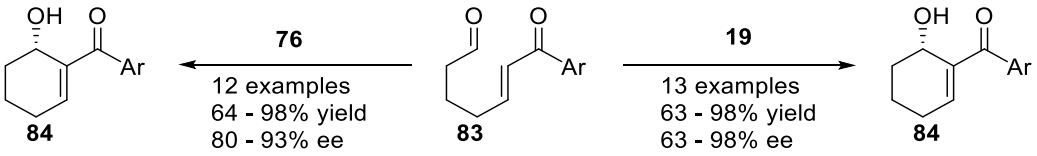

Scheme 13 Intramolecular MBH reaction catalyzed by squaramide **76**[123] or thiourea **19**.[59]

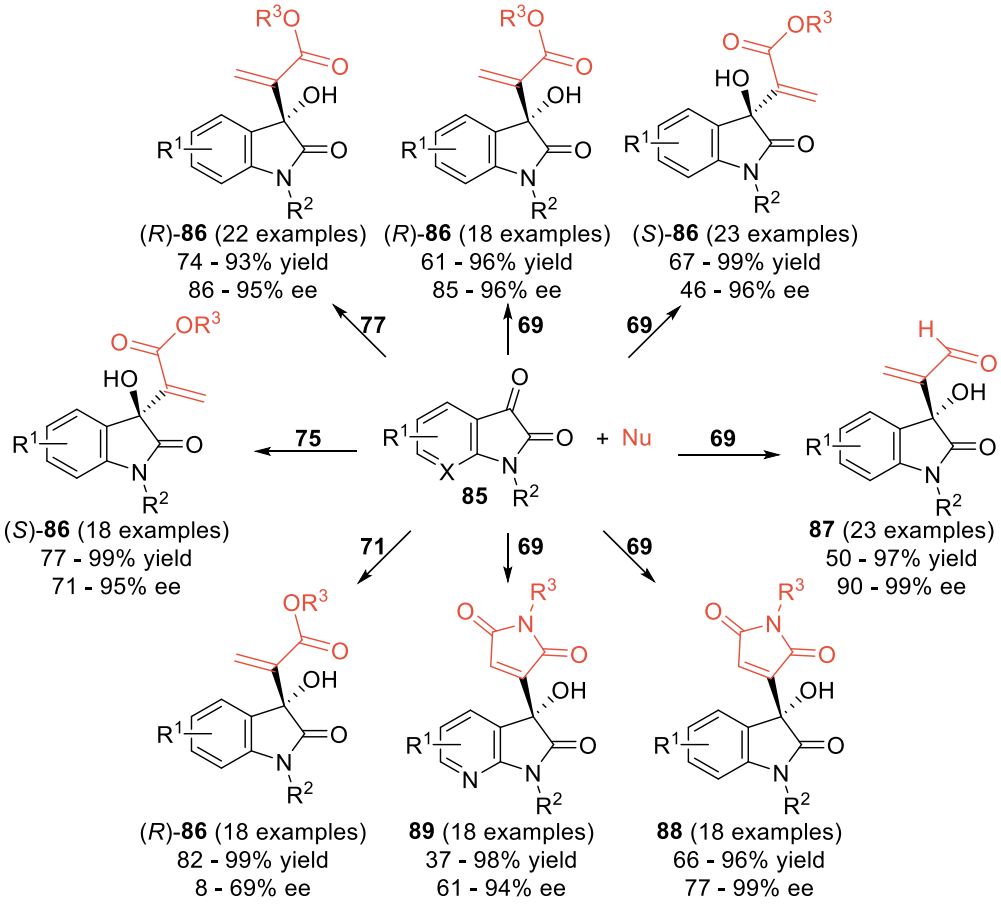

Scheme 14 Construction of a quaternary stereocenter *via* the asymmetric MBH reaction.

In organic synthesis, the enantioselective construction of a quaternary stereocenter is very challenging. Enantiomerically pure 3,3-disubstituted oxindoles **86** – **89** were afforded in the enantioselective MBH reaction of isatins **85** and suitable pronucleophiles catalyzed by β-ICD (**69**),[124–128] thiourea **71**,[129] and squaramides **75**,[130] **77**[131] (Figure 14, Scheme 14).

6.2 Construction of five-membered rings *via* [4+1] cyclization

The reaction between four-atom conjugated π-systems (e.g., compound **93**, Scheme 15) and C_1 synthons (e.g., compound **91**) affording functionalized five-membered rings (e.g., compound **92**) is referred to as [4+1] cyclization. Functionalized five-membered carbo- or heterocyclic compounds are important structural motifs of a variety of natural products and biologically active compounds.[97]

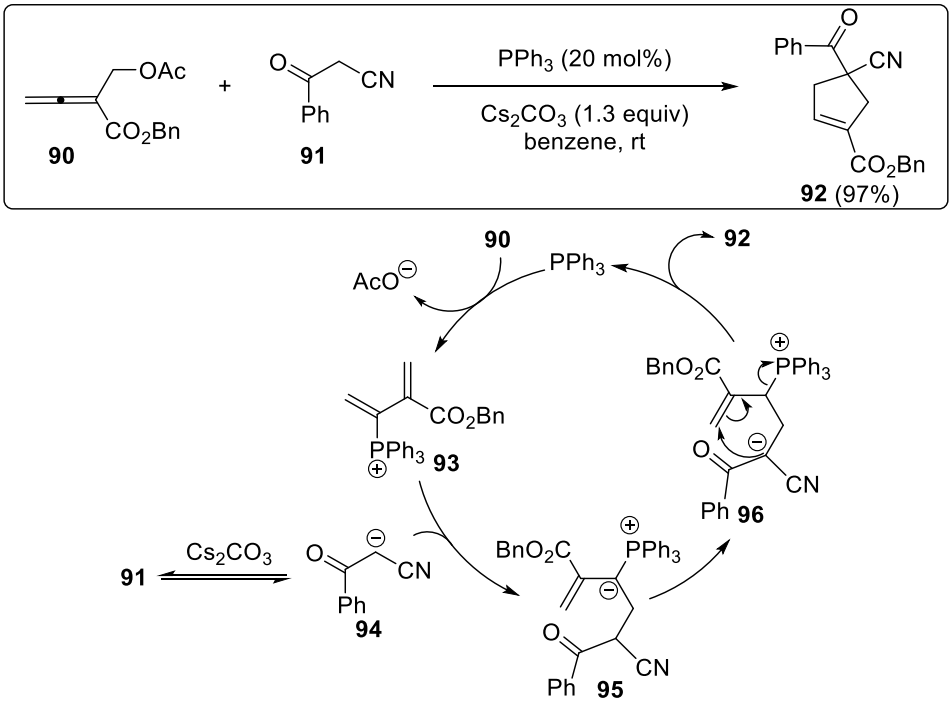

Scheme 15 Mechanism proposed for the [4+1] cyclization of allenoates **90** and 3-oxo-3-phenylpropanenitrile (**91**).

In 2010, Tong was the first who disclosed the PPh_3-catalyzed [4+1] cyclization of allenoates containing β'-*O*-acetyl group **90** with pronucleophiles, such as 3-oxo-3-phenylpropanenitrile (**91**, Scheme 15).[132] The proposed mechanism starts with the nucleophilic addition of PPh_3 to β-position of allenoate **90** which releases acetate and forms electrophilic conjugated π-system **93**. Pronucleophile **91** is activated by a base additive and attacks the γ-position of **93** to afford ylide **95**. The subsequent proton shift gives intermediate **96**. The catalytic cycle is completed by the formation of a five-membered cycle **92** *via* the conjugate addition and elimination of catalyst PPh_3.

In 2014, the first approaches to asymmetric [4+1] cyclizations were developed.[133,134] One of them was the synthesis of spiropyrazolones **99** *via* the [4+1] cyclization catalyzed by bifunctional threonine-derived catalyst **98**. The H-bonding interaction between the catalyst and a substrate was proposed to be crucial for the stereocontrol (Scheme 16).[133]

Some important examples of the highly selective asymmetric [4+1] cyclization catalyzed by binaphthyl-based thiourea/tertiary phosphine catalysts **103**, **106** were published by Shi. The reaction between MBH adducts **101** and electron-deficient 1,3-dienes **102**

afforded cyclopentene derivatives **104** (Scheme 17a).[135] Spirooxindole-dihydrofurans **107** with two adjacent stereocenters were obtained using the MBH adduct **101a** and enones **105** (Scheme 17b).[77] In contrast to the mechanism described in Scheme 15, in which tertiary phosphine is used to form C4 synthon, tertiary phosphine is used to form C1 synthon from the MBH carbonate **101** in these cases. Again, the proposed transition states stress the importance of H-bonding interactions for the stereocontrol.

Early achievements in the field of asymmetric [4+1] cyclizations have proven that [4+1] cyclizations are a powerful approach enabling the construction of five-membered rings structurally unachievable by [3+2] cycloadditions. Further research in this field is therefore highly desirable.

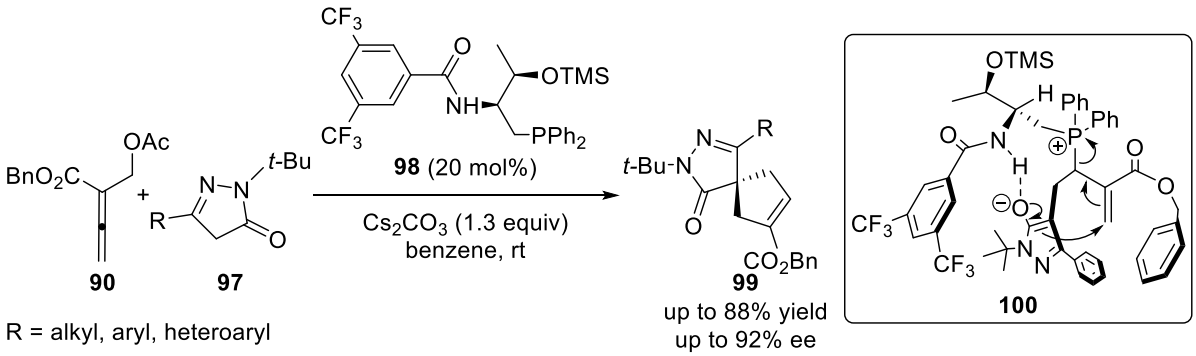

Scheme 16 Synthesis of spiropyrazolones **99** through the catalytic asymmetric [4+1] cyclization.

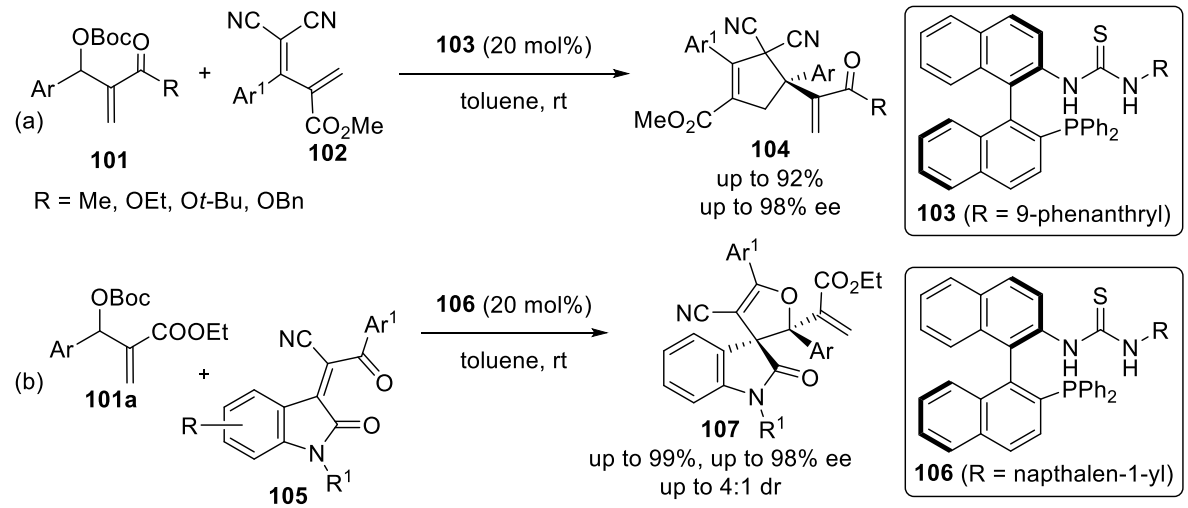

Scheme 17 Asymmetric [4+1] cyclization of MBH carbonates **101** with (a) electron-deficient dienes **102**; (b) isatin-derived enones **105**.

7 Organocatalysts based on saccharides

Saccharides are cheap, readily available biomolecules. Their conformational rigidity (governed by the equatorial presence of substituents and anomeric effect), together with the content of several stereocenters in close proximity and the availability of both enantiomers, makes them promising building blocks for catalyst design. The presence of free hydroxy groups results in water compatibility and enables further modification of catalyst properties *via* substitution. Several successful saccharide-based organocatalysts have been synthesized to this day, and they have been applied to important asymmetric transformations, e.g., aldol,

Michael, Morita-Baylis-Hillman, Biginelli and aza-Henry reactions.[136–138] Representative examples of saccharide-based catalysts are depicted in Figure 15.

The asymmetric epoxidation of alkenes with Oxone represents the most famous application of saccharide-based organocatalysts. The epoxidation using ketone catalyst **108** (Figure 15) was published by Shi already in 1996[2] and it is considered as one of the crucial contributions in the history of organocatalysis.

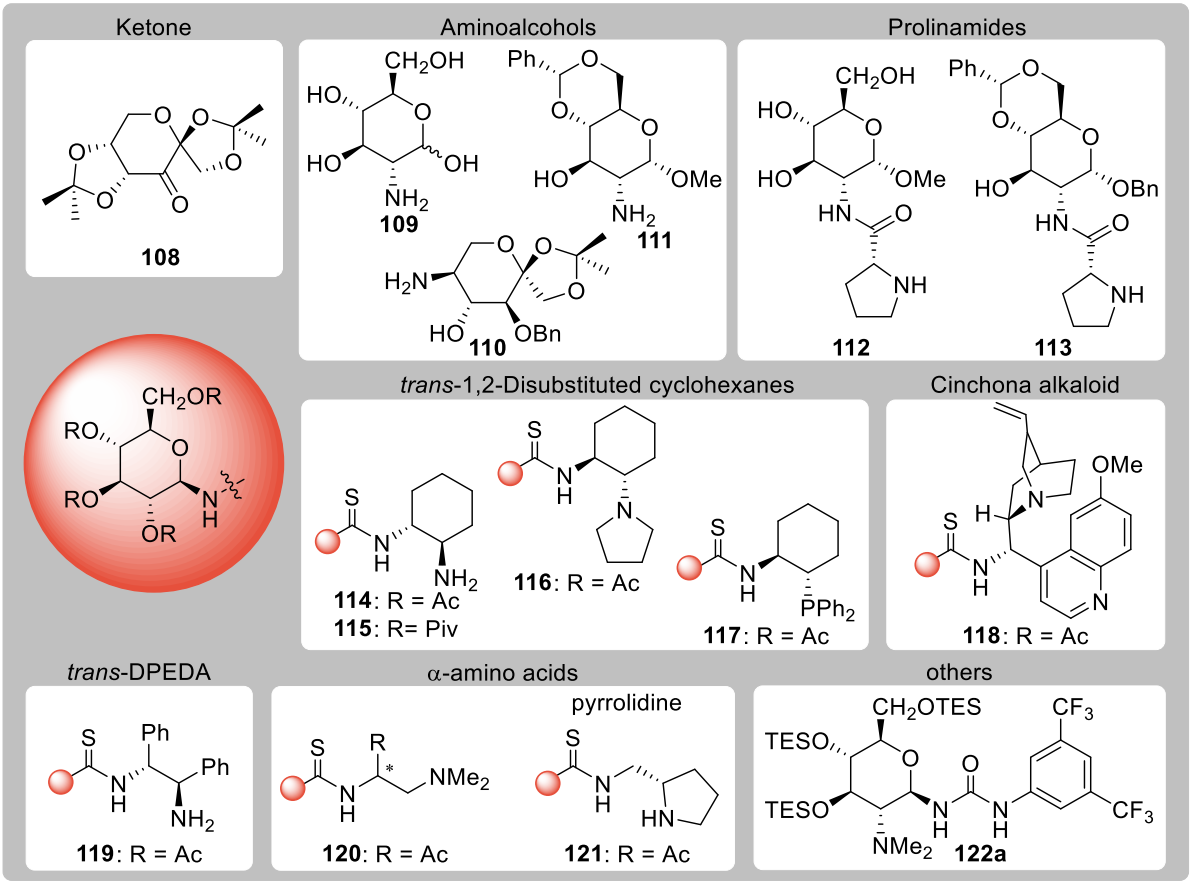

Figure 15 Selected examples of saccharide-based organocatalysts

Amino sugars containing a primary amine group together with free hydroxy group(s) (e.g., compounds **109** – **111**, Figure 15) are catalysts with a high potential for aldol reactions.[138] Proposed mechanism is based on enamine activation of ketone through the amino group and simultaneous activation of aldehyde *via* H-bonding to hydroxy group(s). And indeed, even simple D-glucosamine (**109**) catalyzed the aqueous aldol reaction, although the products were racemic.[139] The employment of protected D-glucosamine derivative **111**[140] and fructose derivative **110**[141] brought an improvement in both yield and enantioselectivity of the aqueous aldol reaction.

Combining the benefits of proline catalytic activity and saccharide water solubility was the main idea behind the development of prolinamide-derived saccharides **112**, **113** (Figure 15). The aqueous aldol reaction between benzaldehyde and acetone catalyzed by **112** (up to 69% yield, 61% ee) brought an improvement in comparison with a similar aqueous reaction catalyzed by L-proline leading to a racemic mixture. On the other hand, the catalytic activity was highly dependent on the water content. The higher the water content, the higher the reaction rate, and the lower the enantioselectivity. The decrease in enantioinduction was

explained as a competition between water molecules and free hydroxy groups of saccharide in the TS stabilization.[142]

The introduction of bulky *O*-protecting groups enabled further improvement of catalytic activity in aqueous aldol reactions. Catalyst **113** proved to be highly effective in the aldol reaction between aryl aldehydes and cyclohexanone co-catalyzed with benzoic acid in water (up to 92% yield, 97:3 anti/syn, 96% ee). Activation of cyclohexanone *via* enamine formation together with simultaneous H-bonding donation from amidic NH and free OH bonds was proposed to explain the observed selectivity; see assembly **A15** in Figure 16.[143]

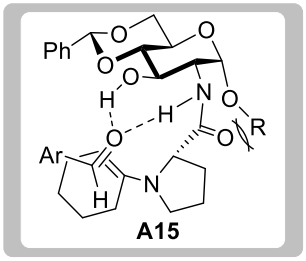

Figure 16 Mechanism **A15** proposed for the aqueous aldol reaction catalyzed by catalyst **113**.

Early examples of saccharide-derived thioureas were inspired by the structure of previously developed powerful organocatalysts (Figure 17). An exchange of *trans*-cyclohexane-1,2-diamine in Jacobsen's Schiff base **123**[25,26,144] for D-glucosamine gave rise to saccharide analogue **124**, which was tested in the Strecker and Mannich reaction.[145] Catalyst **125** was derived from Takemoto's catalyst **16**[42] by replacing 3,5-bis(trifluoromethyl)phenyl with β-D-glucopyranosyl. The saccharide moiety of catalyst **125** is expected to enhance the H-bonding donor ability through an anomeric effect. Catalyst **125** was successfully used in the aza-Henry reaction.[146]

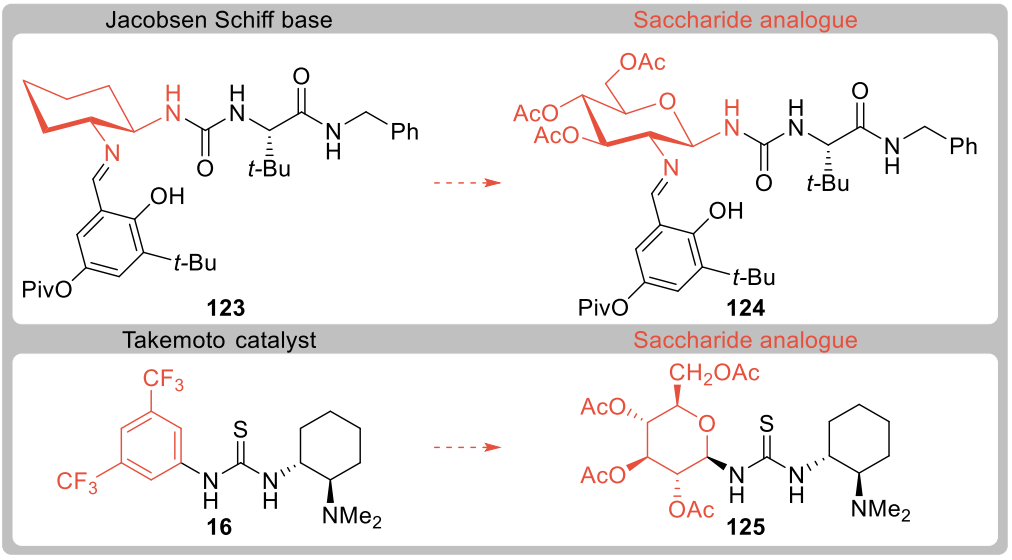

Figure 17 Design of the first saccharide-derived (thio)urea organocatalysts.

Typically, saccharide-based (thio)ureas contain a saccharide group located on the periphery of the catalyst, where it serves as a bulky substituent. The second functional group is connected to a proven chiral scaffold (Figure 15), e.g., *trans*-1,2-disubstituted cyclohexane (such as catalysts **114** – **117**, **125**), *trans*-1,2-disubstituted diphenylethane (such as catalyst **119**), cinchona alkaloids (such as catalyst **118**), α-amino acids (such as catalyst **120**, **121**).

The common feature of (thio)urea-primary amine (e.g., compounds **114**, **115**, **119**) and (thio)urea-secondary amine (e.g., compound **121**) catalysts is enamine activation of pronucleophiles and simultaneous double H-bonding activation of electrophiles (see assemblies **A16**,[147] **A17**,[148] Figure 18). Reactions are usually carried out in the presence of an organic acid (e.g., benzoic acid), which makes the enamine formation easier. We anticipated similar activation modes for our pentose-derived catalysts of type **II** (for the structure, see Figure 29, page 55), which will be discussed later on (Section 9.3.2, page 61).

Catalysts **114**, **115**, **119**, and **121** were successfully applied in Michael[147,149–152] and aldol reactions.[148] Chen reported the synthesis of dihydropyrimidines **128** *via* the asymmetric Biginelli reaction catalyzed by catalyst **114** (Scheme 18).[153]

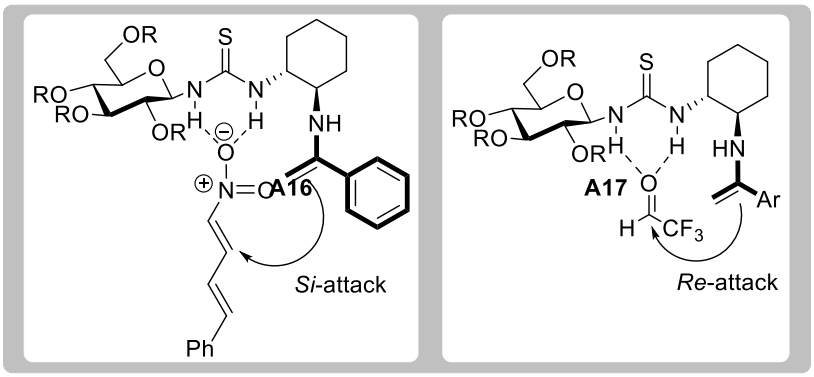

Figure 18 Mechanism **A16** proposed for the Michael addition; mechanism **A17** proposed for the aldol reaction.

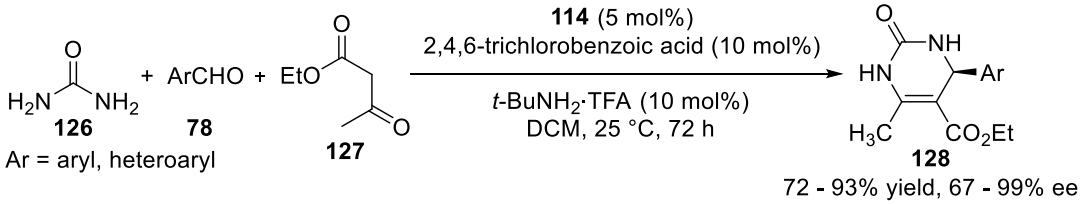

Scheme 18 Asymmetric Biginelli reaction catalyzed by catalyst **114**.

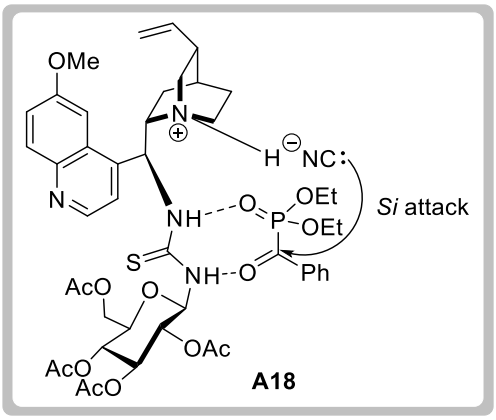

Figure 19 Mechanism **A18** proposed for the addition of HCN to α-keto phosphonates catalyzed by catalyst **118**.

An important class of saccharide-derived (thio)ureas is represented by catalysts containing a tertiary amino group, which is capable of nucleophile deprotonation (e.g., catalysts **116**, **118**, **120**, **122**, **125**). The deprotonation generates a chiral ion pair composed of

the protonated catalyst and an anionic nucleophile, which significantly contributes to the high stereocontrol. For example, cinchona alkaloid-derived catalyst **118** was successfully used in the asymmetric addition of HCN to α-keto phosphonates (Figure 19).[154]

Catalyst **116** was tested in the decarboxylative Mannich reaction of malonic acid half oxyester **130** and cyclic ketimine **129** and applied in a key step of anti-HIV drug **DPC 083** synthesis (Scheme 19).[155]

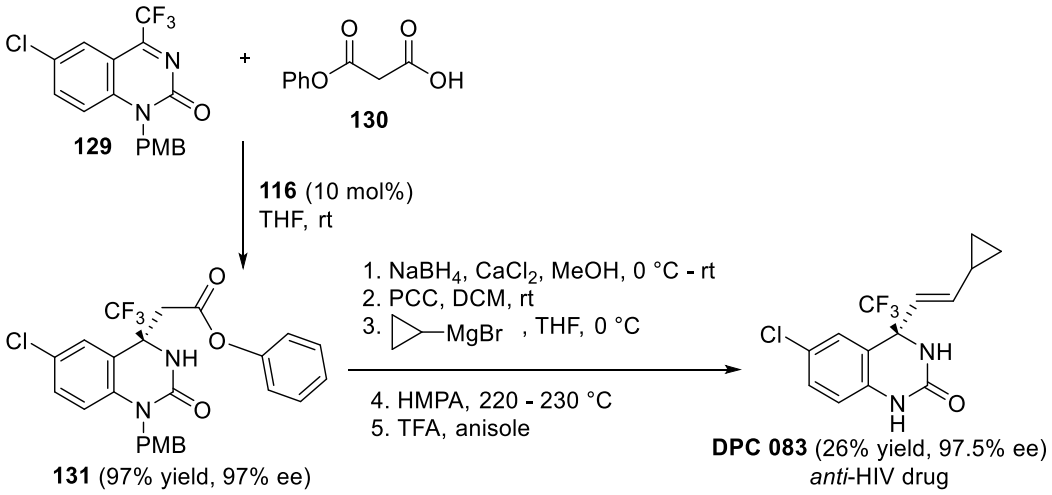

Scheme 19 Synthesis of *anti*-HIV drug **DPC 083**.

Shao synthesized a series of thiourea/tertiary amine catalysts derived from D-glucopyranose and α-amino acids of general structure **120**.[156,157] These catalysts were tested in the asymmetric conjugate addition of acetylacetone to aromatic nitroolefins or to 4-methyl-1-nitropent-1-ene. Catalysts derived from L-Val and L-Phe afforded the best results. Catalysts derived from D-amino acid afforded comparable results and opposite enantiomers of the product in comparison with L-catalysts.[157]

Benaglia, Lay and co-workers designed catalysts derived from D-glucosamine (e.g., **122a**, Figure 15), which represent the first example of catalysts in which both functional groups are bonded to the saccharide scaffold. That was a big breakthrough because the enantioselectivity of such catalysts is directed only by the saccharide unit. Catalysts **122** were tested in the nucleophilic addition of acetylacetone to β-nitrostyrenes (up to 93% yield, up to 83% ee) and of diethyl malonate to *tert*-butyl benzylidenecarbamate (25% yield, 81% ee).[158] The structure of catalysts **122** inspired us to design catalysts of type **I** (Figure 28, page 53).

Catalyst **117** (Figure 15) is the only example of an effective saccharide-based thiourea/tertiary phosphine organocatalyst. The reaction of enantiomerically pure 2-(diphenylphosphino)cyclohexanamine with isothiocyanates derived from D-glucose, D-mannose, and D-galactose led to a series of novel thiourea/tertiary phosphine catalysts. Among them, catalyst **117** showed the highest efficiency while tested in the MBH reaction of various acrylates and benzaldehydes (68 – 96% yield, 50 – 83% ee).[159]

Despite the successful explorations which were done in the field of saccharide-based organocatalysts in recent years, further efforts on new catalysts are required to improve the reactivity and selectivity. The majority of saccharide-based organocatalysts use the saccharide unit as a bulky electron-withdrawing moiety, while there is another chiral scaffold responsible for stereoinduction. Developing novel catalysts, in which the saccharide unit is the sole chiral scaffold, is desirable.

8 Catalytic C–H arylation

During my doctoral studies, I had a great opportunity to do an internship in the Larrosa's group at School of Chemistry at The University of Manchester, where I was dealing with the catalytic asymmetric C–H arylation of (η^6-arene)chromium complexes (see Chapter 10). This chapter is included to provide with the theoretical background for the results presented in Chapter 10.

8.1 Synthetic approaches to biaryls

(Hetero)biaryls are important motifs of pharmaceuticals, agrochemicals, or natural products and organic materials.[160] For that reason, efficient methods for their synthesis are of a great importance. Cross-coupling reactions between aryl(pseudo)halides **132** and organometallic reagents **133** (Scheme 20a), as well as homocoupling reactions between two identical aryl halides or organometallic reagents, represent efficient and highly selective methods for biaryl synthesis under mild conditions, and with high functional group tolerance.[161] The significance of cross-coupling reactions can be well demonstrated by the Nobel price award of the year 2010 for *Pd-catalyzed cross-couplings in organic synthesis*. However, the necessity of functionalization of both starting compounds, which usually requires several steps and suffers from regioselectivity issues, increases the cost and environmental impact of these processes.

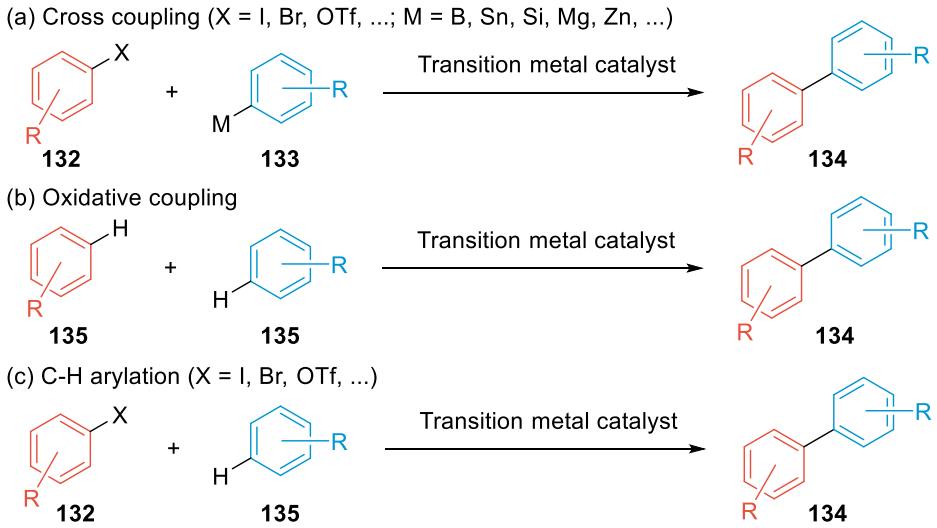

Scheme 20 Approaches to biaryls.

Oxidative couplings present an ideal approach, in which a functionalization is not required at all (Scheme 20b). Unfortunately, due to the strength of the C–H bond, it is disfavoured thermodynamically. For example, the homocoupling of benzene to afford biphenyl and H_2 is thermodynamically disfavoured by 13.8 kJ/mol.[162] Moreover, the presence of several C–H bonds in arenes makes the regioselectivity of the oxidative coupling a considerable issue.

Therefore, the metal-catalyzed C–H arylation (Scheme 20c), in which the organometallic partner is replaced with a simple arene, represents an important compromise to classical cross/homo and oxidative couplings and became one of the key green chemistry research areas demanded by pharmaceutical companies.[163]

8.2 General conditions for C–H arylations

Basic facts concerning the reactivity and selectivity issues of C–H arylations are summarized in this section. More details can be found in the selected comprehensive reviews.[160,164–169].

The low reactivity of C–H bonds together with the difficulties of controlling regioselectivity due to the presence of several C–H bonds in the substrate make the C–H activation step the biggest challenge which C–H arylations faces. Harsh reaction conditions are often necessary. Consequently, low chemoselectivity is observed (a functional group is either more reactive than C–H or decomposes due to harsh conditions).

Transition metals, such as Ru, Rh, and Pd in low oxidation states together with phosphine ligands became privileged catalytic systems for the reaction of aryl iodides, bromides, and recently increasingly used chlorides with suitable coupling partners in either dipolar aprotic solvents (e.g., DMF, DMA, NMP, CH_3CN, DMSO) or nonpolar solvents (e.g., toluene and xylene). The presence of a base, typically K_2CO_3, Cs_2CO_3, KOAc, *t*-BuOK, and CsOPiv together with heating to high temperatures (usually above 100 °C for several hours to days) or microwave heating are often required.[166]

The efficient and regioselective C–H arylation has been developed for intramolecular reactions (Scheme 21a)[170] and for substrates of general structure **138** bearing directing group(s), for highly electron-poor arenes **140**, generally requiring two electron-withdrawing groups (EWG) *ortho* to the C–H bond to be activated, and for electron-rich substrates, such as heterocycles (e.g., indol (**139**), Scheme 21b).[171]

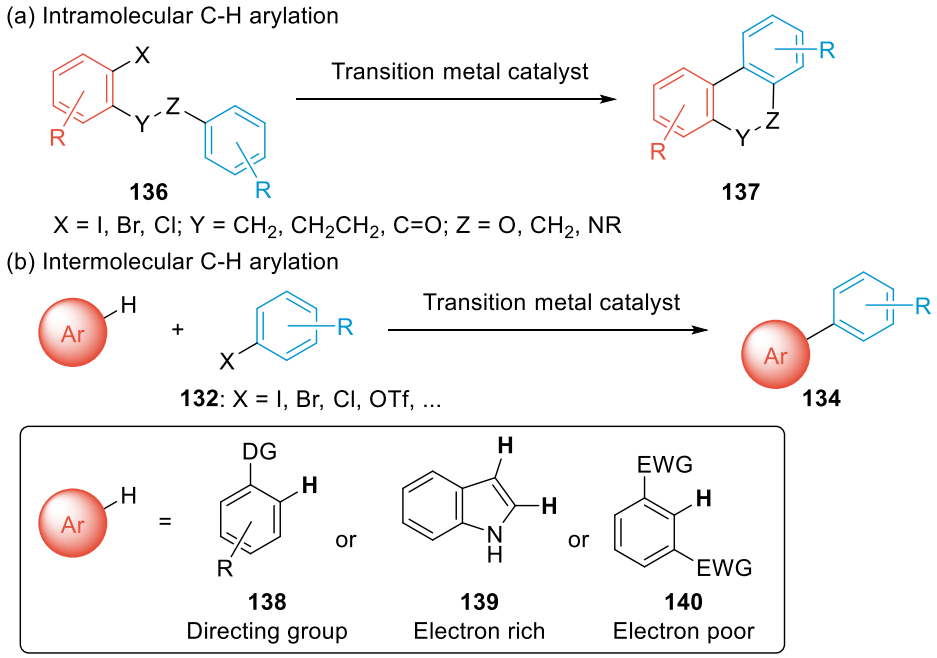

Scheme 21 Approaches to highly regioselective C–H arylation require functionalized starting compounds.

The directing group (DG) is a functional group capable of coordinating the transition metal catalyst and forcing it toward the C–H bond in close proximity, which facilitates the C–H activation and leads to high selectivity. Most DGs are based on an oxygen or nitrogen tether, which directs the metalation to the *ortho* position. Conditions for *meta*- or *para*-selective C–H arylation have also been developed.[160,171] Necessary functionalization of starting compounds is a significant disadvantage of the above-mentioned approaches to the C–H arylation.

However, arenes lacking the described structural patterns are either unreactive or must be used in large excess, for example, as solvents.[171] Typically, fluorobenzene or anisole are highly unreactive and more than 40 equiv are required to promote the C−H arylation, which affords a mixture of *ortho*, *meta* and *para* biaryls (22:3:1 for fluorobenzene and 22:53:25 for anisole, respectively).[172]

Larrosa's group developed the first general methodology for the C−H arylation of non-functionalized monofluorobenzenes **141a** and anisoles **141b** affording excellent yields of *ortho*-substituted biaryls **143** with high selectivity (Scheme 22).[173,174] In these examples, the reactivity of a C−H bond toward the C−H arylation is enhanced *via* π-complexation (e.g., (fluorobenzene)tricarbonylchromium complex is as reactive as pentafluorobenzene).

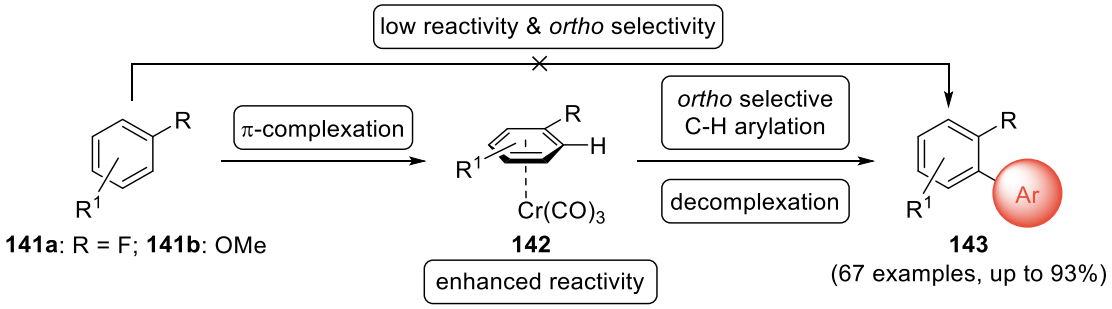

Scheme 22 C−H arylation of non-functionalized arenes **141**.

8.3 Mechanism of C−H activation

A key step of C−H arylations is C−H activation, which usually proceeds through one of the following mechanistic pathways (Figure 20).[175]

1. *The electrophilic aromatic substitution* proceeds *via* the rate-determining addition of an electron-deficient late transition metal to an arene to form unstable Wheland intermediate **144**, which rapidly loses a proton and creates aryl-metal intermediate **145**.
2. *The σ-bond metathesis*, which is typical for electrophilic early transition metals, proceeds *via* four-membered transition state **TS5** that falls into aryl-metal **145** and HX.
3. *The oxidative addition* usually involves electron-rich transition metals in low-valent oxidation states and affords aryl-metal hydride **146**.
4. *The concerted metalation-deprotonation (CMD) mechanism* is characterized by the formation of aryl-metal intermediate **147**, which typically proceeds *via* six-membered carboxylate or carbonate-assisted transition state **TS7**.

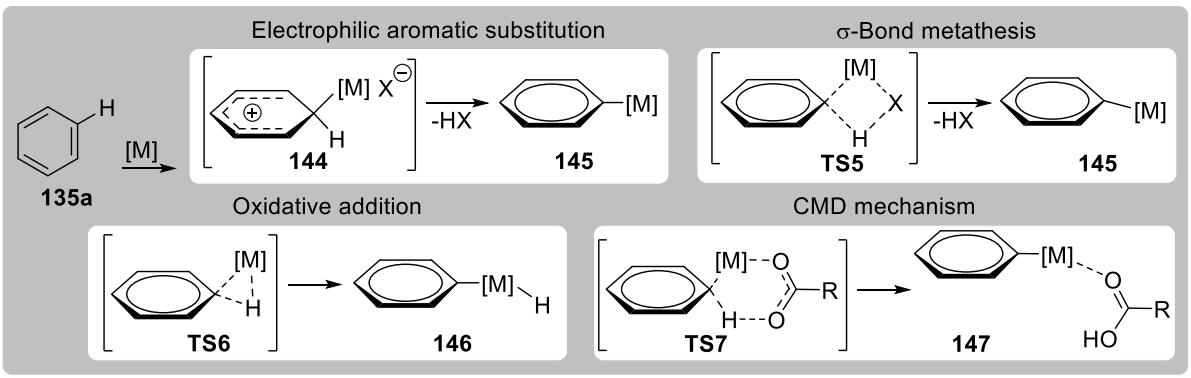

Figure 20 Four major pathways of the C−H activation step.

From the point of view of this thesis, the CMD mechanism deserves special attention because it is the mechanism proposed for the C−H activation of the asymmetric catalytic C−H arylation of (arene)chromium complexes. To provide a deeper understanding of our study in the field of the asymmetric catalytic C−H arylation of (arene)chromium complexes (Chapter 10, page 80), the CMD mechanism is discussed in more detail in the following section.

8.4 Concerted metalation-deprotonation (CMD) mechanism

The CMD mechanism is described as the C–H bond cleavage promoted by the simultaneous metalation and (intramolecular) basic deprotonation (Figure 20).[176,177]

The nature of a base has a significant impact on the reactivity; typically, carboxylates or carbonates are preferred.[176] Pivalic acid (**152**) became a general additive, which enables the development of milder reaction conditions and improvement of regioselectivity in many C−H arylations.[176]

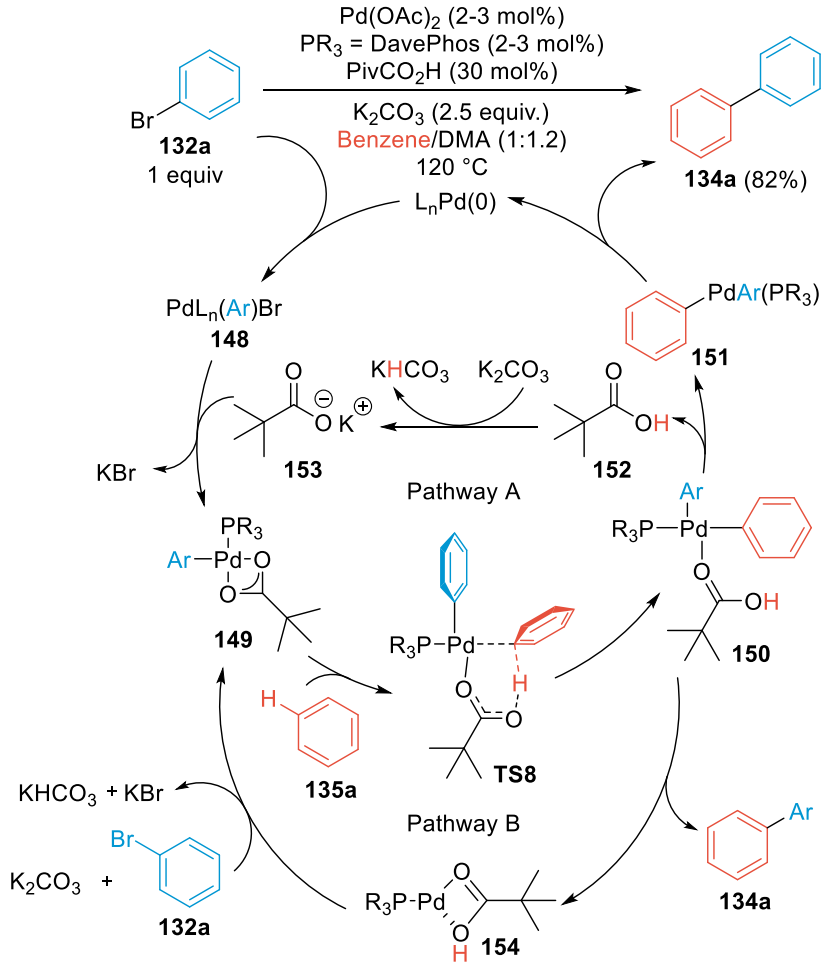

Scheme 23 Mechanism proposed for the Pd-catalyzed direct C−H arylation of benzene.

The positive effect of pivalic acid co-catalyst on the reactivity of benzene (**135a**) in the Pd-catalyzed C−H arylation was first described by Fagnou (Scheme 23). The mechanism in which pivalate **153** serves as a catalytic shuttle from benzene (**135a**) to stoichiometric and insoluble K_2CO_3 was proposed.[172] During the catalytic cycle, pivalic acid (**152**) and pivalate **153** either interact reversibly with the catalyst (pathway A) or remain bound to the catalyst (pathway B). The DFT analysis revealed that pivalate lowers the energy of the CMD transition state **TS8** by 1.3 kcal/mol in comparison to bicarbonate (24.9 vs. 26.2 kcal/mol).

Nowadays, the CMD mechanism is accepted for a variety of catalytic C−H activation, such as catalytic C−H activation of simple arenes in intramolecular C−H arylations, directed catalytic C−H activation of phenylimines, catalytic C−H activation of electron-poor arenes (e.g., pyridine-*N*-oxides, polyhalogenated arenes) and electron-rich heteroaromates.[176]

8.5 Enantioselective C−H functionalization

Although the inert character of C−H bonds makes the development of enantioselective C−H functionalization very challenging, various efficient approaches have already been developed. Two general mechanisms were described for the C−H functionalization: inner and outer sphere mechanism.[178,179] During the inner sphere mechanism, discrete metal-carbon species are formed *via* the direct interaction between a transition metal and a C−H bond (Scheme 24a).[178]

The stereochemistry determining step within the inner sphere mechanism is either C−H activation or migratory insertion. In the first case, the chiral catalyst has to distinguish between two enantiotopic hydrogens. Pd catalysts dominate this area. In the second case, the chiral catalyst directs a coupling partner from one enantiotopic face. Rh and Ir catalysts are typical for the stereochemistry determining migratory insertion.

The outer sphere mechanism utilizes the insertion of metal-bound complexes into a C−H bond. Concerted insertions of Rh carbenoids or nitrenoids are the most typical examples (Scheme 24b).[180]

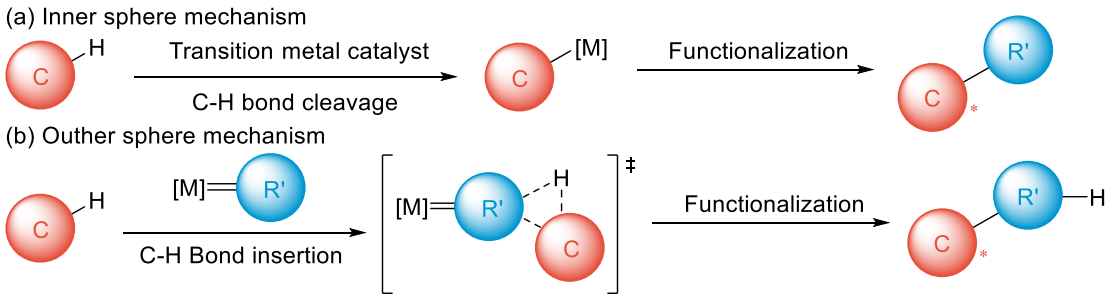

Scheme 24 Mechanistic classification of the enantioselective C−H functionalization catalyzed by transition metals.

The following sections focus on the Pd-catalyzed C−H functionalization proceeding through the inner sphere mechanism with the stereochemistry generating C(sp^2)-H activation step. The emphasis is placed on the synthesis of planar-chiral compounds because it is an area directly connected with Chapter 10, which deals with the catalytic asymmetric C−H arylation of non-functionalized (arene)chromium complexes.

8.5.1 Stereochemistry generating C(sp^2)-H activation

The most common mechanistic scenarios for the Pd-catalyzed enantioselective C−H functionalization with the stereochemistry generating C(sp^2)-H activation step are Pd(0)/Pd(II), Pd(II)/Pd(0), and Pd(II)/Pd(IV) catalytic cycles (Figure 21).[178]

1. The Pd(II)/Pd(0) cycle proceeds via C−H activation followed by transmetalation and reductive elimination. The catalytic cycle is completed by oxidation of Pd(0) to Pd(II) using an external oxidant.
2. The Pd(0)/Pd(II) catalytic cycle starts with oxidative addition affording $RPd^{II}XL_n$ specie, which subsequently cleaves the C−H bond of the coupling partner. The catalytic cycle is completed with reductive elimination.

3. The Pd(II)/Pd(IV) catalytic cycle starts with C−H activation providing $RPd^{II}XL_n$ specie, which undergoes oxidative addition. Reductive elimination completes the catalytic cycle.

While the Pd(0)/Pd(II) catalytic cycle has only been realized in an intramolecular sense, intramolecular as well as intermolecular variants were developed for the other two.

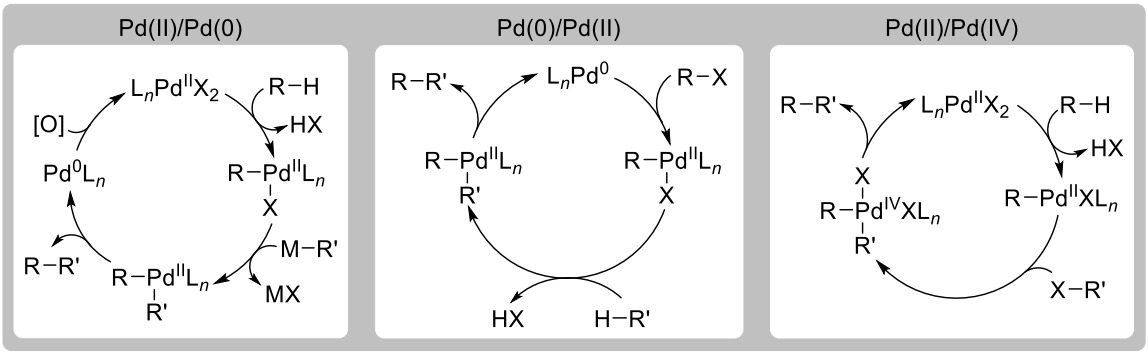

Figure 21 General mechanistic scenarios for the Pd-catalyzed enantioselective C−H functionalization.

8.5.1.1 Pd(II)/Pd(0) catalytic cycle

You's study on the Pd-catalyzed enantioselective C−H arylation of prochiral 2-(diphenylmethyl)pyridine derivatives **155** became the first example of the asymmetric C−H arylation with the stereochemistry determining C−H activation. Alkylated triarylmethanes **158** were synthesized in modest to high ee using mono-*N*-protected amino acids (MPAA) as a suitable chiral ligand for Pd (compound **157** was the best among the tested MPAA), benzoquinone as an additive and Ag_2O as an oxidative agent (Scheme 25).[181]

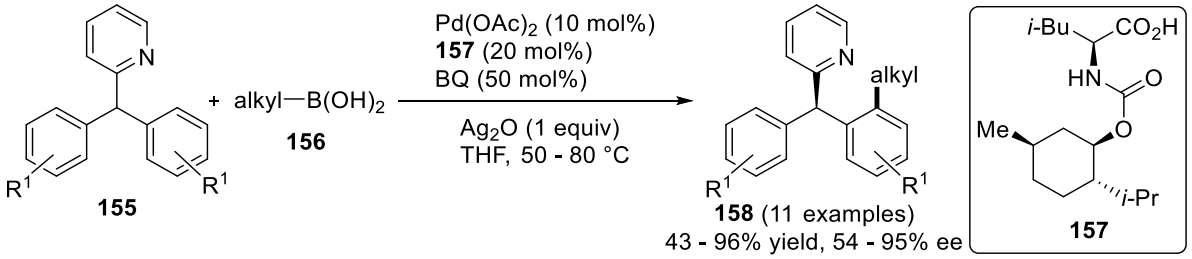

Scheme 25 Asymmetric C−H arylation of 2-(diphenylmethyl)pyridine derivatives **155**.

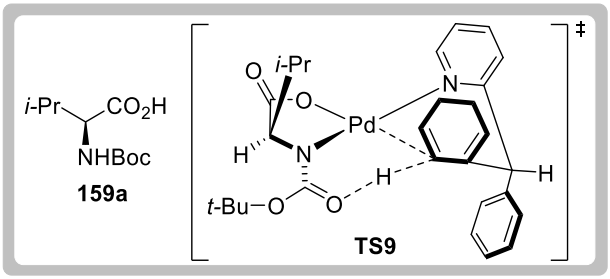

Figure 22 DFT calculated TS for the Pd-catalyzed **159a**-assisted C−H activation.

Subsequent mechanistic studies of the MPAA-assisted C−H activation revealed that the *N*,*O*-bidentate ligand plays a dual role as it stabilizes monomeric Pd complexes and serves as a base, which facilitates C−H activation in the CMD mechanism. Observed (*R*)-enantioselectivity was rationalized by the DFT calculated transition state **TS9** for the Pd-catalyzed alkynylation assisted with chiral ligand **159a**. Pyridine coordinates in a *trans* position relative

to carbamate nitrogen. The *i*-Pr group of chiral ligand **159a** forces the *N*-Boc group below the Pd plane. Boc oxygen is involved in deprotonation, which results in a downward orientation of the C−H bond toward the carbamate oxygen. Therefore, the prochiral carbon at the coplanar *ortho* position has to be oriented downward as well. Conformational requirements direct the remaining aryl group to a less sterically hindered axial position (Figure 22).[178,182]

Carboxylate and *N*-nosyl groups serve as a directing group for the highly enantioselective Pd-catalyzed C−H olefination of diphenylacetic acid[183] and for the Pd-catalyzed coupling between diarylmethylamines and arylboronic acid pinacol ester, respectively.[184]

The Pd(II)/Pd(0) catalytic cycle was successfully applied in the synthesis of planar-chiral ferrocenes (Scheme 26), which have a great potential for asymmetric catalysis as chiral ligands.[185] Tertiary amino group of aminoferrocenes **160** is used as the directing group in the coupling with aryl boronic acid (Scheme 26a),[186] the dehydrogenative Heck coupling (Scheme 26b),[187] and the dehydrogenative cyclization with diarylethynes (Scheme 26c).[188] In all cases, planar-chiral ferrocenes are obtained in moderate to high yields and with excellent enantioselectivities. An exceptional example is represented by an enantioselective oxidative cross-coupling reaction, which is the first developed catalytic biaryl coupling proceeding through C−H activation of both coupling partners (Scheme 26d).[189]

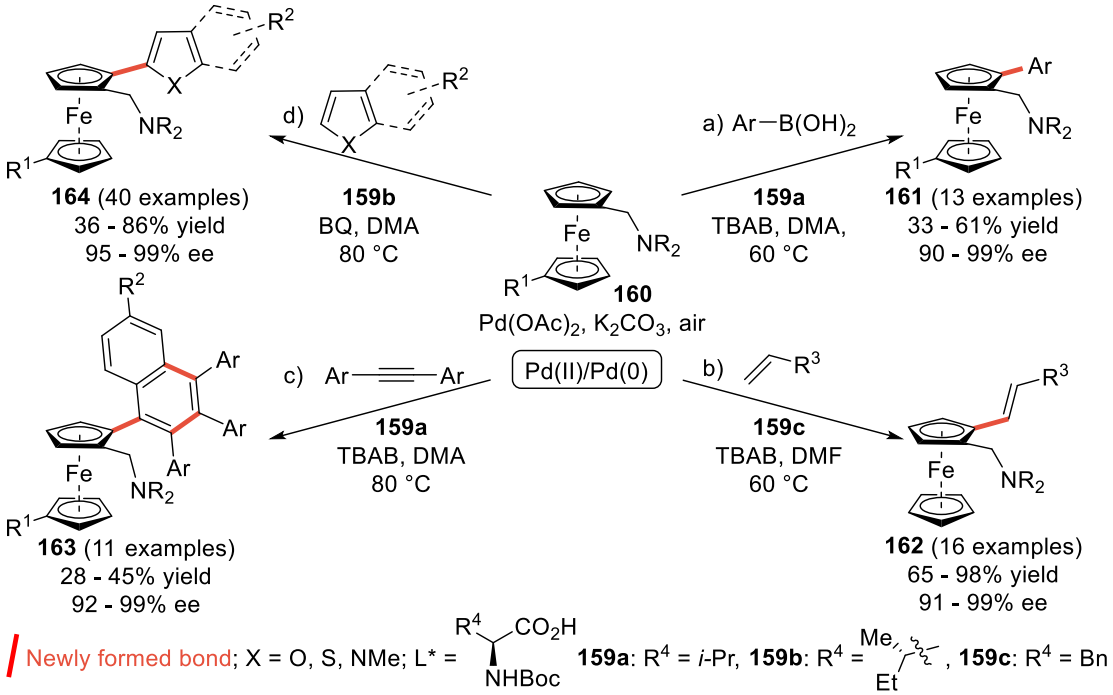

Scheme 26 Synthesis of planar-chiral ferrocenes *via* the Pd(II)/Pd(0) catalytic cycle.

8.5.1.2 Pd(0)/Pd(II) catalytic cycle

The enantioselective intramolecular C−H arylation of vinyl triflates **165** reported by Cramer in 2009 is the first example of the stereochemistry-generating C(sp^2)-H activation proceeding *via* the Pd(0)/Pd(II) catalytic cycle (Scheme 27).[190] TADDOL-derived ligand **166** showed the highest effectivity and gave desired chiral indanes **167** in high yields and enantiomeric excess.

The stereochemistry-generating C(sp^2)-H activation *via* the Pd(0)/Pd(II) catalytic cycle was successfully applied to introduce planar chirality in metallocenes, especially ferrocenes **168** (Scheme 28).[178] The advantage of the Pd(0)/Pd(II) cycle over the previously mentioned Pd(II)/Pd(0) catalytic cycle is that there is no need for an external oxidant resulting

in the absence of side oxidation of ferrocene. The most common conditions use $Pd(OAc)_2$ as a catalyst, BINAP as a stereoselective ligand, and Cs_2CO_3 as an inorganic base.[178]

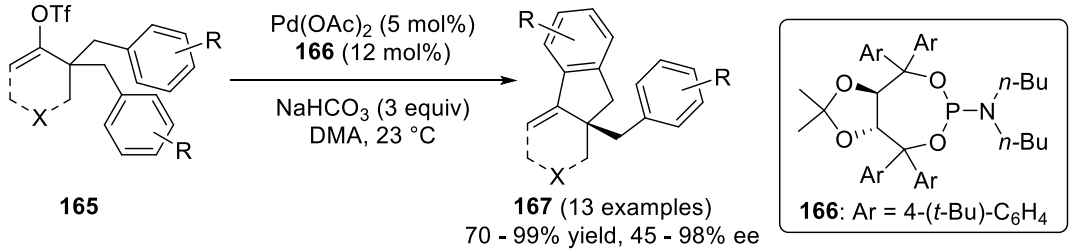

Scheme 27 Enantioselective C−H arylation of vinyl triflates **165** reported by Cramer.

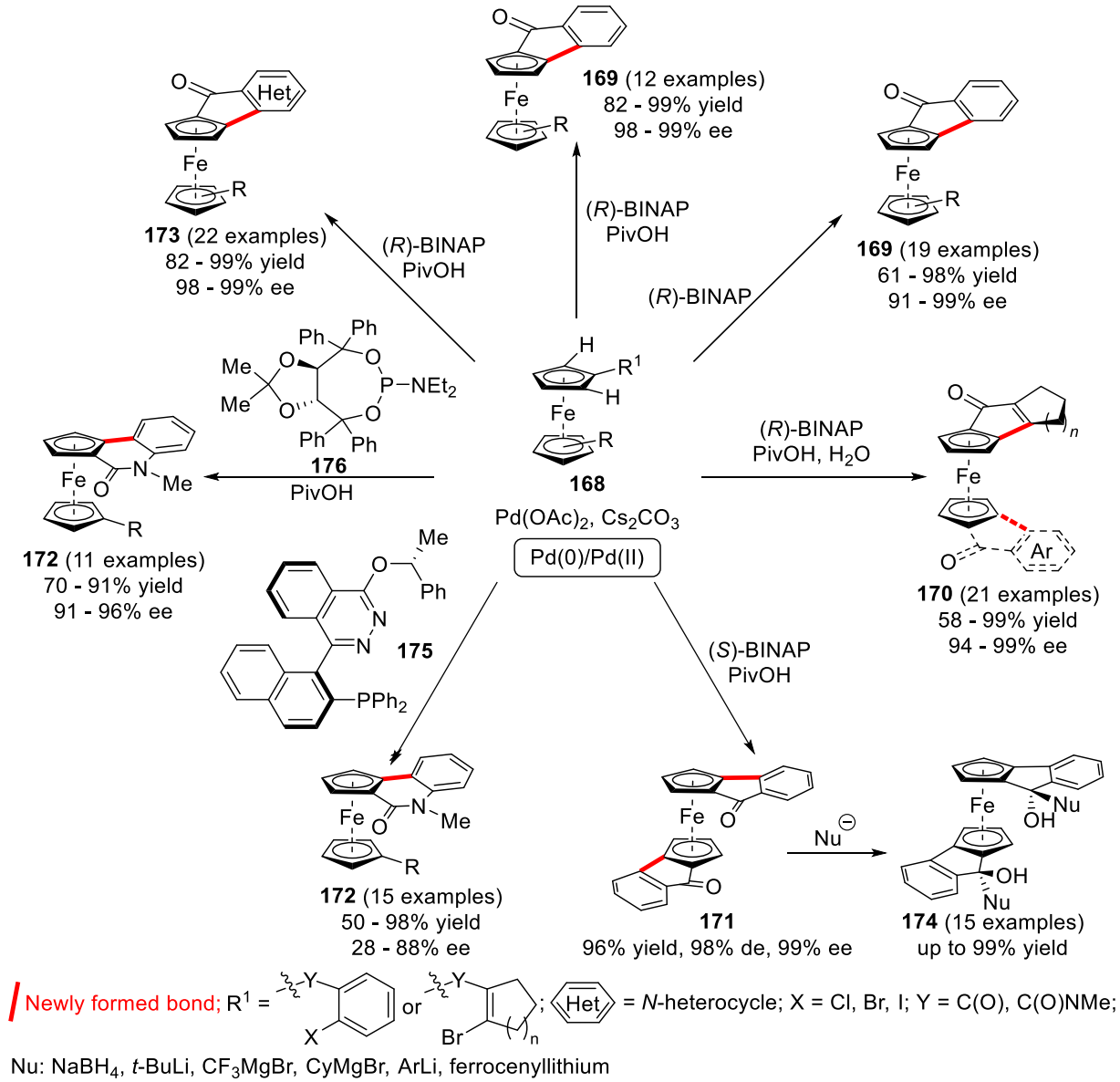

Scheme 28 Synthesis of planar-chiral ferrocenes *via* the Pd(0)/Pd(II) catalytic cycle.

8.5.1.3 Pd(II)/Pd(IV) catalytic cycle

The synthesis of chiral benzofurans **178** represents the first example of the enantioselective C−H activation proceeding *via* the Pd(II)/Pd(IV) catalytic cycle (Scheme 29).[191]

(Diacetoxyiodo)benzene was used as a strong oxidant, which facilitated the reductive elimination by the previous oxidation of Pd(II) to Pd(IV).

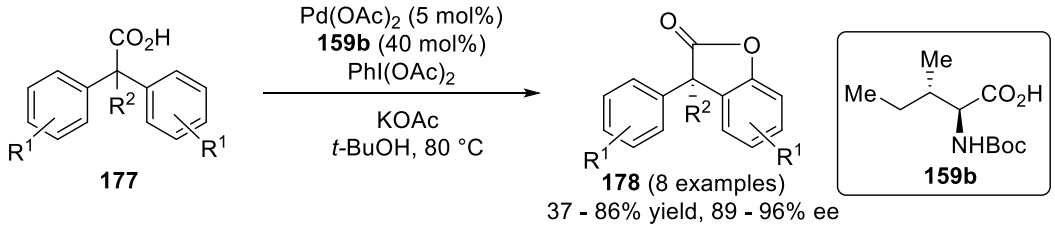

Scheme 29 Desymmetrization of diphenylacetic acid **177** *via* the Pd(II)/Pd(IV) catalytic cycle.

The reaction of diaminoferrocene **160a** with various dialkyl or diaryl 1,2-diketones **179** afforded acylated planar-chiral products **181** in moderate to high yields and enantioselectivities (Scheme 30).[192] Authors suggested that TBHP initiated a radical oxidation of Pd(II) to Pd(III) or Pd(IV) *via* the reaction with 1,2-diketones.

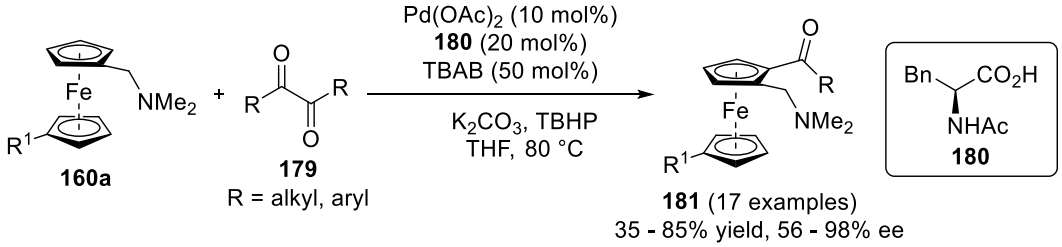

Scheme 30 Pd-catalyzed enantioselective acylation of dimethylaminoferrocenes **160a**.

The above-mentioned examples demonstrate the great potential of enantioselective C–H activation for the synthesis of highly functionalized compounds. Despite these achievements, further research aimed at new catalytic systems with improved reactivity and selectivity and at methodologies with the expanded substrate scope, where functionalization is not necessary, is highly desirable.

8.6 (Arene)chromium complexes as planar-chiral ligands

Planar-chiral compounds, such as metallocenes (especially ferrocene derivatives) and (η^6-arene)chromium complexes, have extensively been applied as stoichiometric auxiliaries and/or starting materials for the asymmetric synthesis of biologically interesting compounds. Moreover, optically active ferrocenes and (η^6-arene)chromium complexes were investigated as chiral ligands for asymmetric catalysis.

Although only a limited number of (η^6-arene)chromium-based chiral ligands was reported to date (for the selected representatives, see Figure 23), easy purification together with unambiguous detection by NMR make those ligands useful in asymmetric synthesis. It can be demonstrated by a broad applicability of the designed ligands in asymmetric C-C bond forming reactions, such as cross-coupling reactions (ligand **182**),[193] nucleophilic substitutions (ligands **182**, **185**, **186**, **190**, **191**),[194–198] 1,4-additions to Michael acceptors (ligands **183**, **190**),[194,199,200] addition of diethylzinc to benzaldehyde (ligand **183**),[199] hydrovinylations (ligand **184**),[201] and 1,2-addition of phenylboroxines to imines (ligand **190**).[194,200]

Moreover, (η^6-arene)chromium-based chiral ligands were successfully applied in the asymmetric hydroboration (ligand **187**),[202] hydrosilylation (ligand **188**),[203] hydroamination (ligand **185**),[196] and in asymmetric reductions (ligands **185** and **189**),[196,204,205]

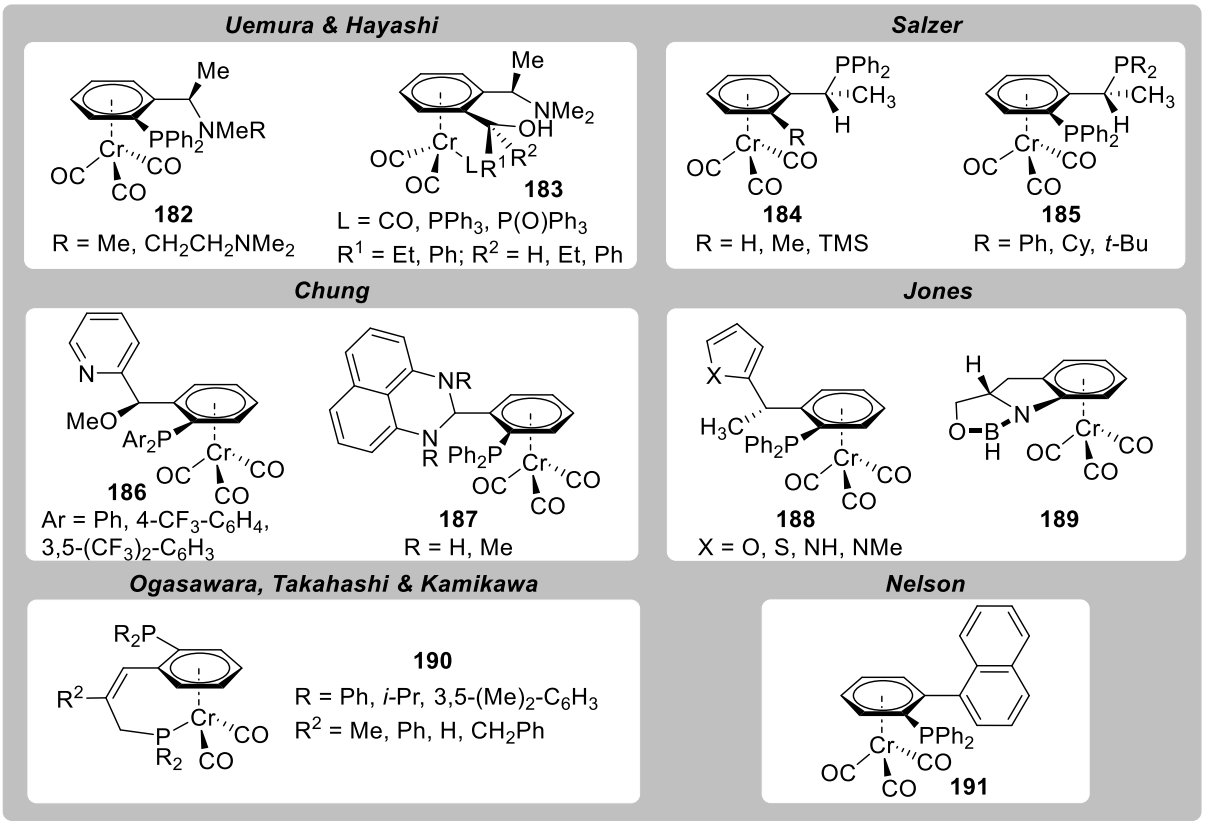

Figure 23 Representative (η^6-arene)chromium-based planar-chiral ligands.

8.6.1 Synthetic approaches to planar-chiral (arene)chromium complexes

Classical approaches to chiral (arene)chromium complexes are diastereo- or enantioselective deprotonation/electrophile quenching, nucleophilic addition/hydride abstraction, diastereoselective complexation, and resolution of racemates (Figure 24).

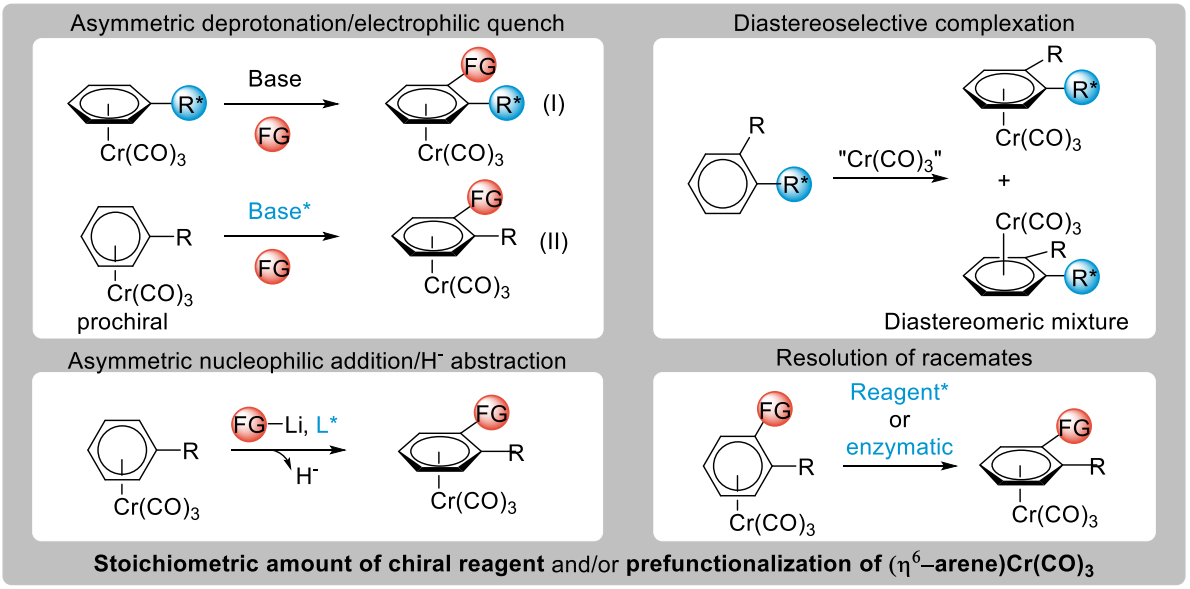

Figure 24 Classical approaches to chiral (arene)chromium complexes.

The employment of stoichiometric chiral reagents or auxiliaries belongs to the main drawbacks of these methods. Moreover, many of the classical approaches use sensitive

organometallic reagents and suffer from poor functional group compatibility and/or low atom economy.

While there are nice methodologies for the catalytic asymmetric C–H functionalization of ferrocenes (see Section 8.5.1, page 45), an access to chiral (arene)chromium complexes *via* asymmetric catalysis is significantly less explored. In 1993, Uemura and Hayashi were the first who reported the desymmetrization of (1,2-dichlorobenzene)chromium complex (**192**) *via* asymmetric Pd-catalyzed cross-coupling with various vinylic metals. The best results were obtained using vinylboronic acid **193** and ligand **194** (Scheme 31).[206]

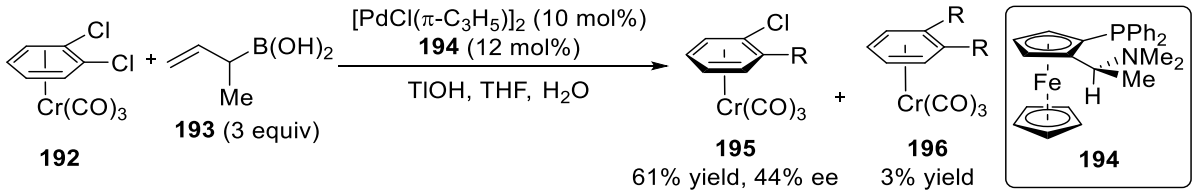

Scheme 31 Pd-catalyzed desymmetrization of (arene)chromium complex **192**.

Later on, the induction of planar chirality was achieved by a transition metal-catalyzed desymmetrization of suitably difunctionalized prochiral (arene)chromium complexes, for example, *via* the intramolecular Mizoroki-Heck reaction,[207] Pd-catalyzed hydrogenolysis of (haloarene)chromium derivatives,[208,209] methoxycarbonylation,[210,211] and the Mo-catalyzed kinetic resolution.[212] Uemura developed an impressive methodology for the synthesis of planar-chiral chromium complexes **198** with enantioselectivity up to 99% ee, which was based on the Au-catalyzed intramolecular nucleophilic addition to (alkynylarene)chromium complexes **197** (Scheme 32).[213,214]

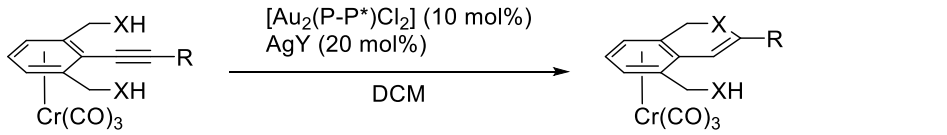

X = O, NBoc; R = alkyl, aryl; Y = BF_4, NTf_2, OTf, SbF_6
P-P* = (*R*)-BINAP, (*R*)-DM-BINAP, (*R*)-3,5-$(Me)_2$-4-MeO-BINAP, (*R*)-SEGPHOS

Scheme 32 Au-catalyzed desymmetrization of (alkynylarene)chromium complexes **197**.

All these methodologies suffer from the necessity of starting compound functionalization (Figure 25). In contrast, the direct catalytic asymmetric synthesis of planar-chiral (arene)chromium complexes has never been reported (Figure 25).

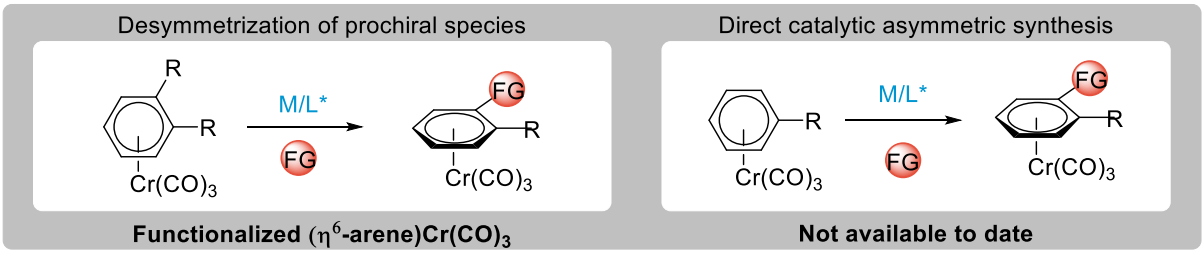

Figure 25 Catalytic desymmetrization vs. direct catalytic asymmetric synthesis.

9 Results & discussion: novel saccharide-derived (thio)urea organocatalysts

9.1 Aim of the work

The first goal of the thesis was designing novel bifunctional (thio)urea catalysts based on a saccharide scaffold.

The second goal was to evaluate the catalytic activity of the prepared saccharide-derived organocatalysts in suitable asymmetric transformations.

The third goal was developing a novel asymmetric transformation using the prepared saccharide-derived organocatalysts.

We chose saccharides as a chiral scaffold for catalyst design because they are readily available biomolecules with remarkable properties, such as conformational rigidity, presence of several adjacent stereocenters, and well-defined three-dimensional arrangement of substituents. Moreover, the availability of various diastereomeric forms enables designing both (*R*)- and (*S*)-selective catalysts. Besides, the presence of several hydroxy groups is promising for the synthesis of water-compatible organocatalysts. These catalysts bring the possibility to use solvents and substrates directly without pre-drying, but also organic reactions carried out in aqueous media are of great importance for green chemistry. In addition, derivatization of hydroxy groups enables changing the steric, electronic, and solubility properties of the saccharide building block for further tuning of catalyst properties.

In contrast to well-developed bifunctional (thio)ureas derived from cinchona alkaloids, steroids, or peptides, little attention has been paid to the synthesis of bifunctional (thio)ureas derived from saccharides.[23]

We proposed three types of novel saccharide-based bifunctional (thio)urea organocatalysts (Figure 26). Organocatalysts of type **I** are C2-symmetrical compounds derived entirely from 2-amino-2-deoxysaccharides. Catalysts of type **II** are composed of two units, namely, pentose in the pyranose form and *trans*-cyclohexane-1,2-diamine. Organocatalysts of type **III** contain a saccharide unit together with an α-amino acid-derived tertiary phosphine.

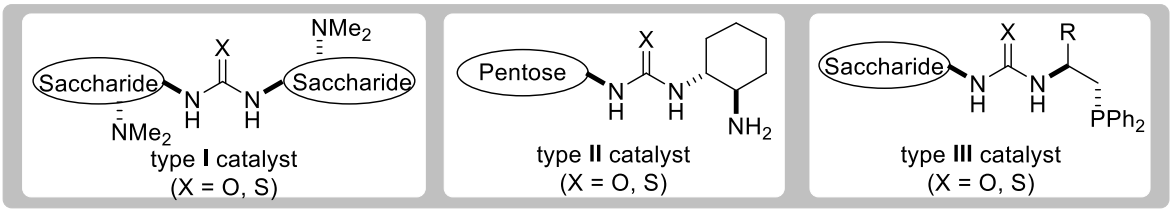

Figure 26 Novel bifunctional (thio)urea catalysts derived from saccharides.

All proposed catalysts of types **I** – **III** are based on β-anomers of saccharides because such configuration provides sterically well accessible thiourea hydrogens, which is crucial for the H-bonding donor ability of the catalysts. Moreover, the acidity of amidic protons is enhanced due to the exo-anomeric effect (delocalization of an unshared pair of electrons of the amidic nitrogen toward the anomeric carbon, Figure 27).[215]

What makes organocatalysts of type **I** distinct is that the saccharide scaffold bears both functional groups and it is the only element which fully determines stereochemistry. To the best of our knowledge, there is only one example of an effective saccharide-based organocatalyst which does not contain any external chiral moiety.[158]

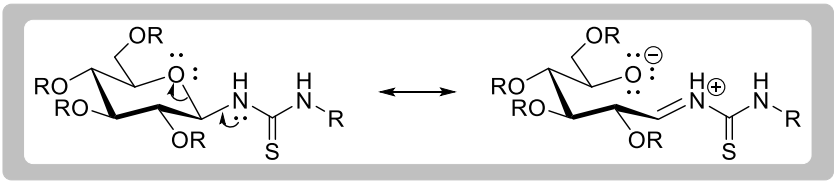

Figure 27 Influence of the exo-anomeric effect on the acidity of amidic protons.

Unlike the majority of saccharide-based organocatalysts presented so far, which are based on hexoses (in particular D-glucose), the catalysts of type **II** are derived from pentoses. Therefore, it might be interesting to study the influence of the replacement of hexoses by pentoses on the properties of organocatalysts and catalytic activity.

Organocatalysts of type **III** consist of a saccharide unit and a chiral tertiary phosphine derived from α-amino acid and they are readily available from naturally occurring molecules: saccharides and α-amino acids. Only one type of bifunctional thiourea/phosphine organocatalyst derived from saccharides and a cyclohexane skeleton has been reported (see catalyst **117**, Figure 15, Chapter 7, page 40) despite tertiary phosphines belonging to an important part of nucleophilic catalysis.

9.2 Design of novel organocatalysts derived from saccharides

9.2.1 Organocatalysts of type I

Catalysts bearing two functional groups arranged in a 1,2-*trans*-cyclohexyl moiety proved to be very effective in asymmetric synthesis. Takemoto's catalyst **16** represents one of these examples (Section 5.4.1, page 25 & Figure 28).[40]

The structure of Takemoto's catalyst **16** inspired Benaglia, Lay and co-workers to prepare catalysts **122** (Chapter 7, page 40 & Figure 28), in which the cyclohexyl moiety is replaced by a saccharide unit.[158] Ureas **122** became the first example of catalysts bearing both functional groups (thiourea and tertiary amine) on the saccharide scaffold.

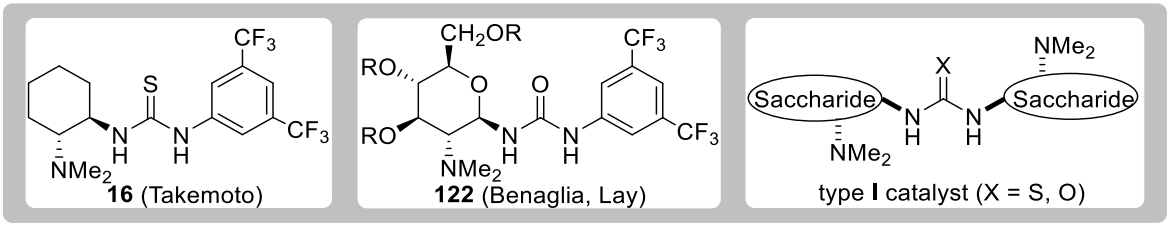

Figure 28 Takemoto's catalyst **16** & catalysts inspired by its structure.

Based on the above-mentioned observations, we proposed C2-symmetrical bifunctional (thio)urea organocatalysts of type **I**, which are entirely derived from saccharides (Figure 28). The introduction of chirality to the achiral substrate *via* C2-symmetrical catalysts proved to be a very effective approach affording excellent enantioinduction. The rotational symmetry of the catalyst reduces the number of catalyst-substrate interactions and thus limits the number of possible reaction pathways resulting in high enantioselectivity.[216] Moreover, using saccharides as the only scaffold brings the advantage of a readily available starting material containing several well-defined stereocenters. In addition, the presence of hydroxy groups is promising in terms of further modifications to tune the catalytic properties. The acidity of amidic protons of type **I** catalysts should be enhanced *via* the exo-anomeric effect. As a result, we anticipated the high catalytic activity of type **I** catalysts.

To get thiourea catalysts of type **I**, one of the most abundant monosaccharides, D-glucosamine (**109**), was chosen as a model substrate. Two approaches starting from D-glucosamine (**109**) were proposed for the synthesis of catalysts **209** (Scheme 33). Both of them contained a sequence of *O*- and *N*-derivatizations, azide introduction, and azido group conversion.

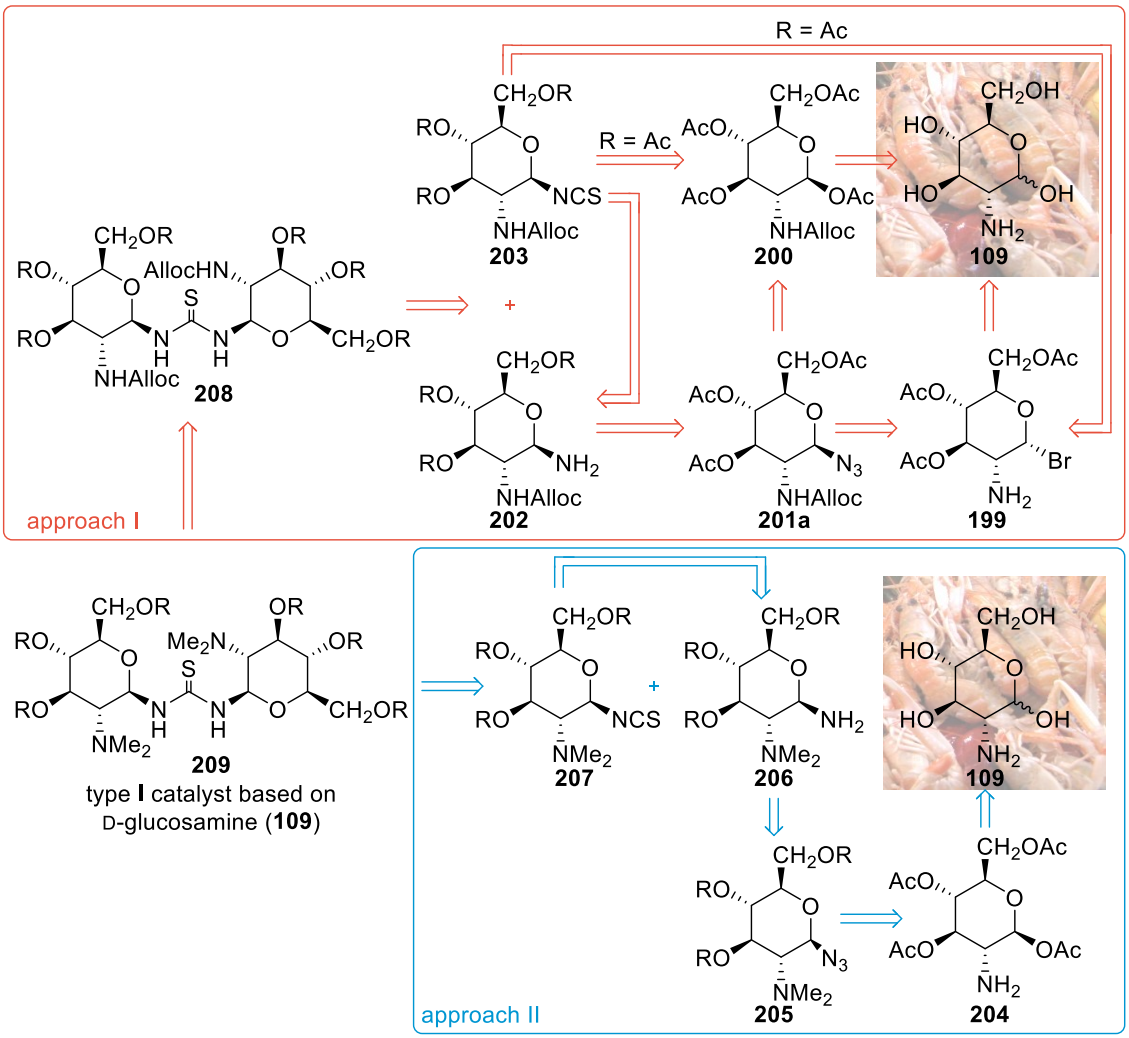

Scheme 33 Retrosynthetic routes to organocatalysts **209**.

The first approach was based on *N*-Alloc-protected derivatives of D-glucosamine. We suggested a synthesis, in which the nucleophilic addition of amine **202** to isothiocyanate **203** afforded C2-symmetrical compound **208**, a precursor of catalyst **209**. Azide **201a** was proposed as a key intermediate for the synthesis of amine **202**, which served as a starting compound for the synthesis of isothiocyanate **203**.

The second approach was based on the direct preparation of C2-symmetrical catalyst **209** *via* the nucleophilic addition between *N*,*N*-dimethylated intermediates: amine **206** and isothiocyanate **207**. Azide **205** was proposed as a key intermediate affording amine **206** *via* azide reduction and isothiocyanate **207** *via* the subsequent NCS group introduction.

9.2.2 Organocatalysts of type II

In 2012, highly effective saccharide-based bifunctional catalysts were presented by Ma's group (Chapter 7, page 39). Ma's catalysts, such as compound **114** (Figure 29), are based on

the proven *trans*-cyclohexane-1,2-diamine chiral scaffold. The saccharide moiety serves as a bulky electron-withdrawing group.[149]

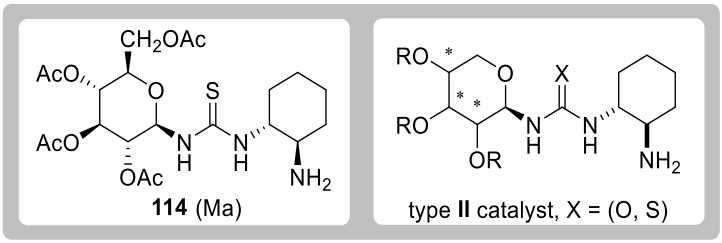

Figure 29 Ma's catalyst and catalyst of type **II** inspired by its structure.

Having this in mind, we proposed thiourea catalyst of type **II** (Figure 29), in which the pentose unit was present as a substitute for D-glucose previously used by Ma. Such a catalyst would reduce the number of functional groups and stereocenters (there is no substituent on C5). Pentoses in the pyranose form do not contain any reactive primary hydroxy groups (usually protected as esters or ethers), which could be reflected in the decreased occurrence of side reactions. In addition, we expected that the absence of a stereocenter on C5 would have the minimal influence on stereoinduction. Similarly as for type **I** catalysts, we anticipated the enhanced acidity of amidic protons due to the exo-anomeric effect.

To prepare type **II** catalyst **215**, we chose D-xylose (**210**) as a representative of pentoses. Easily accessible D-xylose (**210**) is a structural analogue to D-glucose (the same absolute configuration of stereocenters), which made D-xylose a logical first choice. We suggested a synthesis, in which the nucleophilic addition of commercially available diamine **214** to xylopyranosyl isothiocyanate **213** was a crucial step (Scheme 34). The synthesis of isothiocyanate **213** from D-xylose (**210**) was proposed as a sequence of *O*-acetylation, azido group introduction, *O*-deprotection and *O*-substitution, and azido group conversion.

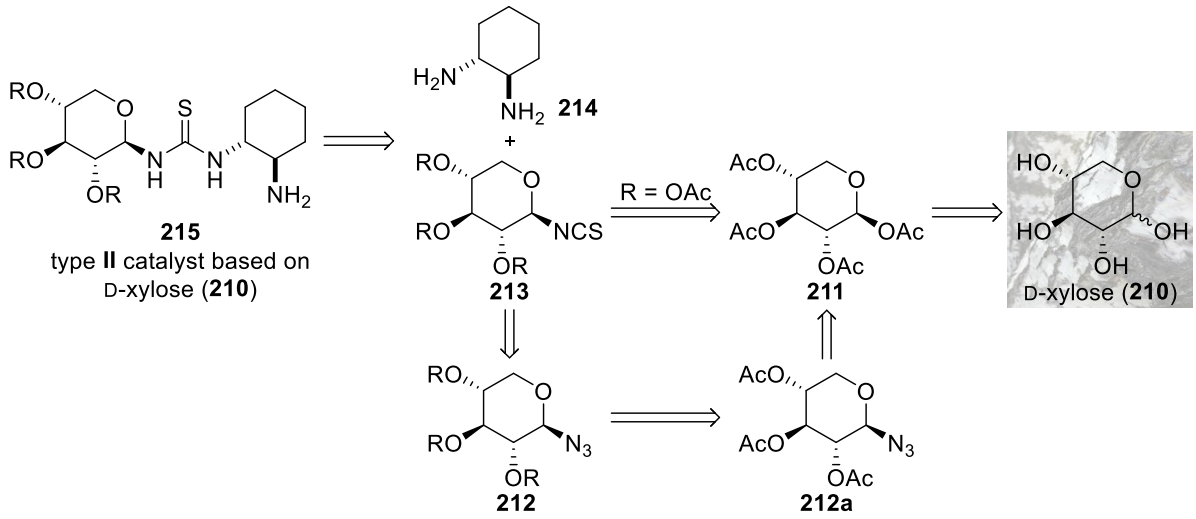

Scheme 34 Retrosynthetic strategy to type **II** organocatalysts.

9.2.3 Organocatalysts of type III

In 2008, Wu's group reported phosphine analogue **19** (Figure 30)[217] of Takemoto's catalyst **16**[42] (Section 5.4.1, page 25) for the enantioselective MBH reaction between aromatic aldehydes and methyl vinyl ketones, which afforded the desired allylic alcohols in up to 91% yield and up to 94% ee. In 2012, the same group introduced saccharide analogue **117** (Chapter

7, page 40) of their catalyst **19** (Figure 30), which was tested in the MBH reaction between acrylates and aromatic aldehydes (up to 96% yield, up to 88% ee).[159]

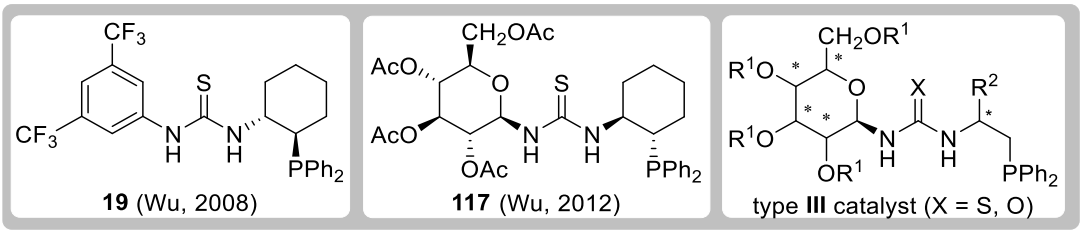

Figure 30 Wu's catalysts and catalyst of type **III** inspired by their structure.

Inspired by their work, we suggested type **III** organocatalysts derived from easily accessible starting compounds: saccharides and α-amino acids (Figure 30). Comparing Wu's catalyst and type **III** organocatalysts, the latter provides straightforward ways of further modifications leading to improved stereocontrol due to the easy availability of various natural and synthetic α-amino acids.

The convergent synthesis of type **III** catalysts was based on the nucleophilic addition of aminophosphine **222** to iso(thio)cyanates **218**, **219**. The most abundant monosaccharide, D-glucose, was chosen as a model substrate. The synthesis of glucopyranosyl iso(thio)cyanates **218**, **219** started from D-glucose, which underwent *O*-acetalization and azidation to get azide **217a**. Intermediate **217a** was subjected to the change of *O*-substituents and the interconversion of azide to iso(thio)cyanate to afford compounds **218**, **219**. The synthesis of aminophosphines **222** started from α-amino acids. A sequence of amino acid reduction, *N*-protection, and hydroxy group derivatization gave intermediates **220**, **221**. The nucleophilic substitution of OR group with a tertiary phosphine and *N*-deprotection afforded desired aminophosphines **222** (Scheme 35).

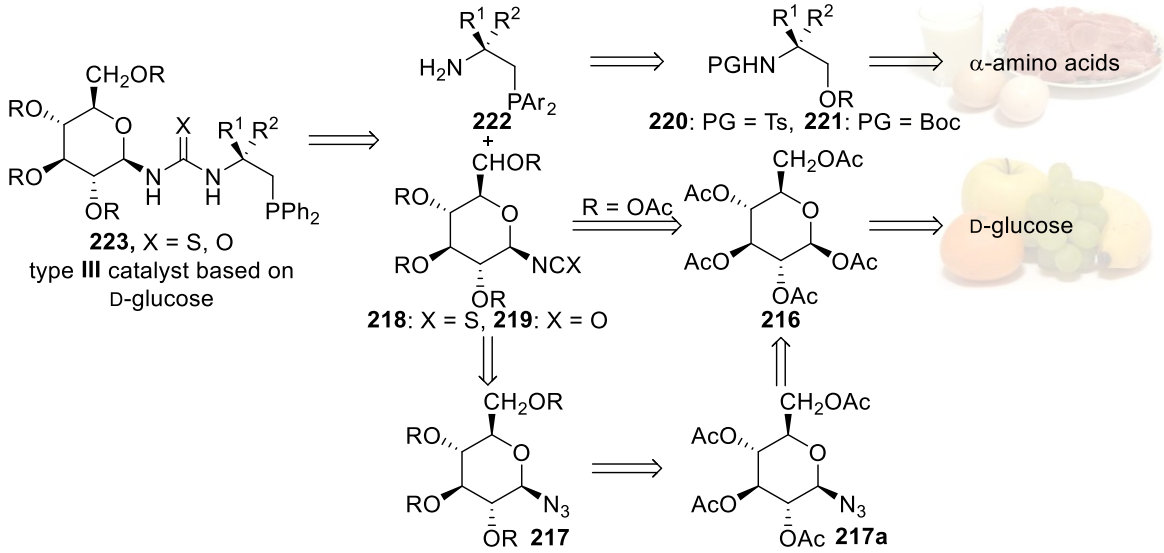

Scheme 35 Retrosynthetic strategy to type **III** organocatalysts.

9.3 The synthesis of novel saccharide-derived bifunctional (thio)urea catalysts

9.3.1 The synthesis of D-glucosamine building blocks for catalysts of type I

The key intermediate for the synthesis of C2-symmetrical organocatalysts **209** based on D-glucosamine is *N*-Alloc-per-*O*-acetylated azide **201a** (for the retrosynthetic strategy, see

Scheme 33, page 54). The Alloc protecting group was chosen because it is a participating group, which is stable under basic and acidic conditions and it can be selectively removed by $Pd(PPh_3)_4$. Two different synthetic pathways to azide **201a** were tested and compared.

The first route started from D-glucosamine hydrochloride (**224**, Scheme 36). To protect the 2-amino group against *N*-acetylation, it was transformed to imine by the reaction of D-glucosamine hydrochloride (**224**) with *p*-anisaldehyde under basic conditions. Subsequently, free hydroxy groups of **225** were acetylated under conditions developed for β-selective acetylation and imine was selectively hydrolysed under acidic conditions to yield per-O-acetylated hydrochloride **227**. The amino group of **227** was protected using allyl chloroformate under basic conditions, and the subsequent reaction with $TMSN_3$ in the presence of $SnCl_4$ afforded desired azide **201a**.[145,218]

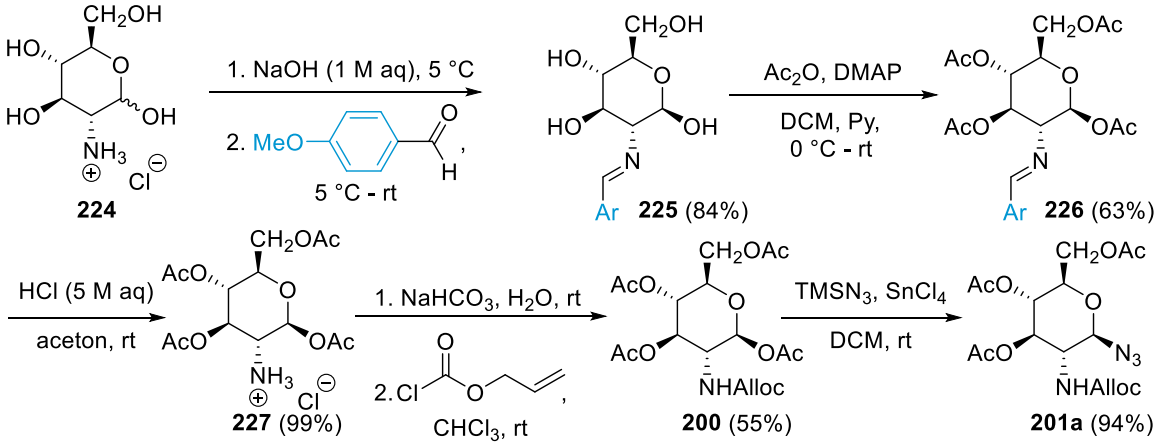

Scheme 36 First synthetic route to azide **201a**.

In the last step, β-anomer of azide **201a** was obtained exclusively due to the participation of the carbamate protecting group during the nucleophilic substitution. The formation of intermediate oxazolidine **229** controls the attack of a nucleophile on anomeric carbon from the equatorial site, leading to the preferential β-anomer formation (Scheme 37).

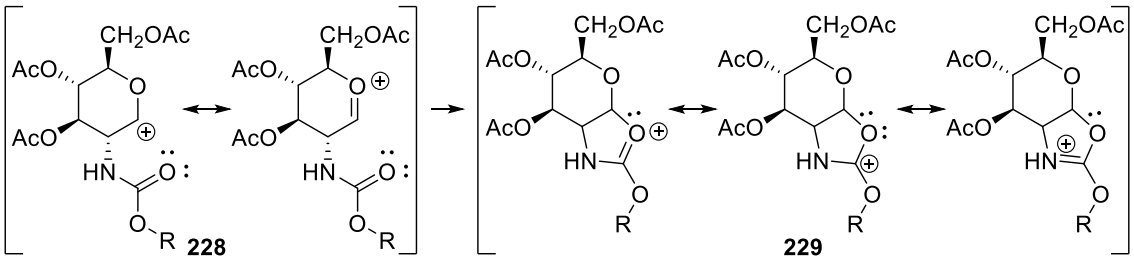

Scheme 37 Formation of carbamate **229** blocks the α-anomeric position.

The second route was based on *O*-acetylation of glucosamine hydrochloride (**224**) using acetyl bromide (the formation of ammonium hydrobromide prevents the acetylation of 2-amino group), the nucleophilic substitution of bromine by $TMSN_3$ in the presence of TBAF and the protection of the amino group with allyl chloroformate (Scheme 38).[219,220] The acetalization in the first step gave α-anomer **230** exclusively due to the large preference of an electronegative halogen for axial orientation. The anomeric effect is the dominant factor in determining the configuration of compound **230**.[221] Azidation proceeded with the inversion of configuration and led exclusively to β-anomer of azide **231**. Interestingly, the second route showed that the presence of the participating group is not necessary for obtaining a pure β-anomer. The presence of a free 2-amino group offers the possibility of shortening the

synthetic route leading to *N*,*N*-dimethylamino azide **205**. The amine **231** was directly subjected to the Eschweiler-Clark methylation, but the reaction failed due to the incompatibility of *O*-acetyl groups with the reaction conditions (see Table 3, page 54).

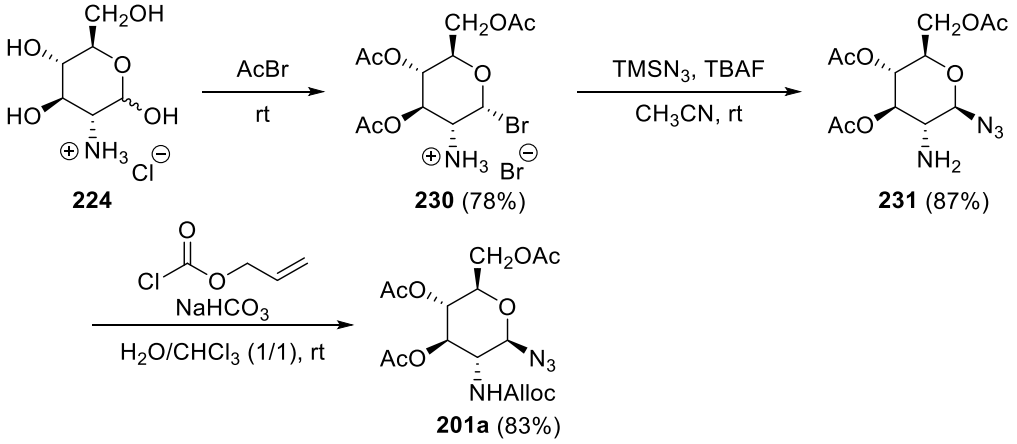

Scheme 38 Second synthetic route to azide **201a**.

The second route was shorter and the desired product was isolated in a higher overall yield (56% compared to 27%). The azide **201a** was suggested as the key intermediate in the synthesis of azides with various *O*-substitutions (e.g., per-*O*-methylated azide **201b** or per-*O*-benzylated azide **201c**).

We expected that the catalytic activity would be influenced by the nature of the *O*-protecting groups. Methyl and benzyl ethers were suggested as suitable *O*-substituents besides *O*-acetyl groups. While the acetyl groups are known to act as H-bonding acceptors and thus support the self-association of (thio)urea catalysts (for details, see Section 5.3, page 23),[24] methyl and benzyl ethers are non-coordinating substituents. The optimal stage for a change of *O*-substituents is before reducing the azido group of **201a** because unlike the amino and NCS groups, the azido group is compatible with O-alkylation and *O*-silylation conditions.

Synthetic routes leading to per-*O*-acetylated catalyst **209a** (R = Ac) do not need the change of *O*-substituents. Together with the possibility of direct NCS group introduction (instead of a two-step interconversion of azide to isothiocyanate), it enables substantial shortening of the reaction pathways. For that reason, we started with the development of conditions for the direct synthesis of per-*O*-acetylated isothiocyanate.

At first, the possibility of nucleophilic substitution of α-bromine of **230** with NCS group was studied using TMSSCN in the presence of TBAF (Scheme 39).

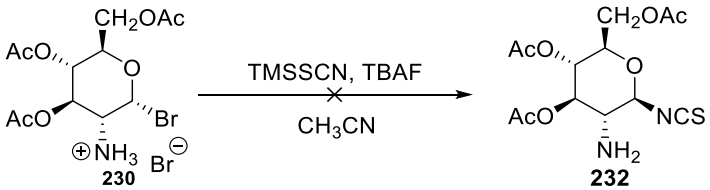

Scheme 39 Direct NCS group introduction *via* nucleophilic substitution.

Although the reaction proceeded under the same conditions as those previously used for azidation (Scheme 38), it did not work for isothiocyanate synthesis, probably due to the lower nucleophilicity or/and higher acid sensitivity of TMSSCN in comparison with $TMSN_3$. The complex mixture of saccharide containing products and decomposed starting compound

230 was obtained. From the ^{1}H NMR spectrum of the reaction mixture, it was evident that partial as well as full *O*-deacetylation (caused by the presence of HBr) occurred during the reaction.

Afterwards, similar conditions as those for azidation of *N*-Alloc-per-*O*-acetylated glucopyranose **200** (Scheme 36) were applied to the direct NCS group introduction. However, the reaction of compound **200** with TMSSCN as a nucleophile in the presence of $SnCl_4$ afforded oxazolidinone **233** in excellent yield (Scheme 40). From these results, it follows that the nucleophilicity of TMSSCN was not sufficient to promote the desired substitution and the nucleophile attacked the allyl group instead of the anomeric carbon.

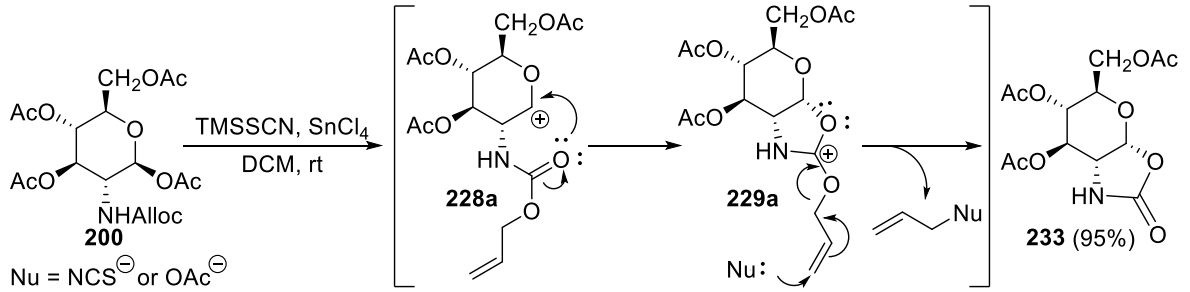

Scheme 40 Mechanism proposed for the formation of oxazolidinone **233**.

As the direct NCS group introduction failed, the possibility of conversion of azide to isothiocyanate *via* the Staudinger reduction followed by the reaction with thiophosgene was tested (Scheme 41). The Staudinger reduction of azide **201a** led to the full conversion of starting compound **201a**, but desired amine **202a** was isolated in low yield due to the decomposition during work-up. Subsequent treatment of intermediate **202a** with thiophosgene did not give product **203a**, and a complex mixture of compounds was observed in ^{1}H NMR spectrum instead.

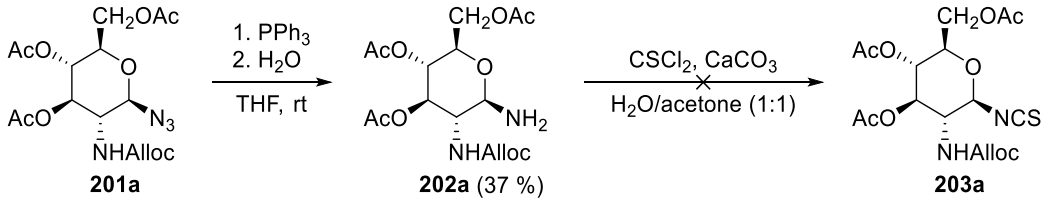

Scheme 41 Staudinger reduction followed by the reaction with thiophosgene.

We believed that the described troubles with the direct NCS group introduction were caused by the incompatibility of *N*-Alloc protecting group with the chosen conditions. Therefore, a change of *N*-Alloc group to *N*,*N*-dimethyl group prior to the NCS group introduction was suggested.

First, Eschweiler-Clark conditions using formaldehyde and $NaCNBH_3$ or HCOOH as a reductive agent were applied to per-*O*-acetylated glucosamine **204** (Scheme 42).[222] Unfortunately, a complex mixture of products of mono- and dimethylation and products of partial or full *O*-deacetylation was observed in ^{1}H NMR spectrum together with the full consumption of starting compound **204**.

The reductive amination of compound **204** using acetaldehyde and $NaCNBH_3$ or Et_3SiH together with $InCl_3$ resulted in a complex mixture. Thus, products of mono- and diethylation and products of partial or full *O*-deacetylation were observed in ^{1}H NMR spectrum together with the full consumption of starting compound **204** (Scheme 43).

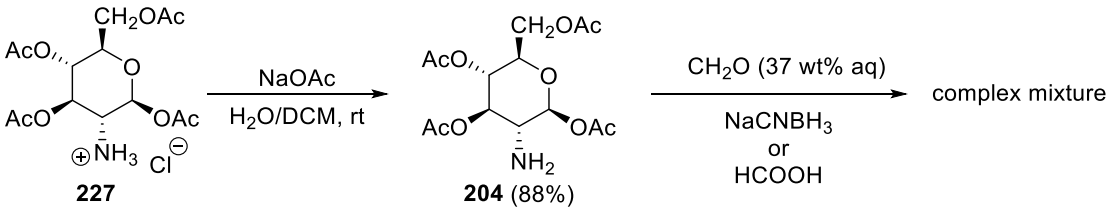

Scheme 42 Eschweiler-Clark methylation of amine **204**.

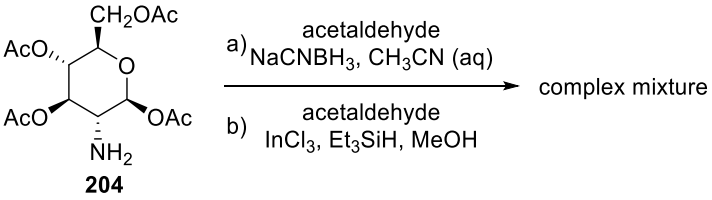

Scheme 43 Alkylation of amine **204**.

Afterwards, the strategy was changed; azide **231** with free 2-amino group was subjected to the Eschweiler-Clark conditions (Table 3). However, this approach did not bring any improvements, and a complex mixture of saccharide products was observed by ^{1}H NMR.

To test the reactivity of 2-amino group, reductive amination of *in situ* formed azide **231** using *m*-anisaldehyde was studied. Azidation of compound **230** followed by imine formation gave product **235**, which upon reduction yielded product **236** in 32% overall yield (Scheme 44).

Table 3 Eschweiler-Clark methylation of amine **231**.

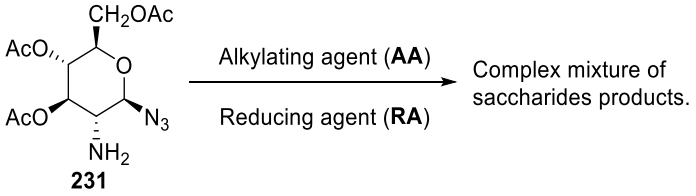

Entry	**AA**	**RA**	Result (analyzed by ^{1}H NMR)
1	Paraformaldehyde	$NaCNBH_3$	Decomposition of starting compound **231**.
2	CH_2O (37 wt% aq)	$NaCNBH_3$	Full consumption of **231**. Monomethylation together with partial and/or full *O*-deacetylation.
3	CH_2O (37 wt% aq)	HCOOH	Complex mixture of azide **231** and other saccharide products.
4	CH_3CHO	$NaCNBH_3$	Full consumption of **231** & complex mixture of saccharide products.

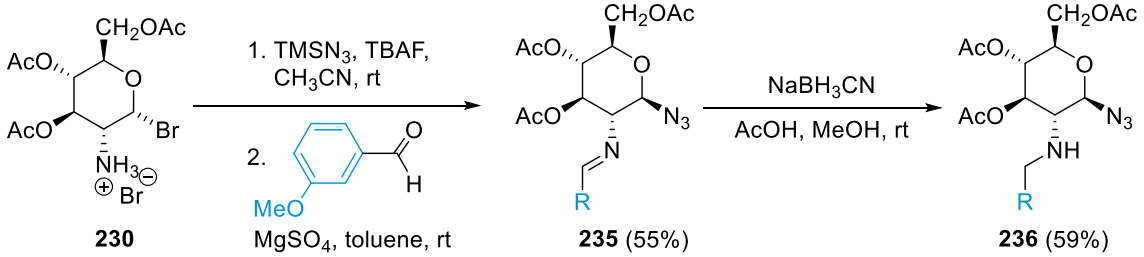

Scheme 44 Reductive amination.

From the above-mentioned results, it seemed that the presence of *O*-acetyl protecting groups was not compatible with the conditions used for *N*,*N*-dialkylation as partial and complete *O*-deacetylation was observed.

Therefore, we focused on *O*-substitution (Scheme 45). The Zemplén deacetylation of per-O-acetylated azide **201a** using MeONa gave azide **237** with free hydroxy groups. However, methyl or benzyl ether synthesis under Williamson's conditions did not lead to desired products **201b** and **201c**, respectively, and a complex mixture of compounds was obtained. In ^{1}H NMR spectrum, partial alkylation of compound **237** together with *N*-Alloc group decomposition were observed.

Unfortunately, due to the described troubles with *N*,*N*-dialkylation and *O*-derivatization, catalysts of type **III** have not been prepared yet. For further study, the change of *N*-Alloc protecting group for another, compatible with Williamson's conditions, is suggested.

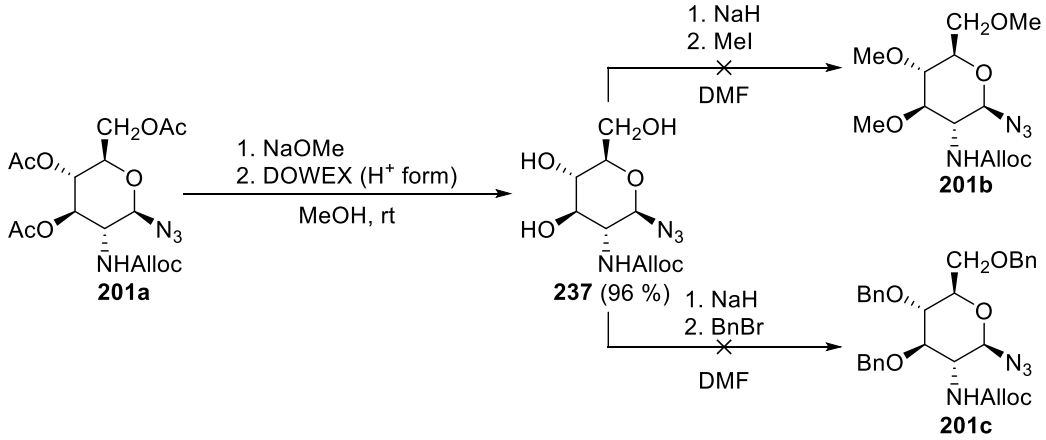

Scheme 45 Zemplén deacetylation followed by the Williamson ether synthesis.

9.3.2 Organocatalysts of type II

9.3.2.1 The synthesis of D-xylose building blocks for catalysts of type II

Retrosynthetic analysis of D-xylose-derived organocatalysts of type **II** consists of the nucleophilic addition of *trans*-cyclohexane-1,2-diamines **214** to xylopyranosyl isothiocyanates **213** (Scheme 34, page 55). Depending on the nature of *O*-substituents, two different pathways were suggested to get isothiocyanates **213** (Scheme 46).

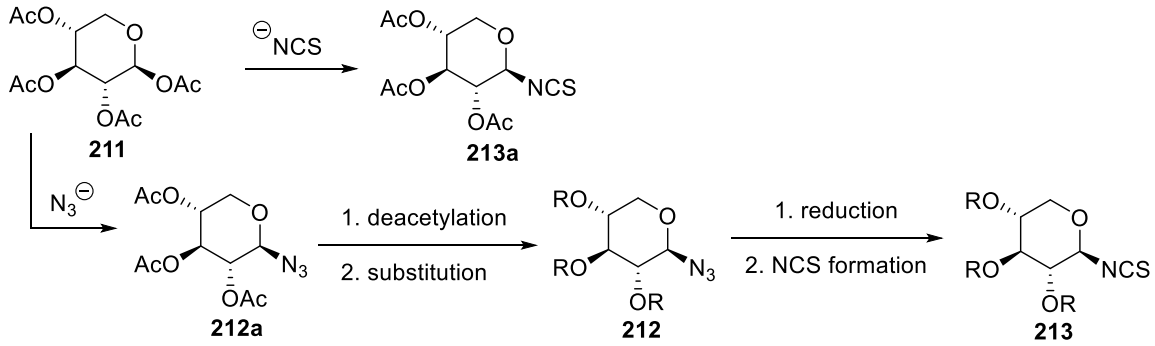

Scheme 46 Synthetic pathways to isothiocyanates **213**.

The direct NCS group introduction was possible to prepare per-*O*-acetyl isothiocyanate **213a**. However, isothiocyanate **213a** cannot stand the conditions for

O-derivatization. Thus, the synthesis of derivatives with different *O*-substituents started from per-*O*-acetylated azide **212a**. The azido group was an eligible substitute for the NCS group because it is compatible with the conditions for *O*-substitution affording azides **212** and it can be converted to isothiocyanate **213** *via* the reduction and subsequent reaction with thiocarbonyldiimidazole.

First, we drew our attention to the synthesis of per-*O*-acetylated xylose-derived organocatalyst **215a**, which is significantly shorter as there is no need for a change of *O*-protecting groups and it enables the direct NCS group introduction. For the synthesis of per-*O*-acetylated β-isothiocyanate **213a**, two different routes were tested starting from per-*O*-acetylated β-xylopyranose **211**. Per-*O*-acetylated β-xylopyranose **211** was prepared from D-xylose (**210**) by the reaction with acetic anhydride in the presence of sodium acetate (Scheme 47). During peracetylation, the formation of α-anomer **238** complicated the purification and decreased the yield of the desired β-anomer. Both anomers were successfully separated by column chromatography.

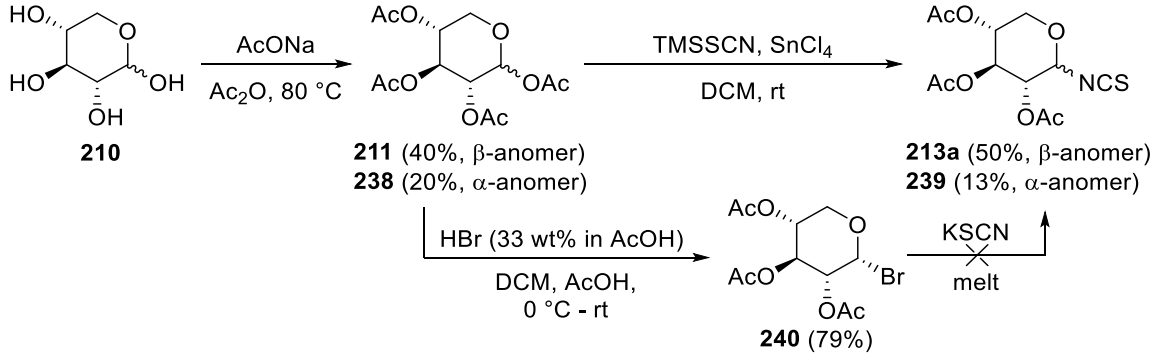

Scheme 47 Synthesis of isothiocyanate **213a**.

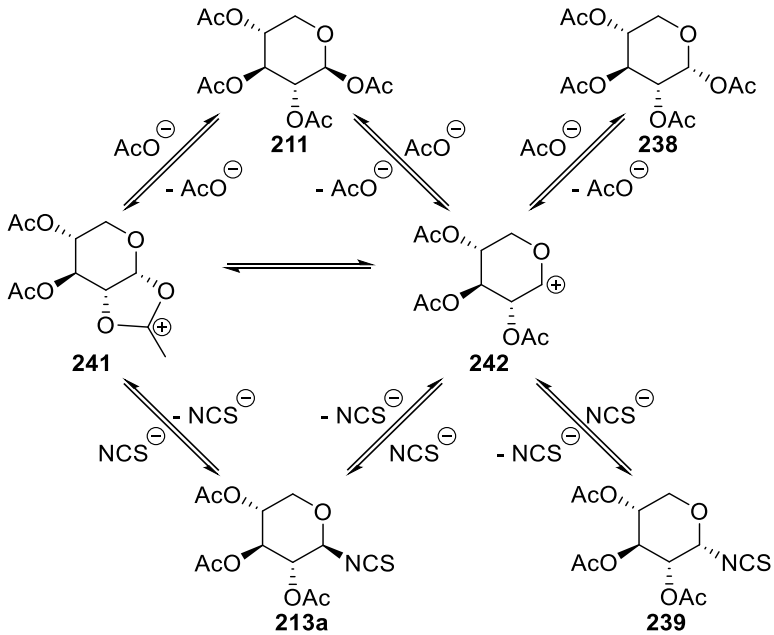

Scheme 48 Mechanism proposed for the anomerization, which proceeded during the direct synthesis of isothiocyanate **213a**.

The possibility of one-step synthesis of isothiocyanate **231a** *via* the reaction of compound **211** with TMSSCN in the presence of $SnCl_4$ was studied (Scheme 47).[223,224]

Reaction was complicated by the formation of α-isothiocyanate **239** and α-per-*O*-acetylated xylopyranose **238**. In analogy to the previously described mechanism for anomerization of glucopyranosyl derivatives,[225,226] mechanism for observed anomerization of starting compound **211** and product **213a** was proposed (Scheme 48). The formation of by-products made the purification difficult and resulted in an average yield of desired β-isocyanate **213a**.

The second route starts similarly from per-*O*-acetylated compound **211**, which gave exclusively α-xylopyranosyl bromide **240** (the anomeric effect is the dominant factor in determining configuration) upon treatment with HBr in acetic acid.[227] Unfortunately, subsequent nucleophilic substitution with KSCN[228] did not lead to desired isocyanate **213a** and the decomposition of starting compound **240** was observed instead (Scheme 47).

The nature of the *O*-protecting group should be reflected in the catalytic activity. As was already mentioned, H-bonding acceptors, such as acetyl groups, can support the self-association of (thio)urea catalysts (Section 5.3, page 24),[24] hence the synthesis of saccharide derivatives with non-coordinating *O*-methyl substituents was suggested.

The azidation of per-*O*-acetylated xylopyranose **211** using $TMSN_3$ in the presence of $SnCl_4$, followed by the Zemplén deacetylation, afforded xylopyranosyl azide **243** in excellent yield. Subsequent methylation of intermediate **243** under Williamson's conditions gave per-*O*-methylated azide **212b** in high yield. Finally, catalytic hydrogenation afforded desired per-*O*-methylated amine **244** in 34% overall yield (Scheme 49).[229]

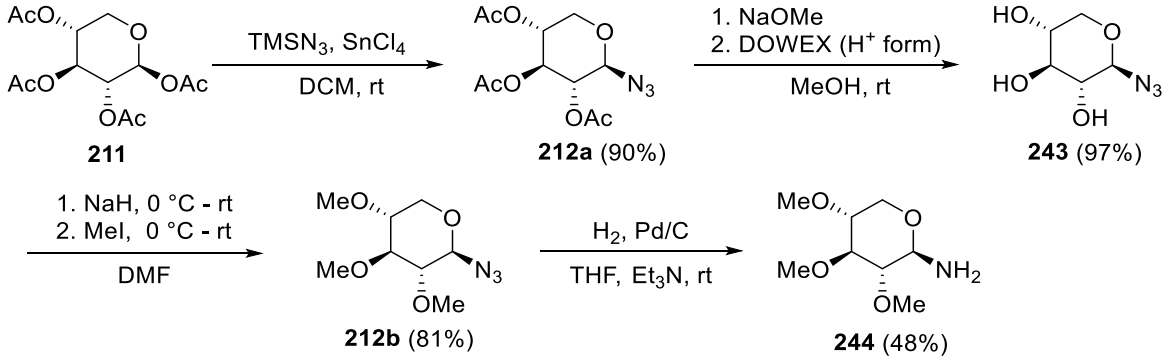

Scheme 49 Preparation of per-*O*-methylated xylopyranosyl amine **244**.

9.3.2.2 Synthesis of thiourea organocatalyst

Per-*O*-acetylated xylopyranosyl catalyst **215a** was prepared from isothiocyanate **213a** and commercially available (*R*),(*R*)-diamine (*R*),(*R*)-**214** in good yield (73%, Scheme 50). Diaminocyclohexane (*R*),(*R*)-**214** was chosen as a nucleophile because (*R*),(*R*)-configuration of the diamine was proven to match with the β-D-glucopyranosyl unit to enhance the stereocontrol.[149,151]

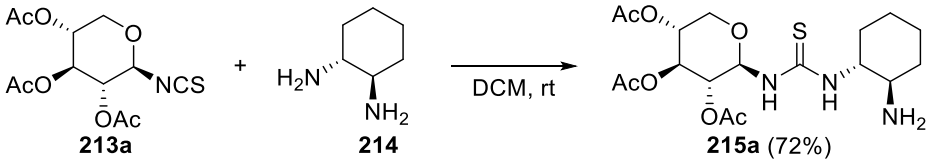

Scheme 50 Synthesis of organocatalysts **215a**.

Catalyst **215a** is a pentose analogue of Ma's glucopyranosyl-based catalyst **114**. Catalyst **114** is one of the first developed primary amine/thiourea bifunctional catalysts (for details, see Chapter 7, page 39). It was originally designed for the asymmetric Michael addition of aromatic ketones **245** to nitroolefins **246** (Scheme 51).[149] High enantioinduction

was explained by simultaneous enamine activation of the pronucleophile and double H-bonding activation of the electrophile, which leads to a well-defined transition state. The nucleophile predominantly approaches from the *Si*-face of nitrostyrene, while the *Re*-face is restricted by the cyclohexyl moiety. In analogy, simultaneous enamine and double H-bonding activation is expected for pentose-derived catalyst **215a**.

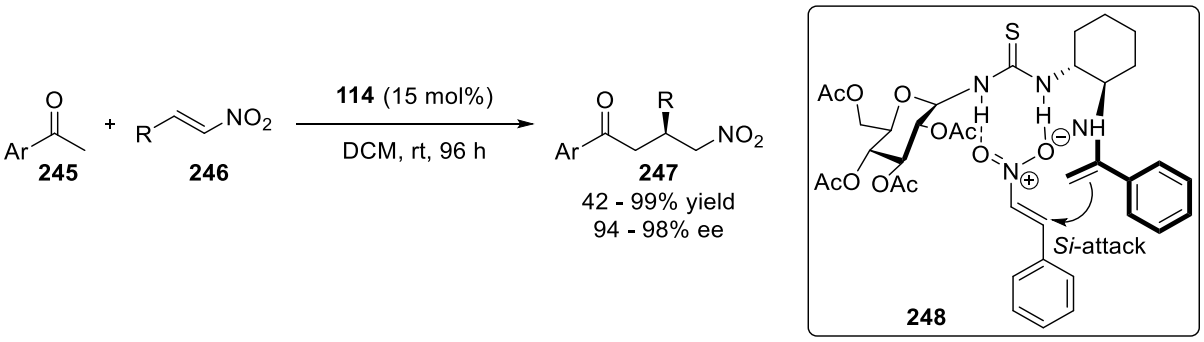

Scheme 51 Asymmetric Michael reaction catalyzed by **114** & proposed mechanism **248**.

9.3.3 Organocatalysts of type III

9.3.3.1 Synthesis of D-glucose building blocks

Retrosynthetic analysis of organocatalysts of type **III** revealed per-*O*-acetylated azide **217a** as an important intermediate for the construction of key building blocks: per-*O*-substituted iso(thio)cyanates **218**, **219** (Scheme 35, page 56).

Intermediate **217a** was synthesized from D-glucose (**249**), which was at first subjected to per-*O*-acetylation under the conditions for selective β-anomer formation using acetic anhydride in the presence of sodium acetate (Scheme 52).[230] The anomeric acetyl group of **216** was then substituted by the azido group using $TMSN_3$ in the presence of $SnCl_4$.[145] The azidation proved to be quick enough to exclude anomerization as only the β-anomer was afforded. The formation of β-anomer **217a** is supported by the participation of the neighbouring acetyl group, which stabilized a nascent cation at the anomeric carbon *via* the formation of cyclic intermediate **250**. It forced the nucleophile to emerge on the anomeric carbon from the opposite side. Intermediate **217a** was prepared from D-glucose (**249**) in two steps in 73% overall yield.

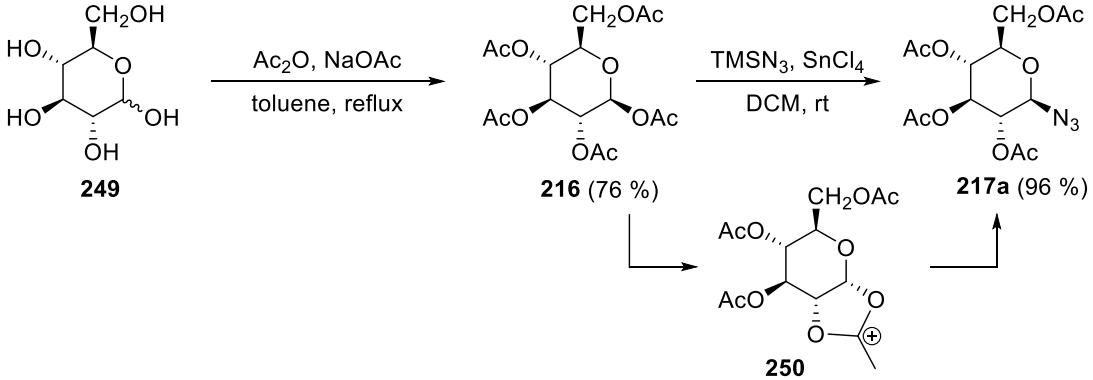

Scheme 52 Synthesis of 2,3,4,6-tetra-*O*-acetylglucopyranosyl azide (**217a**).

To test the influence of *O*-substitution on the catalytic activity, azides **217b** – **217d** were suggested in addition to azide **217a**. While azide **217a** is substituted with electron-withdrawing *O*-acetyl groups, which can act as H-bonding acceptors and coordinate to the

(thio)urea group and consequently suppress the catalytic activity *via* self-association (for details, see Section 5.3), alkyl ethers **217b**, **217c** and silyl ether **217d** contain non-coordinating substituents. Conversely, less polar per-*O*-alkylated and per-*O*-silylated saccharide scaffolds might decrease the H-bonding donor ability of the catalysts. To test the influence of steric bulk of *O*-substituents on catalytic activity, small methyl ether derivative **217b** and a more sterically demanding benzyl ether **217c** were suggested.

To synthesize derivatives **217b – 217d**, the acetic groups of azide **217a** were hydrolyzed under Zemplén deacetylation conditions using sodium methoxide in methanol and subsequent protonation (Scheme 53).[145] Per-*O*-methylated and per-*O*-benzylated azides **217b** and **217c** were prepared from the intermediate **251** using Williamson's protocol for ether synthesis, which is composed of the deprotonation by sodium hydride and the reaction with iodomethane and benzyl bromide, respectively.[231]

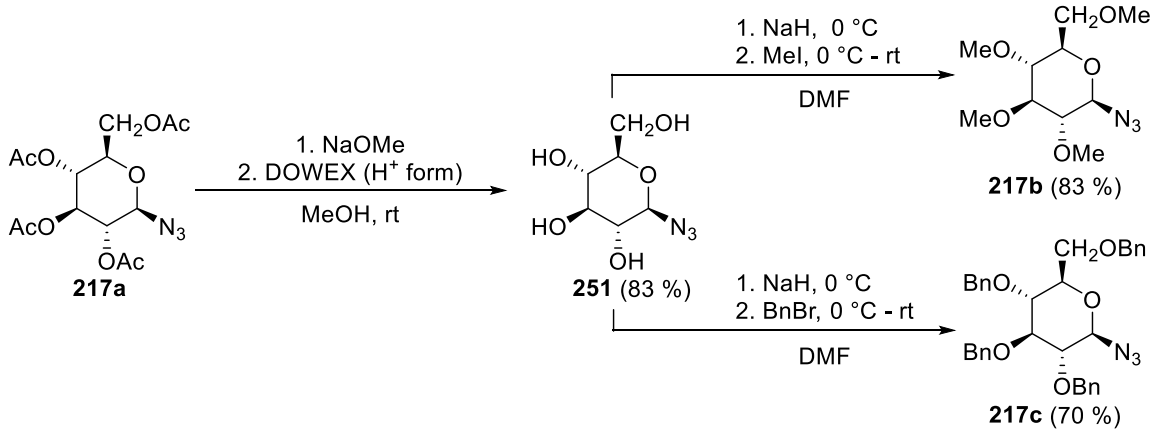

Scheme 53 Synthesis of per-*O*-alkylated glucopyranosyl azides **217b** and **217c**.

Table 4 Routes to per-*O*-silylated azide **217d**.

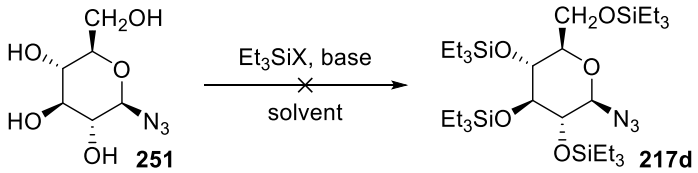

Entry	X	Base	Solvent	Result (analyzed by ^{1}H NMR)
1	Cl	HMDS	Pyridine	Mixture of fully and partly silylated products
2	Cl	Imidazole	DMF	Mixture of fully and partly silylated products
3	Cl	DIPEA	DMF	Mixture of fully and partly silylated products
4	OTf	2,4,6-Collidine	DMF	Mixture of fully and partly silylated products

Four different routes to per-(*O*)-silylated azide **217d** were studied. At the outset, chlorotriethylsilane was used as a protecting agent in the presence of HMDS as a base and pyridine as a basic solvent, but the reaction did not afford desired product **217d** under the chosen conditions (Entry 1, Table 4). Therefore, imidazole or DIPEA in DMF were tried instead. However, in both cases a mixture of fully and partially *O*-silylated products was observed (Entries 2, 3). Every attempt to separate this mixture using column chromatography was unsuccessful. Unfortunately, the same result was obtained when a more reactive silylating agent TESOTf was used in the presence of 2,4,6-collidine in DMF (Entry 4).

The catalytic hydrogenation of azides **217a** – **217c** with Pd/C catalyst gave protected amines **252** in almost quantitative yields (Scheme 54). The yield of *O*-benzylated amine **252c** was lower due to the simultaneous *O*-benzyl group cleavage. Isothiocyanates **218** were synthesized from desired amines **252** and thiocarbonyldiimidazole. Isocyanates **219** were prepared from amines **252** and triphosgene (Scheme 54).[232] Compounds **219** were not purified and were used directly in the subsequent reaction with aminophosphine **222a** (Scheme 64, page 71).

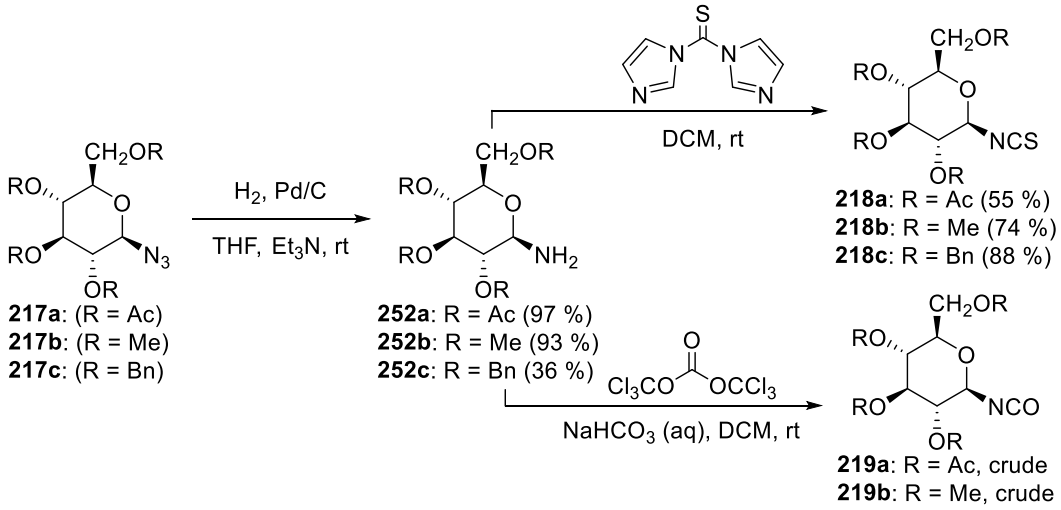

Scheme 54 Synthesis of isothiocyanates **218** and isocyanates 2**19**.

The possibility of direct synthesis of per-*O*-acetylated isothiocyanate **218a** *via* introduction of the NCS group to per-*O*-acetylated glucopyranose **216** was tested. Unlike the two-step interconversion of the azide group, the direct NCS group introduction would lead to substantial shortening of the reaction pathway. However, the reaction of per-*O*-acetylated β-D-glucopyranose **216** with TMSSCN in the presence of $SnCl_4$ was complicated due to the formation of by-products.[224] Main by-product was identified as per-*O*-acetylated α-D-glucopyranose **253** (Scheme 55).

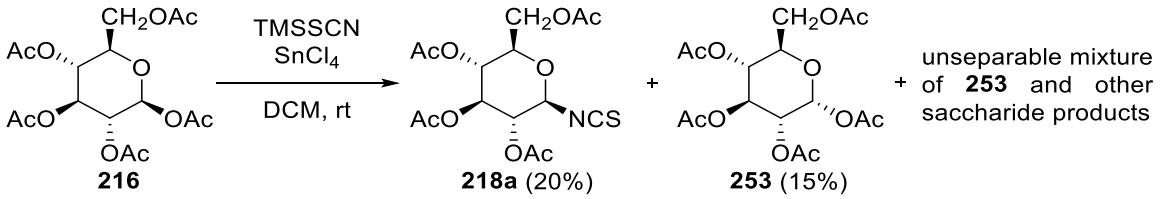

Scheme 55 Direct synthesis of isothiocyanate **218a**.

An anomerization of per-*O*-acetylated β-glucopyranose **216** in the presence of $SnCl_4$ in dry $CHCl_3$ was previously described by Pacsu.[225] On the basis of Magnusson's gas chromatographic investigation,[226] cations **254** and **250** were proposed to be the key intermediates for the formation of α-acetate **253** and of desired product **218a**, respectively (Scheme 56). Moreover, cation **250** is believed to transform into other saccharide products, which are part of an inseparable mixture formed during the synthesis of β-isothiocyanate **218a**.

The formation of by-products made the purification difficult and the yield of isolated β-anomer **218a** was thus very low (20%). Anomerization was not observed during the azidation of per-*O*-acetylated β-D-glucopyranose **216** (Scheme 52, page 64), which uses $TMSN_3$ and a smaller amount of $SnCl_4$. However, the direct NCS group introduction using

TMSSCN and decreased amount of $SnCl_4$ (0.2 equiv instead of 0.83) resulted in suppressed reactivity. Due to the described troubles during the direct synthesis of isothiocyanate **218a**, the four-step preparation starting from D-glucose (**249**) was preferred.

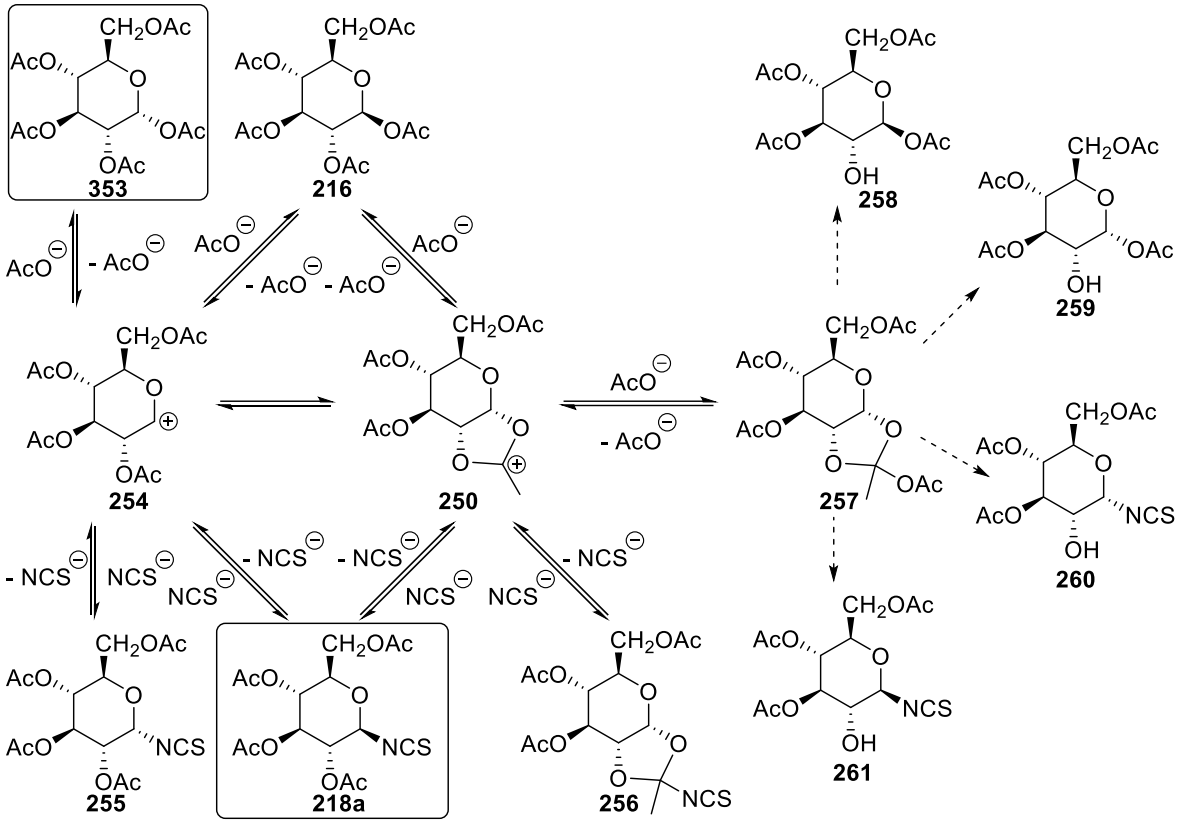

Scheme 56 Mechanism proposed for the anomerization, which proceeded during the direct isothiocyanate synthesis; framed products were isolated and characterised by NMR.

To conclude, three different isothiocyanates **218** were successfully prepared starting from D-glucose (**249**). The four-step synthesis gave isothiocyanate **218a** in 39% yield. Derivatives **218b**, **218c** were prepared in six steps in 35 and 13% overall yield, respectively. Isocyanates **219a**, **219b** were prepared from D-glucose (**249**) in four and six steps, respectively. Crude isocyanates **219** were pure enough to be directly used in the synthesis of urea catalysts of type **III**.

9.3.3.2 Synthesis of α-amino acid building blocks

Generally, the synthesis of α-amino acid building blocks started with a reduction of the corresponding α-amino acid, followed by *N*-protection or *vice versa*. Derivatization of the hydroxy group led to intermediate **220**, **221** bearing a good leaving group, which was subsequently replaced by PAr_2. Finally, *N*-deprotection afforded desired aminophosphines **222** (Scheme 57).

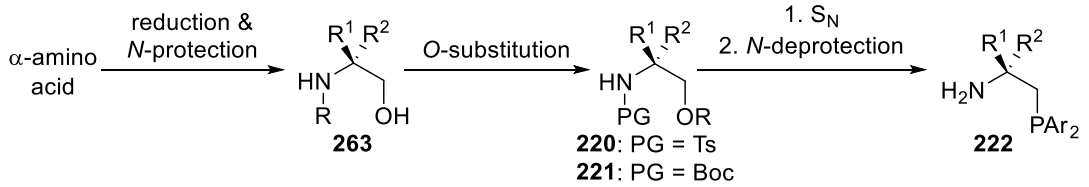

Scheme 57 General approach to aminophosphines **222**.

Two different reduction protocols were tested (Scheme 58). The reduction by $LiAlH_4$ in THF was complicated by coagulation of by-products during work-up and gave a lower yield of amino alcohol **264a** in comparison to the reduction by a mixture of iodine and $NaBH_4$ in THF.[233,234] This is the reason the mixture of iodine and $NaBH_4$, which serves as a source of BH_3, was used for the reduction.

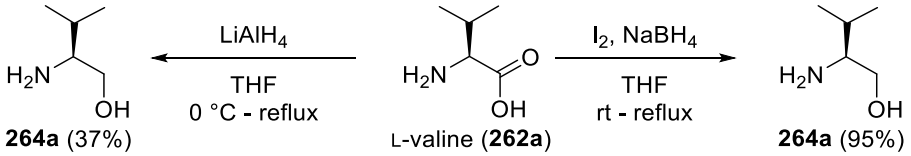

Scheme 58 Methods of α-amino acid reduction.

Following the literature procedure, the tosylation of hydroxy and amino groups of amino alcohols **264**, followed by the basic cyclization of intermediates **220**, afforded aziridines **265**. Aziridine ring was opened by nucleophilic potassium diphenylphosphide. Finally, intermediates **266** were deprotected in hot sulfuric acid (Scheme 59).[235]

Aminophosphines **222** were prepared in five steps starting from the corresponding α-amino acid: aminophosphine **222a** from L-Val in 18% overall yield, its enantiomer **222b** from D-Val in 25% overall yield, aminophosphine **222c** from L-*tert*-Leu in 10% overall yield. Aminophosphine **222d** was prepared by my colleague Jiří Tauchman starting from L-Leu in 23% overall yield.

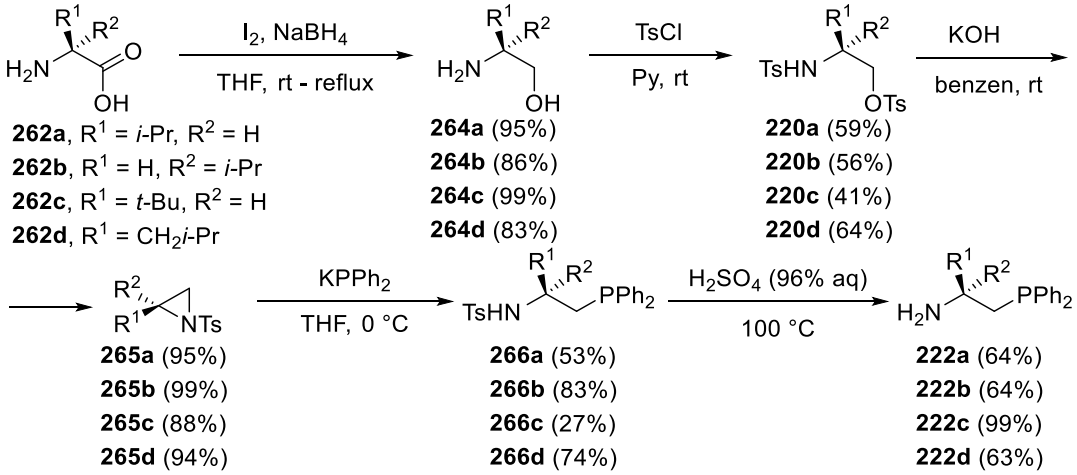

Scheme 59 Preparation of aminophosphines **222** *via* tosylated intermediates.

The above described hydrolysis of *N*-Ts group used harsh conditions (heating in concd sulfuric acid), which resulted in the formation of an aminophosphine oxide by-product. Therefore, an alternative approach based on *N*-Boc-protected intermediates was tested (Scheme 60).[236] At first, the amino group of amino alcohol **264a** was protected using Boc_2O under basic conditions, and the hydroxy group of intermediate **263a** was tosylated using TsCl. The subsequent nucleophilic substitution of OTs group by $KPPh_2$ afforded *N*-Boc-protected intermediate **267**, which was deprotected using trifluoroacetic acid. Aminophosphine **222a** was synthesized starting from L-Val in five steps and in 16% overall yield.

The two routes leading to aminophosphine **222a** are comparable as they are both composed by five steps starting from L-Val and gave desired product **222a** in a similar overall yield (18% vs. 16%, Scheme 59, Scheme 60). The route based on *N*-tosylated intermediates was preferred because of facile isolation and characterization of *N*,*O*-ditosylated compounds **220** and aziridines **265** and because of no need for cooling the reaction mixture to −35 °C.

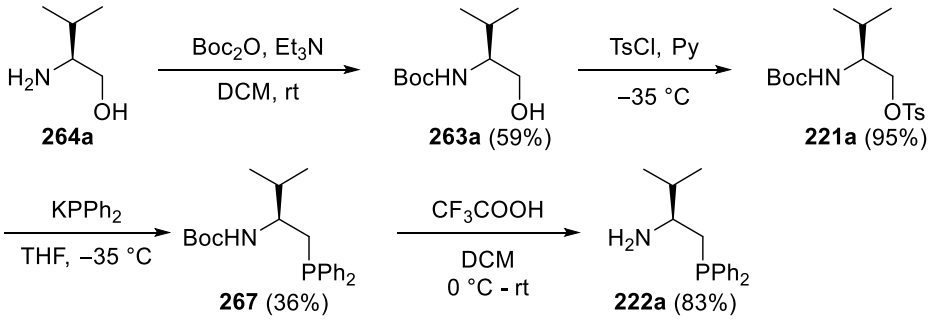

Scheme 60 Alternative synthetic route to aminophosphine **222a**.

An alternative synthetic route was used for the synthesis of L-alanine-derived phosphine **222e** (Scheme 61). The reduction of L-Ala using $LiAlH_4$ as well as I_2 together with $NaBH_4$ gave the corresponding alcohol in low yield. Therefore, L-alanine was *N*-Boc-protected using Boc_2O under basic conditions,[237] *N*-Boc-L-alanine **268e** was transformed to mixed anhydride using $ClCO_2Et$ and NMM and it was reduced using $NaBH_4$ to afford alcohol **263e**.[238] Tosylation of **263e** and the subsequent basic cyclization gave aziridine **269e**,[239] which was opened by the nucleophilic attack of $KPPh_2$.[235] Finally, the removal of Boc-group in the presence of trifluoroacetic acid afforded desired product **222e**.[240] Aminophosphine **222e** was prepared from L-Ala in five steps and 12% overall yield.

When the same protocol was applied to the synthesis of phosphine derived from L-*tert*-Leu, only traces of aziridine **269c** were observed. It is probably due to the proximity of *t*-Bu and Boc groups in the corresponding aziridine **269c**, which brings too much strain to the three-membered ring. Fortunately, the steric strain was not a problem in *N*-tosylated aziridine **265c**, which was obtained by the base-induced cyclization of *N*,*O*-ditosylated amino alcohol **220c** in 68% yield (Scheme 59).

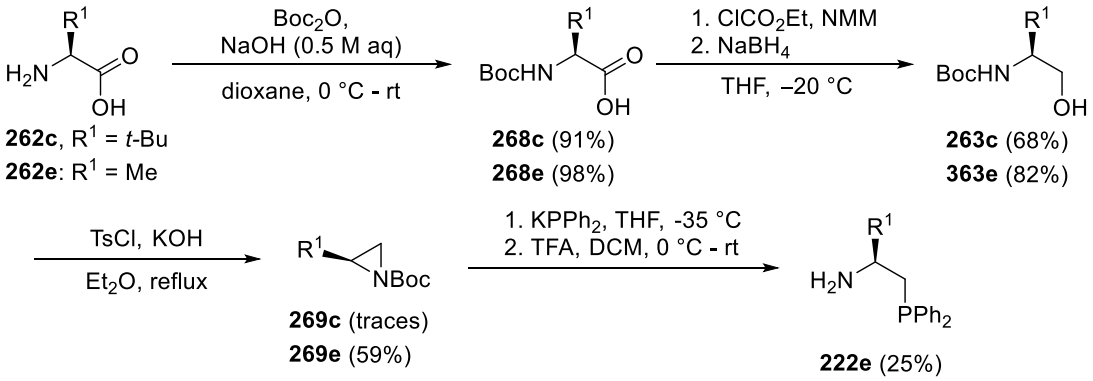

Scheme 61 Preparation of aminophosphines **222** based on Boc-protected intermediates.

Aziridines **265**, **269e** are very useful intermediates for the synthesis of aminophosphines bearing various PAr_2 groups. On that account, the reaction between dimesitylphosphine **270** and sodium in dry THF was tested (Scheme 62). While the control reaction between diphenylphosphine (**272**) and sodium gave the desired product **273** (observed in the ^{31}P NMR spectrum of the reaction mixture measured in dry THF under argon), the reaction with dimesitylphosphine **270** failed, probably due to the steric hindrance of *ortho* methyl groups. The ^{31}P NMR spectrum of the reaction mixture measured in dry THF under argon confirmed an unreacted starting compound. When a stronger base *n*-BuLi was used, the reaction between dimesitylphosphine **270** and *n*-BuLi was followed by the immediate reaction with aziridine **265a**. However, as in the previous case, ^{31}P NMR

analysis showed unreacted starting phosphine **270** and a complex mixture of other products (Scheme 62).

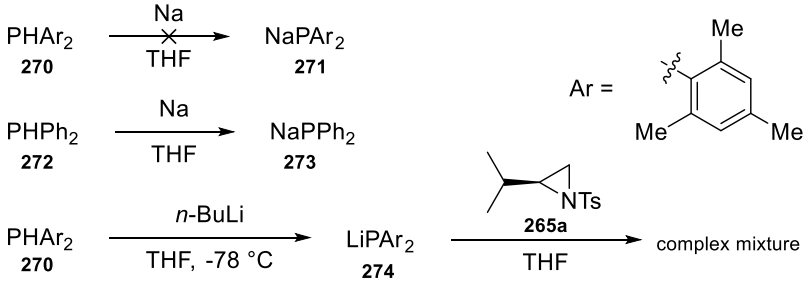

Scheme 62 Preparation of sodium and lithium diphosphides.

9.3.3.3 Synthesis of (thio)urea organocatalysts

Thiourea organocatalysts **275** – **282** were prepared by the nucleophilic addition of corresponding aminophosphines **222** to isothiocyanates **218** in moderate to high yields (35%, 65 – 93%, Scheme 63). Catalyst **277** was prepared in a gram scale starting from D-glucose and L-valine in 25% overall yield. Wu's catalyst **117** was prepared *via* the nucleophilic addition of (1*S*,2*S*)-2-(diphenylphosphino)cyclohexanamine to per-*O*-acetylated isothiocyanate **218a**.[159]

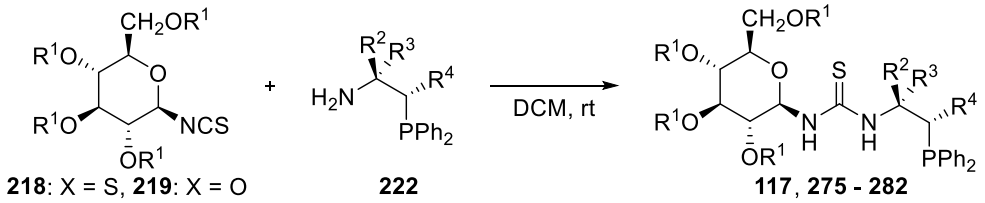

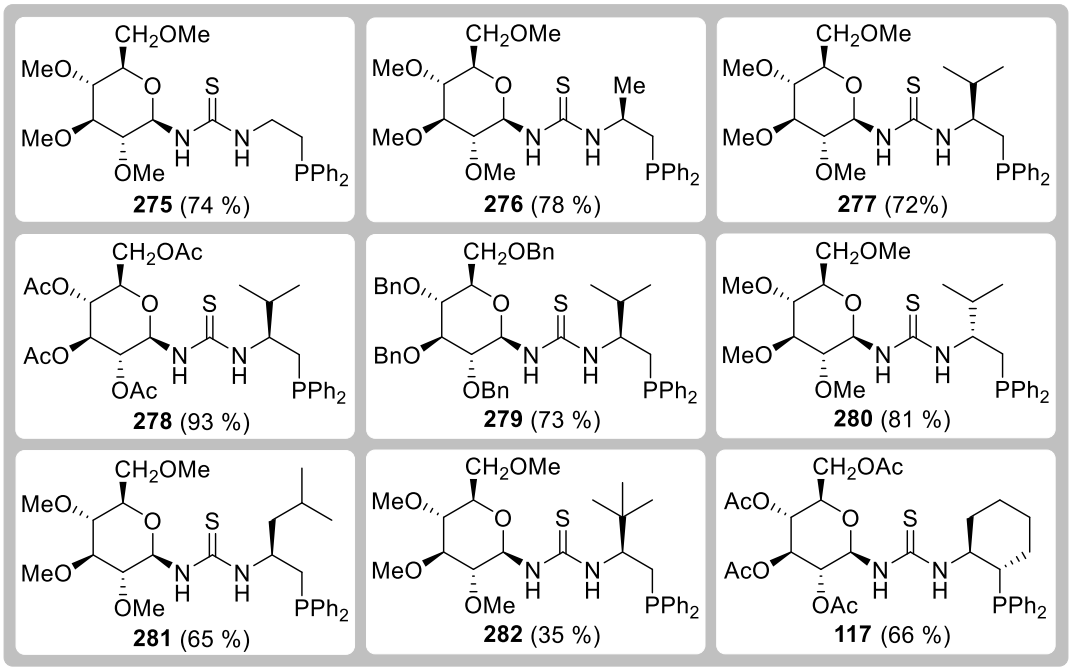

Scheme 63 Prepared thiourea organocatalysts of type **III**.

Two urea catalysts **283** and **284** were prepared in high yields (60% and 79%) by the nucleophilic addition of phosphine **222a** to crude isocyanate **219a** or **219b** (Scheme 64).

The synthetic pathway to iso(thio)cyanates **218** and **219** is described in Section 9.3.3.1 and the synthetic pathway to aminophosphines **222** in Section 9.3.3.2. Compound

2-(diphenylphosphino)ethylamine and (1*S*,2*S*)-2-(diphenylphosphino)cyclohexylamine were purchased from commercial suppliers. The prepared bifunctional organocatalysts exhibited good air and bench stability. The structure of organocatalysts **275** – **284** was confirmed by a single-crystal X-ray diffraction analysis of catalyst **284** (Figure 31).

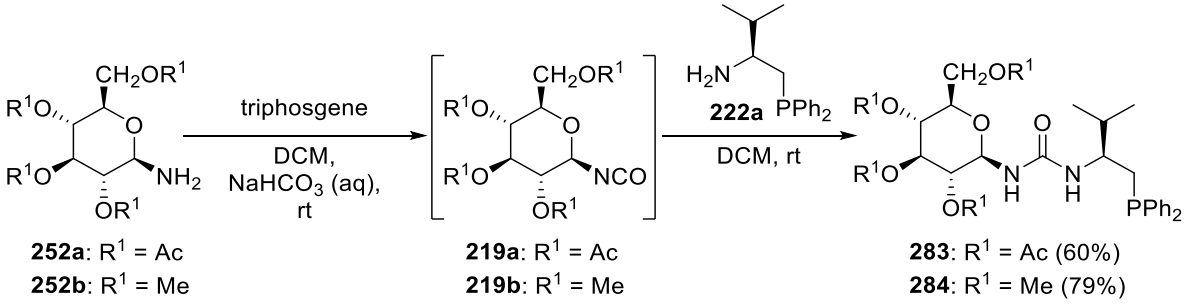

Scheme 64 Prepared urea organocatalysts of type **III**.

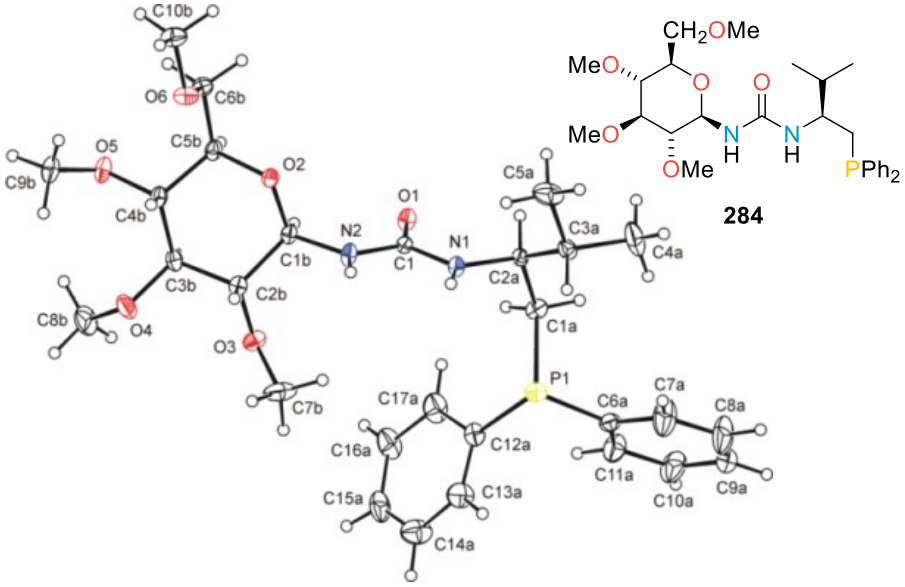

Figure 31 View of molecule **284** with the atom numbering scheme: displacement ellipsoids are drawn at a 30% probability level.

9.4 Evaluation of type III catalysts in the asymmetric MBH reaction

Bifunctional (thio)urea/tertiary phosphine catalysts are known as effective catalysts for the MBH reaction (Section 6.1.3, page 32). For that reason, the catalytic activity of prepared organocatalysts **275** – **284** was tested in the asymmetric MBH reaction between 4-nitrobenzaldehyde (**78a**) and methyl acrylate (**79a**) in THF at room temperature (Table 5). The control reaction without catalyst did not proceed (Entry 1). Thiourea catalysts were more reactive in comparison with urea organocatalysts, and they gave desired allylic alcohol **285** with higher yields as well as enantioselectivities (Entries 5 – 11 vs. 12, 13). These results are not surprising as thioureas are generally considered more reactive than urea catalysts due to the higher acidity of amidic protons (Section 5.3). Indeed, in comparison with urea amidic protons (NH signal observed around 5 and 3.6 ppm), higher acidity of thiourea amidic protons (NH signal observed around 7 and 6.4 ppm) was observed in ^{1}H NMR spectrum of the prepared organocatalysts.

The best results with respect to efficiency and enantioselectivity in the model MBH reaction were achieved with catalyst **277** derived from L-Val (82% ee, Entry 7). Modification

of the diphenylphosphine moiety of the catalyst showed that the reactivity and enantioselectivity are strongly influenced by the steric effects of the alkyl substituent R^2. On the other hand, the glucopyranosyl unit serves as a bulky electron-withdrawing group, affording increased thiourea acidity (Chapter 7) and had only a limited effect on stereoselectivity (Entry 5). In short, the bulkier the R^2 substituent is, the lower the reactivity is, and the higher the enantioselectivity is. As a result, less sterically demanding catalysts **275** (R^2=H), **276** (R^2=Me) and **281** (R^2=CH_2CHMe_2) showed higher reactivity, but lower enantioselectivity (Entries 5,6 and 8) in comparison with **277** (R^2=$CHMe_2$). Conversely, catalyst **282** (R^2=$CHMe_3$) showed reduced reactivity with comparable enantioselectivity (Entry 9).

Table 5 Catalyst screening for the MBH reaction of benzaldehyde **78a** and acrylate **79a**.[a]

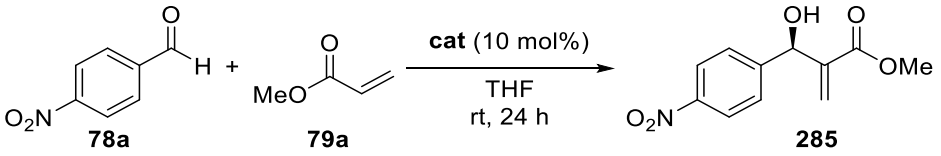

78a **79a** **285**

Entry	Catalyst	Yield (%)[c]	ee[d] (%)
1	—	0	0
2	β-ICD (**69**)[b]	13	6
3	Takemoto (**16**)	0	—
4	Wu (**117**)	80	80
5	**275**	83	12
6	**276**	83	74
7	**277**	68	82
8	**281**	80	71
9	**282**	37	83
10	**278**	22	81
11	**279**	65	80
12	**283**	12	53
13	**284**	25	45

[a] The reaction proceeded with 10 mol% of catalyst, 0.1 mmol of **78a** and 0.5 mmol of **79a** in 1 mL of THF at rt; [b] The reaction time was 72 h; [c] Isolated yield; [d] Chiral HPLC using IC column and a mixture of heptane/*i*-PrOH (80/20) as eluent.

Catalysts **275**, **276**, **281** and **117** showed similar efficiencies after 24 hours, including full conversion of starting compounds (Entries 4 – 6, 8). Besides, Wu's catalyst **117** gave product **285** with high enantioselectivity (80%). Nevertheless, the advantage of type **III** catalysts (here represented by **275** – **284**) consists in the possibility of further modification of catalytic properties *via* the employment of various natural and synthetic amino acids.

Varying the *O*-protecting group on the saccharide unit did not affect the stereochemical outcome of the reaction (Entries 5, 10, 11). However, catalyst **278**, with an electron-withdrawing *O*-acetyl group on the saccharide unit, showed a considerably lower reactivity (Entry 10). It might be due to the interference of the acetoxy group and the acidic thiourea group (Section 5.3, page 23). On the other hand, the presence of a bulkier non-interfering benzyl protecting group on the saccharide unit of the catalyst had only limited effect on the reactivity of catalyst **279** (Entry 11).

The catalytic activity of **277** was compared with that of previously reported organocatalysts (Entries 2, 3, 7). The reaction catalyzed by Takemoto's catalyst **16** (Figure 8, page 25)[40] did not give any product at all (Entry 3). The reaction catalyzed by β-isocupreidine (**69**, Entry 2)[33] showed only poor reactivity under the chosen reaction conditions.

Table 6 Solvent screening.[a]

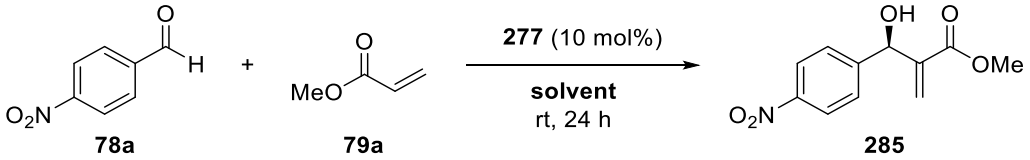

78a **79a** **285**

Entry	Solvent	Yield[b] (%)	ee[c] (%)
1	Toluene	45	82
2	TBME	82	86
3	*i*-Pr_2O	49	79
4	THF	68	82
5	DCM	52	70
6	Chloroform	59	75
7	DMF	81	76
8	DMSO	86	72
9	Acetonitrile	68	61
10	Methanol	22	1

[a] The reaction proceeded with 10 mol% of **277**, 0.1 mmol of **78a** and 0.5 mmol of **79a** in 1 mL of solvent at rt; [b] Isolated yield; [c] Chiral HPLC using IC column and a mixture of heptane/*i*-PrOH (80/20) as eluent.

Based on the described results, catalyst **277** was chosen for further study. At first, the effect of various solvents on the model reaction between *p*-nitrobenzaldehyde (**78a**) and methyl acrylate (**79a**) catalyzed by thiourea **277** was explored (Table 6). Ethereal solvents (Entries 2 – 4) afforded moderate to high yields and high enantiocontrol in the model MBH reaction. The best results with respect to reactivity and enantioselectivity were obtained in TBME and it was chosen for further study (Entry 2). In dipolar aprotic solvents with a high boiling point, the model reaction gave product **285** in the highest yields, but with lower enantiocontrol (Entries 7, 8). In methanol, low conversion, low yield, and no enantiocontrol were observed (Entry 10). The possible explanation is that the presence of methanol caused the destruction of the explicit H-bonding interaction between the catalyst and reactants.[24]

The optimization of further parameters of the asymmetric MBH reaction showed that the higher the temperature is, the higher yield it gives. This effect is accompanied by slightly decreased enantiocontrol (Entries 1 – 3, Table 7). The catalyst loading influenced the yield with only a limited impact on enantioselectivity (Entries 2, 4 – 6). The optimal catalyst loading was established to 10 mol%. Next, we studied the influence of acrylate/*p*-nitrobenzaldehyde ratio on the reaction outcome (Entries 2, 7 – 10). The ratio had only a limited impact on the reaction yield and no effect on the enantiomeric excess, thus we continued with the ratio of **79a**/**78a** (5:1).

Having the optimized reaction conditions in hand, screening of various acrylates was performed (Table 8). MBH alcohols from the reaction with simple alkyl and aryl acrylates were isolated in high yields and with comparable enantioselectivities (Entries 1 – 5). However, an alkyl group of the ester moiety had a significant effect on the reaction rate. With

bulkier ester moieties, such as *t*-butyl, the reaction rate decreased, and product **288** was obtained after prolonged reaction time (3 days, Entry 4).

Hexafluoroisopropyl acrylate is known to be a successful reagent in the MBH reaction of aromatic aldehydes catalyzed with β-ICD (**69**, Section 6.1).[33] However, the reaction of hexafluoroisopropyl acrylate with *p*-nitrobenzaldehyde failed under optimized reaction conditions (when proceeded at room temperature). On that account, the reaction was performed at 0 °C, and the racemic product was isolated in very poor yield (Entry 6).

Table 7 Optimization of reaction conditions.[a]

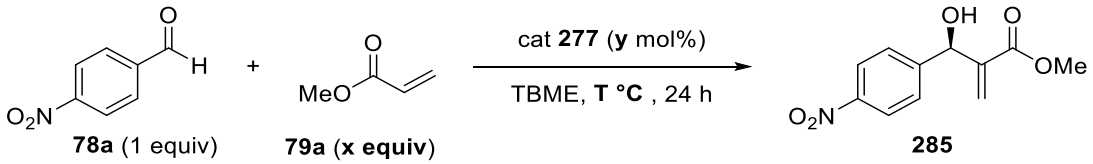

Entry	T (°C)	Acrylate (x equiv)	**277** (y mol%)	Yield[b] (%)	ee[c] (%)
1	0	5	10	12	83
2	25	5	10	82	86
3	50	5	10	90	71
4	25	5	1	13	87
5	25	5	5	35	86
6	25	5	15	74	82
7	25	2	10	70	83
8	25	3	10	72	83
9	25	4	10	78	83
10	25	6	10	78	83

[a] The reaction proceeded with 1 – 10 mol% of **277**, 0.1 mmol of **78a** and 0.1 – 0.6 mmol of **79a** in 1 mL of TBME at reported temperature; [b] Isolated yield; [c] Chiral HPLC using IC column and a mixture of heptane/*i*-PrOH (80/20) as eluent.

Table 8 Asymmetric MBH reaction between **78a** and various acrylates.[a]

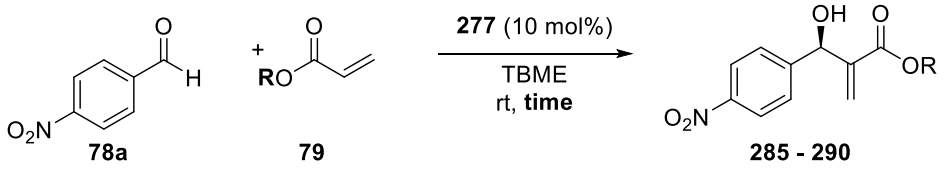

Entry	R	Time (days)	Product	Yield[b] (%)	ee[c] (%)
1	Me	1	**285**	82	86
2	Et	1	**286**	70	85
3	*n*-Bu	1	**287**	75	87
4	*t*-Bu	3	**288**	82	85
5	Bn	1	**289**	83	80
6[d]	$CH(CF_3)_2$	1	**290**	10	2

[a] The reaction proceeded with 10 mol% of **277**, 0.1 mmol of **78a** and 0.5 mmol of acrylate **79** in 1 mL of TBME at rt; [b] Isolated yield; [c] Chiral HPLC using IC column and mixtures of heptane/*i*-PrOH as eluent; [d] The reaction proceeded at 0 °C.

Screening of aromatic aldehydes with various steric and electronic properties revealed that the rate, efficiency and enantiocontrol are highly influenced by the electronic properties and the location of the substituents on the aromatic ring (Table 9). MBH alcohols **285**, **291 - 305** were isolated in moderate to high yields and with high enantioselectivities. Substrates with electron-withdrawing groups, such as nitro, cyano, trifluoromethyl gave the best results in terms of yield and enantiomeric excess (Entries 1 – 6).

Benzaldehyde and aldehydes with similar electronic properties, such as 3-methylphenyl and halogenated aromatic aldehydes (4-fluoro, 4-chloro, 4-bromo) reacted significantly slowly and gave products with low yield and moderate enantioselectivity (Entries 7 – 11). In addition, heterocyclic aromatic aldehydes proved to be suitable substrates for the MBH reaction (Entries 14 – 16).

When aliphatic aldehydes were employed, the corresponding MBH alcohols were not obtained, even after a prolonged reaction time, and decomposition of the starting material was observed instead.

Table 9 Asymmetric MBH reaction between aromatic aldehydes **78** and acrylate **79a**.[a]

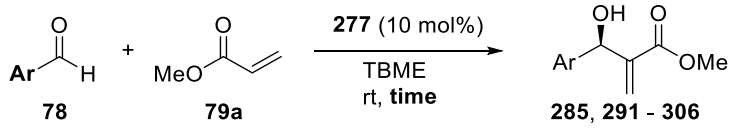

78 **79a** **285**, **291 - 306**

Entry	Ar	Time (days)	Product	Yield[b] (%)	ee[c] (%)
1	(2-NO_2)C_6H_4	2	**291**	69	62
2	(3-NO_2)C_6H_4	1	**292**	62	82
3	(4-NO_2)C_6H_4	1	**285**	82	86
4	(2,4-NO_2)$_2C_6H_4$	3	**293**	41	76
5	(4-CN)C_6H_4	1	**294**	77	84
6	(4-CF_3)C_6H_4	4	**295**	70	83
7	Ph	7	**296**	15	77
8	(3-Me)C_6H_4	4	**297**	11	60
9	(4-F)C_6H_4	4	**298**	24	60
10	(4-Cl)C_6H_4	4	**299**	24	69
11	(4-Br)C_6H_4	4	**300**	36	71
12	β-naphthyl	4	**301**	29	68
13	(*m*-MeO)C_6H_4	4	**302**	24	69
14	3-pyridyl	4	**303**	78	73
15	2-furyl	4	**304**	24	73
16	2-thienyl	4	**305**	28	55
17	(4-NO_2)C_6H_4	1	**306**	85	-85

[a] The reaction proceeded with 10 mol% of **277**, 0.1 mmol of aromatic aldehyde **78** and 0.5 mmol of **79a** in 1 mL of TBME at rt; [b] Isolated yield; [c] Chiral HPLC using IC column and mixtures of heptane/*i*-PrOH as eluent.

Racemic MBH adducts were prepared by the DABCO-catalyzed reaction between aldehydes **78** and acrylates **79** to get a reference samples for HPLC analysis (Scheme 65).[241]

Catalyst **280** was prepared to confirm the decisive influence of the aminophosphine unit in controlling the enantioselectivity and efficiency of the reaction. Catalyst **280** is derived from D-valine, thus it is a pseudoenantiomer of L-valine-derived catalyst **277**. The asymmetric

reaction between 4-nitrobenzaldehyde (**78a**) and methyl acrylate (**79a**) in TBME catalyzed by **280** gave corresponding allylic alcohol **306** in 85% yield and with 85% ee (*S*-enantiomer, entry 17, Table 9). This result confirmed the key role of the nucleophilic aminophosphine unit of the catalyst on the enantiocontrol of the reaction.

78 **79**

Scheme 65 Preparation of racemic MBH carbonates.

The absolute configuration of MBH adducts **285** – **305** was confirmed by chemical correlation with data reported previously[242] and by comparing product **285** of the asymmetric MBH reaction with products of kinetic resolution under the Sharpless asymmetric epoxidation (Scheme 66).[33] (*S*)-Enantiomer **306** of MBH alcohol **285** is more reactive in the epoxidation with TBHP catalyzed by Ti(O*i*-Pr)$_4$ in the presence of L-(+)-diisopropyl tartrate; as a result, starting compound becomes enriched of (*R*)-enantiomer **285**.

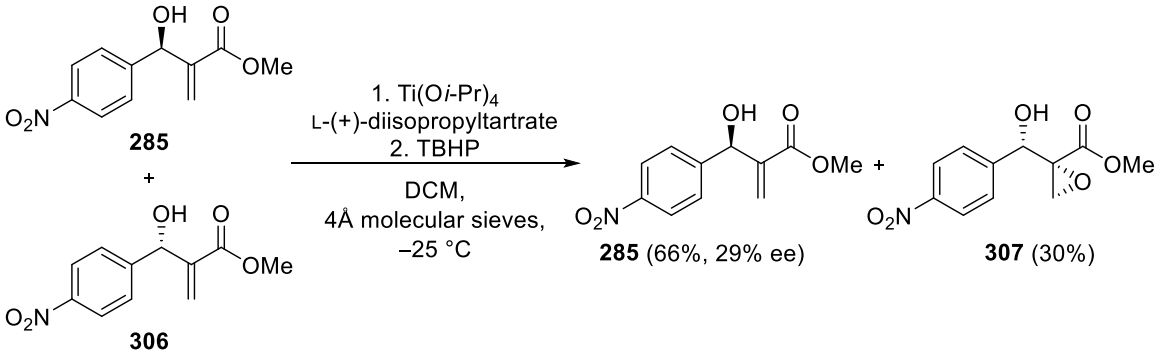

285 + **306**

racemate **285**/**306** (1/1)

Scheme 66 Kinetic resolution under the Sharpless asymmetric epoxidation.

9.5 Application of type III organocatalysts in asymmetric transformations

9.5.1 Asymmetric aza-MBH reaction

The aza-MBH reaction is a formation of α-methylene-β-aminocarbonyls by the creation of C−C bond between α-position of α,β-unsaturated carbonyls and imines in the presence of a nucleophilic catalyst.[102–105]

Powerful methodology for a highly enantioselective organo-co-catalytic aza-MBH reaction between *N*-carbamate protected imines **309** or imines surrogates **308** (α-amido sulfones) and α,β-unsaturated aldehydes **6** has already been developed in our laboratory (Scheme 67).[243] Extensive co-catalyst screening revealed the co-catalytic system of (*S*)-proline and DABCO as the most efficient. When tertiary phosphine BINAP was used instead of DABCO, the reactivity was very low (9% yield of **398**), but the enantioselectivity was excellent (19:1 E/Z and 93% ee).[243]

Comparing the nucleophilicity of the tertiary phosphino group in BINAP and in novel (thio)urea catalysts of type **III**, the latter should be higher due to the presence of one alkyl substituent (Chapter 6, page 29).[89] For that reason, the high catalytic activity of organocatalysts of type **III** was anticipated. The described hypothesis together with the fact

that (thio)ureas are known as efficient catalysts for the aza-MBH reactions[105,102] encouraged us to test catalysts of type **III** in the aza-MBH reaction. The possible structure of the activated pronucleophile was proposed in analogy with previously published results (Scheme 68).[244]

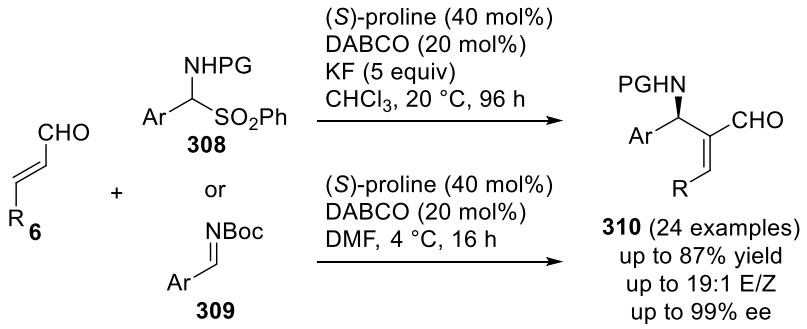

Scheme 67 Organo-co-catalytic aza-MBH reaction previously developed in our laboratory.

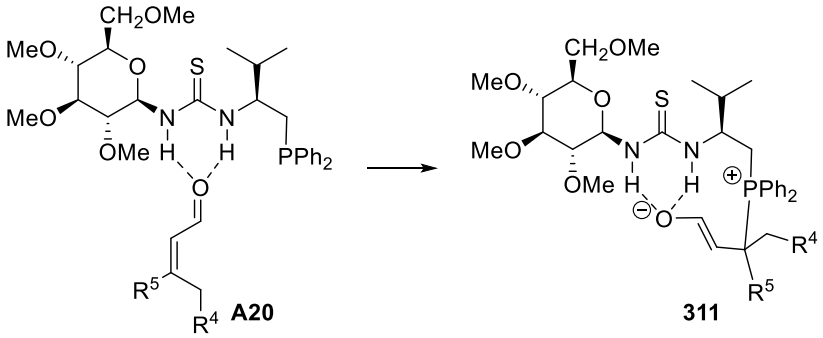

Scheme 68 Nucleophile activation proposed for catalyst **277**.

Imine surrogates showed higher reactivity and better selectivity in previous studies in comparison to imines. On that account, the reaction between α-amido sulfone **308a** and 2-pentenal (**6b**) catalyzed by **277** under previously optimized conditions was examined (Scheme 69a). However, the hydrolysis of imine was observed instead of the aza-MBH reaction. Unfortunately, changing the electrophile for preformed imine **309a** did not bring any improvement (Scheme 69b). Despite additional screening of reaction conditions, we were not able to afford the corresponding aza-MBH adduct **310a**. Further optimization would be necessary for the achievement of the asymmetric aza-MBH reaction.

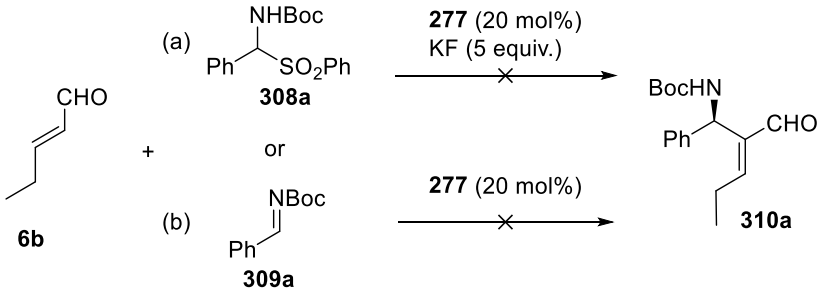

Scheme 69 Aza-MBH reaction catalyzed by **277**.

9.5.2 Asymmetric [4+1] cyclization

Tertiary phosphine catalyzed (asymmetric) [4+1] cyclizations belong to an important class of reactions resulting in highly functionalized five-membered rings (Section 6.2).[94,95] Bifunctional catalysts providing H-bonding interactions with an substrate were proven to be

very effective in asymmetric [4+1] cyclizations as they enable a high level of stereocontrol *via* the formation of well-defined transition states.[77,133,135]

Since Tong's pioneering work on [4+1] cyclization, allenoates became commonly used C_4 synthons.[132] For this reason, we decided to develop a [4+1] cyclization between allenoates **90** and benzothiophene (**317**) catalyzed by organocatalysts of type **III** (e.g., catalyst **277**), leading to spirocompounds **318**.

We anticipated the proposed reaction would follow a similar mechanistic pathway described by Tong (Scheme 15, page 35).[132] In analogy with Lu (Scheme 16, page 36), we speculated that stereoselectivity would be controlled by a well-defined transition state in which H-bonding interactions between benzothiophenone enolate and thiourea would play a crucial role (Scheme 70).

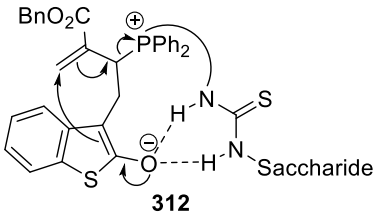

312

Scheme 70 Crucial role of H-bonding interactions in proposed mechanism **312**.

9.5.2.1 Synthesis of starting allenoates

Allenoates were prepared following the known procedure.[245,246] Allenoate **314** was prepared from benzyl bromoacetate (**313**), which was at first converted to stabilized ylide using the nucleophilic substitution followed by basic elimination. The subsequent reaction with acetyl chloride gave allenoate **314**, which underwent the Baylis-Hillman reaction with formaldehyde to yield compound **315** in 14% overall yield (Scheme 71).

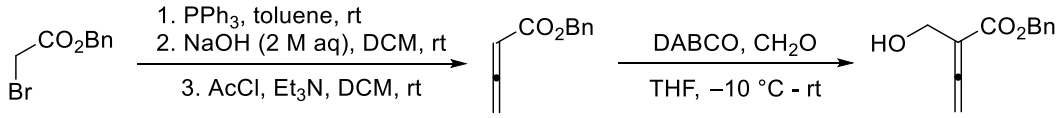

313 **314** (58%) **315** (27%)

Scheme 71 Preparation of allenoate **315**.

The last step was the protection of the free hydroxy group of compound **315**. At first, the Boc protecting group was chosen, but the reaction with Boc_2O in the presence of Et_3N did not proceed. Consequently, a catalytic amount of DMAP was added to the reaction mixture. Unfortunately, DMAP caused decomposition of starting allenoate **315** (Scheme 72a), therefore the acetyl protecting group was chosen instead. The reaction of compound **315** with acetyl chloride in the presence of Et_3N gave protected allenoate **90** (Scheme 72b).[132]

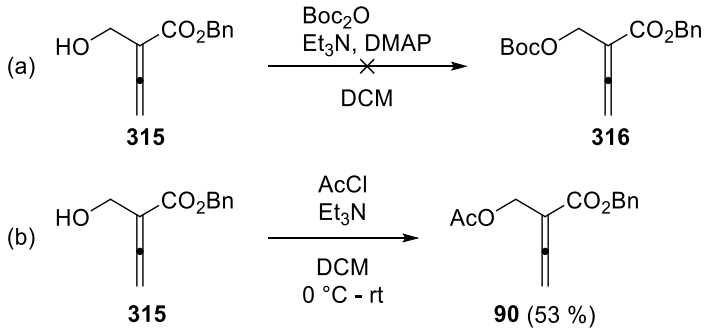

315 **316**

315 **90** (53 %)

Scheme 72 Protection of the free hydroxy group in allenoate **315**.

9.5.2.2 Asymmetric [4+1] cyclization

At the outset, we applied similar conditions as those published by Tong.[132] However, the reaction between allenoates **90** and benzothiophenone (**317**) catalyzed by catalyst **277** did not occur under the chosen reaction conditions (Scheme 73). Further optimization would be necessary to achieve the asymmetric [4+1] cyclization.

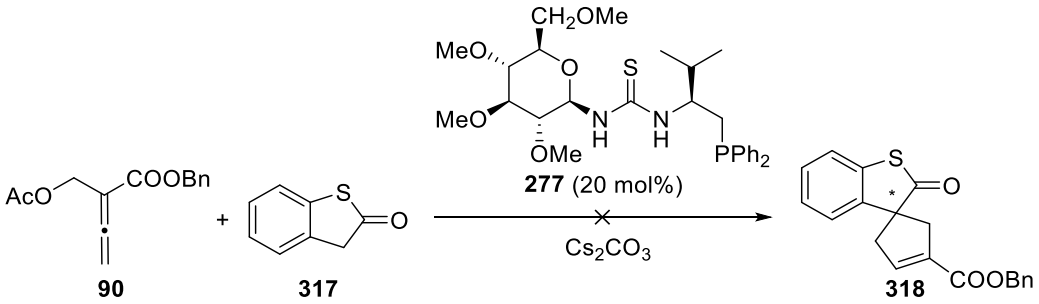

Scheme 73 Asymmetric [4+1] cyclization catalyzed by catalyst **277**.

10 Results & discussion: direct catalytic asymmetric C–H arylation

10.1 Aim of the work

The goal of my internship project in Larrosa's group at the University of Manchester was to develop a methodology for the synthesis of planar-chiral (η^6-arene)chromium complexes *via* a direct catalytic asymmetric C–H arylation of non-functionalized (η^6-arene)chromium complexes (Scheme 74).

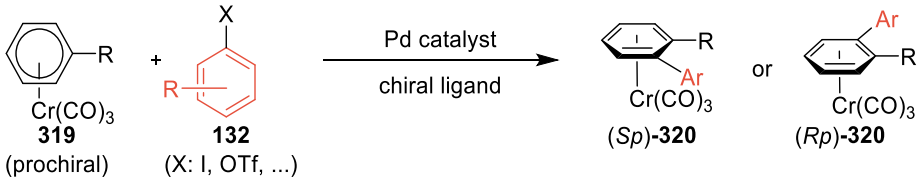

Scheme 74 Direct catalytic asymmetric C–H arylation of non-functionalized complex **319**.

Planar-chiral (η^6-arene)chromium complexes are useful stoichiometric auxiliaries as well as ligands for asymmetric synthesis (for details, see Section 8.6, page 49). However, the majority of synthetic approaches to planar-chiral (η^6-arene)chromium complexes require the employment of stoichiometric chiral reagents or auxiliaries (for details, see Section 8.6.1, page 50). Moreover, many of these classical approaches suffer from poor functional group compatibility and/or low atom economy, and/or the need to use sensitive organometallic reagents. In addition, an access to chiral (arene)chromium complexes *via* asymmetric catalysis is restricted to functionalized starting compounds so far.

To the best of our knowledge, there are no methods reported to synthesize enantioenriched planar-chiral chromium tricarbonyl complexes from non-functionalized precursors in a catalytic fashion (Scheme 74).

10.2 Previous results

In this section, the results of the previous study in the field of asymmetric C–H arylation of (fluorobenzene)tricarbonylchromium complex are briefly summarized. These were conducted in Larrosa's group by Katarina Krämer and Junfei Luo and they are included to provide sufficient background for my approach and results.

Larrosa's group demonstrated that π-complexation to $Cr(CO)_3$ dramatically enhances the reactivity of monofluoroarenes toward a highly *ortho*-selective Pd-catalyzed direct C–H arylation with iodoarenes (Scheme 22, page 43).[173] Catalytic system previously developed for the direct C–H arylation of (monofluoroarene)tricarbonylchromium complexes, i.e., $Pd(PPh_3)_4$, Ag_2CO_3, K_2CO_3, 1-$AdCO_2H$ (Entry 1, Table 10) completed with chiral phosphine was chosen as a reasonable outset for the development of enantioselective C–H arylation.

The initial catalyst $Pd(PPh_3)_4$ was changed to $Pd(dba)_2$ completed with (*S*)-BINAP as a chiral ligand. Catalyst $Pd(dba)_2$ enables facile coordination of the chiral ligand due to the weak coordination between Pd and dibenzylideneacetone. Moreover, it does not contain achiral PPh_3, whose presence in the reaction mixture can lower the enantioselectivity. However, using this catalytic system resulted in no reactivity (Entry 2).

Larrosa's group described that using TMP (2,2,6,6-tetramethylpiperidine) as an additive enhanced the reactivity of η^6-coordinated anisoles toward the direct C–H arylation.[174] By the addition of TMP (2 equiv) the more reactive catalytic system was created and the

reactivity, as well as enantioselectivity, increased (Entry 3). The role of TMP was attributed to the increased solubility of Ag(I) salt, through either coordination or increased solvent polarity. As is common in the Pd-catalyzed C−H functionalization, a stoichiometric Ag_2CO_3 is required as a halide scavenger. In addition, based on recent computational[247–249] and deuteration[250] studies and the results obtained by Larrosa's group during the optimization of the Pd-catalyzed C−H arylation of (arene)tricarbonylchromium complexes, it was proposed that silver could be performing the C−H activation step. Later on, a combination of stoichiometric and kinetic mechanistic studies performed in Larrosa's group showed that (PPh_3)Ag(I)-carboxylates can efficiently carry out C−H activation.[251]

Table 10 Previous results in the field of asymmetric direct C−H arylation.[a, b]

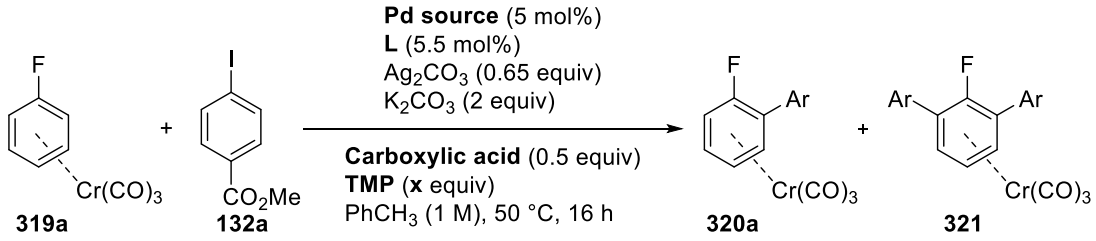

Entry	Pd source	Acid	L	**x**	**320a** (%)	ee[c] (%)	**321** (%)
1	$Pd(PPh_3)_4$	1-$AdCO_2H$	—	0	41	1	31
2	$Pd(dba)_2$	1-$AdCO_2H$	(*S*)-BINAP	0	0	—	0
3	$Pd(dba)_2$	1-$AdCO_2H$	(*S*)-BINAP	2	28	24	9
4	$Pd(dba)_2$	$Cy_2CHCOOH$	(*S*)-BINAP	2	42	64	31
5	$Pd(dba)_2$	$Cy_2CHCOOH$	(*S*)-BINAP(O)	2	50	70	27
6[d]	$Pd(dba)_2$	$Cy_2CHCOOH$	(*S*)-(*H*$_8$)-BINAP(O)	2	41	90	45

[a] The reaction was done with **319a** (0.1 mmol) and **132a** (0.2 mmol) in a GC MS vial; [b] Yields were calculated from ^{1}H NMR spectra of the reaction mixture using 1,3,5-trimethoxybenzene as an inner standard, the unreacted starting material was observed in all cases; [c] Chiral HPLC using IB column and a mixture of hexane/*i*-PrOH (97/3) as an eluent; [d] The reaction proceeded with **319a** (0.1 mmol) and **132a** (2 equiv), $Pd(dba)_2$ (3 mol%), (*S*)-(*H*$_8$)-BINAP(O) (3.3 mol%) at 40 °C for 40 h.

A carboxylic acid is supposed to be involved in the C−H activation step (Figure 32 & Section 8.4, page 44). Thus, the nature of carboxylic acid should have a significant effect on the reactivity and enantioselectivity. This assumption was confirmed by an extensive screening of (a)chiral carboxylic acids. Dicyclohexylcarboxylic acid gave the best results among the tested acids (Entry 4).

Screening of phosphine ligands showed monooxidized phosphine ligands, such as (*S*)-BINAP(O) and (*S*)-(*H*$_8$)-BINAP(O), as the most enantiodiscriminating (Entries 5, 6). The success of monooxidized phosphines was attributed to the weak coordination ability of phosphine oxide, which makes (*H*$_8$)-BINAP(O) a ligand that can act as a bidentate as well as monodentate and thus serves as the ligand for both Pd and Ag. By analogy with previous studies on the Pd-catalyzed C−H activation *via* the CMD mechanism (see Section 8.4, page 44), we proposed a plausible transition state **TS10** for the Ag-catalyzed C−H activation (Figure 32).

In conclusion, the screening of Pd and Ag sources, phosphine ligands, carboxylic acids, and amine additives, discovered a catalytic system based on $Pd(dba)_2$, Ag_2CO_3

(*S*)-(*H*8)-BINAP(O), dicyclohexylcarboxylic acid and TMP as the most effective affording monoarylated product **320a** in 41% yield and 90% ee (Entry 6).

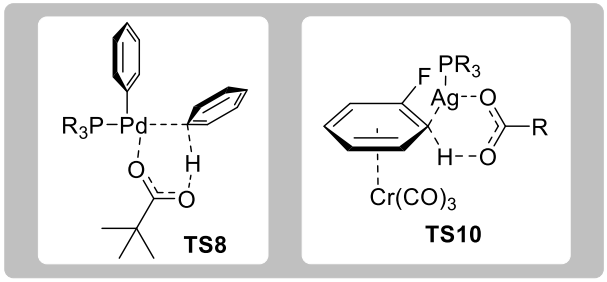

Figure 32 Transition state **TS8** proposed for the Pd-catalyzed C−H activation of benzene;[172] transition state **TS10** proposed for the Ag-catalyzed C−H activation of chromium complex .

I aimed to improve the yield of monoarylated product **320a** while increasing enantioselectivity and reducing bisarylation. Following the above-mentioned results, the optimization of reaction conditions and finding for more effective ligands and Pd-sources were suggested to accomplish the set goal.

10.3 Prochiral chromium tricarbonyl complex

Non-functionalized prochiral (fluorobenzene)tricarbonylchromium (**319a**) was chosen as a model substrate for the asymmetric direct C−H arylation. The presence of C-F bond in the aromatic core brings the advantage of easy derivatization of enantioenriched planar-chiral complexes *via* a nucleophilic aromatic substitution, e.g., phosphination, to obtain arylphosphine derivatives. Furthermore, the conditions for the racemic highly *ortho*-selective direct C−H arylation of (monofluoroarene)tricarbonylchromium complexes **142a** were previously developed in Larrosa's group (Scheme 22, page 43).[173]

The preparation of yellow crystalline (fluorobenzene)tricarbonylchromium **319a** was accomplished by reacting an excess of fluorobenzene (**141a**) with hexacarbonylchromium in a refluxing mixture of *n*-Bu2O/THF (Scheme 75).[173,252]

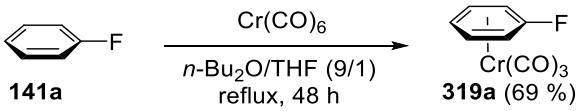

Scheme 75 Preparation of (fluorobenzene)tricarbonylchromium complex **319a.**

10.4 Design of chiral phosphine ligands

First, we focused on the preparation of chiral phosphine ligands. In the preliminary studies, monooxidized phosphine ligand (*H*8)-BINAP(O) (Figure 33) showed high efficiency in the C−H arylation, affording desired planar-chiral product **320a** in moderate yield (41%) and with high enanlioselectivity (90%, Entry 6, Table 10).

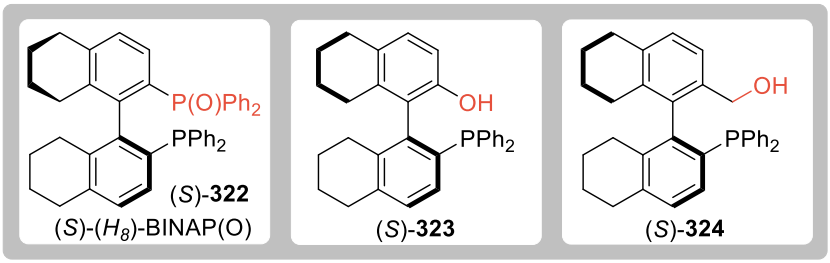

Figure 33 Axially chiral ligands from a family of (*H*8)-BINAP derivatives.

Based on this experience, two axially chiral phosphinoalcohols derived from (*H*8)-BINAP(O) in which the weaker donor site (P(O)Ph2 group) is substituted with the hydroxy or hydroxymethyl group were proposed: phenol-derived ligand **323** and benzyl alcohol-derived ligand **324** (Figure 33).

A stabilization of the CMD transition state *via* the H-bonding interaction between the hydroxy group of ligand **323** or **324** and the fluorine atom of **319a** was suggested for the Ag-catalyzed C−H activation with phosphinoalcohols **323** and **324**. The stabilization would lead to more defined TS (e.g., **TS11**) and thus to higher enantioinduction (Figure 34).

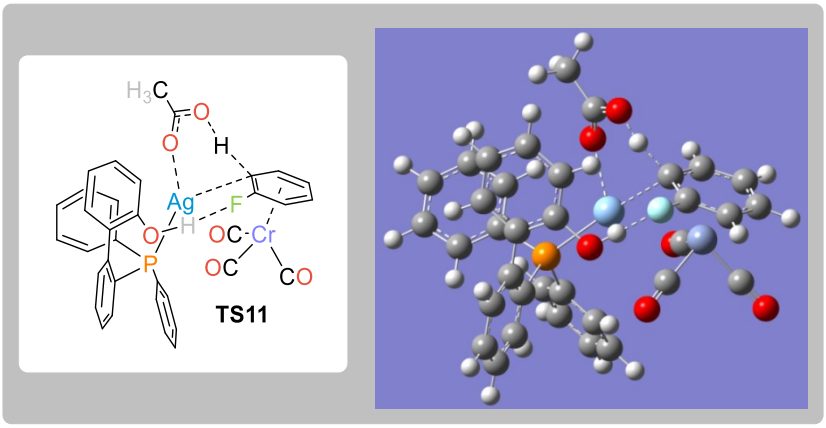

Figure 34 Transition state **TS11** proposed for the Ag-catalyzed C−H activation.

Moreover, monodentate phosphine ligands with a chiral centre on the phosphorus atom, such as phosphine (*S*)-**325** (Figure 35), were proposed. These ligands bring the advantage of the very close proximity of the chiral centre and reactive site, which might lead to higher stereoinduction.

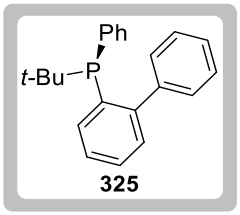

Figure 35 Ligand (*S*)-**325** with a chiral centre on the phosphorus atom.

10.5 Synthesis of axially chiral chiral phosphine ligands

10.5.1 (*S*) and (*R*)-(*H*8)-BINAP(O)

Both enantiomers of (*H*8)-BINAP(O)[253] (*S*)-**322** and (*R*)-**322** were synthesized starting from commercially available (*S*) or (*R*)-BINOL (*S*)-**326**, (*R*)-**326** according to the procedure known for the synthesis of their unsaturated analogue BINAP(O) (Scheme 76).[254,255]

The reaction of (*S*)- or (*R*)-BINOL (*S*)-**326**, (*R*)-**326** with Tf2O in the presence of pyridine afforded bistriflate (*S*)-**327**, (*R*)-**327**, which underwent Pd-catalyzed coupling with diphenylphosphine oxide (**330**, prepared *via* basic hydrolysis of Ph2PCl, see Section 13.2, page 124)[256] to yield monophosphine oxides (*S*)-**328** and (*R*)-**328**, respectively.

The reduction of compounds (*S*)-**328**, (*R*)-**328** with HSiCl3 in the presence of Et3N gave phosphines (*S*)-**329**, (*R*)-**329** and the subsequent Pd-catalyzed coupling with diphenylphosphine oxide (**330**) afforded desired products (*S*)-**322** (46% overall yield) and (*R*)-**322** (15% overall yield).

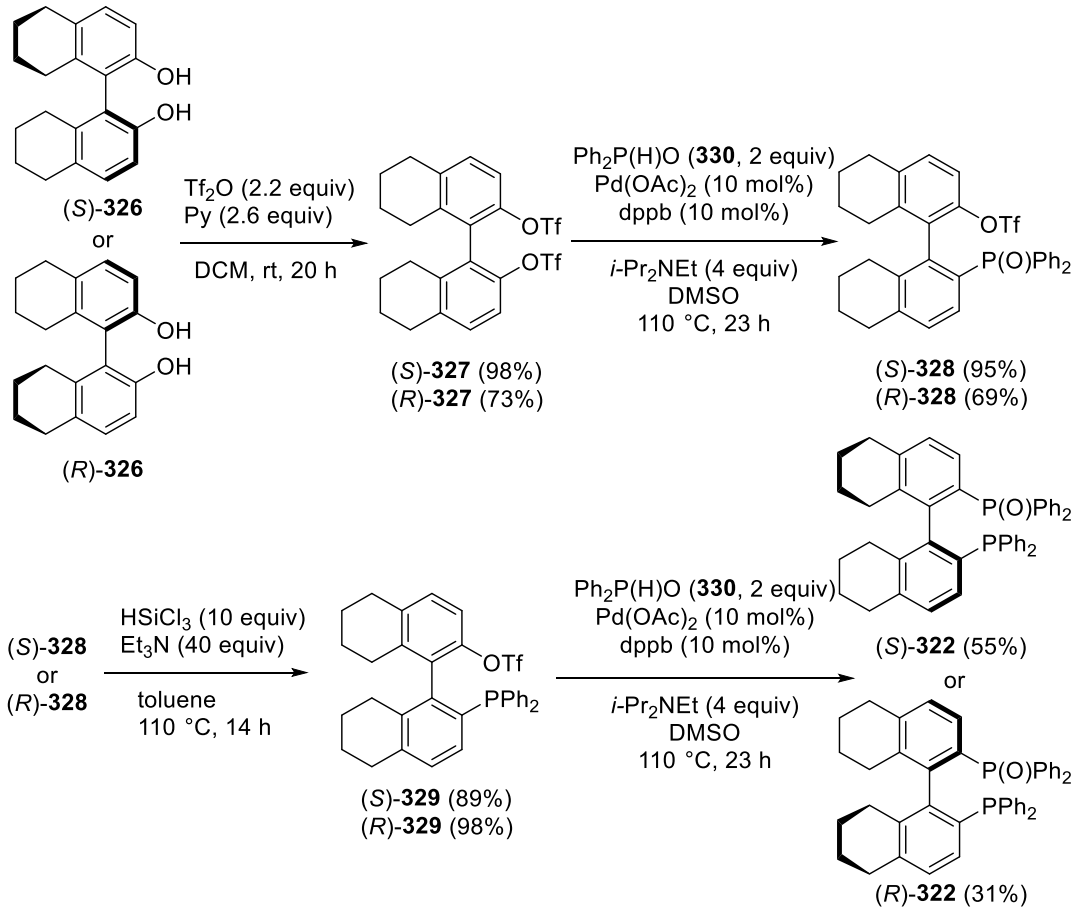

Scheme 76 Preparation of (*S*)- and (*R*)-(*H*8)-BINAP(O) (*S*)-**322** and (*R*)-**322**.

10.5.1.1 Enantiomeric purity of (*S*) and (*R*)-(*H*8)-BINAP(O)

Chiral HPLC analysis revealed that the above-described synthetic route afforded a mixture of (*S*) or (*R*)-(*H*8)-BINAP(O) with an unpredictable enantiomeric excess (ee of (*H*8)-BINAP(O) varied from 18 – 82%). The goal was to determine the synthetic step in which the racemization occurred.

Table 11 Determine of the racemization step *via* chiral HPLC study.[a]

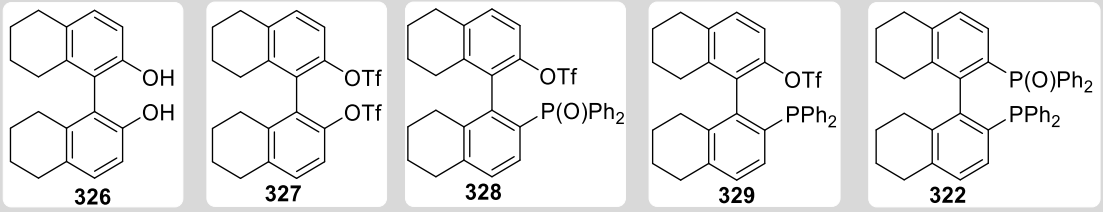

Entry	min[b]			min[c]		min[d]		min[e]		ee (%)
rac	46.0	126.3	Unsuccessful separation	55.9	69.3	20.7	23.7	16.2	34.5	0
(*R*)	x	✓		✓	x	x	✓	✓	✓	82
(*S*)	✓	x		x	✓	✓	x	✓	✓	46

[a] Ee was determined by chiral HPLC using Lux® 5 µm Amylose-1 column, flow rate 0.8 mL/min at 20 °C. using mixtures of [b] 99/1 hexane/*i*-PrOH until 120 min and then 90/10 hexane/*i*-PrOH; [c] 98/2 hexane/*i*-PrOH; [d] 95/5 hexane/*i*-PrOH; [e] 97/3 hexane/*i*-PrOH as eluents.

Compounds **322**, **326** – **329** were prepared again and their enantiomeric purity was verified using chiral HPLC (Table 11). Conditions for successful HPLC separation of bistriflate **327** were not found. Thus, compound (*S*)-**327** was hydrolyzed under basic conditions and the enantiomeric purity of hydrolyzed product (*S*)-**326** was determined instead (Scheme 77). The chiral HPLC study revealed that the first three steps of the synthetic route to (*S*) or (*R*)-(*H8*)-BINAP(O) were stereospecific, as compounds **326** – **329** were afforded as pure (*R*) or (*S*) enantiomers. The racemization occurred in the very last synthetic step.

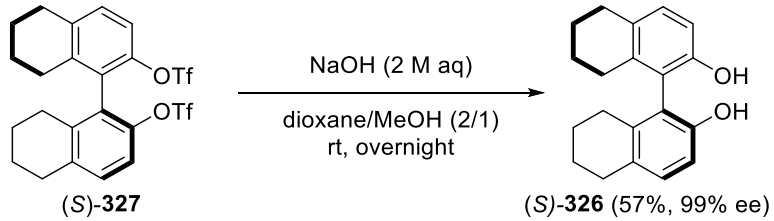

Scheme 77 Basic hydrolysis of bistriflate (*S*)-**327**.

To gain enantiomerically pure (*S*) or (*R*)-(*H8*)-BINAP(O), two approaches were suggested; purification of the prepared ligand (*via* chiral semi-preparative HPLC or *via* recrystallization) and development of a stereospecific coupling of triflate **329** with diphenylphosphine oxide (**330**). Unfortunately, the separation *via* semi-preparative HPLC using OD-H column failed. The purification of the enantiomeric mixture of (*R*)-**322** (18% ee) *via* recrystallization from DCM/hexane (1/1) resulted in needle-like crystals and an amorphous solid. The crystals were separated by tweezers and determined as (*R*)-**322** (70% ee) using chiral HPLC. The amorphous solid was determined as (*R*)-**322** (38% ee) and the filtrate as (*S*)-**322** (−45% ee).

The unsuccessful separation led us to the development of conditions for the stereospecific coupling between (*S*)-**329** and diphenylphosphine oxide (**330**). At first, the influence of temperature was tested and the reaction was proceeded at a lower temperature (80 °C vs. previously used 110 °C, Scheme 76). Secondly, the dppb-based Buchwald catalyst **347** (for the structure, see Scheme 88, page 89) was used instead of $Pd(OAc)_2$ and dppb. However, these changes, affording desired (*S*) or (*R*)-(*H8*)-BINAP(O) **322** in low yields (44%, 20% respectively) with unpredictable enantioselectivity, did not bring any improvements.

Later on, Maria Batuecas, a postdoctoral researcher in Larrosa's group, continued with the project and achieved the stereospecific coupling between (*S*)-**329** and diphenylphosphine oxide (**330**) using Morgans's catalytic system, i.e., $Pd(OAc)_2$/dppp/HCOONa (0.1 equiv/0.1 equiv/0.22 equiv), originally developed for monophosphorylation of [1,1'-binaphthalene]-2,2'-diyl bis(trifluoromethanesulfonate) (Scheme 78).[257]

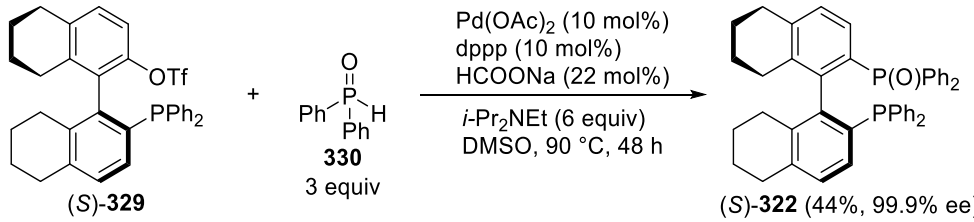

Scheme 78 Stereospecific synthesis of (*S*) or (*R*)-(*H8*)-BINAP(O) **322**.

10.5.2 Synthesis of phenol-derived ligand 323

Ligand (*S*)-**323** was prepared by basic hydrolysis of monophosphine (*S*)-**329** as a white foamy solid (Scheme 79). Effectivity of ligand (*S*)-**323** was tested in the direct C−H arylation of

(fluorobenzene)tricarbonylchromium complex **319a**. Using a catalytic system composed from XPhos-based Buchwald's catalyst **345**, ligand (*S*)-**323**, Ag_2CO_3, K_2CO_3, Cy_2CHCO_2H, and TMP (for detail, see Entry 12, Table 16, page 93), racemic product **320a** was obtained in a very low yield. Poor efficiency of ligand **323** might be caused by the high acidity of the phenolic hydroxy group, which is reflected in the deprotonation of the hydroxy group under reaction conditions. Consequently, the proposed stabilizing H-bonding interaction between the hydroxy group and the fluorine atom (see Figure 34) could not be formed.

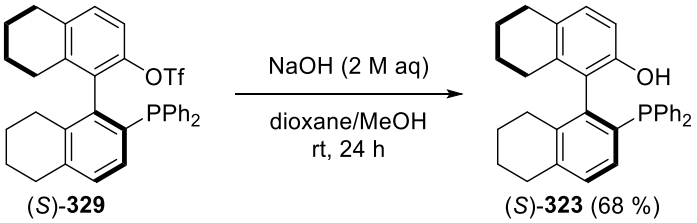

Scheme 79 Preparation of phenol-derived ligand (*S*)-**323**.

10.5.3 Synthesis of benzyl alcohol-derived ligand 324

Ligand **324** (Figure 33, page 82) was devised as a less acidic analogue of ligand **323** (the benzylic hydroxy group is less acidic in comparison to the phenolic hydroxy group). We expected ligand **324** could remain protonated under C−H arylation conditions.

The preparation of ligand **324** started from bistriflate (*S*)-**327** or (*R*)-**327**, which underwent the Pd-catalyzed carbonylation (Scheme 80). During the reaction, dicarbonylated by-product **332** was formed.[258] Subsequent Pd-catalyzed coupling between methyl ester **331** and diphenylphosphine oxide **330** gave product (*S*)-**333** (56% overall yield) or (*R*)-**333** (13% overall yield).

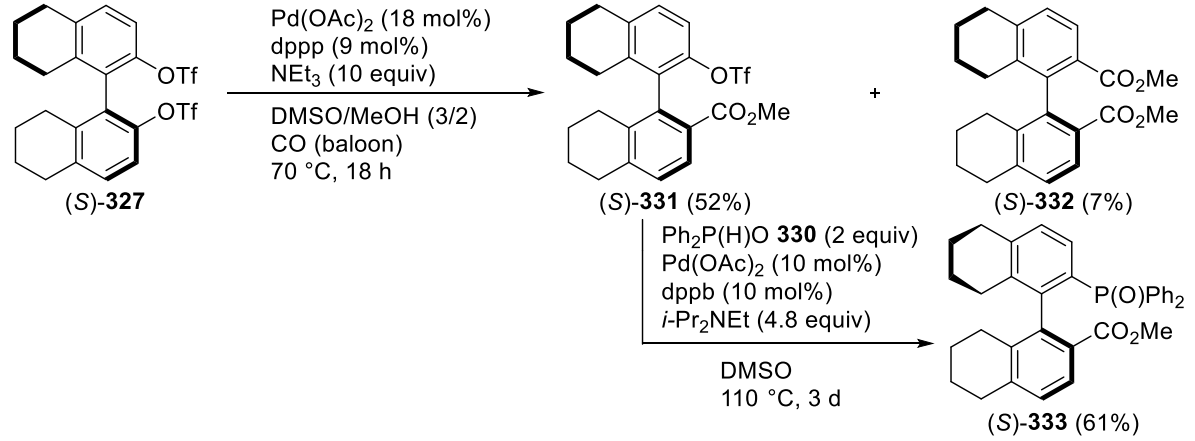

Scheme 80 Synthetic route to intermediate (*S*)-**333**.

Afterwards, the conditions for ester reduction were screened. The reduction did not proceed when either borane or sodium borohydride in combination with iodine were used as reducing agents (Scheme 81).[259]

The simultaneous reduction of both functional groups using $LiAlH_4$ was tested. The preferential reduction of ester group afforded product (*S*)-**334** (34% yield) and only traces of desired product (*S*)-**324** were observed by ^1H and ^{31}P NMR (Scheme 82). Hayashi reported the synthesis of an unsaturated analogue of (*S*)-**324** based on the preferential reduction of phosphine oxide using $HSiCl_3$ and Et_3N followed by the reduction of the ester group by

$LiAlH_4$.[260] Unfortunately, I had to leave Larrosa's group before I could apply Hayashi's approach on the synthesis of ligand (*S*)-**324**.

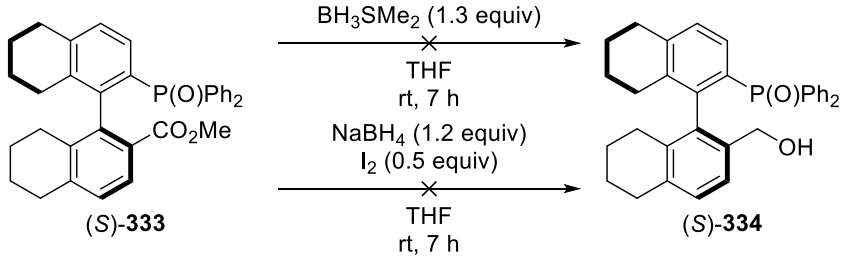

Scheme 81 Reduction of the ester group of (*S*)-**333**.

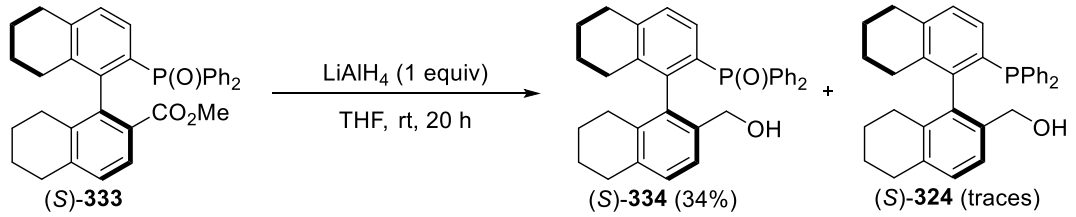

Scheme 82 Reduction of compound (*S*)-**333** by $LiAlH_4$.

10.5.4 Ligand with a chiral centre on the phosphorus atom

To prepare ligand (*S*)-**325**, a synthetic pathway based on the resolution of racemic *tert*-butyl(phenyl)phosphine oxide (*rac*-**336**) and the subsequent stereospecific reduction were suggested. Racemic phosphine oxide *rac*-**336** was prepared *via* the reaction of chlorodiphenylphosphine (**335**) with *t*-BuLi followed by acidic hydrolysis (Scheme 83).

In 2014, Couzijn and Minnaard reported a dynamic kinetic resolution (DKR) based on the formation of crystalline diastereomeric complexes of phosphine oxides with enantiomerically pure dibenzoyl tartaric acid and radical-mediated racemization using iodine.[261] Using their procedure for the resolution of racemic phosphine oxide *rac*-**336** afforded compound (*R*)-**336** (46% yield, 65% ee) and compound (*S*)-**336** (45% yield, −78% ee, Scheme 83).

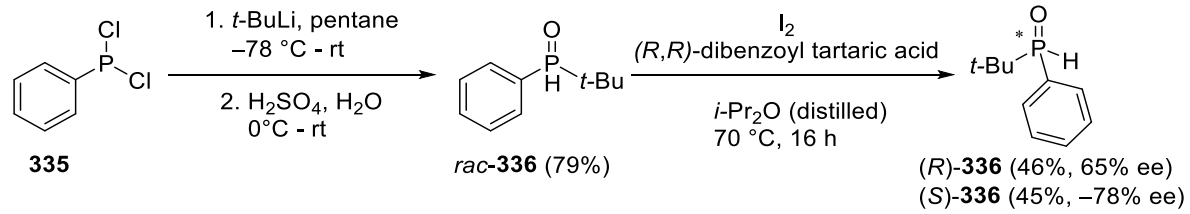

Scheme 83 Preparation of enantiomerically pure *tert*-butyl(phenyl)phosphine oxide.

At this stage, before the optimization of the conditions for the DKR, the enantioselectivity of subsequent coupling was studied (Scheme 84). The Pd-catalyzed coupling between phosphine oxide (*R*)-**336** (54% ee) and triflate **337** (prepared by the reaction of 2-phenylphenol and Tf_2O in the presence of pyridine, see Section 13.4, page 128)[262] in the presence of dppb or Xantphos chiral ligand afforded product (*R*)-**338** with 41% and 11% ee, respectively,[263,264] leading to the conclusion that the racemization occurred during the Pd-catalyzed coupling. When 2-iodobiphenyl (**339**) was used as a coupling partner instead of triflate **337**,[264] unreacted starting compound **336** and traces of desired product **338** were observed by ^{1}H NMR analysis (Scheme 85).

Due to the described difficulties in the synthesis of enantiomerically pure phosphine oxide **338**, we decided to prepare racemic tertiary phosphine *rac*-**325** and test its activity in the C−H arylation of (fluorobenzene)tricarbonylchromium complex at first. Racemic phosphine oxide *rac*-**325** was prepared using the Pd-catalyzed coupling between triflate **337** and racemic phosphine oxide *rac*-**336**.[264] Reduction of intermediate *rac*-**338** by the reaction with TMDS catalyzed either by $Ti(OTf)_4$ or $Cu(OTf)_2$ left mainly the unreacted starting compound **338** and only a small amount (39%) or traces of desired phosphine *rac*-**325**, respectively (Scheme 86).[265,266]

Unfortunately, racemic tertiary phosphine *rac*-**325** showed a very poor reactivity while tested in the direct C−H arylation of (fluorobenzene)tricarbonylchromium (**319a**) (see Entry 5, Table 16, page 93).

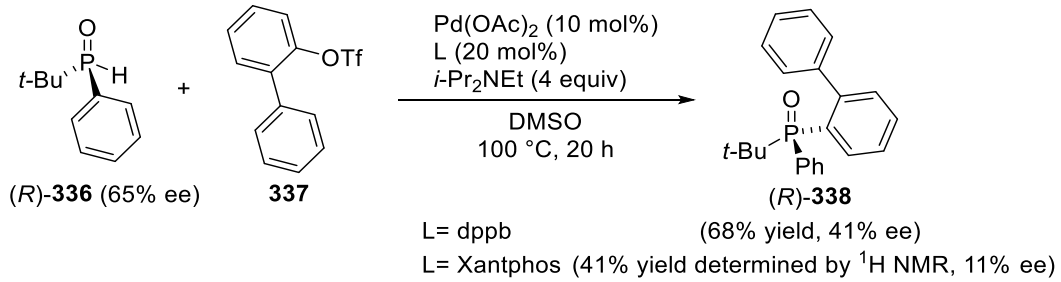

Scheme 84 Pd-Catalyzed coupling between phosphine oxide (*R*)-**336** and triflate **337**.

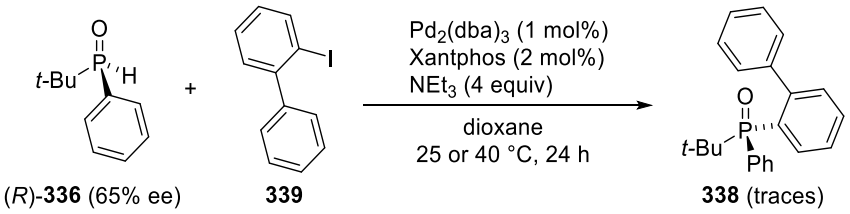

Scheme 85 The Pd-catalyzed coupling of phosphine oxide **336** and 2-iodobiphenyl (**339**).

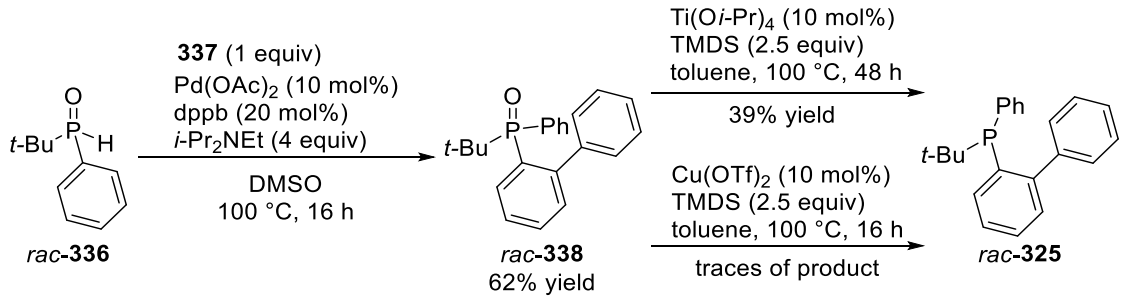

Scheme 86 Synthetic approach to racemic phosphine ligand *rac*-**325**.

10.6 Synthesis of Buchwald-type catalysts

Commercially available sources of Pd(0), such as $Pd_2(dba)_3$ and $Pd(PPh_3)_4$, contain achiral ligands. Ligands such as dba and PPh_3 can interfere with the reactions in which the Pd(0) source is used as catalyst.[267] In response, Buchwald developed a novel Pd(0) source based on *N*-methyl-2-aminobiphenyl **340**, which undergoes a rapid base-induced *in situ* formation of LPd(0) connected with the generation of unreactive by-product *N*-methyl carbazole **341** (Scheme 87).[268,269] Buchwald's precatalysts **340** are easy to prepare, compatible with a broad range of ligands and highly efficient in Pd-catalyzed C-C and C-N bond-forming reactions.

The synthesis of Buchwald's precatalysts **344** – **348** started from dimeric palladacycle **343**, which was prepared by my colleague Daniel Whitaker *via* the reaction of *N*-methyl-2-aminobiphenyl (**342**) with methanesulfonic acid followed by heating of the resulting solution with $Pd(OAc)_2$. The reaction of dimeric palladacycle **343** with various phosphines afforded Buchwald's catalysts **344** – **348** in excellent yields (Scheme 88). Catalyst **348** was prepared by Daniel Whitaker using the same procedure. Prepared Buchwald's catalysts **344** – **346**, and **348** were tested in the enantioselective C−H arylation (for details, see Table 15, page 92).

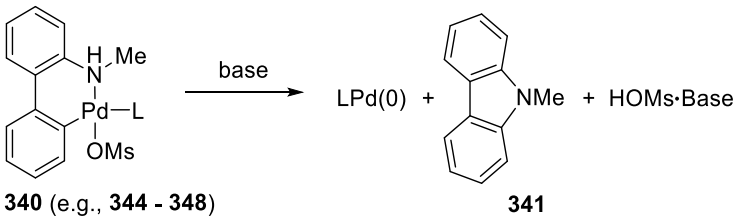

Scheme 87 The formation of Pd(0) source from Buchwald's precatalysts **340**.

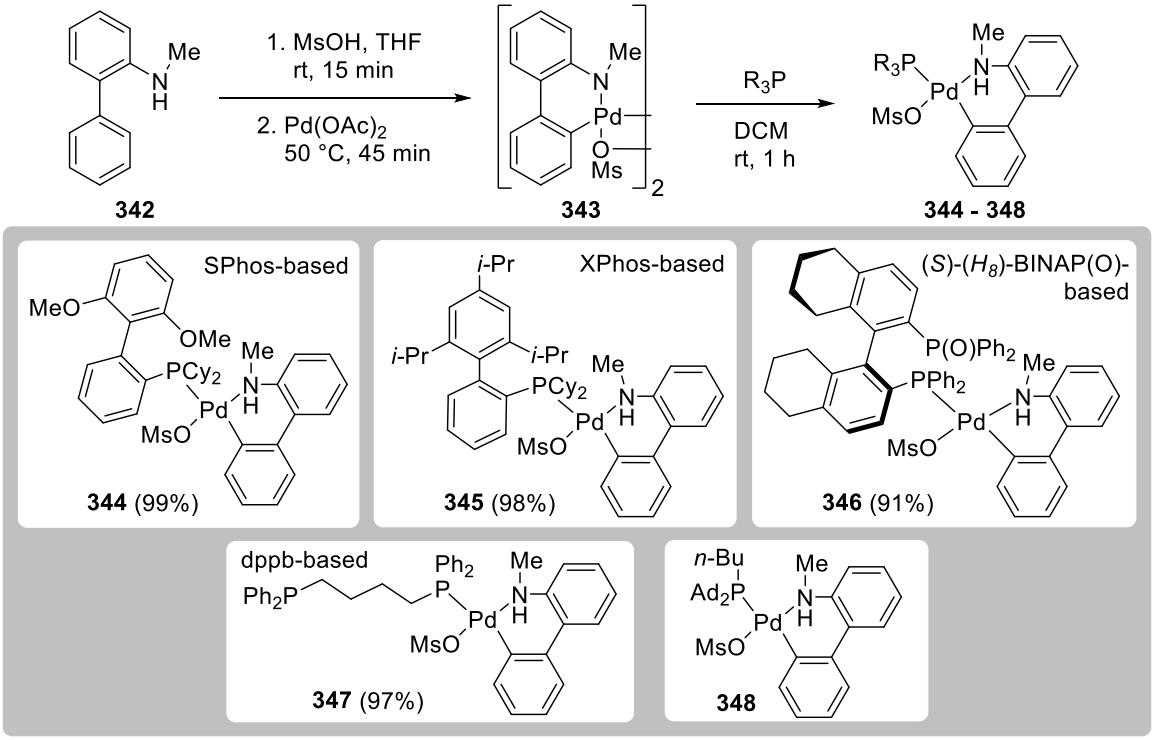

Scheme 88 The preparation of Buchwald's catalysts **344** – **348**.

10.7 Asymmetric C−H arylation using commercial Pd sources

At first, the C−H arylation of (flurobenzene)tricarbonylchromium complex **319a** was repeated under conditions previously optimized in Larrosa's group (for details, see Table 10, page 81). I afforded corresponding products **320a** and **321** in similar yields with slightly decreased enantioselectivity (Scheme 89). Then I concentrated on the optimization of reaction conditions.

TMP enhanced the reactivity of chromium complex **319a** in the C−H arylation (Entry 2 vs. Entry 3, Table 10, page 81), but it is an achiral additive and thus it might decrease enantioinduction. For that reason, the possibility to replace TMP with a chiral phosphine ligand was tested (Table 12). However, even when 48 mol% of (*S*)-(*H8*)-BINAP(O) was used,

the catalytic system was almost unreactive (Entry 4). The results presented in Table 12 emphasize the importance of TMP for increased reactivity and support the hypothesis that TMP coordinates and solubilizes an Ag(I)-carboxylate, which facilitates the C-H activation.

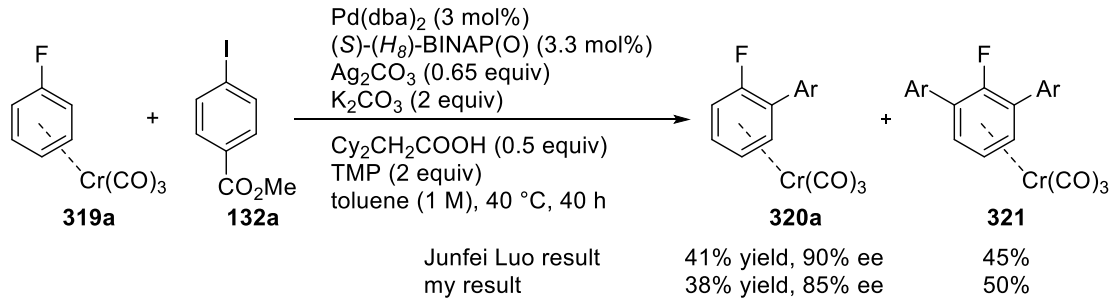

Scheme 89 Enantioselective C−H arylation under previously optimized conditions.

Table 12 Replacement of TMP with (*S*)-(*H8*)-BINAP(O).[a, b]

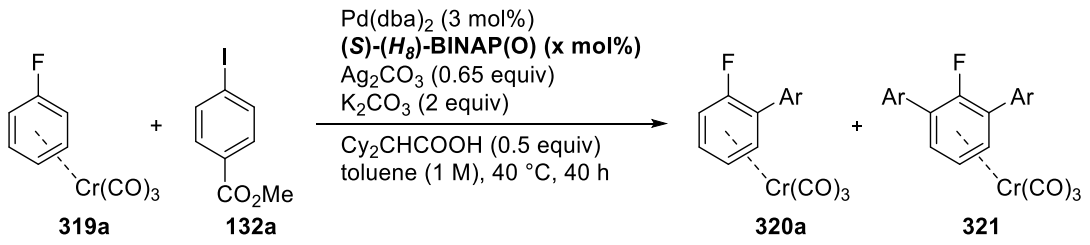

Entry	L (x mol%)	**320a** (%)	ee[c] (%)	**321** (%)	**319a** (%)	**132a** (%)
1	12	4	4	0	96	96
2	24	7	5	traces	91	85
3	36	8	5	traces	91	91
4	48	9	17	traces	88	90

[a] The reaction was done with **319a** (0.1 mmol) and **132a** (0.2 mmol) in a microwave tube; [b] Yields were calculated from ^{1}H NMR spectra of the reaction mixture using 1,3,5-trimethoxybenzene as an inner standard; [c] Chiral HPLC using IB column and a mixture of hexane/*i*-PrOH (97/3) as an eluent.

Next, the effect of dilution was studied (Table 13). The higher is the dilution, the lower is the enantioselectivity and the reduced is the extent of bisarylation. The yield of product **320a** was not affected by the dilution. The difference between the results presented in Scheme 89 and Table 13 (Entry 1) led us to explore the reproducibility of the studied system.

To check reproducibility, doubled experiments were performed. For the doubled experiments, the reaction between chromium complex **319a** and methyl *p*-iodobenzoate (**132a**) was set up twice under the same conditions using the same reagents at the same time (Table 14). The reproducibility of a pair of reactions within the doubled experiments was excellent as similar yields of products **320a**, **321** and enantioselectivity of product **321** were observed (Entries 1, 2). When the doubled experiments were performed in a glove box, the enantioselectivity slightly decreased (Entries 3, 4). In all cases, enantioselectivity was lower in comparison with those results depicted in Scheme 89.

From the above-mentioned results, it turned out that the unreliable reproducibility is most likely associated with the different batches of (*S*)-(*H8*)-BINAP(O) which were used. Soon after, it was discovered that the synthetic pathway, which was used for the preparation of (*S*)-(*H8*)-BINAP(O) (see Section 10.5.1, page 83), gave the ligand with an unpredictable ee (see Section 10.5.1.1). However, even when the issue of enantiomeric purity of

(*S*)-(*H*8)-BINAP(O) was solved, reproducibility troubles persisted. Finally, Maria Batuecas, a postdoctoral researcher in Larrosa's group, showed that reproducibility is the best when the reaction is set up in the glove box with all reagents dried and water (1 equiv) is added into the reaction mixture (Scheme 90, page 95).

Table 13 Effect of dilution on the C−H arylation.[a, b]

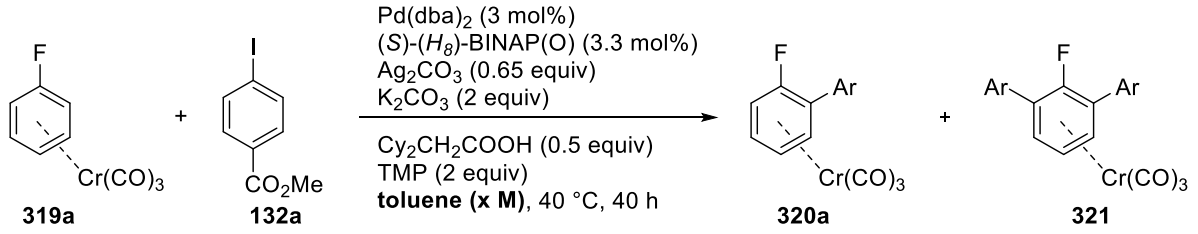

319a **132a** **320a** **321**

Entry	Molarity	**320a** (%)	ee[c] (%)	**321** (%)
1	1M	43	74	36
2	0.5M	43	66	19
3	0.2M	42	56	15

[a] The reaction was done with **319a** (0.1 mmol) and **132a** (0.2 mmol) in a microwave tube; [b] Yields were calculated from ^{1}H NMR spectra of the reaction mixture using 1,3,5-trimethoxybenzene as an inner standard; the unreacted starting material was observed in all cases; [c] Chiral HPLC using IB column and a mixture of hexane/*i*-PrOH (97/3) as an eluent.

Table 14 Doubled experiments.[a, b]

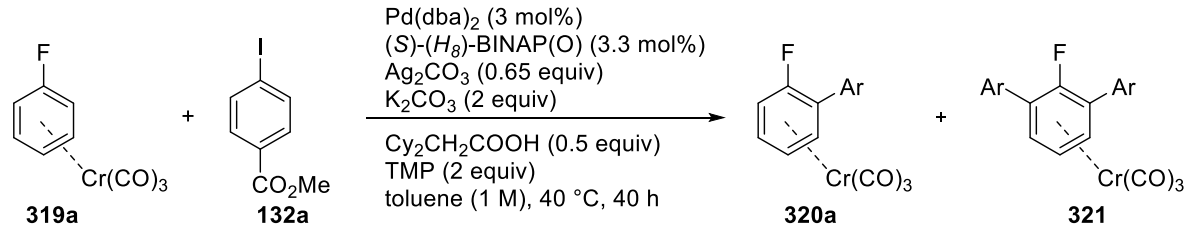

319a **132a** **320a** **321**

Entry	**320a** (%)	ee[c] (%)	**321** (%)
1	44	70	29
2	43	70	27
3[e]	45	67	34
4[e]	44	66	31

[a] The reaction was done with **319a** (0.1 mmol) and **132a** (0.2 mmol) in a microwave tube; [b] Yields were calculated from ^{1}H NMR spectra of the reaction mixture using 1,3,5-trimethoxybenzene as an inner standard; the unreacted starting material was observed in all cases; [c] Chiral HPLC using IB column and a mixture of hexane/*i*-PrOH (97/3) as an eluent; [e] The reaction was set up in a glove box.

10.8 Asymmetric C−H arylation using Buchwald-type catalysts

To improve the reaction conditions, Buchwald catalysts were chosen as a substitute for the combination of Pd(0) source and chiral ligand. As the outset, catalyst **346** with built-in (*S*)-(*H*8)-BINAP(O) ligand was used as a substitute for Pd(dba)2 and (*S*)-(*H*8)-BINAP(O) in the reaction of (fluorobenzene)tricarbonylchromium complex **319a** and methyl 4-iodobenzoate (**132a**) under previously optimized conditions (Entry 2, Table 15). A decrease in reactivity together with a significant drop of enantioselectivity in comparison to the

reaction with $Pd(dba)_2$ and separate (*S*)-(*H*$_8$)-BINAP(O) were observed (Entry 1 vs. Entry 2). The same scenario with an even bigger decrease of reactivity and selectivity was observed using catalyst **345** with built-in XPhos ligand (Entry 3).

To mimic the previously optimized conditions as much as possible, dba was added, leading to a slightly improved enantioinduction (Entry 4). To our surprise, the combination of Buchwald's catalyst **344**, **345**, **348** and (*S*)-(*H*$_8$)-BINAP(O) afforded yields and enantioselectivities of monoarylated product **320a** similar to the results obtained in the reaction with $Pd(dba)_2$ and (*S*)-(*H*$_8$)-BINAP(O) (Entries 5 – 7 vs. Entry 1), while the undesired bisarylation was suppressed. High enantioselectivity and the simultaneous decrease in the yield of diarylated product **321** made these results very promising. Catalytic system composed of Buchwald's catalyst **346** and XPhos or SPhos ligand showed low reactivity and enantioselectivity (Entries 8, 9). Results presented in Entries 5 – 9 strongly support the proposal that (*S*)-(*H*$_8$)-BINAP(O) serves as the ligand for silver and that the silver complex is responsible for C−H activation.

Table 15 Screening of Buchwald's catalysts and external ligands.[a], [b]

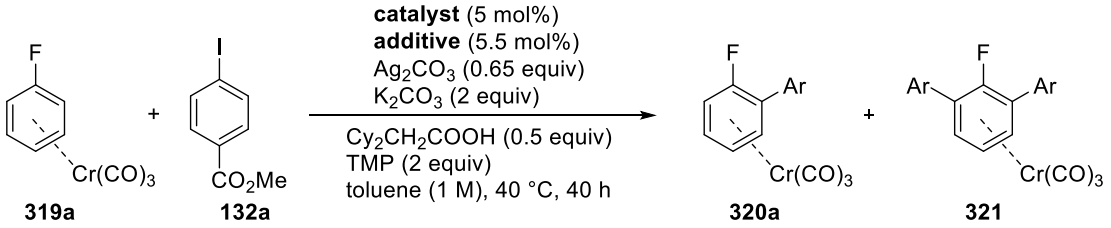

Entry	cats	additive	**320a** (%)	ee[c] (%)	**321** (%)
1	$Pd(dba)_2$	(*S*)-(*H*$_8$)-BINAP(O)	38	84	50
2	**346**	—	38	22	28
3	**345**	—	16	1	11
4	**346**	dba	37	30	20
5	**345**	(*S*)-(*H*$_8$)-BINAP(O)	43	80	17
6	**344**	(*S*)-(*H*$_8$)-BINAP(O)	42	80	22
7	**348**	(*S*)-(*H*$_8$)-BINAP(O)	43	72	13
8	**346**	XPhos	35	32	17
9	**346**	SPhos	39	24	22
10	$Pd(dba)_2$	(*S*)-(*H*$_8$)-BINAP(O) + XPhos	38	31	16
11	$Pd(dba)_2$	XPhos	29	3	19

[a] The reaction was done with **319a** (0.1 mmol) and **132a** (0.2 mmol) in a microwave tube; [b] Yields were calculated from ^{1}H NMR spectra of the reaction mixture using 1,3,5-trimethoxybenzene as an inner standard; the unreacted starting material was observed in all cases; [c] Chiral HPLC using IB column and a mixture of hexane/*i*-PrOH (97/3) as an eluent.

The direct asymmetric C−H arylation of (flurobenzene)tricarbonylchromium complex **319a** using $Pd(dba)_2$, (*S*)-(*H*$_8$)-BINAPO and XPhos proceeded with a significantly decreased enantiocontrol in comparison to the reaction catalyzed by XPhos-based catalyst **345** and (*S*)-(*H*$_8$)-BINAPO (Entry 10 vs. Entry 5). This result demonstrated the essential role of Buchwald's catalyst for high enantioinduction. Finally, the importance of external (*S*)-(*H*$_8$)-BINAP(O) for the stereocontrol was shown (Entry10 vs. Entry 11).

10.8.1.1 Ligand screening

As was shown in Table 15, the enantiocontrol of the C−H arylation is strongly dependent on the nature of the external ligand. Therefore, ligand screening for the reaction between chromium complex **319a** and methyl *p*-iodobenzoate (**132a**) catalyzed by XPhos-based Buchwald's catalyst **345** was done (Table 16). The majority of the tested ligands were bidentate ligands based on a biphenyl atropoisomeric backbone with similar bite angles to BINAP because it showed high efficiency in the previous studies (Figure 36).

Table 16 Ligand screening.[a], [b]

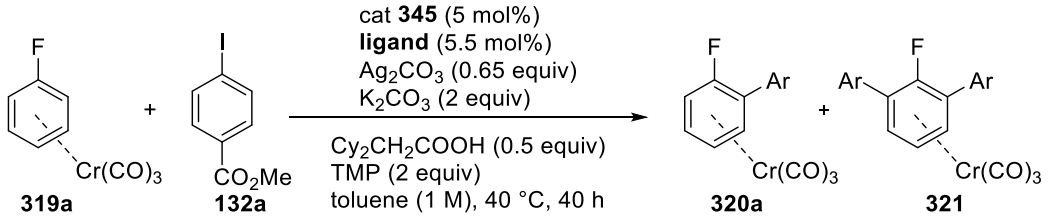

Entry	Ligand	**320a** (%)	ee[c] (%)	**321** (%)
1	**349**	35	0	10
2	**350**	46	3	16
3	**351**	48	-50	3
4	**352**	1	-	0
5	(*rac*)-**325** (10 mol%)	8	0	traces
6	**353**	42	32	16
7	**355**	43	15	22
8	**354**	46	67	21
9	**322**	41	79	32
10	**356**	48	-7	24
11	**357**	44	-9	28
12	**323**	7	2.6	traces
13	**358**	38	37	29

[a] The reaction was done with **319a** (0.1 mmol) and **132a** (0.2 mmol) in a microwave tube; [b] Yields were calculated from ^{1}H NMR spectra of the reaction mixture using 1,3,5-trimethoxybenzene as an inner standard; the unreacted starting material was observed in all cases; [c] Chiral HPLC using IB column and a mixture of hexane/*i*-PrOH (97/3) as an eluent.

Ligands **349**, **350** with slightly smaller bite angle than BINAP gave mono arylated product **320a** in acceptable yields 35%, 46%, respectively, but the product was racemic (Entries 1 – 2, Table 16). Ligand **351** which differed in electronic properties, gave product **320a** in comparable yield and with significantly increased enantioselectivity and excellent selectivity toward monoarylation (Entry 3). Reactions in the presence of bidentate phosphine **352**, which is based on central chirality, did not proceed (Entry 4). The racemic monodentate ligand *rac*-**325** showed very poor reactivity (Entry 5). The reaction in the presence of (*S*)-BINAP(O) and (*S*)-(*H*$_8$)-BINAP(O) gave the monoarylated product with the highest enantioselectivities (Entries 8 – 9). Enantioselectivities obtained with these ligands were much higher than those obtained with their diphosphine analogues (*S*)-BINAP and (*S*)-(*H*$_8$)-BINAP (Entries 6 – 7). These results highlighted the importance of the presence of both weak and strong donor atoms in the ligand to achieve a high stereoinduction.

The (*H8*)-BINAP(O) derivatives **356**, **357**, in which a weaker donor site is replaced with ether and ester, respectively, showed similar reactivity to (*S*)-(*H8*)-BINAP(O), together with a poor enantioselectivity (Entry 10, 11). The phenol-derived ligand **323** gave a low reactivity and the formation of racemic product **320a** was observed (Entry 12). These results indicate that the phosphine oxide functional group of the ligand is essential for a high enantioinduction. Changing of phenyl groups in $P(O)Ph_2$ to more sterically demanding 3,5-dimethylphenyl (ligand **358**) led to a decreased enantioselectivity (Entry 9 vs. Entry 13).

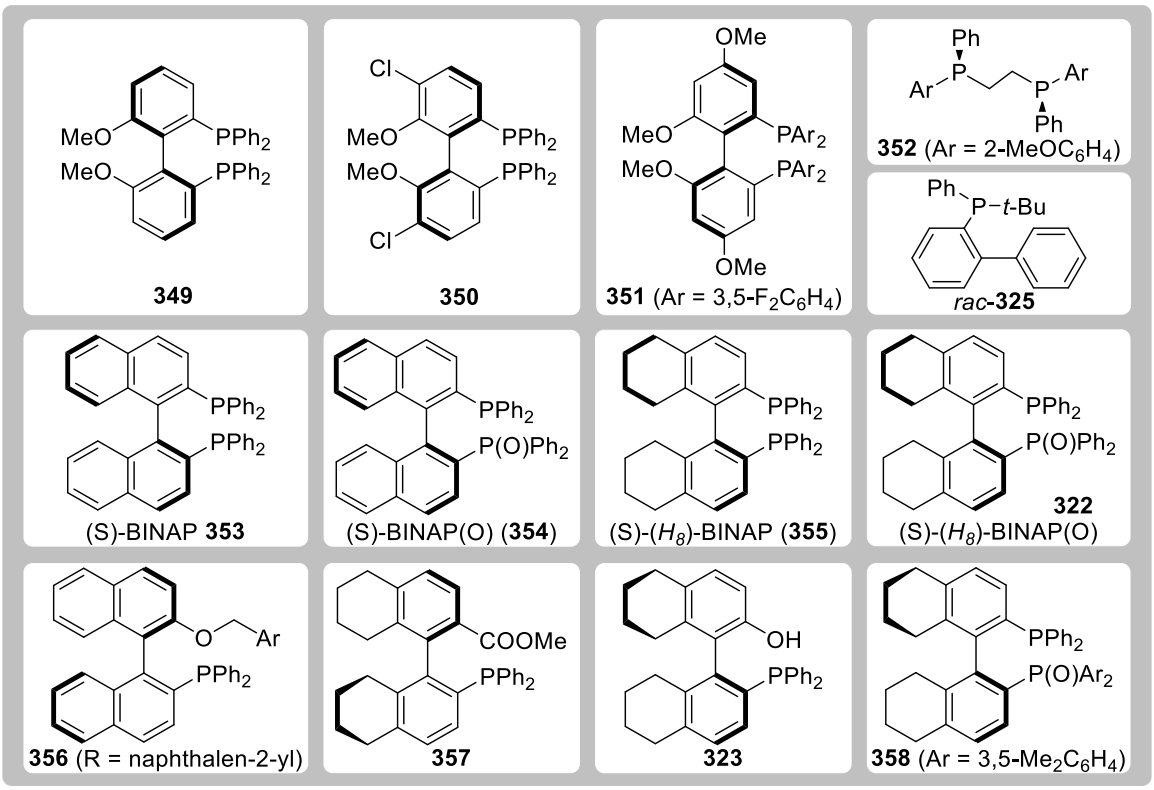

Figure 36 Ligands used for ligand screening.

Table 17 Influence of TMP loading.[a], [b]

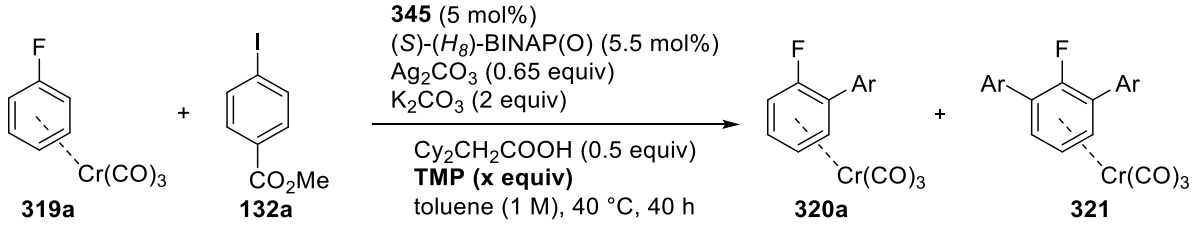

Entry	TMP (x equiv)	**320a** (%)	ee[c] (%)	**321** (%)
1	0	5	0	0
2	0.5	7	2	traces
3	1	44	73	35
4	2	41	79	32

[a] The reaction was done with **319a** (0.1 mmol) and **132a** (0.2 mmol) in a microwave tube; [b] Yields were calculated from ^{1}H NMR spectra of the reaction mixture using 1,3,5-trimethoxybenzene as an inner standard; the unreacted starting material was observed in all cases; [c] Chiral HPLC using IB column and a mixture of hexane/*i*-PrOH (97/3) as an eluent.

Next, the influence of a loading of achiral TMP on the C−H arylation between chromium complex **319a** and methyl *p*-iodobenzoate (**132a**) was studied (Table 17). As in previous cases (Table 12, page 90), the catalytic system was poorly reactive without TMP as well as with only 0.5 equiv of TMP (Entries 1 – 2). Using 1 or 2 equiv of TMP led to a high catalytic activity and enantioinduction with the optimum at 2 equiv of TMP (Entries 3 – 4)

10.9 Proposed mechanism and optimized conditions

For the sake of completeness of the studied topic, the optimized conditions (Scheme 90) and the proposed mechanism obtained after my departure from Larrosa's group are briefly described below.

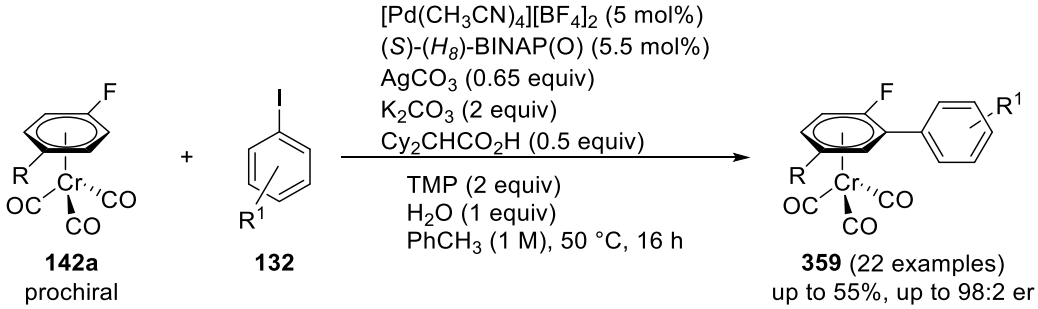

Scheme 90 Catalytic asymmetric C−H arylation under optimized conditions.

A mechanism based on the bimetallic catalytic cycle was proposed (Scheme 91). The oxidative addition of a (*S*)-(*H8*)-BINAP(O)-Pd(0) **360** followed by transmetalation affords carboxylate-Pd derivative **363**. In the parallel catalytic cycle, intermediate **365** is formed by C−H activation of the (arene)chromium complex; presumably, through the carboxylate-assisted CMD mechanism (Section 8.4, page 44). Transmetalation from **365** to palladium aryl carboxylate **363** affords intermediate **364**, which releases the desired product and catalyst **360** in the reductive elimination. There are two possible enantiodetermining steps in the proposed mechanism. Either the enantioselective C−H activation by silver carboxylate **366** is followed by fast transmetalation to intermediate **363** or fast reversible C−H activation is followed by the enantiodetermining transmetalation. Further experiments are necessary to fully understand this process.

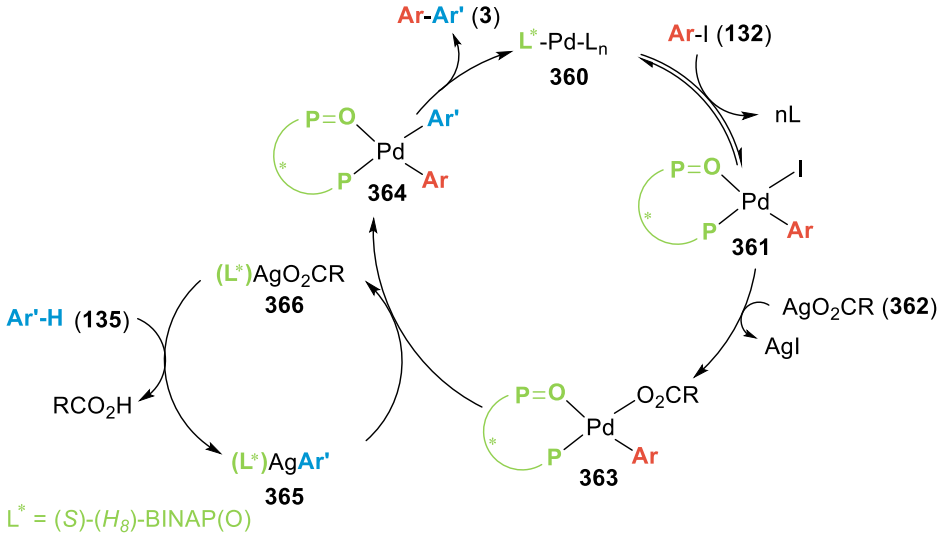

Scheme 91 Mechanism proposed for the catalytic asymmetric C−H arylation.

11 Conclusion

Despite the fact that saccharides have properties suitable for catalyst design, only limited attention has been paid to the synthesis of bifunctional (thio)ureas derived from saccharides so far. We designed three types of novel saccharide-derived bifunctional (thio)urea organocatalysts: C2-symmetrical thiourea/tertiary amines entirely based on the structure of 2-amino-2-deoxy saccharides, thiourea/primary amines derived from pentopyranose and a cyclohexane skeleton and (thio)urea/tertiary phosphines containing both saccharide and α-amino acid unit.

Two retrosynthetic strategies for the synthesis of C2-symmetrical D-glucosamine-derived organocatalysts were developed: based on *N*-Alloc-protected and *N*,*N*-dimethylated intermediates, respectively. During the synthesis, we revealed the incompatibility of *O*-acetyl protecting groups with conditions for *N*,*N*-dimethylation and *N*-Alloc protecting group with conditions for *O*-substitution. To overcome the incompatibility issues, suitable *N*-protecting groups need to be found.

Novel xylopyranosyl-derived thiourea/primary amine catalyst was prepared starting from D-xylose in three steps and in 15% overall yield. In analogy with Ma's study,[149] creation of a well-defined transition state *via* simultaneous enamine activation of a pronucleophile and double H-bonding activation of an electrophile is anticipated. Thus, xylopyranosyl-derived catalyst could be applied for various Michael additions, such as the Michael addition of aromatic ketones to nitrostyrene.

We prepared novel bifunctional (thio)urea-tertiary phosphine organocatalysts, which were readily available from naturally occurring biomolecules such as D-glucose, glycine, L-alanine, L-valine, L-leucine. The efficiency of the organocatalysts was demonstrated in the asymmetric MBH reaction of aromatic aldehydes with acrylates. The L-valine-derived thiourea/phosphine catalyst was the most suitable for the MBH reaction, affording allylic MBH alcohols in high yields (up to 85%) and with high enantioselectivities (up to 87% ee). Obtained results were published in *Synlett* **2015**, *26*, 2690 – 2696. Future work could focus on developing new asymmetric transformations (e.g., [4+1] cyclization) catalyzed by novel bifunctional (thio)urea-tertiary phosphine organocatalysts.

During my internship in Larrosa's group at the University of Manchester, I explored a one-step construction of planar-chiral chromium complexes *via* the direct catalytic asymmetric C−H arylation of prochiral (η^6-fluorobenzene)tricarbonylchromium complexes under mild conditions. Planar-chiral H_8-BINAP derivatives, ligand with a chiral centre on the phosphorus atom and Buchwald's catalysts were prepared and tested. The combination of XPhos-based Buchwald's catalyst and (*S*)-H_8-BINAP(O) seemed as the most promising, affording the monoarylated product with 80% ee in 43% yield with a significantly decreased extent of undesired bisarylation. The results became part of the paper published in *ACS Catalysis* **2019**, *9*, 5268 – 5278. The future work in this field is aimed at the application of new planar-chiral chromium complexes as ligands to asymmetric catalysis.

12 Experimental part: novel saccharide-derived (thio)urea organocatalysts

Reagents were purchased from common commercial suppliers and used without further purification unless otherwise stated. Solvents were either purchased from commercial suppliers in HPLC-grade or purified by standard techniques. Dry solvents for the reactions were obtained using standard protocols, e.g., distillation from sodium/benzophenone (THF, toluene) or CaH_2 (DCM), standing over molecular sieves (DMF), standing over molecular sieves and subsequent distillation (MeOH). All air and moisture sensitive reactions were performed under a dry argon atmosphere. Glassware was flame-dried under vacuum and allowed to cool under vacuum/argon prior to use. Solvents were evaporated using a rotary evaporator and all products were dried using a high vacuum.

Column chromatography was performed on silica gel (40 – 63 μL). Solvents for column chromatography were distilled prior to use. Analytical thin-layer chromatography (TLC) was performed on pre-coated aluminium-backed silica gel F_{254} plates with visualization under UV light (λ = 254 nm). Spot detection was completed by immersion in AMC (phosphomolybdenic acid (25 g), $Ce(SO_4)_2 \bullet H_2O$ (10g), sulfuric acid (1.2 M aq, 1 L)) or $KMnO_4$ or a solution of ninhydrin (0.2% in *n*-butanol) followed by heating using heat gun.

NMR spectra were recorded on Varian UNITY INOVA (300 MHz) or Bruker AVANCE III (600 MHz) instruments at 25 °C (unless otherwise stated) using $CDCl_3$, CD_3OD, C_6D_6 and D_2O as solvents. Chemical shifts (δ) are reported in parts per million (ppm) from low to high field and referenced to the residual solvent peak ($CDCl_3$: δ 7.26/77.16 $^1H/^{13}C$ NMR; CD_3OD: 3.31 ^1H NMR; C_6D_6: 7.16 ^1H NMR; D_2O: 4.79 ^1H NMR). Chemical shifts of phosphorus spectra are referenced relative to the external standard 85% H_3PO_4 ($CDCl_3$: δ = 0 ppm). Coupling constants (*J*) are reported in Hertz (Hz). Standard abbreviations indicating multiplicity were used as follows: m = multiplet, q = quartet, t = triplet, d = doublet, s = singlet, br = broad signal, dd = doublet of doublet, dt = doublet of triplet, ddd = doublet of doublet of doublet.

High resolution mass spectra (HRMS) were recorded using the electrospray ionization (ESI) technique with a time of flight (TOF) analyzer. Mass spectroscopy (MS) was recorded either using the electrospray ionization technique with ion trap (IT) or TOF analyzer or using the electron impact (EI) ionization technique with TOF analyzer. Infrared (IR) spectra were recorded in KBr using the diffuse reflectance (DRIFT) technique and measured on a Nicolet Avatar 370 FTIR spectrometer. Infrared spectra are quoted in cm^{-1}.

High performance liquid chromatography (HPLC) was performed on SHIMADZU chromatograph with SPD-M20A spectrophotometric detector using Chiralpak® IC, Chiralpak® IA, Chiralpak® IB columns at 25 °C and mixtures of HPLC-grade heptane and propan-2-ol as an an eluent. The detailed conditions are given in the characterization part of the products. Enantiomeric ratios of the enantioenriched products were determined by comparison of the asymmetric products with the racemic ones. Optical rotations (α) were measured using a Rudolph Research Analytical Autopol III Polarimetr, $[\alpha]_D^{25}$ values are given in $10^{-1} \cdot \mathrm{deg} \cdot \mathrm{cm}^2 \cdot \mathrm{g}^{-1}$ and sample concentrations are denoted as *c* (g/100 mL).

12.1 Synthesis of type I organocatalysts

2-Amino-2-deoxy-3,4,6-tri-*O*-acetyl-α-D-glucopyranosyl bromide hydrobromide (230):

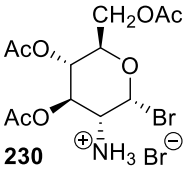

230

Under argon, a solution of D-glucosamine hydrochloride (**224**, 3.0 g, 13.9 mmol) was dissolved in acetyl bromide (10.8 mL, 146.1 mmol). The reaction mixture was stirred at rt overnight. The reaction mixture solidified during that time. The solid was dissolved in hot $CHCl_3$ and purified by hot filtration. Et_2O was added to the filtrate and the precipitate formed was separated by filtration and washed with Et_2O until the filtrate became colourless. Vacuum drying of the precipitate afforded **230** as a white solid (4.9 g, 78% yield): ^{1}H NMR (300 MHz, $CDCl_3$) δ 8.68 (s, 3H), 7.06 (s, 1H), 5.47 (t, *J* = 9.5 Hz, 1H), 5.22 (t, *J* = 9.5 Hz, 1H), 4.40 – 4.21 (m, 2H), 4.14 (d, *J* = 10.9 Hz, 1H), 3.91 (s, 1H), 2.24 (s, 3H), 2.10 (s, 3H), 2.06 (s, 3H). ^{1}H NMR corresponds to the literature.[219]

2-Amino-2-deoxy-3,4,6-tri-*O*-acetyl-β-D-glucopyranosyl azide (231):

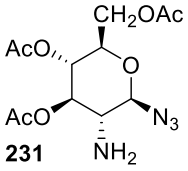

231

Under argon, trimethylsilyl azide (0.03 mL, 0.22 mmol) and TBAF (1 M in THF, 0.22 mL) were added to a suspension of hydrobromide **230** (100 mg, 0.22 mmol) in dry acetonitrile (1 mL) in a flame-dried vial. The reaction mixture was stirred at rt for 6 h. The solvent was eliminated under reduced pressure and the residue was purified by silica gel column chromatography (EtOAc) to afford **231** as a white crystals (64 mg, 87% yield): ^{1}H NMR (300 MHz, $CDCl_3$) δ 5.17 (t, *J* = 9.5 Hz, 1H), 5.03 (t, *J* = 9.6 Hz, 1H), 4.76 (d, *J* = 8.8 Hz, 1H), 4.31 (dd, *J* = 12.2, 4.4 Hz, 1H), 4.14 (d, *J* = 12.6 Hz, 1H), 3.86 – 3.76 (m, 1H), 2.93 (t, *J* = 9.4 Hz, 1H), 2.46 (br s, 2H), 2.10 (s, 6H), 2.03 (s, 3H). ^{1}H NMR corresponds to the literature.[220]

2-Deoxy-2-(4-methoxybenzylidene)amino-β-D-glucopyranose (225):

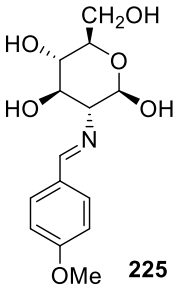

225

A solution of NaOH (1 M aq, 120 mL) was cooled to 5 °C in an ice bath. While stirring vigorously, D-glucosamine hydrochloride (**224**, (21.6 g, 100.0 mmol) and anisaldehyde (12.5 mL, 102.7 mmol) were added. The reaction mixture was stirred vigorously at 5 °C for 5 min and at rt for 3 h. Ice water (130 mL) was added and the solid was separated by filtration. The crude product was washed with Et_2O and dried over KOH in a desiccator to afford **225** as white crystals (25.0 g, 84% yield). ^{1}H NMR (300 MHz, CD_3OD) confirmed the formation of imine 9.82 (s, 1H).

1,3,4,6-Tetra-*O*-acetyl-2-deoxy-2-(4-methoxybenzylidene)amino-β-D-glucopyranose (226):

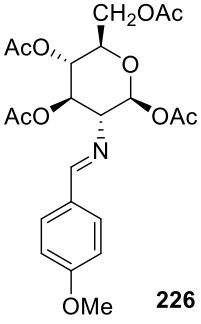

226

Under argon, dry pyridine (32.0 mL, 39.7 mmol) was added to a solution of Schiff base **225** (12.0 g, 40.4 mmol) in dry DCM (50 mL) and the reaction mixture was cooled to 0 °C in an ice bath. Acetic anhydride (24.7 mL, 261.5 mmol), followed by a solution of DMAP (276 mg, 2.26 mmol) in dry DCM (2 mL), were added. The reaction mixture was stirred at rt overnight. Then it was cooled to 0 °C in an ice bath and EtOH (15 mL) was added. The reaction mixture was stirred at 0 °C for 3 h. After that time, the solvent was eliminated under reduced pressure and the reside was codistillated with toluene (35 mL) five times. Et_2O (21 mL) was added and the resulting solution was placed in a freezer to solidify. Recrystallization from EtOH and drying over KOH in desiccator afforded **226** as white needles (11.7 g, 63% yield): $[\alpha]_D^{25} = +12.5$ (*c* 0.44, MeOH); ^{1}H NMR (300 MHz, CD_3OD) δ 8.30 (s, 1H), 7.74 – 7.67 (m, 2H), 7.04 – 6.97 (m, 2H), 5.98 (d, *J* = 8.3 Hz, 1H), 5.45 (t, *J* = 9.6 Hz, 1H), 5.12 (t, *J* = 9.7 Hz, 1H), 4.37 (dd, *J* = 12.4, 4.4 Hz, 1H), 4.18 (d, *J* = 2.3 Hz, 1H), 4.15 – 4.06 (m, 1H), 3.87 (s, 3H), 3.52 (dd, *J* = 9.8, 8.4 Hz, 1H), 2.08 (s, 3H), 2.04 (s, *3*H), 2.02 (s, 3H), 1.88 (s, 3H).

1,3,4,6-Tetra-*O*-acetyl-2-amino-2-deoxy-β-D-glucopyranose hydrochloride (227):

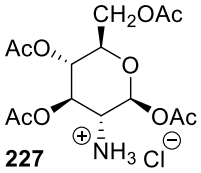

227

Per-*O*-acetylated Schiff base **226** (11.5 g, 2.7 mmol) was dissolved in acetone (120 mL) and a solution of HCl (5 M aq) was added dropwise until the reaction mixture became solid. The reaction mixture was placed in a freezer for 3 h and then it was diluted with acetone. The solid was separated by filtration, washed with Et_2O and dried under high vacuum to afford **227** as white crystals (9.4 g, 99% yield): $[\alpha]_D^{25} = +35.9$ (*c* 0.39, MeOH); ^{1}H NMR (300 MHz, CD_3OD) δ 5.89 (d, *J* = 8.8 Hz, 1H), 5.38 (dd, *J* = 10.5, 9.1 Hz, 1H), 5.09 (dd, *J* = 10.0, 9.2 Hz, 1H), 4.31 (dd, *J* = 12.6, 4.5 Hz, 1H), 4.12 (dd, *J* = 12.6, 2.3 Hz, 1H), 4.03 (ddd, *J* = 10.1, 4.5, 2.3 Hz, 1H), 3.64 (dd, *J* = 10.5, 8.8 Hz, 1H), 2.20 (s, 3H), 2.10 (s, 3H), 2.04 (s, 3H), 2.03 (s, 3H).

1,3,4,6-Tetra-*O*-acetyl-2-allyloxycarbonylamino-2-deoxy-β-D-glucopyranose (200):

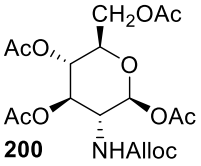

200

Hydrochloride **227** (9.3 g, 24.4 mmol) was dissolved in water (95 mL) and $NaHCO_3$ (7.8 g, 93.7 mmol) was added in 5 portions to afford a yellow foam, which was subsequently dissolved in $CHCl_3$ (95 mL). Allyl chloroformate (3.9 mL, 36.6 mmol) was added and the reaction mixture was stirred at rt for 5 h. The layers were separated and the aqueous layer was extracted with $CHCl_3$ (5 x 20 mL). The combined organic layer was washed with brine and water, dried over anhydrous $MgSO_4$, and concentrated under reduced pressure. The crude solid was purified by recrystallization from Et_2O to afford **200** as white needles (4.7 g). The filtrate was concentrated under reduced pressure and the residue was purified by gradient silica gel column chromatography (DCM/EtOAc 5/1 to DCM/EtOAc 1/1) to afford **200** as a white solid (1.1 g). Total yield of product **200** was (5.8 g, 55% yield): $[\alpha]_D^{25} = +15.2$ (*c* 0.33, MeOH); ^{1}H NMR (300 MHz, $CDCl_3$) δ 6.00 – 5.78 (m, 1H), 5.70 (d, *J* = 9.0 Hz, 1H), 5.36 – 5.05 (m, 4H), 4.92 – 4.74 (m, 1H), 4.56 (d, *J* = 4.7 Hz, 2H), 4.28 (dd, *J* = 12.5, 4.6 Hz, 1H), 4.11 (dd, *J* = 12.5, 1.9 Hz, 1H), 3.93 (dd, *J* = 18.9, 9.7 Hz, 1H), 3.81 (ddd, *J* = 9.6, 4.5, 2.2 Hz, 1H), 2.12 (s, 3H), 2.09 (s, 3H), 2.04 (s, 3H), 2.03 (s, 3H). ^{1}H NMR corresponds to the literature.[145]

2-Allyloxycarbonylamino-2-deoxy-3,4,6-tri-*O*-acetyl-β-D-glucopyranosyl azide (201a):

First route

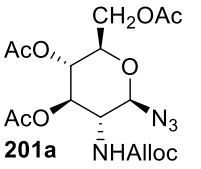

201a

$NaHCO_3$ (694 mg, 8.3 mmol) was added to a solution of azide **231** (711 mg, 2.2 mmol) in a mixture of $CHCl_3$ (8 mL) and water (8 mL). After stirring at rt for 5 min, allyl chloroformate (0.34 mL, 3.2 mmol) was added and the reaction mixture was stirred at rt for 2 h. The layers were separated and the aqueous layer was extracted with DCM (5 x 15 mL). The combined organic layer was washed with brine and water, dried over anhydrous $MgSO_4$, and concentrated under reduced pressure to afford **201a** (737 mg, 83% yield) as a yellowish solid.

Second route

Under argon, $TMSN_3$ (0.48 mL, 3.6 mmol) and $SnCl_4$ (0.05 mL, 0.5 mmol) were added to a solution of compound **200** (1 g, 2.4 mmol) in dry DCM (17 mL). The reaction mixture was stirred at rt overnight. The reaction mixture was poured into a solution of $NaHCO_3$ (50 mL, sat aq) and the resulting mixture was stirred until the evolution of CO_2 was ceased. The layers were separated and the aqueous layer was extracted with DCM (5 x 20 mL). The combined organic layer was washed with brine and water, dried over anhydrous $MgSO_4$, and concentrated under reduced pressure to afford **201a** as a white solid (939 mg, 94% yield): $[\alpha]_D^{25} = -15.2$ (*c* 0.33, MeOH); ^{1}H NMR (300 MHz, $CDCl_3$) δ 5.89 (ddd, *J* = 16.2, 10.6, 5.5 Hz, 1H), 5.35 – 5.17 (m, 3H), 5.08 (t, *J* = 9.6 Hz, 1H), 5.00 – 4.88 (m, 1H), 4.84 –

4.72 (m, 1H), 4.59 (d, J = 4.5 Hz, 2H), 4.28 (dd, J = 12.4, 4.9 Hz, 1H), 4.16 (dd, J = 12.5, 2.3 Hz, 1H), 3.78 (ddd, J = 10.0, 4.8, 2.3 Hz, 1H), 3.59 (d, J = 9.1 Hz, 1H), 2.10 (s, 3H), 2.04 (s, 3H), 2.03 (s, 3H). ^{1}H NMR corresponds to the literature.[145] Azide **201a** decomposed during storage (even in a freezer).

2-Allyloxycarbonylamino-2-deoxy-3,4,6-tri-*O*-acetyl-β-D-glucopyranosyl isothiocyanate (203a):

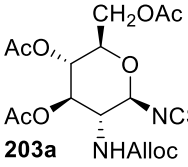

203a

Under argon, $SnCl_4$ (0.11 mL, 0.9 mmol) was added to a solution of compound **200** (500 mg, 1.2 mmol) in dry DCM (7 mL). After stirring at rt for 5 min, TMSSCN (0.18 mL, 1.3 mmol) was added and the reaction mixture was stirred at rt for 20 h. Then it was poured into a solution of $NaHCO_3$ (25 mL, sat aq). The layers were separated and the aqueous layer was extracted with DCM (5 x 10 mL). The combined organic layer was washed with water, dried over anhydrous $MgSO_4$, and silica gel (1 g) was added. The solvent was eliminated under reduced pressure and the residue was purified by silica gel column chromatography (DCM/EtOAc 5/1) to afford a white solid, which was not desired product **203a**, but **(1,2-dideoxy-3,4,6-tri-*O*-acetyl-α-D-glucopyranoso)[2,1-*d*]-1,3-oxazolidin-2-one (233)** was obtained instead**:** (360 mg, 95% yield); ^{1}H NMR (300 MHz, $CDCl_3$) δ 5.98 (d, J = 7.2 Hz, 1H), 5.61 (br s, 1 H), 5.10 (dd, J = 6.2, 9.5 Hz, 1H), 4.83 (dd, J = 4.2, 6 Hz, 1H), 4.34 (dd, J = 5.3, 12.5 Hz, 1H), 4.20 (dd, J = 2.6, 12.5 Hz, 1H), 4.10 – 4.06 (m, 1H), 3.90 – 3.87 (m, 1H), 2.13 (s, 3H), 2.10 (s, 3H), 2.09 (s, 3H); ^{13}C NMR (75 MHz, $CDCl_3$) δ 170.5, 170.1, 169.5, 156.7, 96.2, 72.3, 68.2, 66.5, 62.4, 53.7, 20.7, 20.6. ^{1}H NMR and ^{13}C NMR correspond to the literature.[270]

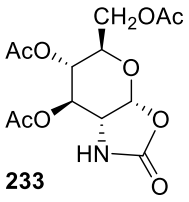

233

2-Allyloxycarbonylamino-2-deoxy-3,4,6-tri-*O*-acetyl-β-D-glucopyranosylamine (202a):

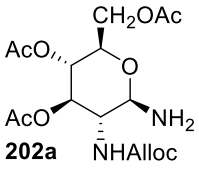

202a

Under argon, azide **201a** (250 mg, 0.60 mmol) and PPh_3 (174 mg, 0.66 mmol) were dissolved in dry THF (5 mL). The reaction mixture was stirred at rt for 17 h. Water (0.5 mL) was added and stirring was continued for 30 min. A mixture of HCl (concd, 6 mL) and water (6 mL) was added and the resulting solution was extracted with DCM (3 x 15 mL). A solution of NH_3 (2 M aq) was added to the aqueous layer until pH of 12 – 13 and the resulting mixture was extracted with DCM (5 x 10 mL). The combined organic layer was dried over Na_2SO_4 and concentrated under reduced pressure to afford **202a** as a white foam (87 mg, 37% yield): ^{1}H NMR (300 MHz, $CDCl_3$) δ 5.88 – 5.74 (m, 1H), 5.28 – 5.22 (m, 1H), 5.22 – 5.15 (m, 1H), 5.11 (dd, J = 10.4, 1.3 Hz, 1H), 5.07 – 4.97 (m, 2H), 4.46 (d, J = 5.3 Hz, 2H), 4.22 (dd, J = 12.3, 4.9, 1H), 4.14 – 4.04 (m, 1H), 3.99 (dd, J = 11.8, 2.5 Hz, 1H), 3.92 – 3.77 (m, 1H), 3.51 – 3.38 (m, 1H), 2.00 (s, 3H), 1.96 (s, 3H), 1.94 (s, 3H); MS (ESI) m/z: $[M+2H+Na]^{3+}$ calcd for $C_{16}H_{26}N_2NaO_9$ = 413.15, found = 413.00.

1,3,4,6-Tetra-*O*-acetyl-2-amino-2-deoxy-β-D-glucopyranose (204):

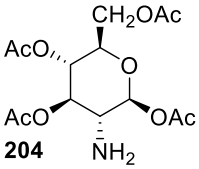

204

NaOAc (2.7 g, 33.0 mmol) was added to a suspension of D-glucosamine hydrochloride (**227**, 4.0 g, 10.4 mmol) in a mixture of DCM (27 mL) and water (23 mL). The reaction mixture was stirred at rt for 45 min. The layers were separated and the aqueous layer was extracted with DCM (3 x 30 mL). The combined organic layer was dried over anhydrous $MgSO_4$ and concentrated under reduced pressure. The residue was washed with Et_2O to afford **204** as a white solid (3.19 g, 88% yield): ^{1}H NMR (300 MHz, $CDCl_3$) δ 5.50 (d, J = 8.6 Hz, 1H), 5.08 – 5.01 (m, 2H), 4.31 (dd, J = 12.5, 4.6 Hz, 1H), 4.08 (dd, J = 12.5, 2.2 Hz, 1H), 3.82 (ddd, J = 9.8, 4.5, 2.3 Hz, 1H), 3.15 – 2.95 (m, 1H), 2.17 (s, 3H), 2.09 (s, 3H), 2.07 (s, 3H), 2.03 (s, 3H). ^{1}H NMR corresponds to the literature.[271]

2-(3-Methoxybenzylidene)amino-2-deoxy-3,4,6-tri-*O*-acetyl-β-D-glucopyranosyl azide (235):

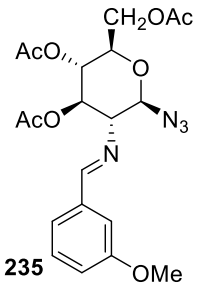

Under argon, $TMSN_3$ (0.06 mL, 0.44 mmol) and TBAF (1 M in THF, 0.44 mL) were added to a solution of compound **230** (200 mg, 0.44 mmol) in dry acetonitrile (1.5 mL). The reaction mixture was stirred at rt for 3 h. Then the solvent was eliminated under reduced pressure. Under argon, anhydrous $MgSO_4$ (2 spoons), dry toluene (2 mL), and 3-anisaldehyde (0.05 mL, 0.44 mmol) were added to the residue. The reaction mixture was stirred at rt overnight. Then it was filtrated through a celite pad using EtOAc as an eluent and concentrated under reduced pressure. The residue was purified by gradient silica gel column chromatography (hexane/EtOAc to EtOAc) to afford **235** as a white solid (109 mg, 55% yield): $[\alpha]_D^{25}$ = +13.7 (*c* 0.26, MeOH); ^{1}H NMR (300 MHz, $CDCl_3$) δ 8.19 (s, 1H), 7.36 – 7.21 (m, 3H), 7.01 (ddd, *J* = 8.2, 2.6, 1.2 Hz, 1H), 5.46 – 5.34 (m, 1H), 5.10 (dd, *J* = 19.2, 9.3 Hz, 2H), 4.36 (dd, *J* = 12.4, 4.8 Hz, 1H), 4.18 (dd, *J* = 12.4, 2.2 Hz, 1H), 3.93 (ddd, *J* = 10.1, 4.8, 2.2 Hz, 1H), 3.84 (s, 3H), 3.34 – 3.23 (m, 1H), 2.11 (s, 3H), 2.03 (s, 3H), 1.88 (s, 3H); HRMS (ESI-TOF) m/z: $[M+H]^+$ calcd for $C_{20}H_{25}N_4O_8$ = 449.1667, found = 449.1668.

2-(3-Methoxybenzyl)amino-2-deoxy-3,4,6-tri-*O*-acetyl-β-D-glucopyranosyl azide (236):

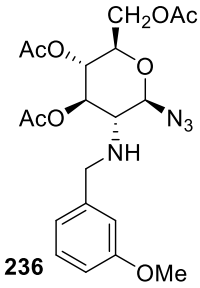

Under argon, compound **235** (88 mg, 0.2 mmol) was suspended in dry MeOH (8.5 mL) and the suspension was slowly heated to 50 °C (oil bath temperature) to dissolve it. The solution was cooled to rt and acetic acid (0.85 mL, 14.9 mmol), followed by $NaBH_3CN$ (92 mg, 1.5 mmol), were added. The resulting reaction mixture was stirred at rt for 15 min. Then water (50 mL) was added and the resulting solution was extracted with DCM (5 x 10 mL). The combined organic layer was washed with brine, dried over Na_2SO_4, and concentrated under reduced pressure. The residue was purified by silica gel column chromatography (EtOAc) to afford **236** as white solid (53 mg, 59% yield): ^{1}H NMR (300 MHz, $CDCl_3$) δ 7.28 – 7.19 (m, 1H), 6.98 – 6.70 (m, 3H), 5.10 – 4.91 (m, 2H), 4.60 (d, *J* = 6.8 Hz, 1H), 4.28 (dd, *J* = 12.4, 4.9 Hz, 1H), 4.12 (dd, *J* = 12.4, 2.3 Hz, 1H), 3.98 – 3.87 (m, 1H), 3.86 – 3.68 (m, 5H), 2.73 (t, *J* = 9.5 Hz, 1H), 2.08 (s, 3H), 2.01 (s, 3H), 1.99 (s, 3H), 1.56 (s, 1H); HRMS (ESI-TOF) m/z: $[M+H]^+$ calcd for $C_{20}H_{27}N_4O_8$ = 451.1823; found = 451.1821.

2-Allyloxycarbonylamino-2-deoxy-β-D-glucopyranosyl azide (237):

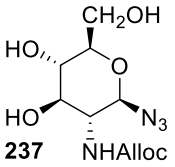

Under argon, the freshly prepared NaOMe (1 M in dry MeOH, 0.82 mL) was added to a solution of azide **201a** (918 mg, 2.2 mmol) in dry MeOH (17 mL). The reaction mixture was stirred at rt overnight and acidified by DOWEX® (H^+ form) until a pH of 3 – 4. Filtration through a sintered funnel and concentration under reduced pressure afforded **237** as a red solid (610 mg, 96% yield): ^{1}H NMR (300 MHz, CD_3OD) δ 5.96 (ddd, *J* = 22.2, 10.6, 5.4 Hz, 1H), 5.34 (d, *J* = 17.4 Hz, 1H), 5.20 (d, *J* = 10.5 Hz, 1H), 4.64 – 4.47 (m, 3H), 3.97 – 3.85 (m, 1H), 3.72 (dd, *J* = 12.1, 4.9 Hz, 1H), 3.51 – 3.28 (m, 4H).

12.2 Synthesis of type II organocatalyst

1,2,3,4-Tetra-*O*-acetyl-β-D-xylopyranosa (211):

Under argon, sodium acetate (4.3 g, 82.0 mmol) and D-xylose (**210**, 6.0 g, 40.0 mmol) were suspended in acetic anhydride (38 mL, 0.4 mol). The reaction mixture was stirred at 80 °C (oil bath temperature) for 4 h and then it was cooled to rt. The reaction mixture was poured

into a solution of Na_2CO_3 (40 mL, sat aq) cooled to 0 °C using an ice bath and extracted with DCM (3 x 30 mL). The combined organic layer was dried over anhydrous $MgSO_4$ and concentrated under reduced pressure. The residue was purified by gradient silica gel column chromatography (hexane/EtOAc 3/1 to hexane/EtOAc 1/3) to afford β-anomer **211** and α-anomer **238**. β-anomer **211** as a white solid (5.2 g, 40% yield): ^{1}H NMR (300 MHz, $CDCl_3$) δ 5.72 (d, *J* = 6.9 Hz, 1H), 5.21 (t, *J* = 8.3 Hz, 1H), 5.03 (dd, *J* = 8.4, 6.9 Hz, 1H), 5.02 – 4.93 (m, 1H), 4.15 (dd, *J* = 12.0, 5.0 Hz, 1H), 3.52 (dd, *J* = 12.0, 8.4 Hz, 1H), 2.11 (s, 3H), 2.06 (s, 3H), 2.05 (s, 6H). ^{1}H NMR corresponds to the literature.[272]

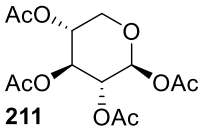

211

1,2,3,4-Tetra-*O*-acetyl-α-D-xylopyranosa (238) as a white solid (2.6 g, 20% yield): ^{1}H NMR (300 MHz, $CDCl_3$) δ 6.23 (d, *J* = 3.7 Hz, 1H), 5.44 (t, *J* = 9.8 Hz, 1H), 5.06 – 4.91 (m, 2H), 3.91 (dd, *J* = 11.2, 5.9 Hz, 1H), 3.69 (t, *J* = 10.9 Hz, 1H), 2.13 (s, 3H), 2.12 (s, 3H), 2.09 (s, 3H), 2.07 (s, 3H). ^{1}H NMR corresponds to the literature.[273]

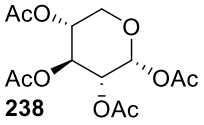

238

2,3,4-Tri-*O*-acetyl-α-D-xylopyranosyl bromide (240):

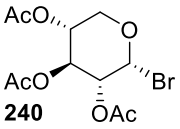

240

Acetic acid (0.3 mL, 5.2 mmol) was added to a solution of compound **211** (1.5 g, 4.7 mmol) in DCM (10 mL). The reaction mixture was cooled to 0 °C using an ice bath and a solution of HBr (33% in AcOH, 3 mL) was added slowly. The reaction mixture was stirred at 0 °C for 1 h and then at rt for 1 h. The reaction mixture was diluted by DCM (20 mL), washed with water, $NaHCO_3$ (sat aq), and brine. The organic layer was separated, dried over anhydrous $MgSO_4$, and concentrated under reduced pressure to afford **240** as a yellowish solid (1.3 g, 79% yield): ^{1}H NMR (300 MHz, $CDCl_3$) δ 6.58 (d, *J* = 4.0 Hz, 1H), 5.56 (t, *J* = 9.8 Hz, 1H), 5.04 (ddd, *J* = 10.9, 9.6, 6.0 Hz, 1H), 4.77 (dd, *J* = 10.0, 4.0 Hz, 1H), 4.05 (dd, *J* = 11.3, 6.0 Hz, 1H), 3.92 – 3.83 (m, 1H), 2.10 (s, 3H), 2.05 (s, 3H), 2.05 (s, 3H). ^{1}H NMR corresponds to the literature.[227]

2,3,4-Tri-*O*-acetyl-β-D-xylopyranosyl isothiocyanate (213a):

Under argon, $SnCl_4$ (0.36 mL, 3.0 mmol) was added to a solution of compound **211** (1.2 g, 3.7 mmol) in dry DCM (24 mL). After stirring at rt for 5 min, TMSSCN (0.58 mL, 4.1 mmol) was added. The reaction mixture was stirred at rt overnight. Then it was poured into a solution of $NaHCO_3$ (50 mL, sat aq) and the resulting mixture was stirred at rt for 2 h. The layers were separated and the aqueous layer was extracted with DCM (5 x 20 mL). The combined organic layer was washed with water, dried over anhydrous $MgSO_4$, and concentrated under reduced pressure. The residue was purified by silica gel column chromatography (hexane/EtOAc 4/1) to afford β-anomer **213a** and α-anomer **239**. β-anomer **213a** as a white solid (584 mg, 50% yield): ^{1}H NMR (600 MHz, $CDCl_3$) δ 5.13 (t, *J* = 7.1 Hz, 1H), 5.06 (d, *J* = 6.2 Hz, 1H), 4.95 (t, *J* = 6.5 Hz, 1H), 4.91 (dt, *J* = 7.3, 4.4 Hz, 1H), 4.20 (dd, *J* = 12.3, 4.38 Hz, 1H), 3.53 (dd, *J* = 12.4, 7.4 Hz,1H) 2.11 (s, 3H), 2.09 (s, 3H), 2.06 (s, 3H). ^{13}C NMR (151 MHz, $CDCl_3$) δ 169.6, 169.6, 169.1, 142.8, 82.9, 70.3, 69.5, 67.4, 63.1, 20.7, 20.6, 20.6.

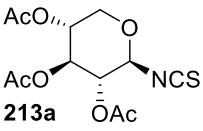

213a

2,3,4-Tri-*O*-acetyl-α-D-xylopyranosyl isothiocyanate (239) as a white solid (201 mg, 13% yield): ^{1}H NMR (600 MHz, $CDCl_3$) δ 5.76 (d, *J* = 4.2 Hz, 1H), 5.41 (t, *J* = 9.7 Hz, 1H), 5.00 – 4.94 (m, 1H), 4.92 (dd, *J* = 9.8, 4.2 Hz, 1H), 3.96 (dd, *J* = 11.6, 5.8 Hz, 1H), 3.72 (t, *J* = 11.4 Hz, 1H), 2.12 (s, 3H), 2.05 (s, 3H), 2.04 (s, 3H). ^{13}C NMR (151 MHz, $CDCl_3$) δ 169.8, 169.8, 169.7, 144.1, 82.3, 70.6, 69.1, 68.3, 61.2, 20.6, 20.6, 20.4.

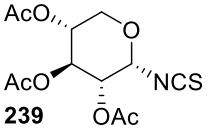

239

2,3,4-Tri-*O*-acetyl-β-D-xylopyranosyl azide (212a):

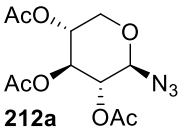

212a

Under argon, $TMSN_3$ (0.3 mL, 2.4 mmol) and $SnCl_4$ (0.04 mL, 0.3 mmol) were added to a solution of compound **211** (500 mg, 1.6 mmol) in dry DCM (8 mL). The reaction mixture was stirred at rt overnight and then it was poured into a solution of $NaHCO_3$ (16 mL, sat aq). The resulting mixture was stirred at rt for 1 h. The layers were separated and the aqueous layer was extracted with DCM (3 x 15 mL). The combined organic layer was washed with brine and water, dried over anhydrous $MgSO_4$, and concentrated under reduced pressure to afford **212a** as a colourless oil (424 mg, 90% yield): ^{1}H NMR (300 MHz, $CDCl_3$) δ 5.19 (t, *J* = 8.9 Hz, 1H), 4.98 (td, *J* = 9.2, 5.3 Hz, 1H), 4.88 (dd, *J* = 8.8, 8.1 Hz, 1H), 4.63 (d, *J* = 8.0 Hz, 1H), 4.21 (dd, *J* = 11.7, 5.3 Hz, 1H), 3.44 (dd, *J* = 11.7, 9.6 Hz, 1H), 2.08 (s, 3H), 2.05 (s, 3H), 2.04 (s, 3H). ^{1}H NMR corresponds to the literature.[274]

β-D-xylopyranosyl azide (243):

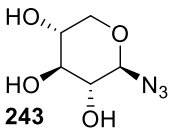

243

Under argon, freshly prepared NaOMe (1 M in dry MeOH, 0.49 mL) was added to a solution of azide **212a** (394 mg, 1.3 mmol) in dry MeOH (10 mL). The reaction mixture was stirred at rt overnight and then it was acidified by DOWEX® (H^+ form) until a pH of 6. Filtration through a sintered funnel and concentration under reduced pressure afforded **243** as a brownish oil (223 mg, 97% yield). ^{1}H NMR (300 MHz, CD_3OD) confirmed complete hydrolysis of acetyl groups.

2,3,4-Tri-*O*-methyl-β-D-xylopyranosyl azide (212b):

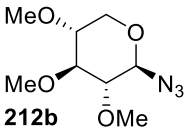

212b

Under argon, a solution of azide **243** (221 mg, 1.3 mmol) in dry DMF (50 mL) was cooled to 0 °C using an ice bath and NaH (204 mg, 60% dispersion in mineral oil, 5.1 mmol) was added. The reaction mixture was stirred at 0 °C for 10 min and at rt for 1 h. Then the reaction mixture was cooled to 0 °C using an ice bath and MeI (0.33 mL, 5.3 mmol) was added. The reaction mixture was stirred at 0 °C for 10 min and at rt overnight. Then water (50 mL) was added and the resulting solution was extracted with DCM (5 x 10 mL). The combined organic layer was dried over anhydrous $MgSO_4$ and concentrated under reduced pressure. The residue was purified by silica gel column chromatography (hexane/EtOAc 1/1) to afford **212b** as a colourless viscous oil (243 mg, 81% yield): ^{1}H NMR (300 MHz, $CDCl_3$) δ 4.42 (d, *J* = 8.3 Hz, 1H), 4.04 (dd, *J* = 9.8, 3.5 Hz, 1H), 3.60 (s, 3H), 3.57 (s, 3H), 3.46 (s, 3H), 3.30 – 3.06 (m, 3H), 2.94 – 2.84 (m, 1H).

2,3,4-Tri-*O*-methyl-β-D-xylopyranosylamine (244):

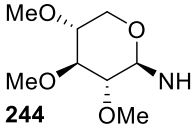

244

In a flame-dried flask, Et_3N (0.17 mL, 1.2 mmol) was added to a suspension of azide **212b** (243 mg, 1.1 mmol) and Pd/C (24 mg, 10%, 10% w/w) in dry THF (5 mL). The reaction flask was evacuated and backfilled with hydrogen. This process was repeated three times. The reaction mixture was stirred under hydrogen atmosphere at rt overnight. The resulting suspension was filtered through a two-layer pad (upper Na_2SO_4, lower celite) using DCM (30 mL) as an eluent and concentrated under reduced pressure to afford **244** as a colourless oil (102 mg, 48% yield): ^{1}H NMR (300 MHz, $CDCl_3$) δ 3.92 (d, *J* = 8.4 Hz, 1H), 3.63 (s, 3H), 3.62 (s, 3H), 3.59 – 3.54 (m, 1H), 3.50 (d, *J* = 1.9 Hz, 1H), 3.47 (s, 3H), 3.30 – 3.18 (m, 1H), 3.18 – 3.10 (m, 1H), 2.72 (t, *J* = 8.5 Hz, 1H), 1.87 (br s, 2H).

***N*-[(1*R*,2*R*)-2-Aminocyclohexyl]-*N*'-(2,3,4-tri-*O*-acetyl-β-D-xylopyranosyl)thiourea (215a):**

Under argon, (1*R*,2*R*)-cyclohexane-1,2-diamine (**214**, 43 mg, 0.38 mmol) was dissolved in dry DCM (10 mL) and a solution of isothiocyanate **213a** (100 mg, 0.32 mmol) in dry DCM (5 mL) was added slowly during 1h. The reaction mixture was stirred at rt for 1.5 h and

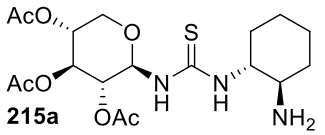

215a

concentrated under reduced pressure. The crude product was purified by silica gel column chromatography (hexane/EtOAC 1/1 and subsequently MeOH) to afford **215a** as a yellow solid (98 mg, 72% yield): $[\alpha]_D^{25} = +16.7$ (*c* 0.57, MeOH); IR (KBr) 600, 755, 905, 937, 982, 1039, 1066, 1114, 1228, 1332, 1368, 1562, 1754, 2857, 2932, 3046, 3279, 3318 cm^{-1}; ^1H NMR (400 MHz, $CDCl_3$) 5.74 (d, *J* = 9.1 Hz, 1H), 5.31 (t, *J* = 9.4 Hz, 1H), 5.07 – 4.79 (m, 2H), 4.18 – 3.92 (m, 2H), 3.44 (t, *J* = 10.5 Hz, 2H), 2.59 (br s, 1H), 2.12 – 2.08 (m, 1H), 2.03 (s, 3H), 2.02 (s, 3H), 2.01 (s, 3H), 1.94 (br s, 1H), 1.78 – 1.64 (m, 2H), 1.45 – 1.04 (m, 5H); ^{13}CNMR (101 MHz, $CDCl_3$) δ 179.8, 170.5, 170.0, 169.8, 77.2, 72.7, 69.1, 64.2, 55.0, 34.8, 31.9, 24.6, 24.5, 20.8, 20.7, 20.7; HRMS (ESI-TOF) m/z: $[M+H]^+$ calcd for $C_{18}H_{30}N_3O_7S$ = 432.17990, found = 432.17978.

12.3 Synthesis of the saccharide unit of type III catalysts

1,2,3,4,6-Penta-*O*-acetyl-β-D-glucopyranosa (216):

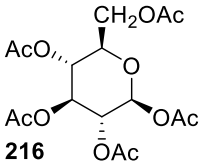

216

A round-bottomed flask equipped with a reflux condenser was charged with D-glucose (**249**, 15.0 g, 83.2 mmol) and toluene (120 mL), acetic anhydride (50.4 mL, 532.8 mmol), followed by sodium acetate (2.5 g, 30.8 mmol), were added. Using an oil bath, the reaction mixture was refluxed for 4 h and water (45 mL) was added. The resulting solution was neutralized by the addition of NaOH (120 mL, 3 wt% aq). The organic layer was separated, dried over anhydrous $MgSO_4$, and concentrated under reduced pressure. The residue was recrystallized from EtOH to afford **216** as a white solid (24.8 g, 76% yield): $[\alpha]_D^{25} = +8.7$ (*c* 0.46, $CHCl_3$); ^1H NMR (300 MHz, $CDCl_3$) δ 5.71 (d, *J* = 8.2 Hz, 1H), 5.29 – 5.19 (m, 1H), 5.17 – 5.05 (m, 2H), 4.29 (dd, *J* = 12.5, 4.5 Hz, 1H), 4.11 (dd, *J* = 12.5, 2.2 Hz, 1H), 3.83 (ddd, *J* = 9.9, 4.5, 2.2 Hz, 1H), 2.11 (s, 3H), 2.08 (s, 3H), 2.03 (s, 6H), 2.01 (s, 3H); MS (ESI) m/z: $[M+Na]^+$calcd for $C_{16}H_{22}NaO_{11}$ = 413.1, found = 413.0. ^1H NMR corresponds to the literature.[275]

2,3,4,6-Tetra-*O*-acetyl-β-D-glucopyranosyl azide (217a):

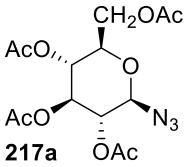

217a

Under argon, $TMSN_3$ (6.0 mL, 45.6 mmol) and $SnCl_4$ (0.7 mL, 6.1 mmol) were added to a solution of compound **216** (11.9 g, 30.4 mmol) in dry DCM (150 mL). The reaction mixture was stirred at rt overnight. Then it was poured into a solution of $NaHCO_3$ (150 mL, sat aq). The layers were separated and the aqueous layer was extracted with DCM (3 x 30 mL). The combined organic layer was dried over anhydrous $MgSO_4$ and concentrated under reduced pressure to afford **217a** as a white solid (10.9 g, 96% yield): $[\alpha]_D^{25} = -17.1$ (*c* 0.35, $CHCl_3$); ^1H NMR (300 MHz, $CDCl_3$) δ 5.21 (t, *J* = 9.4 Hz, 1H), 5.10 (t, *J* = 9.7 Hz, 1H), 4.95 (t, *J* = 9.2 Hz, 1H), 4.64 (d, *J* = 8.8 Hz, 1H), 4.27 (dd, *J* = 12.5, 4.8 Hz, 1H), 4.16 (dd, *J* = 12.5, 2.4 Hz, 1H), 3.79 (ddd, *J* = 9.9, 4.7, 2.4 Hz, 1H), 2.10 (s, 3H), 2.07 (s, 3H), 2.03 (s, 3H), 2.00 (s, 3H); MS (ESI) m/z: $[M+Na]^+$ calcd for $C_{14}H_{19}N_3NaO_9$= 396.1, found = 396.0. ^1H NMR corresponds to the literature.[276]

β-D-glucopyranosyl azide (251):

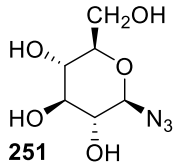

251

Under argon, freshly prepared NaOMe (1 M in dry MeOH, 11 mL) was added to a solution of azide **217a** (10.9 g, 29.2 mmol) in dry MeOH (210 mL). The reaction mixture was stirred at rt overnight. Then it was acidified by DOWEX® (H^+ form) until a pH of 6, filtrated through a celite pad using MeOH as an eluent, and concentrated under reduced pressure. The residue was purified by silica gel column chromatography (DCM/MeOH

5/1) to afford **251** as a yellow viscous oil (5.0 g, 83% yield): $[\alpha]_D^{25} = -20.8$ (*c* 0.36, MeOH); ^{1}H NMR (300 MHz, D_2O) δ 4.75 (d, *J* = 8.8 Hz, 1H), 3.93 (dd, *J* = 12.4, 2.0 Hz, 1H), 3.75 (dd, *J* = 12.4, 5.5 Hz, 1H), 3.59 – 3.23 (m, 4H); MS (ESI) m/z: $[M+Na]^+$ calcd for $C_6H_{11}N_3NaO_5$ = 228.1, found = 228.1.

12.3.1 Typical procedure to prepare azides 217b, 217c

Under argon, a solution of azide **251** (2.1 g, 10.2 mmol) in dry DMF (50 mL) was cooled to 0 °C using an ice bath and NaH (1.6 g, 60% dispersion in mineral oil, 40.0 mmol) was added. The reaction mixture was stirred at 0 °C for 2 h. Then MeI (3.6 mL, 57.3 mmol) was added and the reaction mixture was stirred at 0 °C for 20 min and at rt overnight. Water (50 mL) was added and the resulting solution was extracted with DCM (5 x 15 mL). The combined organic layer was dried over anhydrous $MgSO_4$ and concentrated under reduced pressure. The residue was purified by silica gel column chromatography (hexane/EtOAc 4/1) to afford **217b** (2.2 g, 83% yield).

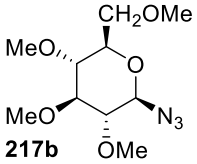

217b

2,3,4,6-Tetra-*O*-methyl-β-D-glucopyranosyl azide (217b): Colourless oil (2.2 g, 83% yield); $[\alpha]_D^{25} = -20.9$ ° (*c* 0.46, $CHCl_3$); ^{1}H NMR (300 MHz, C_6D_6) δ 4.12 (d, *J* = 8.5 Hz, 1H), 3.48 (s, 3H), 3.42 (dd, *J* = 5.1, 2.9 Hz, 2H), 3.39 (s, 3H), 3.38 (s, 3H), 3.22 (dd, *J* = 9.8, 8.9 Hz, 1H), 3.14 (s, 3H), 3.10 – 3.01 (m, 1H), 3.06 (t, *J* = 8.7 Hz, 1H), 2.95 – 2.86 (m, 1H); MS (ESI) m/z: $[M+Na]^+$calcd for $C_{10}H_{19}N_3NaO_5$ = 284.1, found = 284.0. ^{1}H NMR corresponds to the literature.[277]

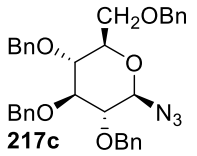

217c

2,3,4,6-Tetra-*O*-benzyl-β-D-glucopyranosyl azide (217c): Colourless oil (1.9 g, 70% yield); ^{1}H NMR (300 MHz, $CDCl_3$) δ = 7.38 – 7.24 (m, 18H), 7.20 – 7.12 (m, 2H), 4.90 (d, *J* = 8.0 Hz, 1H), 4.88 (d, *J* = 7.7 Hz, 1H), 4.83 (d, *J* = 7.7 Hz, 1H), 4.80 (d, *J* = 7.5 Hz, 1H), 4.76 (d, *J* = 10.7 Hz, 1H), 4.63 (d, *J* = 8.8 Hz, 1H), 4.63 (s, *J* = 11.3 Hz, 1H), 4.55 (d, *J* = 12.5 Hz, 1H), 4.55 (d, *J* = 10.1 Hz, 1H), 3.78 – 3.61 (m, 4H), 3.56 – 3.50 (m, 1H), 3.42 – 3.34 (m, 1H). ^{1}H NMR corresponds to the literature.[278]

12.3.2 Typical procedure to prepare amines 252

In a flame-dried flask, Et_3N (0.3 mL, 2.1 mmol) was added to a suspension of azide **217b** (520 mg, 2.0 mmol) and Pd/C (52 mg, 10%, 10% w/w) in dry THF (8 mL). The reaction flask was evacuated and backfilled with hydrogen. This process was repeated three times. The reaction mixture was stirred under hydrogen atmosphere at rt for a reported time. The resulting suspension was filtered through a two-layer pad (upper Na_2SO_4, lower celite) using DCM (30 mL) as an eluent and evaporated to afford product **252b** (434 mg, 93% yield).

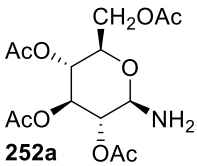

252a

2,3,4,6-Tetra-*O*-acetyl-β-D-glucopyranosylamine 252a: The reaction mixture was stirred overnight. A white solid (4.1 g, 97% yield): $[\alpha]_D^{25} = +13.8°$ (*c* 0.29, $CHCl_3$); ^{1}H NMR (300 MHz, $CDCl_3$) δ 5.24 (t, *J* = 9.5 Hz, 1H), 5.03 (t, *J* = 9.7 Hz, 1H), 4.82 (t, *J* = 9.4 Hz, 1H), 4.22 (dd, *J* = 12.3, 4.8 Hz, 1H), 4.19 (d, *J* = 9 Hz, 1H), 4.10 (dd, *J* = 12.3, 2.2 Hz, 1H), 3.68 (ddd, *J* = 10.1, 4.8, 2.4 Hz, 1H), 2.09 (s, 3H), 2.06 (s, 3H), 2.02 (s, 3H), 2.00 (s, 3H); MS (ESI) m/z: $[M+Na]^+$ calcd for $C_{14}H_{21}NNaO_9$= 370.1, found = 370.1. ^{1}H NMR corresponds to the literature.[279]

2,3,4,6-Tetra-*O*-methyl-β-D-glucopyranosylamine (252b): The reaction time was 15 h. A white solid (434 mg, 93% yield): $[\alpha]_D^{25} = -20.9$ (*c* 0.46, $CHCl_3$); ^{1}H NMR (600 MHz, $CDCl_3$) δ 3.95 (d, *J* = 8.7 Hz, 1H), 3.64 (s, 3H), 3.62 (s, 3H), 3.61 – 3.58 (m, 1H), 3.53 (s,

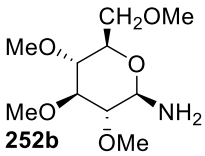

252b

3H), 3.53 – 3.50 (m, 1H), 3.40 (s, 3H), 3.29 (ddd, *J* = 9.8, 4.9, 1.9 Hz, 1H), 3.19 (t, *J* = 8.9 Hz, 1H), 3.12 (t, *J* = 9.4 Hz, 1H), 2.74 (t, *J* = 8.8 Hz, 1H), 1.85 (br s, 2H); ^{13}C NMR (151 MHz, $CDCl_3$) δ 87.5, 85.9, 85.4, 79.8, 75.3, 71.6, 60.8, 60.7, 60.3, 59.3; HRMS (ESI-TOF) m/z: $[M+Na]^+$ calcd for $C_{10}H_{21}NNaO_5$ = 258.1312, found = 258.1312.

2,3,4,6-Tetra-*O*-benzyl-β-D-glucopyranosylamine (252c): The reaction time was 1.5 h. A white solid (344 mg, 36% yield): $[\alpha]_D^{25}$ = +19.8 (*c* 0.43, $CHCl_3$); ^{1}H NMR (600 MHz, $CDCl_3$) δ 7.40 – 7.37 (m, 2H), 7.35 – 7.27 (m, 16H), 7.13 (dd, *J* = 7.0, 2.5 Hz, 2H), 5.00 (d, *J* = 10.9 Hz, 1H), 4.95 (d, *J* = 10.9 Hz, 1H), 4.86 – 4.81 (m, 2H), 4.79 (d, *J* = 10.9 Hz, 1H), 4.58 (AB spin system, J_{AB} = 12.3 Hz, Δν = 36.7 Hz, 2H), 4.50 (dd, *J* = 10.8, 4.3 Hz, 1H), 4.12 (d, *J* = 8.6 Hz, 1H), 3.71 (dd, *J* = 10.4, 1.8 Hz, 1H), 3.69 (s, 1H), 3.68 – 3.63 (m, 1H), 3.59 (t, *J* = 9.4 Hz, 1H), 3.49 (ddd, *J* = 9.8, 4.7, 2.0 Hz, 1H), 3.22 (t, *J* = 8.8 Hz, 1H), 1.95 (br s, 2H); ^{13}C NMR (151 MHz, $CDCl_3$) δ 138.6, 138.4, 138.1, 137.9, 128.4, 128.4, 128.3, 128.2, 127.9, 127.9, 127.8, 127.7, 127.7, 127.6, 86.2, 85.8, 83.5, 78.2, 75.7, 75.6, 75.0, 74.9, 73.5, 69.0; MS (ESI) m/z: $[M+Na]^+$ calcd for $C_{34}H_{37}NNaO_5$ = 562.3, found 562.2.

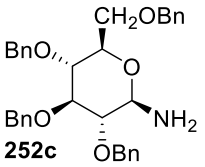

252c

12.3.3 Typical procedure to prepare isothiocyanates 218

Under argon, amine **252** (10.5 mmol) and thiocarbonyldiimidazole (3.38 g, 19.0 mmol) were dissolved in dry DCM (75 mL). The reaction mixture was stirred at rt for 14 h. The resulting mixture was diluted with DCM (75 mL) and HCl (2.5 M aq, 75 mL) was added. The layers were separated and the aqueous layer was extracted with DCM (5 x 15 mL). The combined organic layer was washed with $NaHCO_3$ (sat aq) and water, dried over anhydrous $MgSO_4$, and concentrated under reduced pressure. The residue was purified according to the protocol reported below.

2,3,4,6-Tetra-*O*-methyl-β-D-glucopyranosylisothiocyanate (218b): The residue was purified by silica gel column chromatography (hexane/EtOAc 3/1) to afford **218b** as a pale yellow solid (2.15 g, 74% yield): $[\alpha]_D^{25}$ = +39.7 (*c* 0.29, $CHCl_3$); IR (KBr) 492, 510, 570, 797, 890, 925, 937, 958, 988, 1027, 1078, 1111, 1138, 1171, 1183, 1198, 1210, 1272, 1302, 1350, 1383, 1395, 1452, 2059, 2065, 2095, 2154, 2253, 2735, 2839, 2887, 2920, 2977, 3001 cm^{-1}; ^{1}H NMR (600 MHz, $CDCl_3$) δ 4.65 (d, *J* = 8.5 Hz, 1H), 3.66 (s, 3H), 3.64 (s, 3H), 3.61 (dd, *J* = 10.8, 1.9 Hz, 1H), 3.55 (dd, *J* = 10.8, 4.4 Hz, 1H), 3.53 (s, 3H), 3.40 (s, 3H), 3.29 (ddd, *J* = 9.1, 4.4, 2.0 Hz, 1H), 3.20 – 3.14 (m, 2H), 3.08 (t, *J* = 8.6 Hz, 1H); ^{13}C NMR (151 MHz, $CDCl_3$) δ 141.5, 87.0, 85.1, 84.3, 78.8, 76.8, 70.7, 61.2, 61.0, 60.6, 59.4; HRMS (ESI-TOF) m/z: $[M+Na]^+$ calcd for $C_{11}H_{19}NNaO_5S$ = 300.0876, found = 300.0877.

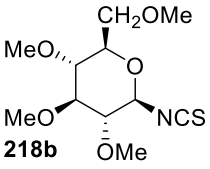

218b

2,3,4,6-Tetra-*O*-benzyl-β-D-glucopyranosylisothiocyanate (218c): The residue was purified by silica gel column chromatography (hexane/EtOAc 3/1) to afford mixture of both anomers (β/α ratio was 9/1)[280] as a colourless oil (291 mg, 88% yield): $[\alpha]_D^{25}$ = +15.9 (*c* 0.44, $CHCl_3$); IR (KBr) 701, 740, 749, 914, 1009, 1033, 1090, 1213, 1299, 1359, 1455, 1497, 1583, 1604, 1733, 1808, 1870, 2035, 2800, 2863, 2905, 3031, 3060, 3084 cm^{-1}; MS (ESI-TOF) m/z: $[M+Na]^+$calcd for $C_{35}H_{35}NNaO_5S$ = 604.2, found = 604.2; ^{1}H NMR (600 MHz, $CDCl_3$) of pure β-anomer **218c**: δ 7.40 – 7.28 (m, 18H), 7.18 – 7.14 (m, 2H), 4.95 – 4.81 (m, 6H), 4.64 (d, *J* = 12.2 Hz, 1H), 4.58 – 4.55 (m, 2H), 3.72 (dd, *J* = 7.4, 3.1 Hz, 2H), 3.70 – 3.64 (m, 2H), 3.56 (t, *J* = 8.7 Hz, 1H), 3.50 (ddd, *J* = 9.4, 4.0, 2.1 Hz, 1H); ^{13}C NMR (151 MHz, $CDCl_3$) δ 141.4, 138.1, 137.7, 137.7, 137.2, 128.5, 128.4, 128.4, 128.4, 128.4, 128.1, 128.0, 127.9, 127.9, 127.8, 127.7, 127.6, 85.3, 84.9, 82.4, 77.1, 75.7, 75.7, 75.1, 73.6, 68.1.

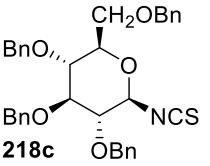

218c

2,3,4,6-Tetra-*O*-acetyl-β-D-glucopyranosyl isothiocyanate (218a): The crude product was dissolved in hot toluene (5 mL) and hot filtration was done. Codistillation with $CHCl_3$ afforded **218a** as a pale yellow solid (186 mg, 55% yield): $[\alpha]_D^{25}$ = +13.8 (*c* 0.29, $CHCl_3$); ^{1}H NMR (600 MHz, $CDCl_3$) δ 5.24 – 5.16 (m, 1H), 5.10 (dd, *J* = 14.1, 4.8 Hz, 2H), 5.04 – 4.98 (m, 1H), 4.24 (dd, *J* = 12.5, 4.8 Hz, 1H), 4.14 (dt, *J* = 12.4, 3.3 Hz, 1H), 3.75 (d, *J* = 9.9 Hz, 1H), 2.11 (s, 3H), 2.10 (s, 3H), 2.03 (s, 3H), 2.02 (s, 3H); ^{13}C NMR (151 MHz, $CDCl_3$) δ 170.6, 170.1, 169.2, 169.0, 144.3, 83.5, 74.0, 72.5, 71.9, 67.6, 61.5, 20.7, 20.5; MS (ESI) m/z: $[M+Na]^+$ calcd for $C_{15}H_{19}NNaO_9S$ = 412.1, found = 412.1. ^{1}H and ^{13}C NMR correspond to the literature.[281]

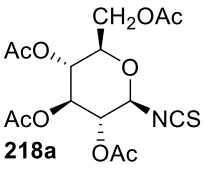

218a

*Alternative route to compound **218a**.*

Under argon, $SnCl_4$ (1.24 mL, 10.6 mmol) was added to a solution of compound **216** (5.0 g, 12.8 mmol) in dry DCM (80 mL). After stirring at rt for 5 min, TMSSCN (2.0 mL, 14.5 mmol) was added and the reaction mixture was stirred at rt overnight. Then it was poured into a solution of $NaHCO_3$ (150 mL, sat aq). The layers were separated and the aqueous layer was extracted with DCM (3 x 20 mL). The combined organic layer was dried over anhydrous $MgSO_4$ and concentrated under reduced pressure. The residue was purified by silica gel column chromatography (DCM/EtOAc 1/1) afforded **218a** as a white solid (1.01 g, 20% yield) and **1,2,3,4,6-penta-*O*-acetyl-α-D-glucopyranose (253)** as a white solid (735 mg, 15% yield): $[\alpha]_D^{25}$ = +84,4 (*c* 0.39; CH_3Cl), ^{1}H NMR (300 MHz, $CDCl_3$) δ 6.33 (d, *J* = 3.6 Hz, 1H), 5.47 (t, *J*= 9.9 Hz, 1H), 5.19 – 5.03 (m, 2H), 4.27 (dd, *J* = 12.6, 4.3 Hz, 1H), 4.14 – 4.06 (m, 2H), 2.09 (s, 3H), 2.04 (s, 3H), 2.03 (s, 3H), 2.02 (s, 3H). ^{1}H NMR corresponds to the literature.[282]

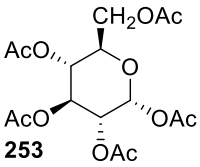

253

12.4 Synthesis of the amino acid unit of type III catalysts

12.4.1 Typical procedure to prepare α-amino alcohols 264

A flame-dried round-bottomed flask equipped with a reflux condenser was charged with (*S*)-valine (**262a**, 446 mg, 3.8 mmol), evacuated, and backfilled with argon. Dry THF (20 mL) was added. $NaBH_4$ (360 mg, 9.5 mmol) was added to the suspension under argon flow. After stirring at rt for 5 min, iodine (844 mg, 6.7 mmol) was added slowly under argon flow. The reaction mixture was stirred at rt for 15 min (until the iodine colour was discoloured). Then it was refluxed in an oil bath for 21 hours. NaOH (2 M aq, 13 mL) was added slowly and the reaction mixture was stirred at 90 °C (oil bath temperature) for 1 h. The reaction mixture was cooled to rt and extracted with Et_2O (5 x 15 mL). The combined organic layer was dried over anhydrous $MgSO_4$ and concentrated under reduced pressure to afford **264a**.

(*S*)-Valinol (264a) as a yellow oil (819 mg, 95% yield): ^{1}H NMR (300 MHz, $CDCl_3$) δ 3.65 (dd, *J* = 10.6, 3.9 Hz, 1H), 3.31 (dd, *J* = 10.6, 8.8 Hz, 1H), 2.64 – 2.51 (m, 1H), 2.43 (br s, 3H), 1.69 – 1.46 (m, 1H), 0.92 (d, *J* = 4.5 Hz, 3H), 0.90 (d, *J* = 4.5 Hz, 3H). ^{1}H NMR corresponds to the literature.[283]

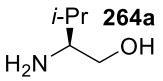

(*R*)-Valinol (264b) as a yellow oil (336 mg, 86% yield): ^{1}H NMR (300 MHz, $CDCl_3$) δ 3.64 (dd, *J* = 10.6, 3.8 Hz, 1H), 3.30 (dd, *J* = 10.6, 8.7 Hz, 1H), 2.63 – 2.50 (m, 1H), 2.37 (br s, 3H), 1.67 – 1.46 (m, 1H), 0.92 (d, *J* = 4.3 Hz, 3H), 0.89 (d, *J* = 4.2 Hz, 3H). ^{1}H NMR corresponds to the literature.[283]

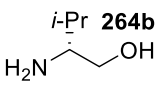

(*S*)-*tert*-Leucinol (264c) as a colourless oil (945 mg, 99% yield): ^{1}H NMR (300 MHz, $CDCl_3$) δ 3.70 (dd, *J* = 10.2, 3.9 Hz, 1H), 3.20 (t, *J* = 10.2 Hz, 1H), 2.50 (dd, *J* = 10.1, 3.9 Hz, 1H), 1.81 (br s, 3H), 0.89 (s, 9H). ^{1}H NMR corresponds to the literature.[284]

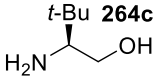

(*S*)-Leucinol (264d) as a colourless oil (746 mg, 83% yield): ^{1}H NMR (300 MHz, $CDCl_3$) δ 3.56 (dd, *J* = 10.6, 3.9 Hz, 1H), 3.20 (dd, *J* = 10.6, 8.8 Hz, 1H), 2.94 – 2.83 (m, 1H), 2.09 (br s, 3H), 1.69 – 1.62 (m, 1H), 1.20 (t, *J* = 7.1 Hz, 2H),0.92 (d, *J* = 6.6 Hz, 3H), 0.90 (d, *J* = 6.6 Hz, 3H). ^{1}H NMR corresponds to the literature.[285]

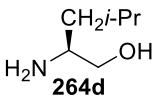

*Alternative route to (S)-valinol (**264a**)*

A flame-dried round-bottomed flask equipped with a reflux condenser was charged with (*S*)-valine (**262a**, 761 mg, 6.5 mmol), evacuated and backfilled with argon. Dry THF (6 mL) was added and the resulting suspension was cooled to 0 °C using an ice bath. A freshly prepared solution of $LiAlH_4$ (435 mg, 9.1 mmol) in dry THF (6 mL) was cooled to 0 °C and added slowly to the suspension of the amino acid. The reaction mixture was stirred at 0 °C for 1 h and at rt for 1 h, and then it was refluxed for 16 h. The reaction mixture was cooled to rt and diluted with Et_2O (90 mL). Water (23 mL), followed by NaOH (7.5 mL, 15 wt% aq), were added slowly. The reaction mixture was filtered through a celite pad using Et_2O (30 mL) as an eluent. Filtrate was concentrated under reduced pressure to afford (*S*)-valinol (**264a**) as a yellow oil (245 mg, 37% yield).

12.4.2 Preparation of tosylated intermediates 220, 265, 266 and *N*-Boc-protected compounds 221a, 263a, 267

Intermediates **220a**, **220c**, **265a**, **265c**, **266a**, **266c** (Scheme 59, page 68) were prepared according to the reported procedure and ^{1}H NMR spectra of these compounds correspond to the literature.[235] An analogous approach was applied to the synthesis of D-Val-derived compounds **220b**, **265b**, **266b**. Compounds **220b** and **220a**, **265b** and **265a**, **266b** and **266a** are enantiomers and thus they have similar ^{1}H NMR spectra. The synthetic pathway was applied by my colleague Jiří Tauchman to the preparation of compounds **220d**, **265d**, **266d**.

An alternative route to aminophosphine **222a** (Scheme 60, page 69) was realized according to the reported procedure and ^{1}H NMR spectra of compounds **221a**, **263a** and **267** correspond to the literature.[236]

12.4.3 Typical procedure to prepare aminophosphines 222

In a flame-dried flask, the mixture of tosylated aminophosphine **266b** (637 mg, 1.5 mmol) and H_2SO_4 (9.6 mL, 96% aq) was stirred at 100 °C (oil bath temperature) for 5 h. The reaction mixture was cooled to 0 °C using an ice bath. Crushed ice (9 g) and distilled water (40 mL) were added. The resulting solution was extracted with EtOAc (2 x 30 mL). Aqueous layer was separated and KOH was added until a pH of 11. The alkaline solution was extracted with EtOAc (3 x 20 mL). The combined organic layer (from the second extraction) was washed with brine, dried over anhydrous $MgSO_4$, and concentrated under reduced pressure. The residue was purified by gradient silica gel column chromatography (hexane/EtOAc 1/1 with 10% of Et_3N to ethyl acetate with 10% of Et_3N) to afford **222b** (261 mg, 64% yield).

(*S*)-1-Diphenylphosphino-3-methylbutan-2-amine (222a) as a pale yellow oil (1655 mg, 64% yield): $[\alpha]_D^{25}$ = +86.9 (*c* 0.31, $CHCl_3$); ^{1}H NMR (600 MHz, $CDCl_3$) δ 7.50 – 7.45 (m, 2H), 7.44 – 7.38 (m, 2H), 7.37 – 7.27 (m, 6H), 2.64 (ddd, *J* = 13.3, 8.4, 4.0 Hz, 1H), 2.37 – 2.29 (m, 1H), 1.99 – 1.91 (m, 1H), 1.75 – 1.66

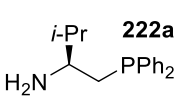

(m, 1H), 1.36 (s, 2H), 0.91 (d, J = 6.8 Hz, 3H), 0.88 (d, J = 6.8 Hz, 3H); ^{13}C NMR (151 MHz, $CDCl_3$) δ 139.3 (d, J = 12.1 Hz), 138.1 (d, J = 13.0 Hz), 133.1 (d, J = 19.4 Hz), 132.4 (d, J = 18.2 Hz), 128.8 (s), m (128.5, 128.4, 128.4, 128.3, 128.3), 54.0 (d, J = 13.1 Hz), 34.8 (d, J = 11.7 Hz), 34.4 (d, J = 7.4 Hz), 18.8 (s), 17.1 (s); ^{31}P NMR (121 MHz, $CDCl_3$) δ −21.4 (s); MS (ESI) m/z: $[M+H]^+$ calcd for $C_{17}H_{23}NP$ = 272.2, found = 272.1. ^{1}H and ^{13}C NMR correspond to the literature.[235]

(*R*)-1-Diphenylphosphino-3-methylbutan-2-amine (222b) as a pale yellow oil (261 mg, 64% yield): $[\alpha]_D^{25}$ = −76.7 (*c* 0.88, $CHCl_3$); ^{1}H NMR (600 MHz, $CDCl_3$) δ 7.49 – 7.44 (m, 2H), 7.43 – 7.38 (m, 2H), 7.37 – 7.27 (m, 6H), 2.69 – 2.62 (m, 1H), 2.36 – 2.29 (m, 1H), 2.10 – 1.87 (m, 3H), 1.79 – 1.69 (m, 1H), 0.91 (d, J = 6.8 Hz, 3H), 0.88 (d, J = 6.8 Hz, 3H); ^{13}C NMR (151 MHz, $CDCl_3$) δ 139.2 (d, J = 12.0 Hz), 138.0 (d, J = 12.8 Hz), 133.2 (d, J = 19.4 Hz), 132.4 (d, J = 18.3 Hz), 128.9 (s), m (128.5, 128.5, 128.4, 128.4, 128.4), 54.1 (d, J = 13.4 Hz), 34.5 (d, J = 12.1 Hz), 34.2 (d, J = 7.4 Hz), 18.8 (s), 17.1 (s); ^{31}P NMR (121 MHz, $CDCl_3$) δ −21.7 (s).

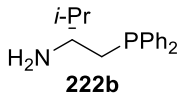

222b

(*S*)-1-Diphenylphosphino-3,3-dimethylbutan-2-amine (222c) as a white solid (462 mg, 99% yield): $[\alpha]_D^{25}$ = +92.4 (*c* 0.60, $CHCl_3$); ^{1}H NMR (300 MHz, $CDCl_3$) δ 7.57 – 7.42 (m, 4H), 7.42 – 7.27 (m, 6H), 2.60 – 2.42 (m, 2H), 1.82 – 1.72 (m, 1H), 1.44 (s, 2H), 0.90 (s, 9H); ^{31}P NMR (121 MHz, $CDCl_3$) δ −21.0 (s); HRMS (ESI-TOF) m/z: $[M+H]^+$ calcd for $C_{18}H_{25}NP$ = 286.1719, found = 286.1720. ^{1}H NMR corresponds to the literature.[235]

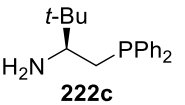

222c

(*S*)-1-Diphenylphosphino-4-methylpentan-2-amine (222d) as a pale yellow oil (503 mg, 63% yield): $[\alpha]_D^{25}$ = +37.0 (*c* 0.27, $CHCl_3$); ^{1}H NMR (600 MHz, $CDCl_3$) δ 7.47 7.39 (m, 4H), 7.36 – 7.27 (m, 6H), 2.94 – 2.83 (m, 1H), 2.30 – 2.26 (m, 1H), 2.05 (dd, J = 13.5, 8.5 Hz, 1H), 1.99 (br s, 2H), 1.74 – 1.65 (m, 1H), 1.41 – 1.37 (m, 1H), 1.35 – 1.30 (m, 1H), 0.81 (t, J = 5.8 Hz, 6H); ^{13}C NMR (151 MHz, $CDCl_3$) δ 138.5 (d, J = 11.7 Hz), 137.9 (d, J = 12.3 Hz), 132.5 (d, J = 19.1 Hz), 132.2 (d, J = 18.5 Hz), 128.3 (s), 128.2 (s), m (128.0, 128.0, 128.0, 127.9), 48.3 (d, J = 10.5 Hz), 46.5 (d, J = 14.4 Hz), 38.0 (d, J = 12.4 Hz), 24.4 (s), 22.7 (s), 21.6 (s); ^{31}P NMR (121 MHz, $CDCl_3$) δ −22.8 (s); MS (ESI) m/z: $[M+H]^+$ calcd for $C_{18}H_{25}NP$ = 286.2, found = 286.1.

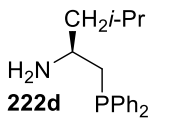

222d

(*S*)-1-Diphenylphosphinopropan-2-amine (222e):

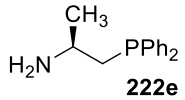

222e

Under argon, a solution of aziridine **269e** (517 mg, 3.29 mmol) in dry THF (18 mL) in a flame-dried Schlenk flask was cooled to −35 °C in a cryocooler. Then $KPPh_2$ (0.5 M in THF, 6.6 mL) was added dropwise and the reaction mixture was stirred at −35 °C for 16 h. The reaction mixture was warmed to rt, filtered through a celite pad using DCM as an eluent, and concentrated under reduced pressure. Under argon, the crude *N*-Boc-protected phosphine (350 mg, 1.02 mmol) was dissolved in dry DCM (10 mL). The solution was cooled to 0 °C using an ice bath and CF_3COOH (3.9 mL, 0.05 mmol) was added slowly. The reaction mixture was stirred at 0 °C for 1 h and at rt overnight. Water (20 mL) was added and the aqueous layer was separated. NaOH (20 mL, 10 wt% aq) was added to the separated aqueous layer and the resulting mixture was extracted with DCM (5 x 15 mL). The combined organic layer was washed with $NaHCO_3$ (sat aq) and water, dried over anhydrous $MgSO_4$, and concentrated under reduced pressure. The residue was purified by gradient silica gel column chromatography (hexane/EtOAc 1/1 to EtOAc) to afford **222e** as a pale yellow oil (200 mg, 25% yield): ^{1}H NMR (600 MHz, $CDCl_3$) δ 7.48 – 7.39 (m, 4H), 7.36 – 7.28 (m, 6H), 3.06 – 2.95 (m, 1H), 2.25 – 2.19 (m, 1H), 2.11 (dd, J = 13.6, 7.8 Hz, 1H), 1.46 (s, 2H), 1.19 (d, J = 6.3 Hz, 3H); ^{13}C NMR (151 MHz, $CDCl_3$) δ 138.8 (d, J = 11.9 Hz), 138.5 (d, J = 12.3 Hz), 132.9 (d, J =

19.1 Hz), 132.6 (d, J = 18.7 Hz), 128.7 (s), m (128.5, 128.5, 128.4, 128.4, 128.4), 45.0 (d, J = 15.8 Hz), 40.1 (d, J = 12.7 Hz), 25.5 (d, J = 8.2 Hz); ^{31}P NMR (121 MHz, $CDCl_3$) δ −21.7 (s); MS (ESI) m/z: $[M+H]^+$ calcd for $C_{15}H_{19}NP$ = 244.1, found = 244.1.

12.4.4 Preparation of *N*-Boc protected amino acids 268.

Alanine-derived compound **268e** was prepared according to the reported procedure and its ^{1}H NMR spectrum corresponds to the literature.[237] An analogous procedure was used for the preparation of *tert*-leucine-derived compound **268c**.

(*S*)-2-(*tert*-Butoxycarbonyl)amino-3,3-dimethylbutanoic acid (268c) as a colourless oil (105 mg, 91% yield): ^{1}H NMR (300 MHz, $CDCl_3$) δ 5.11 (d, J = 9.5 Hz, 1H), 4.10 (d, J = 6.2 Hz, 1H), 1.45 (s, 9H), 1.11 (s, 9H). ^{1}H NMR corresponds to the literature.[286]

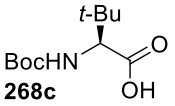

268c

12.4.5 Preparation of *N*-Boc protected amino alcohols 263.

Alanine-derived compound **263e** was prepared according to the reported procedure and its ^{1}H NMR spectrum corresponds to the literature.[238] An analogous procedure was used for the preparation of *tert*-leucine-derived compound **263c**.

***tert*-Butyl (*S*)-(1-hydroxy-3,3-dimethylbutan-2-yl)carbamate (263c)** as a yellowish solid (400 mg, 68% yield): ^{1}H NMR (300 MHz, $CDCl_3$) δ 5.67 (d, J = 8.0 Hz, 1H), 3.91 – 3.71 (m, 1H), 3.52 – 3.46 (m, 2H), 2.30 (br s, 1H), 1.45 (s, 9H), 0.94 (s, 9H). ^{1}H NMR corresponds to the literature.[287]

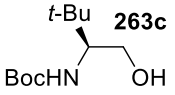

12.4.6 Preparation of aziridines 269.

Alanine-derived aziridine **269e** was prepared according to the reported procedure and its ^{1}H NMR spectrum corresponds to the literature.[239] An analogous procedure was used for the preparation of *tert*-leucine-derived aziridine **269c**. However, only traces of compound **269c** were obtained.

12.5 Typical procedure to prepare thiourea organocatalysts of type III

Under argon, a solution of aminophosphine **222a** (1.14 g, 4.2 mmol) in dry DCM (10 mL) was added slowly to a solution of isothiocyanate **218b** (1.16 g, 4.2 mmol) in dry DCM (10 mL) in a dry Schlenk flask. The reaction mixture was stirred at rt for 5 h. The solvent was eliminated under reduced pressure and the residue was purified by gradient silica gel column chromatography (hexane/EtOAc 4/1 to hexane/EtOAc 1/1) to afford catalyst **277** (1.65 g, 72% yield).

***N*-[({2-(Diphenylphosphino)ethyl}amino)carbonothioyl]-2,3,4,6-tetra-*O*-methyl-β-D-glucopyranosylamine (275)** as a colourless solid (136 mg, 74% yield): $[\alpha]_D^{25}$ = −22.4 (*c* 0.34, $CHCl_3$); IR (KBr) 510, 698, 737, 946, 988, 1018, 1066, 1093, 1120, 1159, 1186, 1281, 1341, 1383, 1392, 1434, 1464, 1479, 1541, 1817, 1885, 1957, 2836, 2911, 2932, 2983, 3052, 3069, 3312 cm^{-1}; ^{1}H NMR (600 MHz, $CDCl_3$) δ 7.47 – 7.40 (m, 4H), 7.35 – 7.28 (m, 6H), 7.05 (br s, 1H), 6.54 (br s, 1H), 3.72 – 3.61 (m, 6H), 3.55 (s, 3H), 3.53 – 3.48 (m, 4H), 3.43 – 3.38 (m, 1H), 3.30 (s, 3H), 3.27 (t, J = 8.9 Hz, 1H), 3.11 (t, J = 9.4 Hz, 1H), 3.03 (t, J = 8.9 Hz, 1H), 2.45 – 2.33 (m, 2H), 1.76 (br s, 1H); ^{13}CNMR (151 MHz, $CDCl_3$) δ 183.8 (s), 137.7 – 137.5 (m), 132.8 (d, J = 5.8 Hz), 132.7 (d, J = 5.7 Hz), 128.8 (s), 128.6 (d, J = 2.5 Hz), 128.5 (d, J = 2.6 Hz), 86.8 (s), 83.5 (s), 82.0 (s), 79.8 (s), 75.7 (s), 71.0 (s), 60.8 (s), 60.5 (s), 60.0 (s), 59.0

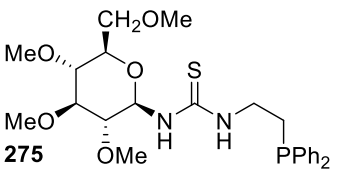

275

(s), 42.4 (d, J = 19.0 Hz), 27.9 (d, J = 13.3 Hz); ^{31}P NMR (121 MHz, $CDCl_3$) δ −21.5 (s); HRMS (ESI-TOF) m/z: $[M+H]^+$ calcd for $C_{25}H_{36}N_2O_5PS$ = 507.2077, found = 507.2076.

***N*-[({(*S*)-1-[(Diphenylphosphino)methyl]ethyl}amino)carbonothioyl]-2,3,4,6-tetra-*O*-methyl-β-D-glucopyranosylamine (276)** as a white solid (103 mg 78% yield): $[\alpha]_D^{25}$ = −17.2 (*c* 0.29, $CHCl_3$); IR (KBr) 513, 698, 740, 946, 985, 1024, 1093, 1120, 1153, 1189, 1275, 1323, 1344, 1377, 1437, 1452, 1482, 1541, 1715, 1811, 1888, 1957, 2833, 2908, 2932, 2980, 3055, 3072, 3306 cm^{-1}; ^{1}H NMR (600 MHz, $CDCl_3$) δ 7.53 (qd, J = 3.8, 2.1 Hz, 2H), 7.40 (qd, J = 3.9, 2.2 Hz, 2H), 7.36 – 7.27 (m, 6H), 7.02 (br s, 1H), 6.38 (br s, 1H), 4.69 (br s, 1H), 4.52 (br s, 1H), 3.63 (s, 3H), 3.61 (dd, J = 10.4, 2.1 Hz, 1H), 3.55 (s, 3H), 3.51 (s, 3H), 3.52 – 3.48 (m, 1H), 3.36 (ddd, J = 9.8, 5.2, 2.0 Hz, 1H), 3.29 (s, 3H), 3.24 (t, J = 8.9 Hz, 1H), 3.13 (t, J = 9.4 Hz, 1H), 3.08 (t, J = 8.5 Hz, 1H), 2.59 (ddd, J = 13.8, 5.6, 1.2 Hz, 1H), 2.22 (dd, J = 13.8, 7.8 Hz, 1H), 1.30 (d, J = 6.6 Hz, 3H); ^{13}C NMR (151 MHz, $CDCl_3$) δ 182.5 (s), 138.6 (d, J = 11.4 Hz), 137.6 (d, J = 11.7 Hz), 133.0 (d, J = 19.4 Hz), 132.7 (d, J = 19.1 Hz), 128.8 (s), 128.6 – 128.3 (m), 86.8 (s), 83.6 (s), 82.2 (s), 79.6 (s), 75.9 (s), 70.9 (s), 60.7 (s), 60.5 (s), 60.2 (s), 59.0 (s), 49.3 (d, J = 16.7 Hz), 36.0 (d, J = 15.0 Hz), 21.4 (d, J = 9.1 Hz); ^{31}P NMR (121 MHz, $CDCl_3$) δ −24.3 (s); HRMS (ESI-TOF) m/z: $[M+H]^+$ calcd for $C_{26}H_{38}N_2O_5PS$ = 521.2234, found = 521.2234.

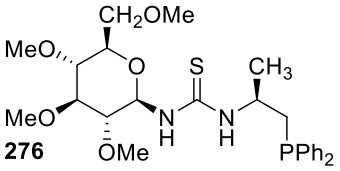

276

***N*-[({(*S*)-1-[(Diphenylphosphino)methyl]-2-methylpropyl}amino)carbonothioyl]-2,3,4,6-tetra-*O*-methyl-β-D-glucopyranosylamine (277)** as a colourless viscous oil. The oil was freeze-dried to afford a white solid **277** (1.65 g, 72% yield): $[\alpha]_D^{25}$ = −26.1 (*c* 0.35, $CHCl_3$); IR (KBr) 507, 698, 740, 937, 985, 1030, 1096, 1165, 1186, 1251, 1308, 1347, 1368, 1389, 1431, 1455, 1479, 1541, 1550, 1616, 1739, 1814, 1885, 1960, 2833, 2902, 2929, 2953, 3052, 3072, 3306 cm^{-1}; ^{1}H NMR (600 MHz, $CDCl_3$) δ 7.55 – 7.49 (m, 2H), 7.48 – 7.41 (m, 2H), 7.37 – 7.27 (m, 6H), 7.14 (br s, 1H), 6.24 (br s, 1H), 4.46 (br s, 1H), 4.38 (br s, 1H), 3.63 (s, 3H), 3.60 (s, 3H), 3.58 (dd, J = 14.3, 3.7 Hz, 1H), 3.50 (s, 3H), 3.48 (dd, J = 10.5, 5.5 Hz, 1H), 3.33 (ddd, J = 9.7, 5.2, 1.9 Hz, 1H), 3.26 (s, 3H), 3.23 – 3.11 (m, 3H), 2.39 – 2.26 (m, 2H), 2.16 (dq, J = 13.3, 6.8 Hz, 1H), 0.89 (d, J = 6.9 Hz, 3H), 0.87 (d, J = 6.8 Hz, 3H); ^{13}C NMR (151 MHz, $CDCl_3$) δ 183.7 (s), 138.5 (d, J = 15.6 Hz), 138.3 (d, J = 12.0 Hz), 133.0 (s), 132.9 (s), 128.6 (s), 128.5 – 128.3 (m), 87.1 (s), 84.1 (s), 81.9 (s), 79.5 (s), 76.4 (s), 70.9 (s), 60.8 (s), 60.7 (s), 60.5 (s), 59.0 (s), 58.0 (d, J = 14.0 Hz), 31.4 (d, J = 6.5 Hz), 31.2 (d, J = 13.6 Hz), 18.6 (s), 17.5 (s); ^{31}P NMR (121 MHz, $CDCl_3$) δ −24.4 (s); HRMS (ESI-TOF) m/z: $[M+H]^+$ calcd for $C_{28}H_{42}N_2O_5PS$ = 549.2546, found = 549.2546.

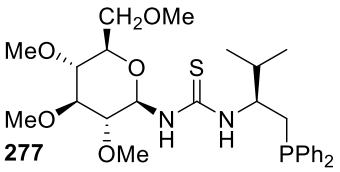

277

***N*-[({(*S*)-1-[(Diphenylphosphino)methyl]-2-methylpropyl}amino)carbonothioyl]-2,3,4,6-tetra-*O*-acetyl-β-D-glucopyranosylamine (278)** as a white solid (97 mg, 93% yield): $[\alpha]_D^{25}$ = +13.7 (*c* 0.26, $CHCl_3$); IR (KBr) 600, 698, 746, 911, 1036, 1099, 1230, 1374, 1431, 1464, 1482, 1535, 1751, 2869, 2953, 3001, 3049, 3075, 3354 cm^{-1}; ^{1}H NMR (600 MHz, $CDCl_3$, 50 °C) δ 7.49 – 7.41 (m, 4H), 7.35 (br s, 6H), 6.03 (br s, 2H), 5.65 (br s, 1H), 5.33 (t, J = 9.4 Hz, 1H), 5.08 (t, J = 9.7 Hz, 1H), 4.85 (br s, 1H), 4.34 (d, J = 9.1 Hz, 1H), 4.14 (d, J = 12.3 Hz, 1H), 3.85 – 3.81 (m, 1H), 2.36 (dd, J = 13.9, 5.2 Hz, 1H), 2.29 – 2.22 (m, 1H), 2.10 – 1.99 (m, 14H), 0.90 (d, J = 7.0 Hz, 3H), 0.88 (d, J = 6.8 Hz, 3H); ^{13}C NMR (151 MHz, $CDCl_3$, 50 °C) δ 183.2 (s), 171.2 (s), 170.5 (s), 169.7 (s), 169.5 (s), 138.2 (d, J = 14.6 Hz), 133.1 (d, J = 19.4 Hz), 132.9 (d, J = 19.3 Hz), 129.0 – 128.6 (m), 83.2 (s), 73.5 (s), 72.9 (s),

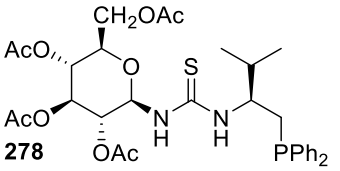

278

71.0 (s), 68.6 (s), 61.9 (s), 57.6 (d, *J* = 11.6 Hz), 32.1 (br s), 29.7 (s), 20.6 (s), 20.6 (s) 20.5 (s), 20.5 (s), 18.9 (s), 17.6 (br s); ^{31}P NMR (121 MHz, $CDCl_3$, 50 °C) δ −23.8 (s); HRMS (ESI-TOF) m/z: $[M+H]^+$ calcd for $C_{32}H_{42}N_2O_9PS$ = 661.2343, found = 661.2346.

***N*-[({(*S*)-1-[(Diphenylphosphino)methyl]-2-methylpropyl}amino)carbonothioyl]-2,3,4,6-tetra-*O*-benzyl-β-D-glucopyranosylamine (279)** as a white solid (236 mg, 73% yield): $[\alpha]_D^{25}$ = −7.5 (*c* 0.47, $CHCl_3$); IR (KBr) 507, 603, 695, 740, 824, 863, 911, 1006, 1027, 1090, 1153, 1210, 1245, 1362, 1431, 1452, 1494, 1538, 1811, 1885, 1948, 2866, 2905, 2953, 3025, 3063, 3300 cm^{-1}; ^{1}H NMR (600 MHz, $CDCl_3$) δ 7.58 – 7.53 (m, 2H), 7.46 – 7.41 (m, 2H), 7.41 – 7.23 (m, 22H), 7.23 – 7.18 (m, 2H), 7.12 (br s, 3H), 6.17 (br s, 1H), 4.92 (dd, *J* = 22.8, 11.0 Hz, 2H), 4.85 (dd, *J* = 28.4, 10.4 Hz, 2H), 4.78 (d, *J* = 10.8 Hz, 1H), 4.58 (br s, 1H), 4.46 (t, *J* = 10.1 Hz, 3H), 4.38 (d, *J* = 12.1 Hz, 1H), 3.80 (br s, 1H), 3.73 (t, *J* = 8.9 Hz, 1H), 3.65 (t, *J* = 12.6 Hz, 3H), 3.55 – 3.49 (m, 1H), 2.35 – 2.24 (m, 2H), 2.11 (dd, *J* = 12.0, 6.5 Hz, 1H), 0.84 (d, *J* = 6.9 Hz, 3H), 0.81 (d, *J* = 6.8 Hz, 3H); ^{13}C NMR (151 MHz, $CDCl_3$) δ 183.9 (s), 138.6 (d, *J* = 11.7 Hz), 138.2 (s), 138.1 (d, *J* = 11.9 Hz), 137.7 (s), 137.5 (s), 137.4 (s), 85.6 (s), 84.5 (s), 78.7 (s), 77.5 (s), 76.5 (s), 75.6 (s), 75.0 (br s), 73.3 (s), 68.1 (s), 57.9 (d, *J* = 14.3 Hz), 31.1 – 31.4 (m), 18.6 (s), 17.6 (s); ^{31}P NMR (121 MHz, $CDCl_3$, 50 °C) δ −25.0 (s); HRMS (ESI-TOF) m/z: $[M+Na]^+$ calcd for $C_{52}H_{57}N_2NaO_5PS$ = 875.3618, found = 875.3620.

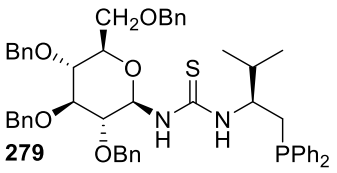

279

***N*-[({(*R*)-1-[(Diphenylphosphino)methyl]-2-methylpropyl}amino)carbonothioyl]-2,3,4,6-tetra-*O*-methyl-β-D-glucopyranosylamine (280)** as a white solid (254 mg, 81% yield): $[\alpha]_D^{25}$ = −44.1 (*c* 0.34, $CHCl_3$); IR (KBr) 477, 507, 614, 665, 695, 740, 860, 937, 949, 985, 1021, 1093, 1156, 1186, 1248, 1308, 1335, 1386, 1416, 1485, 1538, 1544, 1613, 1661, 1808, 1876, 1954, 2833, 2896, 2902, 2932, 2959, 3043, 3069, 3117, 3132, 3303 cm^{-1}; ^{1}H NMR (600 MHz, $CDCl_3$) δ 7.50 – 7.42 (m, 4H), 7.37 – 7.29 (m, 6H), 7.02 (br s, 1H), 6.21 (br s, 1H), 4.47 (br s, 1H), 3.85 (br s, 1H), 3.62 (s, 3H), 3.57 – 3.53 (m, 4H), 3.50 (s, 3H), 3.44 (dd, *J* = 10.1, 6.6 Hz, 1H), 3.33 (s, 3H), 3.26 – 3.18 (m, 1H), 3.12 (t, *J* = 8.7 Hz, 1H), 2.98 (dd, *J* = 16.0, 7.1 Hz, 1H), 2.94 (t, *J* = 8.8 Hz, 1H), 2.43 (ddd, *J* = 14.2, 4.4, 2.0 Hz, 1H), 2.26 (dd, *J* = 14.2, 8.6 Hz, 1H), 2.21 (dd, *J* = 12.7, 6.3 Hz, 1H), 0.93 (d, *J* = 1.6 Hz, 3H), 0.92 (d, *J* = 1.7 Hz, 3H); ^{13}C NMR (151 MHz, $CDCl_3$) δ 183.5 (s), 139.0 (d, *J* = 10.8 Hz), 138.4 (d, *J* = 12.3 Hz), 132.9 (d, *J* = 8.9 Hz), 132.8 (d, *J* = 8.8 Hz), 128.8 (s), 128.7 – 128.5 (m), 87.1 (s), 83.2 (s), 81.6 (s), 80.0 (s), 75.9 (s), 71.3 (s), 60.7 (s), 60.6 (s), 60. 6 (s), 59.0 (s), 58.7 (d, *J* = 14.2 Hz), 31.7 (d, *J* = 8.8 Hz), 30.4 (d, *J* = 14.0 Hz), 18.4 (s), 18.1 (s); ^{31}P NMR (121 MHz, $CDCl_3$) δ −23.8 (s); HRMS (ESI-TOF) m/z: $[M+Na]^+$ calcd for $C_{28}H_{41}N_2NaO_5PS$ = 571.2366, found = 571.2366.

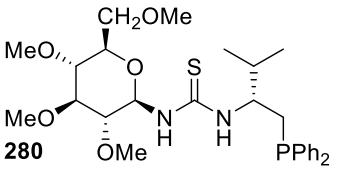

280

***N*-[({(*S*)-1-[(Diphenylphosphino)methyl]-3-methylbutyl}amino)carbonothioyl]-2,3,4,6-tetra-*O*-methyl-β-D-glucopyranosylamine (281)** as a white solid (134 mg, 65% yield): $[\alpha]_D^{25}$ = −26.7 (*c* 0.38, $CHCl_3$); IR (KBr) 504, 695, 719, 737, 749, 806, 911, 937, 952, 985, 1078, 1099, 1156, 1186, 1230, 1272, 1284, 1335, 1368, 1437, 1458, 1470, 1485, 1535, 1547, 1604, 1616, 1811, 1885, 1954, 2830, 2869, 2902, 2929, 2950, 3031, 3052, 3066, 3297 cm^{-1}; ^{1}H NMR (600 MHz, $CDCl_3$) δ 7.55 (td, *J* = 7.7, 1.6 Hz, 2H), 7.41 (td, *J* = 7.9, 1.5 Hz, 2H), 7.31 (ddd, *J* = 17.1, 14.3, 6.9 Hz, 6H), 7.08 (br s, 1H), 6.17 (br s, 1H), 4.60 (br s, 1H), 4.34 (br s, 1H), 3.63 (s, 3H), 3.60 (dd, *J* = 10.3, 1.9 Hz, 1H), 3.56 (br s, 3H), 3.51 (s, 3H), 3.50 – 3.46 (m, 1H), 3.31 (s, 3H), 3.29 (dd, *J* = 5.5, 1.9 Hz, 1H), 3.20 (t, *J* = 8.9 Hz, 1H), 3.13 (t, *J* =

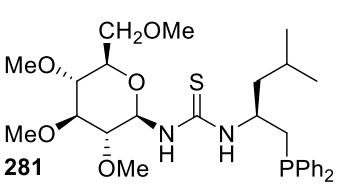

281

9.2 Hz, 1H), 3.07 (br s, 1H), 2.54 (dd, *J* = 13.6, 3.0 Hz, 1H), 2.34 (dd, *J* = 13.2, 6.9 Hz, 1H), 1.65 (s, 1H), 1.56 (br s, 1H), 1.53 – 1.45 (m, 1H), 0.85 (d, *J* = 6.1 Hz, 3H), 0.80 (d, *J* = 6.0 Hz, 3H); ^{13}C NMR (151 MHz, $CDCl_3$) δ 183.08 (s), 139.07 – 138.76 (m), 137.86 (d, *J* = 11.5 Hz), 133.29 (d, *J* = 19.8 Hz), 132.60 (d, *J* = 18.8 Hz), 128.81 (s), 128.61 – 128.24 (m), 87.16 (s), 83.92 (s), 82.17 (s), 79.59 (s), 76.30 (s), 70.90 (s), 60.8 – 60.7 (m), 60.52 (s), 59.11 (s), 52.04 (d, *J* = 9.1 Hz), 44.46 (d, *J* = 9.2 Hz), 34.55 (d, *J* = 14.5 Hz), 25.04 (s), 22.89 (s), 22.28 (s); ^{31}P NMR (121 MHz, $CDCl_3$) δ −25.0 (s); HRMS (ESI-TOF) m/z: $[M+H]^+$ calcd for $C_{29}H_{44}N_2O_5PS$ = 563.2703, found = 563.2704.

***N*-[({(*S*)-1-[(Diphenylphosphino)methyl]-2,2-dimethylpropyl}amino)carbonothioyl]-2,3,4,6-tetra-*O*-methyl-β-D-glucopyranosylamine (282)** as a white solid (27 mg, 35% yield): $[\alpha]_D^{25}$ = +15.8 (*c* 0.70, $CHCl_3$); IR (KBr) 698, 746, 937, 952, 988, 1069, 1090, 1159, 1192, 1210, 1260, 1332, 1353, 1371, 1434, 1473, 1479, 1551, 1619, 1643, 1712, 2830, 2935, 2947, 2953, 3055, 3073, 3237, 3425, 3482 cm^{-1}; ^{1}H NMR (600 MHz, $CDCl_3$) δ 7.57 – 7.51 (m, 2H), 7.45 – 7.40 (m, 2H), 7.34 – 7.26 (m, 6H), 7.22 (br s, 1H), 6.32 (br s, 1H), 4.54 – 4.47 (m, 1H), 4.42 (br s, 1H), 3.63 (s, 3H), 3.63 (s, 3H), 3.59 – 3.54 (m, 1H), 3.50 (s, 3H), 3.47 – 3.42 (m, 1H), 3.35 (ddd, *J* = 8.1, 7.7, 5.0 Hz, 1H), 3.22 (s, 3H), 3.25 – 3.16 (m, 1H), 3.14 – 3.07 (m, 1H), 3.07 – 3.03 (m, 1H), 2.55 – 2.47 (m, 1H), 1.99 – 1.91 (m, 1H), 0.91 (s, 9H); ^{13}C NMR (151 MHz, $CDCl_3$) δ 185.0 (s), 139.9 (d, *J* = 13.3 Hz), 138.5 (d, *J* = 14.9 Hz), 133.5 (d, *J* = 19.3 Hz), 132.6 (d, *J* = 18.9 Hz), 128.7 (s), 128.3 (s), 128.2 (s), 128.1 (s), 87.3 (s), 84.1 (s), 81.9 (s), 79.9 (s), 76.4 (s), 71.1 (s), 60.9 (s), 60.8 (s), 60.7 (s), 60.6 (s), 58.9 (s), 36.1 (d, *J* = 6.5 Hz), 31.7 (d, *J* = 14.2 Hz), 26.4 (s); ^{31}P NMR (121 MHz, $CDCl_3$) δ – 23.5 (s); HRMS (ESI-TOF) m/z: $[M+H]^+$ calcd for $C_{29}H_{44}N_2O_5PS$ = 563.2703, found = 563.2704.

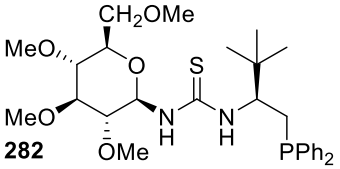

282

***N*-[({(1*S*,2*S*)-2-(Diphenylphosphino)cyclohexyl}amino)carbonothioyl]-2,3,4,6-tetra-*O*-acetyl-β-D-glucopyranosylamine (117)**[159] as a white solid (79 mg, 66% yield): $[\alpha]_D^{25}$ = +45.0 (*c* 1.00, $CHCl_3$); ^{1}H NMR (600 MHz, $CDCl_3$, 40 °C) δ 7.52 – 7.44 (m, 4H), 7.41 – 7.32 (m, 6H), 6.11 (br s, 1H), 5.91 (br s, 1H), 5.77 (t, *J* = 8.8 Hz, 1H), 5.35 (t, *J* = 9.5 Hz, 1H), 5.10 (t, *J* = 9.7 Hz, 1H), 4.88 (br s, 1H), 4.35 (d, *J* = 9.4 Hz, 1H), 4.15 (d, *J* = 12.1 Hz, 1H), 3.85 (d, *J* = 8.4 Hz, 1H), 2.35 (br s, 1H), 2.06 (s, 3H), 2.03 (s, 3H), 2.02 (s, 3H), 2.01 (s, 3H), 1.82 (br s, 1H), 1.73 (br s, 1H), 1.63 (br s, 1H), 1.57 (s, 1H), 1.41 – 1.23 (m, 5H); ^{13}C NMR (151 MHz, $CDCl_3$, 40 °C) δ 181.9 (s), 171.3 (s), 170.5 (s), 169.8 (s), 169.6 (s), 136.3 (d, *J* = 13.4 Hz), 134.6 (d, *J* = 20.7 Hz), 132.7 (d, *J* = 18.5 Hz), 129.3 (s), 128.8 (d, *J* = 5.5 Hz), 128.6 (s), 128.4 (d, *J* = 7.3 Hz), 83.1 (s), 73.5 (s), 72.8 (s), 71.0 (s), 68.4 (s), 61.8 (s), 54.6 (s), 40.6 (s), 32.7 (s), 26.9 (s), 25.0 (s), 23.9 (s), 20.7 (s), 20.7 (s), 20.6 (s), 20.5 (s); ^{31}P NMR (121 MHz, $CDCl_3$, 40 °C) δ −9.3 (s); HRMS (ESI-TOF) m/z: $[M+H]^+$ calcd for $C_{33}H_{42}N_2O_9PS$ = 673.2343, found = 673.2345.

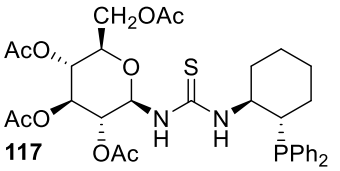

117

12.6 Typical procedure to prepare urea organocatalysts of type III

Amine **252b** (100 mg, 0.43 mmol) and triphosgene (126 mg, 0.43 mmol) were added to a mixture of DCM (3 mL) and $NaHCO_3$ (1 mL, sat aq). The reaction mixture was stirred at rt for 2 h and water (10 mL) was added. The layers were separated and the aqueous layer was extracted with DCM (3 x 10 mL). The combined organic layer was dried over anhydrous $MgSO_4$ and concentrated under reduced pressure. Under argon, the residue was dissolved in DCM (1 mL) and a solution of aminophosphine **222a** (87 mg, 0.32 mmol) in DCM (1 mL) was added dropwise. The reaction mixture was stirred at rt for 18 h and concentrated under

reduced pressure. The residue was purified by silica gel column chromatography (hexane/EtOAc 1/1) to afford product **284**.

***N*-[({(*S*)-1-[(Diphenylphosphino)methyl]-2-methylpropyl}amino)carbonyl]-2,3,4,6-tetra-*O*-acetyl-β-D-glucopyranosylamine (283)** as a white solid (79 mg, 60% yield): $[\alpha]_D^{25}$ = +18.9 (*c* 0.27, $CHCl_3$); IR (KBr) 606, 695, 743, 911, 1036, 1102, 1227, 1365, 1434, 1467, 1485, 1553, 1652, 1700, 1751, 2872, 2959, 3052, 3072, 3354 cm^{-1}; ^1H NMR (600 MHz, $CDCl_3$) δ 7.44 – 7.39 (m, 4H), 7.38 – 7.30 (m, 6H), 5.32 (t, *J* = 9.5 Hz, 1H), 5.20 (t, *J* = 9.4 Hz, 1H), 5.07 (t, *J* = 9.8 Hz, 1H), 5.01 – 4.97 (m, 1H), 4.89 (t, *J* = 9.4 Hz, 1H), 4.38 (br s, 1H), 4.35 (dd, *J* = 12.5, 4.4 Hz, 1H), 4.08 (dd, *J* = 12.4, 2.0 Hz, 1H), 3.81 (ddd, *J* = 10.1, 4.3, 2.2 Hz, 1H), 3.69 (s, 1H), 2.26 (ddd, *J* = 13.9, 4.8, 2.6 Hz, 1H), 2.13 – 2.10 (m, 1H), 2.08 (s, 3H), 2.07 (s, 3H), 2.04 (s, 3H), 2.03 (s, 3H), 1.93 – 1.86 (m, 1H), 0.86 (d, *J* = 3.4 Hz, 3H), 0.85 (d, *J* = 3.4 Hz, 3H); ^{13}C NMR (151 MHz, $CDCl_3$) δ 171.3 (s), 170.6 (s), 169.9 (s), 169.6 (s), 155.5 (s), 138. 6 (d, *J* = 12.0 Hz), 138.2 (d, *J* = 13.1 Hz), 133.0 (d, *J* = 19.3 Hz), 132.6 (d, *J* = 18.9 Hz), 128.9 (s), 128.7 – 128.5 (m), 80.3 (s), 73.2 (s), 72.9 (s), 70.6 (s), 68.3 (s), 61.8 (s), 53.1 (br s), 32.8 (d, *J* = 13.6 Hz), 32.6 (d, *J* = 7.4 Hz), 20.9 (s), 20.9 (s), 20.7 (s), 20.6 (s), 18.8 (s), 17.4 (s); ^{31}P NMR (121 MHz, $CDCl_3$) δ −23.6 (s); HRMS (ESI-TOF) m/z: $[M+H]^+$ calcd for $C_{32}H_{42}N_2O_{10}P$ = 645.2572, found = 645.2574.

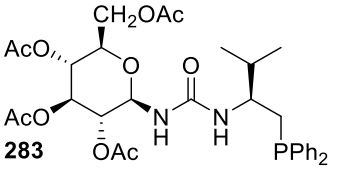

***N*-[({(*S*)-1-[(Diphenylphosphino)methyl]-2-methylpropyl}amino)carbonyl]-2,3,4,6-tetra-*O*-methyl-β-D-glucopyranosylamine (284)** crystallized from $CHCl_3$ as a white glacial solid (124 mg, 79% yield): mp 137 – 138 °C; $[\alpha]_D^{25}$ = +22.6 (*c* 0.27, $CHCl_3$); IR (KBr) 510, 701, 740, 934, 952, 988, 1027, 1069, 1099, 1144, 1165, 1186, 1242, 1263, 1308, 1368, 1389, 1416, 1437, 1464, 1482, 1565, 1640, 1811, 1888, 1957, 2830, 2893, 2905, 2932, 2956, 3046, 3072, 3309 cm^{-1}; ^1H NMR (600 MHz, $CDCl_3$) δ 7.47 (tt, *J* = 5.1, 2.0 Hz, 2H), 7.41 (tt, *J* = 6.0, 2.3 Hz, 2H), 7.36 – 7.27 (m, 6H), 4.98 (d, *J* = 6.9 Hz, 1H), 4.82 (d, *J* = 7.0 Hz, 1H), 4.61 (t, *J* = 8.0 Hz, 1H), 3.75 (br s, 1H), 3.64 (s, 3H), 3.60 (dd, *J* = 10.4, 2.0 Hz, 1H), 3.54 (s, 3H), 3.53 – 3.50 (m, 1H), 3.52 (s, 3H), 3.35 – 3.31 (m, 1H), 3.31 (s, 3H), 3.24 (t, *J* = 8.9 Hz, 1H), 3.21 – 3.15 (m, 1H), 2.98 (t, *J* = 8.9 Hz, 1H), 2.23 (d, *J* = 7.2 Hz, 2H), 2.02 – 1.94 (m, 1H), 0.85 (d, *J* = 1.1 Hz, 3H), 0.84 (d, *J* = 1.2 Hz, 3H); ^{13}C NMR (151 MHz, $CDCl_3$) δ 157.0 (s), 138.7 (d, *J* = 12.5 Hz), 132.9 (d, *J* = 19.3 Hz), 132.8 (d, *J* = 19.1 Hz), 128.7 – 128.4 (m), 87.1 (s), 82.7 (s), 82.0 (s), 79.4 (s), 75.8 (s), 70.9 (s), 60.7 (s), 60.4 (s), 60.2 (s), 59.1 (s), 52.9 (d, *J* = 14.2 Hz), 32.2 (s), 32.05 (d, *J* = 7.8 Hz), 18.9 (s), 17.3 (s); ^{31}P NMR (121 MHz, $CDCl_3$) δ −23.7 (s); HRMS (ESI-TOF) m/z: $[M+H]^+$ calcd for $C_{28}H_{42}N_2O_6P$ = 533.2775, found = 533.2776.

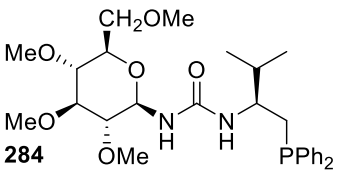

12.7 General procedure for the asymmetric MBH reaction

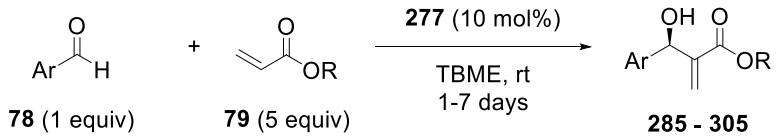

Scheme 92 Enantioselective MBH reaction catalyzed by catalyst **277**.

Acrylate **79** (0.50 mmol) was added to a solution of organocatalyst **277** (5.5 mg, 0.01 mmol) in TBME (1 mL) in a dry screw neck glass vial (5 mL). The vial was closed with a hole cap equipped with an inserted septum. The resulting solution was stirred at rt for 15 min and

aldehyde **78** (0.10 mmol) was added *via* a syringe and the cap was wrapped with parafilm. The reaction mixture was stirred at rt for a reported time (Table 8, Table 9, page 74). The solvent was eliminated under reduced pressure and the residue was purified by silica gel column chromatography (hexane/EtOAc 4/1 unless otherwise stated) to provide the title compound.

Methyl 2-[(*R*)-hydroxy(4-nitrophenyl)methyl]acrylate (285) as a yellow solid (19.5 mg, 82% yield): $[\alpha]_D^{25} = -57.3$ (*c* 0.52, MeOH, 86% ee); ^{1}H NMR (600 MHz, $CDCl_3$) δ 8.22 (d, *J* = 8.7 Hz, 2H), 7.59 (d, *J* = 8.6 Hz, 2H), 6.41 (s, 1H), 5.89 (s, 1H), 5.64 (d, *J* = 6.1 Hz, 1H), 3.76 (s, 3H), 3.34 (d, *J* = 6.3 Hz, 1H); ^{13}C NMR (151 MHz, $CDCl_3$) δ 166.4, 148.5, 147.5, 140.9, 127.3, 123.6, 72.8, 52.2; MS (EI-TOF) m/z: $[M]^{+\bullet}$calcd for $C_{11}H_{11}NO_5$ = 237.1, found = 237.1; HPLC (Chiralpak® IC column, heptane/propan-2-ol 80/20, flow rate 1.0 mL/min at 25 °C, detection at 220 nm): t_R = 6.69 min (minor), t_R = 8.04 min (major). ^{1}H and ^{13}C NMR correspond to the literature.[121]

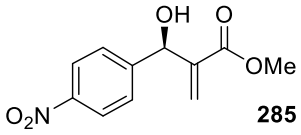

285

Ethyl 2-[(*R*)-hydroxy(4-nitrophenyl)methyl]acrylate (286) as a yellow oil (18.1 mg, 70% yield): $[\alpha]_D^{25} = -65.8$ (*c* 0.78, MeOH, 85% ee); ^{1}H NMR (600 MHz, $CDCl_3$) δ 8.19 (dd, *J* = 8.8, 1.1 Hz, 2H), 7.57 (dd, *J* = 8.3, 0.5 Hz, 2H), 6.39 (s, 1H), 5.85 (s, 1H), 5.62 (d, *J* = 6.1 Hz, 1H), 4.18 (q, *J* = 7.1 Hz, 2H), 3.39 (br s, 1H), 1.25 (t, *J* = 7.1 Hz, 3H); ^{13}C NMR (151 MHz, $CDCl_3$) δ 166.0, 148.7, 147.4, 141.2, 127.3, 127.0, 123.5, 72.7, 61.3, 14.0; MS (EI-TOF) m/z: $[M]^{+\bullet}$ calcd for $C_{12}H_{13}NO_5$ = 251.1, found = 251.1; HPLC (Chiralpak® IC column, heptane/propan-2-ol 80/20, flow rate 1.0 mL/min at 25 °C, detection at 220 nm): t_R = 6.18 min (minor), t_R = 7.51 min (major). ^{1}H and ^{13}C NMR correspond to the literature.[288]

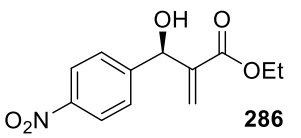

286

Butyl 2-[(*R*)-hydroxy(4-nitrophenyl)methyl]acrylate (287): The residue was purified by silica gel column chromatography (hexane/EtOAc 5/1) to afford a yellow oil (20.7 mg, 75% yield): $[\alpha]_D^{25} = -51.2$ (*c* 0.65, MeOH, 87% ee); ^{1}H NMR (600 MHz, $CDCl_3$) δ 8.22 – 8.19 (m, 2H), 7.59 – 7.56 (m, 2H), 6.39 (s, 1H), 5.84 (s, 1H), 5.62 (d, *J* = 6.2 Hz, 1H), 4.13 (t, *J* = 6.6 Hz, 2H), 3.34 (d, *J* = 6.3 Hz, 1H), 1.63 – 1.58 (m, 2H), 1.37 – 1.29 (m, 2H), 0.91 (t, *J* = 7.4 Hz, 3H); ^{13}C NMR (151 MHz, $CDCl_3$) δ 166.0, 148.6, 141.0, 127.3, 127.2, 123.6, 73.0, 65.2, 30.4, 19.1, 13.6; MS (EI-TOF) m/z: $[M]^{+\bullet}$calcd for $C_{14}H_{17}NO_5$ = 279.1, found = 279.1; HPLC (Chiralpak® IC column, heptane/propan-2-ol 90/10, flow rate 1.0 mL/min at 25 °C, detection at 220 nm): t_R = 8.82 min (minor), t_R = 10.78 min (major). ^{1}H NMR corresponds to the literature.[120]

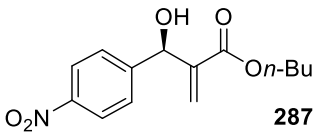

287

***tert*-Butyl 2-[(*R*)-hydroxy(4-nitrophenyl)methyl]acrylate (288)** The residue was purified by silica gel column chromatography (hexane/EtOAc 5/1) to afford a white solid (21.2 mg, 82% yield): $[\alpha]_D^{25} = -66.1$ (*c* 0.31, MeOH, 85% ee); ^{1}H NMR (600 MHz, $CDCl_3$) δ 8.21 (d, *J* = 8.7 Hz, 2H), 7.57 (d, *J* = 8.5 Hz, 2H), 6.30 (s, 1H), 5.74 (s, 1H), 5.56 (d, *J* = 6.6 Hz, 1H), 3.40 (d, *J* = 6.6 Hz, 1H), 1.43 (s, 9H); ^{13}C NMR (151 MHz, $CDCl_3$) δ 165.3, 149.0, 147.4, 142.3, 127.2, 126.6, 123.6, 82.4, 73.2, 28.0; MS (EI-TOF) m/z: $[M]^{+\bullet}$ calcd for $C_{14}H_{17}NO_5$ = 279.1, found = 279.1; HPLC (Chiralpak® IA column, heptane/propan-2-ol 90/10, flow rate 1.0 mL/min at 25 °C, detection at 220 nm): t_R = 7.83 min (minor), t_R = 8.84 min (major). ^{1}H and ^{13}C NMR correspond to the literature.[289]

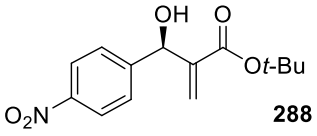

288

Benzyl 2-[(*R*)-hydroxy(4-nitrophenyl)methyl]acrylate (289) as a white solid (25.8 mg, 83% yield): $[\alpha]_D^{25} = -43.5$ (*c* 0.35, MeOH, 80% ee); ^{1}H NMR (600 MHz, $CDCl_3$) δ 8.20 – 8.16 (m, 2H), 7.56 – 7.52 (m, 2H), 7.36 – 7.32 (m, 3H), 7.28 – 7.25 (m, 2H), 6.45 (s, 1H), 5.89 – 5.88 (m, 1H), 5.64 (d, *J* = 6.3 Hz, 1H), 5.16 (s, 2H), 3.17 (d, *J* = 6.3 Hz, 1H); ^{13}C NMR (151 MHz, $CDCl_3$) δ 165.7, 148.5, 147.5, 141.0, 135.1, 128.6, 128.6, 128.3, 127.6, 127.3, 123.6, 72.8, 67.0; MS (EI-TOF) m/z: $[M]^{+\bullet}$ calcd for $C_{17}H_{15}NO_5$ = 313.1, found = 313.1; HPLC (Chiralpak® IC column, heptane/propan-2-ol 80/20, flow rate 1.0 mL/min at 25 °C, detection at 220 nm): t_R = 6.37 min (minor), t_R = 7.34 min (major). ^{1}H and ^{13}C NMR correspond to the literature.[121]

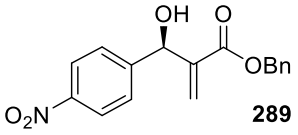

289

Hexafluoroisopropyl 2-[(*R*)-hydroxy(4-nitrophenyl)methyl]acrylate (290) as a pale yellow oil (11.7 mg, 10% yield, 2% ee): ^{1}H NMR (300 MHz, $CDCl_3$) δ 8.27 – 8.18 (m, 2H), 7.61 – 7.52 (m, 2H), 6.66 (d, *J* = 0.7 Hz, 1H), 6.26 (d, *J* = 1.3 Hz, 1H), 5.83 – 5.64 (m, 2H), 2.71 (d, *J* = 5.1 Hz, 1H); ^{19}F NMR (282 MHz, $CDCl_3$) δ −73.1 – (−73.3) (m); HPLC (Chiralpak® AD column, heptane/propan-2-ol 95/5, flow rate 1.0 mL/min at 25 °C, detection at 220 nm): t_R = 10.98 min (minor), t_R = 13.34 min (major). ^{1}H NMR corresponds to the literature.[290]

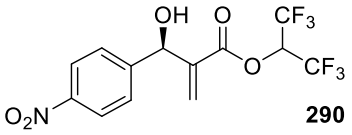

290

Methyl 2-[(*R*)-hydroxy(2-nitrophenyl)methyl]acrylate (291) as a yellow solid (16.1 mg, 69% yield): $[\alpha]_D^{25} = -143.2$ (*c* 0.37, MeOH, 62% ee); ^{1}H NMR (600 MHz, $CDCl_3$) δ 7.92 (dd, *J* = 8.2, 1.2 Hz, 1H), 7.73 (dd, *J* = 7.9, 1.3 Hz, 1H), 7.62 (td, *J* = 7.6, 1.2 Hz, 1H), 7.46 – 7.42 (m, 1H), 6.34 (s, 1H), 6.18 (s, 1H), 5.71 – 5.70 (m, 1H), 3.70 (s, 3H), 3.57 (br s, 1H); ^{13}C NMR (151 MHz, $CDCl_3$) δ 166.4, 148.3, 140.7, 136.1, 133.4, 128.9, 128.7, 126.4, 124.5, 67.6, 52.1; MS (ESI-TOF) m/z: $[M+Na]^+$calcd for $C_{11}H_{11}NNaO_5$ = 260.1, found = 260.1; HPLC (Chiralpak® IB column, heptane/propan-2-ol 95/5, flow rate 1.0 mL/min at 25 °C, detection at 220 nm): t_R = 15.69 min (minor), t_R = 16.85 min (major). ^{1}H and ^{13}C NMR correspond to the literature.[121]

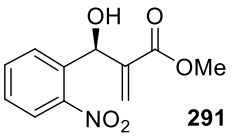

291

Methyl 2-[(*R*)-hydroxy(3-nitrophenyl)methyl]acrylate (292) as a colourless oil (14.8 mg, 62% yield): $[\alpha]_D^{25} = -65.1$ (*c* 0.32, MeOH, 82% ee); ^{1}H NMR (600 MHz, $CDCl_3$) δ 8.27 (s, 1H), 8.16 (dd, *J* = 8.1, 1.3 Hz, 1H), 7.76 (d, *J* = 7.7 Hz, 1H), 7.54 (t, *J* = 7.9 Hz, 1H), 6.43 (s, 1H), 5.91 (s, 1H), 5.64 (d, *J* = 6.2 Hz, 1H), 3.76 (s, 3H), 3.28 (d, *J* = 6.3 Hz, 1H); ^{13}C NMR (151 MHz, $CDCl_3$) δ 166.4, 148.3, 143.5, 140.8, 132.6, 129.4, 127.4, 122.8, 121.5, 72.8, 52.2; MS (ESI-TOF) m/z: $[M+Na]^+$calcd for $C_{11}H_{11}NNaO_5$ = 260.1, found = 260.1; HPLC (Chiralpak® IC column, heptane/propan-2-ol 80/20, flow rate 1.0 mL/min at 25 °C, detection at 220 nm): t_R = 7.22 min (minor), t_R = 8.24 min (major). ^{1}H and ^{13}C NMR correspond to the literature.[121]

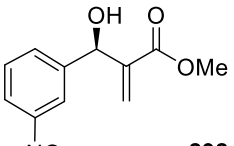

292

Methyl 2-[(*R*)-hydroxy(2,4-dinitrophenyl)methyl]acrylate (293) as a pale yellow oil (11.5 mg, 41% yield): $[\alpha]_D^{25} = -187.2$ (*c* 0.47, MeOH, 76% ee); ^{1}H NMR (300 MHz, $CDCl_3$) δ 8.79 (d, *J* = 2.3 Hz, 1H), 8.48 (dd, *J* = 8.6, 2.2 Hz, 1H), 8.04 (d, *J* = 8.7 Hz, 1H), 6.40 (s, 1H), 6.29 (d, *J* = 4.7 Hz, 1H), 5.75 (s, 1H), 3.76 (s, 3H), 3.50 (d, *J* = 5.1 Hz, 1H); HPLC (Chiralpak® IB column, heptane/propan-2-ol 90/21, flow rate 1.0 mL/min at 25 °C, detection at 220 nm): t_R = 15.62 min (major), t_R = 20.14 min (minor).

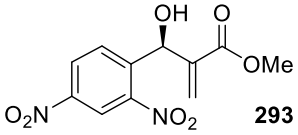

293

Methyl 2-[(*R*)-(4-cyanophenyl)(hydroxy)methyl]acrylate (294) as a colourless oil

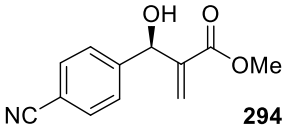

294

(16.9 mg, 77% yield): $[\alpha]_D^{25} = -72.0$ (*c* 0.63, MeOH, 84% ee); ^{1}H NMR (600 MHz, $CDCl_3$) δ 7.64 – 7.62 (m, 2H), 7.50 (d, *J* = 8.1 Hz, 2H), 6.37 (s, 1H), 5.85 (t, *J* = 0.8 Hz, 1H), 5.57 (d, *J* = 6.0 Hz, 1H), 3.73 (s, 3H), 3.30 (d, *J* = 6.1 Hz, 1H); ^{13}C NMR (151 MHz, $CDCl_3$) δ 166.4, 146.6, 141.0, 132.2, 127.2, 127.1, 118.7, 111.5, 72.8, 52.2; MS (ESI-IT) m/z: calcd for $[M+Na]^+$ $C_{12}H_{11}NNaO_3$ = 240.1, found = 240.2; HPLC (Chiralpak® IC column, heptane/propan-2-ol 80/20, flow rate 1.0 mL/min at 25 °C, detection at 220 nm): t_R = 7.93 min (minor), t_R = 9.78 min (major). ^{1}H and ^{13}C NMR correspond to the literature.[121]

Methyl 2-{(*R*)-hydroxy[4-(trifluoromethyl)phenyl]methyl}acrylate (295) as a yellow oil,

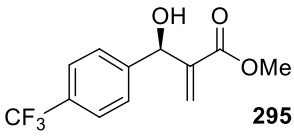

295

(20.5 mg, 70% yield): $[\alpha]_D^{25} = -56.3$ (*c* 0.40, MeOH, 83% ee); ^{1}H NMR (600 MHz, $CDCl_3$) δ 7.60 (d, *J* = 8.1 Hz, 2H), 7.50 (d, *J* = 8.0 Hz, 2H), 6.36 (s, 1H), 5.84 (s, 1H), 5.59 (d, *J* = 5.8 Hz, 1H), 3.73 (s, 3H), 3.30 (d, *J* = 6.0 Hz, 1H); ^{13}C NMR (151 MHz, $CDCl_3$) δ 166.5 (s), 145.2 (s), 141.3 (s), 129.9 (q, *J* = 32.4 Hz), 126.8 (s), 126.8 (s), 125.4 (m), 125.0 (s), 123.2 (s), 72.8 (s), 52.1 (s); MS (ESI-IT) m/z: calcd for $[M+Na]^+$ $C_{12}H_{11}F_3NaO_3$ = 283.1, found = 283.2; HPLC (Chiralpak® IC column, heptane/propan-2-ol 90/10, flow rate 1.0 mL/min at 25 °C, detection at 220 nm): t_R = 4.94 min (minor), t_R = 6.48 min (major). ^{1}H and ^{13}C NMR correspond to the literature.[121]

Methyl 2-[(*R*)-hydroxy(phenyl)methyl]acrylate (296) as a white solid (11.9 mg, 15%

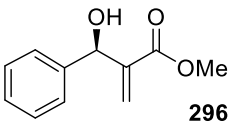

296

yield): $[\alpha]_D^{25} = -67.9$ (*c* 0.28, MeOH, 77% ee); ^{1}H NMR (600 MHz, $CDCl_3$) δ 7.40 – 7.33 (m, 4H), 7.31 – 7.27 (m, 1H), 6.34 (s, 1H), 5.83 (t, *J* = 1.1 Hz, 1H), 5.57 (d, *J* = 5.6 Hz, 1H), 3.73 (s, 3H), 3.00 (d, *J* = 5.7 Hz, 1H); ^{13}C NMR (151 MHz, $CDCl_3$) δ 166.8, 141.8, 141.2, 128.4, 127.8, 126.5, 126.2, 73.3, 52.0; MS (ESI-IT) m/z: calcd for $[M+Na]^+$ $C_{11}H_{12}NaO_3$ = 215.1, found 215.1; HPLC (Chiralpak® IC column, heptane/propan-2-ol 90/10, flow rate 1.0 mL/min at 25 °C, detection at 220 nm): t_R = 8.92 min (minor), t_R = 15.34 min (major). ^{1}H and ^{13}C NMR correspond to the literature.[121]

Methyl 2-[(*R*)-hydroxy(3-methylphenyl)methyl]acrylate (297) as a colourless oil (5.0 mg,

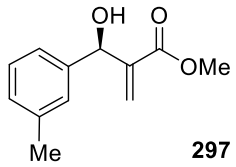

297

11% yield, 60% ee): ^{1}H NMR (300 MHz, $CDCl_3$) δ 7.25 – 7.06 (m, 4H), 6.35 (s, 1H), 5.84 (s, 1H), 5.54 (s, 1H), 3.73 (s, 3H), 2.94 (br s, 1H), 2.35 (s, 3H); HPLC (ChiralPak IC column, heptane/propan-2-ol 80/20, flow rate 1.0 mL/min at 25 °C, detection at 220 nm): t_R = 6.22 min (minor), t_R = 9.09 min (major). ^{1}H NMR corresponds to the literature.[291]

Methyl 2-[(*R*)-(4-fluorophenyl)(hydroxy)methyl]acrylate (298) as a colourless oil

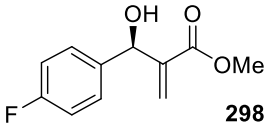

298

(10.5 mg, 24% yield): $[\alpha]_D^{25} = -57.5$ (*c* 0.44, MeOH, 60% ee); ^{1}H NMR (600 MHz, $CDCl_3$) δ 7.37 – 7.33 (m, 2H), 7.06 – 7.01 (m, 2H), 6.34 (s, 1H), 5.82 (t, *J* = 1.1 Hz, 1H), 5.55 (d, *J* = 5.5 Hz, 1H), 3.73 (s, 3H), 3.01 – 2.99 (m, 1H); ^{13}C NMR (151 MHz, $CDCl_3$) δ 166.7 (s), 163.1 (s), 161.5 (s), 141.7 (s), 136.9 (d, *J* = 2.8 Hz), 128.3 (d, *J* = 8.1 Hz), 126.2 (s), 115.3 (d, *J* = 21.5 Hz), 72.7 (s), 52.0 (s); MS (ESI-IT) m/z: calcd for $[M+Na]^+$ $C_{11}H_{11}FNaO_3$ = 233.1, found = 233.2; HPLC (Chiralpak® IC column, heptane/propan-2-ol 95/5, flow rate 1.0 mL/min at 25 °C, detection at 220 nm): t_R = 10.00 min (minor), t_R = 18.69 min (major). ^{1}H and ^{13}C NMR correspond to the literature.[121]

Methyl 2-[(*R*)-(4-chlorophenyl)(hydroxy)methyl]acrylate (299) as a colourless oil (4.1 mg, 24% yield): $[\alpha]_D^{25} = -61.0$ (*c* 0.21, MeOH, 69% ee); ^{1}H NMR (600 MHz, $CDCl_3$) δ 7.32 – 7.31 (m, 4H), 6.32 (s, 1H), 5.82 (t, *J* = 1.0 Hz, 1H), 5.53 (d, *J* = 5.8 Hz, 1H), 3.73 (s, 3H), 3.06 (d, *J* = 5.8 Hz, 1H); ^{13}C NMR (151 MHz, $CDCl_3$) δ 166.6, 141.6, 139.7, 133.6, 128.6, 127.9, 126.4, 72.8, 52.1; MS (ESI-IT) m/z: calcd for $[M+Na]^+$ $C_{11}H_{11}ClNaO_3$ = 249.0, found = 249.2; HPLC (Chiralpak® IC column, heptane/propan-2-ol 90/10, flow rate 1.0 mL/min at 25 °C, detection at 220 nm): t_R = 6.65 min (minor), t_R = 9.97 min (major). ^{1}H and ^{13}C NMR correspond to the literature.[121]

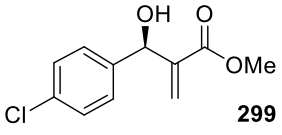

299

Methyl 2-[(*R*)-(4-bromophenyl)(hydroxy)methyl]acrylate (300) as a colourless oil (19.5 mg, 36% yield): $[\alpha]_D^{25} = -58.2$ (*c* 0.58, MeOH, 71% ee); ^{1}H NMR (600 MHz, $CDCl_3$) δ 7.49 – 7.46 (m, 2H), 7.28 – 7.25 (m, 2H), 6.34 (s, 1H), 5.82 (t, *J* = 1.1 Hz, 1H), 5.52 (d, *J* = 5.8 Hz, 1H), 3.73 (s, 3H), 3.05 (d, *J* = 5.8 Hz, 1H); ^{13}C NMR (151 MHz, $CDCl_3$) δ 166.6, 141.5, 140.3, 131.5, 128.3, 126.5, 121.8, 72.8, 52.1; MS (ESI-TOF) m/z: calcd for $[M+Na]^+$ $C_{11}H_{11}BrNaO_3$ = 293.0, found = 293.0; HPLC (Chiralpak® IC column, heptane/propan-2-ol 90/10, flow rate 1.0 mL/min at 25 °C, detection at 220 nm): t_R = 6.66 min (minor), t_R = 9.48 min (major). ^{1}H and ^{13}C NMR correspond to the literature.[121]

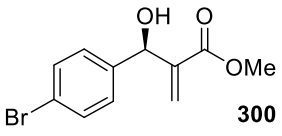

300

Methyl 2-[(*R*)-hydroxy(naphthalen-2-yl)methyl]acrylate (301) as a white solid (14.0 mg, 29% yield): $[\alpha]_D^{25} = -72.1$ (*c* 0.70, MeOH, 68% ee); ^{1}H NMR (600 MHz, $CDCl_3$) δ 7.88 – 7.81 (m, 4H), 7.50 – 7.46 (m, 3H), 6.39 – 6.38 (m, 1H), 5.88 (t, *J* = 1.1 Hz, 1H), 5.74 (d, *J* = 5.5 Hz, 1H), 3.73 (s, 3H), 3.15 (td, *J* = 5.4, 1.8 Hz, 1H); ^{13}C NMR (151 MHz, $CDCl_3$) δ 166.8, 141.8, 138.6, 133.2, 133.0, 128.2, 128.1, 127.6, 126.4, 126.2, 126.0, 125.5, 124.6, 73.4, 52.0; MS (ESI-IT) m/z: calcd for $[M+Na]^+$ $C_{15}H_{14}NaO_3$ = 265.1, found = 265.1; HPLC (Chiralpak® IC column, heptane/propan-2-ol 90/10, flow rate 1.0 mL/min at 25 °C, detection at 220 nm): t_R = 11.75 min (minor), t_R = 16.12 min (major). ^{1}H and ^{13}C NMR correspond to the literature.[121]

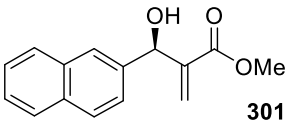

301

Methyl 2-[(*R*)-hydroxy(3-methoxyphenyl)methyl]acrylate (302) as a colourless oil (10.9 mg, 24% yield): $[\alpha]_D^{25} = -48.2$ (*c* 0.42, MeOH, 69% ee); ^{1}H NMR (300 MHz, $CDCl_3$) δ 7.30 – 7.22 (m, 1H), 6.97 – 6.92 (m, 2H), 6.83 (dd, *J* = 8.2, 1.6 Hz, 1H), 6.36 – 6.32 (m, 1H), 5.56 – 5.52 (m, 1H), 5.54 (d, *J* = 5.9 Hz, 1H), 3.81 (s, 3H), 3.74 (s, 3H), 3.02 (d, *J* = 5.8 Hz, 1H); HPLC (Chiralpak® IC column, heptane/propan-2-ol 90/10, flow rate 1.0 mL/min at 25 °C, detection at 220 nm): t_R = 16.88 min (minor), t_R = 22.68 min (major). ^{1}H NMR corresponds to the literature.[292]

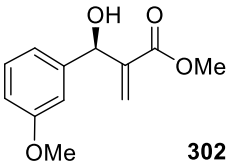

302

Methyl 2-[(*R*)-hydroxy(pyridin-3-yl)methyl]acrylate (303): The residue was purified by gradient silica gel column chromatography (hexane/EtOAc 4/1 to 1/1) to afford a white solid (31.3 mg, 78% yield): $[\alpha]_D^{25} = -65.9$ (*c* 0.38, MeOH, 73% ee); ^{1}H NMR (600 MHz, $CDCl_3$) δ 8.57 (d, *J* = 2.0 Hz, 1H), 8.49 (dd, *J* = 4.8, 1.5 Hz, 1H), 7.73 (dt, *J* = 7.9, 1.7 Hz, 1H), 7.27 (dd, *J* = 7.9, 4.9 Hz, 1H), 6.39 (s, 1H), 5.91 (s, 1H), 5.60 (s, 1H), 3.73 (s, 3H), 3.72 (br s, 1H); ^{13}C NMR (151 MHz, $CDCl_3$) δ 166.4, 150.0, 148.4, 141.3, 137.0, 134.3, 126.6, 123.4, 71.2, 52.1; MS (ESI-IT) m/z: $[M+H]^+$calcd for $C_{10}H_{12}NO_3$ = 194.1, found = 194.3; HPLC (Chiralpak® IC column, heptane/propan-2-ol 80/20, flow rate 1.0 mL/min at 25 °C, detection at 220 nm): t_R = 17.51 min (minor), t_R = 27.84 min (major). ^{1}H and ^{13}C NMR correspond to the literature.[121]

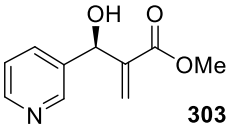

303

Methyl 2-[(*S*)-furan-2-yl(hydroxy)methyl]acrylate (304): as a colourless oil (6.7 mg, 24% yield): $[\alpha]_D^{25} = -64.2$ (*c* 0.27, MeOH, 73% ee); ^{1}H NMR (600 MHz, $CDCl_3$) δ 7.37 (dd, *J* = 1.8, 0.8 Hz, 1H), 6.38 (s, 1H), 6.33 (dd, *J* = 3.2, 1.8 Hz, 1H), 6.25 (d, *J* = 3.3 Hz, 1H), 5.94 (t, *J* = 1.1 Hz, 1H), 5.59 (d, *J* = 6.5 Hz, 1H), 3.76 (s, 3H), 3.15 (d, *J* = 6.7 Hz, 1H); ^{13}C NMR (151 MHz, $CDCl_3$) δ 166.4, 154.1, 142.3, 139.4, 126.8, 110.4, 107.2, 67.4, 52.0; MS (ESI-IT) m/z: calcd for $[M+Na]^+$ $C_9H_{10}NaO_4$ = 205.1, found = 205.2; HPLC (Chiralpak® IC column, heptane/propan-2-ol 80/20, flow rate 1.0 mL/min at 25 °C, detection at 220 nm): t_R = 8.77 min (major), t_R = 24.83 min (minor). ^{1}H and ^{13}C NMR correspond to the literature.[293]

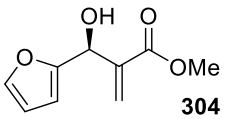

304

Methyl 2-[(*S*)-thiophen-2-yl(hydroxy)methyl]acrylate (305): as a colourless oil (12.0 mg, 28% yield): $[\alpha]_D^{25} = -46.0$ (*c* 0.38, MeOH, 55% ee); ^{1}H NMR (300 MHz, $CDCl_3$) δ 7.28 – 7.24 (m, 1H), 6.99 – 6.94 (m, 2H), 6.37 – 6.35 (m, 1H), 5.95 (t, *J* = 1.0 Hz, 1H), 5.77 (d, *J* = 6.7 Hz, 1H), 3.76 (s, 3H), 3.31 (d, *J* = 6.7 Hz, 1H); HPLC (Chiralpak® IC column, heptane/propan-2-ol 90/10, flow rate 1.0 mL/min at 25 °C, detection at 220 nm): t_R = 10.16 min (minor), t_R = 14.26 min (major). ^{1}H NMR corresponds to the literature.[293]

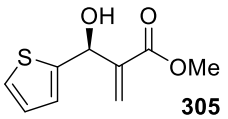

305

12.8 General procedure for the racemic MBH reaction

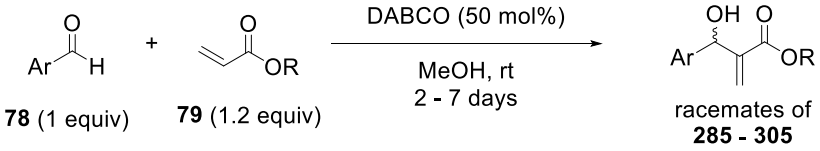

78 (1 equiv) **79** (1.2 equiv) racemates of **285 - 305**

Scheme 93 Racemic MBH reaction

Racemic MBH alcohols were prepared according to Hiemstra *et al.*[241] Acrylate **79** (3 mmol) was added to a solution of aldehyde **78** (2.5 mmol) and DABCO (0.75 mmol) in dry MeOH (7.5 mL). The reaction mixture was stirred at rt for 2 – 7 days. The crude product was purified by silica gel column chromatography (hexane/EtOAc mixtures) to provide the title compound.

Racemic MBH alcohols **285** – **289** and **291** – **305** were successfully prepared. However, the described procedure was not suitable for the preparation of hexafluoroisopropyl 2-[hydroxy(4-nitrophenyl)methyl]acrylate (*rac*-**290**, Scheme 94a) because a side reaction occurred and methyl 2-[hydroxy(4-nitrophenyl)methyl]acrylate (*rac*-**285**) was prepared instead. An analogous transesterification was already described by Hatakeyama (Scheme 94b).[33] MBH alcohol *rac*-**290** was prepared using modified reaction conditions (THF at 0 °C for 2 h instead of MeOH at rt for 2 days).

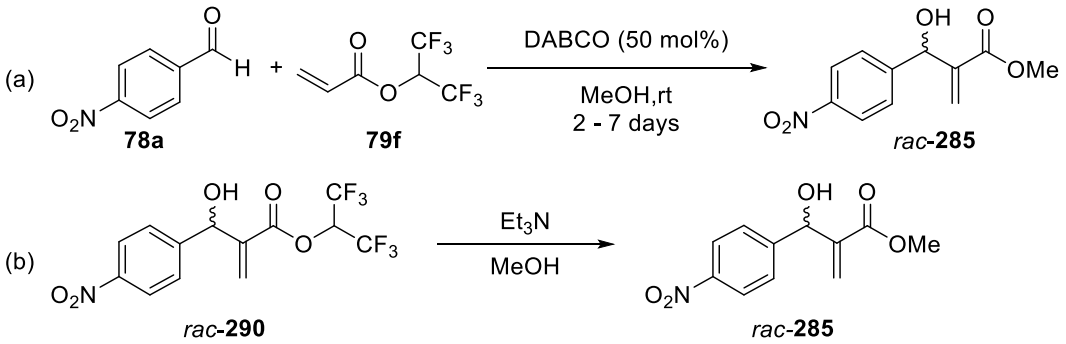

Scheme 94 Transesterification of *rac*-**290** under conditions: (a) used for the preparation of racemic MBH alcohols; (b) described by Hatakeyama.

12.9 Kinetic resolution *via* the Sharpless asymmetric epoxidation

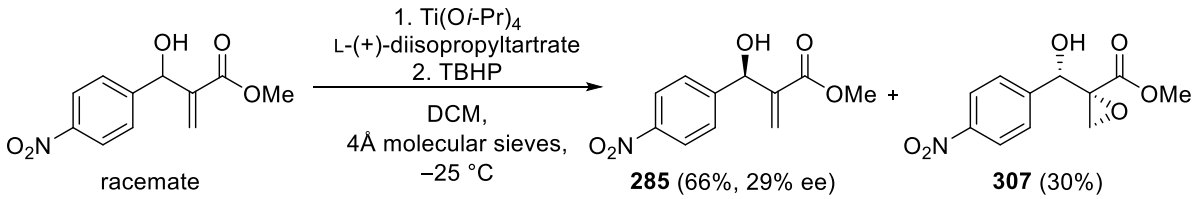

Scheme 95 Kinetic resolution under the Sharpless asymmetric epoxidation.

Following the reported procedure,[33] under argon, Ti(O*i*-Pr)$_4$ (0.47 mL, 1.59 mmol) and L-(+)-diisopropyl tartrate (0.34 mL, 1.91 mmol) were added to a stirring suspension of powdered and activated 4Å molecular sieves (1.6 g) in dry DCM (20 mL) cooled to −25 °C in a cryocooler. The reaction mixture was stirred at −25 °C for 30 min and a solution of racemic methyl 2-[hydroxy(4-nitrophenyl)methyl]acrylate (*rac*-**285**, 754 mg, 3.18 mmol) in dry DCM (8 mL) was added and the reaction mixture was stirred at −25 °C for 1h. Afterwards, a solution of TBHP (5.5 M in decane, 0.35 mL) was added dropwise and the reaction mixture was stirred at −25 °C for 16 h. Then acetone (14 mL) and distilled water (3 mL) were added and after warming up to rt, the resulting emulsion was filtered through a celite pad using EtOAc as an eluent. The filtrate was dried over anhydrous $MgSO_4$ and concentrated under reduced pressure. The residue was purified by gradient silica gel column chromatography (hexane/EtOAc 20/1 to hexane/EtOAc 1/1) to afford enantioenriched MBH alcohol **285** and oxirane **307**. **Methyl 2-[hydroxy(4-nitrophenyl)methyl]acrylate** (**285**) as a yellow oil (499 mg, 66% yiled): $[\alpha]_D^{25} = -22.2$ (*c* 0.63, MeOH, 29% ee); HPLC (Chiralpak® IC column, heptane/propan-2-ol 80/20, flow rate 1.0 mL/min at 25 °C, detection at 220 nm): t_R = 6.62 min (minor), t_R = 7.90 min (major). **Methyl (*R*)-2-[(*S*)-hydroxy(4-nitrophenyl)methyl]oxirane-2-carboxylate** (**307**) as colourless oil (244 mg, 30% yield): $[\alpha]_D^{25} = -21.4$ (*c* 0.56, $CHCl_3$); ^{1}H NMR (300 MHz, $CDCl_3$) δ 8.20 (d, *J* = 8.8 Hz, 2H), 7.64 (d, *J* = 8.7 Hz, 2H), 5.14 (br s, 1H), 3.73 (s, 3H), 3.33 – 3.06 (br s, 1H), 3.19 (d, *J* = 5.6 Hz, 1H), 2.93 (d, *J* = 5.6 Hz, 1H).^{1}H NMR corresponds to the literature.[294]

12.10 Preparation of allenoates

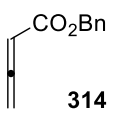

Benzyl buta-2,3-dienoate (314): Benzyl bromoacetate (**313**, 15.9 mL, 100.0 mmol) was added slowly over 15 min to a solution of PPh_3 (26.9 g, 100.0 mmol) in toluene (200 mL). The reaction mixture was stirred at rt overnight. The precipitate formed was filtered, washed with toluene (5 x 30 mL), and vacuum dried to afford phosphonium salt as a white solid (46.4 g, 94% yield). NaOH (2 M aq, 50 mL) was added slowly to a solution of phosphonium salt (25.0 g, 50.9 mmol) in DCM (50 mL). The reaction mixture was stirred at rt for 24 h. The layers were separated and the aqueous layer was extracted with DCM (3 x 30 mL). The combined organic layer was dried over anhydrous $MgSO_4$ and concentrated under reduced pressure to afford benzyl (triphenylphosphoranylidene)acetate as a white solid (20.7 g, 99% yield).[248] Under argon, Et_3N (3.0 mL, 21.4 mmol) was added slowly to a solution of benzyl (triphenylphosphoranylidene)acetate (8.8 g, 21.4 mmol) in dry DCM (40 mL). After stirring at rt for 5 min, acetyl chloride (1.52 mL, 21.4 mmol) was added dropwise. The reaction mixture was stirred at rt for 1 h and concentrated under reduced pressure. Hexane (130 mL) was added and the residue was allowed to stand for 2 h, while it was shaken periodically to facilitate precipitation. The precipitate was removed by filtration and washed with hexane. The filtrate was concentrated under reduced pressure and the residue was purified by silica gel column chromatography (hexane/EtOAc 4/1) to afford **314** as a colourless oil (2.1 g, 58%

yield): ^{1}H NMR (300 MHz, $CDCl_3$) δ 7.42 – 7.29 (m, 5H), 5.69 (t, *J* = 6.5 Hz, 1H), 5.24 (d, *J* = 6.5 Hz, 2H), 5.20 (s, 2H). ^{1}H NMR corresponds with the literature.[246]

Benzyl 2-(hydroxymethyl)buta-2,3-dienoate (315): Paraformaldehyde and DABCO were pre-dried under vacuum at 50 °C (oil bath temperature) for 30 min. Under argon, a suspension of paraformaldehyde (1.81 g, 60.3 mmol) in dry THF (40 mL) was cooled to −10 °C in a cryocooler. A solution of DABCO (258 mg, 2.3 mmol) in dry THF (15 mL) and a solution of allenoate **314** (2 g, 11.5 mmol) in dry THF (15 mL) were added to the suspension at −10 °C. The reaction mixture was allowed to warm up to rt and stirred at rt for 1.5 h. A solution of NH_4Cl (40 mL, sat aq) was added and the resulting solution was extracted with EtOAc (5 x 15 mL). The combined organic layer was washed with brine, dried over anhydrous $MgSO_4$, and concentrated under reduced pressure. The crude product was purified by gradient silica gel column chromatography (hexane/EtOAc 4/1 to hexane/EtOAc 2/1) to afford **315** as a white solid (675 mg, 27% yield): ^{1}H NMR (300 MHz, $CDCl_3$) δ 7.35 – 7.22 (m, 5H), 5.23 (t, *J* = 2.2 Hz, 2H), 5.20 (s, 2H), 4.33 (s, 2H), 3.06 (s, 1H). ^{1}H NMR corresponds to the literature.[246]

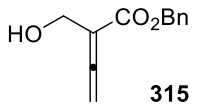

315

Benzyl 2-(acetoxymethyl)buta-2,3-dienoate (90): Under argon, a solution of allenoate **315** (385 mg, 1.89 mmol) in dry DCM (3 mL) was cooled to 0 °C in an ice bath. A solution of acetyl chloride (0.15 mL, 2.07 mmol) in dry DCM (1 mL), followed by a solution of Et_3N (0.20 mL, 2.07 mmol) in dry DCM (1 mL), were added slowly. The reaction mixture was stirred at 0 °C for 20 min and at rt for 30 min. Then EtOAc was added and the precipitate formed was filtered off and washed with EtOAc. The filtrate was concentrated under reduced pressure and the residue was purified by silica gel column chromatography (hexane/EtOAc 10/1) to afford **90** as a colourless oil (241 mg, 53% yield): ^{1}H NMR (300 MHz, $CDCl_3$) δ 7.37 – 7.29 (m, 5H), 5.29 (t, *J* = 2.2 Hz, 2H), 5.21 (s, 2H), 4.80 (t, *J* = 2.2 Hz, 2H), 2.03 (s, 3H). ^{1}H NMR corresponds to the literature.[132]

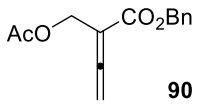

90

12.11 X-ray Diffraction Data

Single-crystal X-ray diffraction data for **284** were obtained from Bruker ApexII-CCD diffractometer by monochromatized MoKα radiation ($\lambda = 0.71073$ Å) at 150(2)K. The structure was solved by direct methods (SHELXS)[295] and refined by full-matrix least squares based on F^2 (SHELXL97). The hydrogen atoms were fixed into idealised positions (riding model) and assigned temperature factors $H_{iso}(H) = 1.2\ U_{eq}$ (pivot atom). One of the phenyl rings is disordered over two equally occupied positions.

Crystal data for **284**: $C_{28}H_{41}N_2O_6P$, $M_r = 532.60$, Triclinic, $P1$ (No 1), a = 4.7183 (2) Å, $b = 10.3408$ (4) Å, $c = 15.0173$ (6) Å, $\alpha = 89.561$ (2) °, $\beta = 82.906$ (2) °, $\gamma = 79.299$ (2) °, $V = 714.37$ (5) Å^3, $Z = 1$, $D_x = 1.238$ mg · m^{-3}, colourless crystal of dimensions 0.52 × 0.23 × 0.12 mm, multi-scan absorption correction ($\mu = 0.14$ mm^{-1}), $T_{min} = 0.932$, $T_{max} = 0.983$; a total of 9139 measured reflections ($\theta_{max} = 26°$), from which 4891 were unique ($R_{int} = 0.017$) and 4505 observed according to the $I > 2\sigma(I)$ criterion. The refinement converged ($\Delta/\sigma_{max} < 0.001$) to $R = 0.034$ for observed reflections and $wR(F^2) = 0.080$, $GOF = 1.03$ for 376 parameters and all 4891 reflections. The final difference map displayed no peaks of chemical significance ($\Delta\rho_{max} = 0.16$, $\Delta\rho_{min}$ −0.17 e.Å^{-3})

Crystallographic data (excluding structure factors) for the structures has been deposited with the Cambridge Crystallographic Data Centre with CCDC number 1038565. Copies of the data can be obtained, free of charge, on application to Cambridge Crystallographic Data Centre, 12 Union Road, Cambridge CB2 1EZ, UK, (fax: +44-(0)1223-336033 or e-mail: deposit@ccdc.cam.ac.uk).

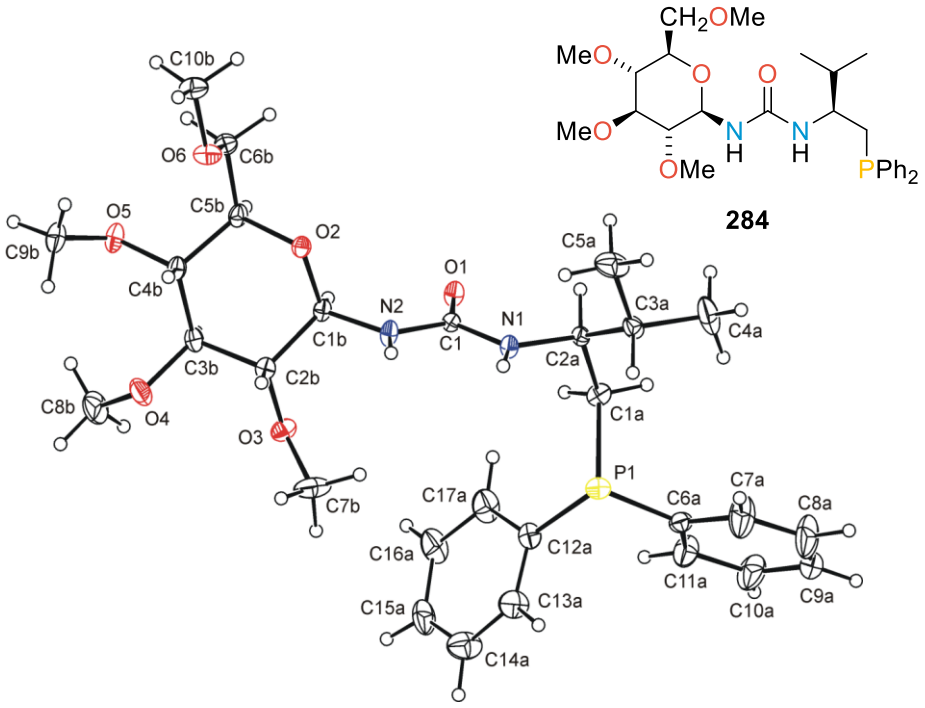

Figure 37 View on the molecule of **284** with the atom numbering scheme. The displacement ellipsoids are drawn with a 30% probability level. The second position of disordered atoms C13b, C14b, C16b, C17b are omitted for clarity.

13 Experimental part: direct catalytic asymmetric C–H arylation

Reagents were purchased from common commercial suppliers and used without further purification unless otherwise stated. Anhydrous solvents were either purchased from commercial suppliers or obtained by Grubbs solvent purification system and stored over molecular sieves under argon atmosphere. All reactions involving chromium complexes were carried out in the dark, covered with aluminium foil. All air and moisture sensitive reactions were performed under a dry argon or nitrogen atmosphere. Glassware was flame-dried under vacuum and allowed to cool under vacuum/argon prior to use. Solvents were evaporated using a rotary evaporator and all products were dried using a high vacuum.

Column chromatography was performed on silica gel (40 – 63 μL). Column chromatography was carried out using a Biotage Isolera Four purification system, employing Biotage ZIP cartridges. Analytical thin layer chromatography was performed on pre-coated aluminium-backed silica gel F_{254} plates with visualization under UV light (λ = 254 nm).

NMR spectra were recorded on Bruker AV–400/AV–500 instrument at a constant temperature of 300 K using $CDCl_3$, acetone-d_6 or CD_3OD as solvents. Chemical shifts (δ) are reported in parts per million (ppm) from low to high field and referenced to the residual solvent peak ($CDCl_3$: δ 7.26/77.16; acetone-d_6 δ 2.05/206.3; CD_3OD δ 3.31/49.0 for $^1H/^{13}C$ NMR, respectively). Chemical shifts of phosphorus spectra are referenced relative to the external standard 85% H_3PO_4 ($CDCl_3$: δ = 0 ppm). Coupling constants (*J*) are reported in Hertz (Hz). Standard abbreviations indicating multiplicity were used as follows: m = multiplet, q = quartet, t = triplet, d = doublet, s = singlet, br = broad signal, dd - doublet of doublet, dt - doublet of triplet, ddd - doublet of doublet of doublet. High Resolution Mass Spectroscopy (HRMS) were recorded on Thermo Finnigan MAT95XP or Thermo Scientific Exactive Plus EMR using the electrospray ionization (ESI) technique.

High performance liquid chromatography (HPLC) was performed on Agilent Technologies chromatographs (Series 1260; G1315D - 1260 DAD VL) using Chiralpak® AD-H, Chiralpak® IB, and Amylose-1 columns at 20 °C and mixtures of HPLC-grade hexane and propan-2-ol as an eluent. The detailed conditions are given in the characterization part of the products. Enantiomeric ratios of the enantioenriched products were determined by comparison of the asymmetric products/reaction mixtures with the racemic ones.

13.1 Preparation of (arene)tricarbonylchromium complex

(Fluorobenzene)tricarbonylchromium (319a)[173]: A flame-dried round-bottom flask equipped with a reflux condenser was charged with $Cr(CO)_6$ (1100 mg, 5.1 mmol), evacuated, and backfilled with argon. The fluorobenzene (**141a**, 4.5 mL, 47.5 mmol) was added to the flask, followed by the addition of anhydrous di-*n*-butyl ether (30.6 mL) and dry THF (3.4 mL). The resulting suspension was subjected to three freeze-pump-thaw cycles (30 minutes each), the reaction vessel was wrapped with aluminium foil and then refluxed (oil bath temperature was 160 °C) for 48 h. The solution was then cooled down to rt and filtered through a short pad of silica gel using toluene (50 mL) as an eluent. The organic layer was then concentrated under reduced pressure. Recrystallization from hexane afforded the product **319a** as a yellow solid (820 mg, 76% yield): ^1H NMR (400 MHz, $CDCl_3$) δ 5.50 (dt, *J* = 6.4, 3.1 Hz, 2H), 5.36 – 5.30 (m, 2H), 4.86 (dt, *J* = 6.1, 2.8 Hz, 1H).

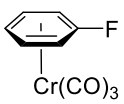

319a

13.2 Synthesis of (*S*) and (*R*)-(*H8*)-BINAP(O)

5,5',6,6',7,7',8,8'-Octahydro-[1,1'-binaphthalen]-2,2'-diyl bis(trifluoromethanesulfonate) (327):

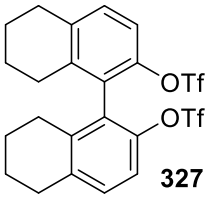

327

Under nitrogen, pyridine (1.8 mL, 22.1 mmol) was added to a solution of (*S*)-(H_8)-BINOL (*S*)-**326** (2.50 g, 8.5 mmol) in dry DCM (88 mL). After stirring at rt for 5 min, the solution was cooled to 0 °C using an ice bath and Tf_2O (3.1 mL, 18.7 mmol) was added slowly and the reaction mixture was stirred at rt for 20 h. After this time, the reaction mixture was filtered through a pad of silica gel using hexane (60 mL) as an eluent. The filtrate was concentrated under reduced pressure to afford exclusively (*S*)-**327** as a white solid (4.60 g, 98% yield). Starting from (*R*)-enantiomer (*R*)-**326**, compound (*R*)-**327** was yielded exclusively as a white solid (3.45 g, 73% yield): ^{1}H NMR (400 MHz, $CDCl_3$) δ 7.19 (AB spin system, J_{AB} = 8.7 Hz, Δν = 36.9 Hz, 4H), 2.85 (t, *J* = 6.3 Hz, 4H), 2.35 (AB spin system of triplets, J_{AB} = 17.3 Hz, Δν = 53.2 Hz, *J* = 6.3 Hz, 4H), 1.87 – 1.62 (m, 8H); ^{13}C NMR (101 MHz, $CDCl_3$) δ 144.9 (s), 139.4 (s), 138.4 (s), 131.0 (s), 127.2 (s), 118.4 (q, *J* = 319.9 Hz), 118.2 (s), 29.5 (s), 27.6 (s), 22.5 (s), 22.5 (s); ^{19}F NMR (376 MHz, $CDCl_3$) δ −74.8 (s); HRMS (ESI) m/z: $[M+H]^+$ calcd for $C_{23}H_{21}O_6F_6S_2$ = 559.0678, found = 559.0673.

2'-(Diphenylphosphoryl)-5,5',6,6',7,7',8,8'-octahydro-[1,1'-binaphthalen]-2-yl trifluoromethanesulfonate (328):

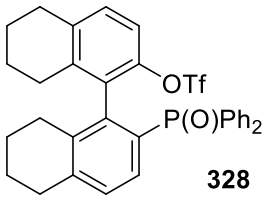

328

Under nitrogen, dry *i*-Pr_2NEt (1.9 mL, 10.71 mmol) was added to a solution of (*S*)-**327** (1500 mg, 2.69 mmol), diphenylphosphine oxide (1086 mg, 5.37 mmol), $Pd(OAc)_2$ (60 mg, 0.27 mmol), and 1,4-bis(diphenylphosphino)butane (114.5 mg, 0.27 mmol) in dry DMSO (13 mL). The reaction mixture was stirred at rt for 20 min and then at 110 °C (oil bath temperature) for 23 h. After this time, the reaction mixture was cooled down to rt and water (60 mL) was added. The resulting solution was extracted with Et_2O (5 x 20 mL). The combined organic layer was dried over anhydrous $MgSO_4$ and concentrated under reduced pressure. The residue was purified by silica gel column chromatography (hexane/EtOAc 4/1) to afford exclusively (*S*)-**328** as a white solid (1548 mg, 95% yield). Starting from (*R*)-enantiomer (*R*)-**327**, compound (*R*)-**328** was yielded exclusively as a white solid (1124 mg, 69% yield): ^{1}H NMR (400 MHz, $CDCl_3$) δ 7.66 – 7.56 (m, 2H), 7.52 – 7.44 (m, 3H), 7.44 – 7.36 (m, 3H), 7.34 – 7.26 (m, 2H), 7.19 – 7.08 (m, 2H), 6.58 (AB spin system, J_{AB} = 8.5 Hz, Δν = 115.2 Hz, 2H), 2.89 – 2.80 (m, 2H), 2.80 – 2.72 (m, 2H), 2.52 – 2.28 (m, 2H), 2.15 – 1.99 (m, 2H), 1.83 – 1.50 (m, 8H); ^{13}C NMR (101 MHz, $CDCl_3$) δ 145.5 – 117.0 (25C, aromatic carbons and OSO_2CF_3, observed complexity due to C−P splitting), 30.4 (s), 29.6 (s), 28.0 (s), 27.0 (s), 23.0 (s), 22.6 (s), 22.5 (s), 22.5 (s); ^{19}F NMR (376 MHz, $CDCl_3$) δ −75.1 (s); ^{31}P NMR (162 MHz, $CDCl_3$) δ 27.4 (s); HRMS (ESI) m/z: $[M+H]^+$ calcd for $C_{33}H_{31}O_4F_3PS$ = 611.1627, found = 611.1622; HPLC (Lux® 5 µm Amylose-1 column, hexane/propan-2-ol 98/2, flow rate 0.8 mL/min at 20 °C, detection at 280 nm): t_R = 55.9 min (*R*), t_R = 69.3 min (*S*).

2'-(Diphenylphosphino)-5,5',6,6',7,7',8,8'-octahydro-[1,1'-binaphthalen]-2-yl trifluoromethanesulfonate (329):

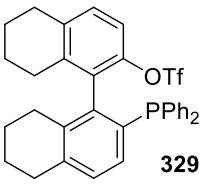

329

Under nitrogen, a solution of (*S*)-**328** (950 mg, 1.6 mmol) and dry Et_3N (8.7 mL, 62.2 mmol) in dry toluene (30 mL) was subjected to three freeze-pump-thaw cycles (30 minutes each) and cooled to 0 °C in an ice bath. Trichlorosilane (1.6 mL, 15.6 mmol) was added slowly. The reaction mixture was stirred at 0 °C for 10 min and then at 110 °C (oil

bath temperature) for 14 h. After this time, the reaction mixture was cooled down to rt, diluted with Et_2O, and filtered through a pad of silica gel using EtOAc (40 mL) as an eluent. The filtrate was dried over anhydrous $MgSO_4$ and concentrated under reduced pressure to afford exclusively (*S*)-**329** as a white solid (826 mg, 89% yield). Starting from (*R*)-enantiomer (*R*)-**328**, compound (*R*)-**329** was yielded exclusively as a white solid (909 mg, 98% yield): ^{1}H NMR (400 MHz, $CDCl_3$) δ 7.34 – 7.23 (m, 6H), 7.23 – 7.11 (m, 5H), 7.11 – 7.04 (m, 2H), 7.03 – 6.96 (m, 1H), 2.89 – 2.69 (m, 4H), 2.45 – 2.32 (m, 1H), 2.20 – 2.00 (m, 2H), 1.90 – 1.36 (m, 8H), 1.25 – 1.09 (m, 1H); ^{13}C NMR (101 MHz, $CDCl_3$) δ 145.5 – 116.0 (25C, aromatic carbons and OSO_2CF_3, observed complexity due to C−P splitting), 30.1 (s), 29.6 (s), 27.8 (s), 27.5 (s), 23.1 (s), 22.8 (s), 22.5 (s), 22.4 (s); ^{19}F NMR (376 MHz, $CDCl_3$) δ −75.0 (s); ^{31}P NMR (162 MHz, $CDCl_3$) δ −14.5 (s); HRMS (ESI) m/z: $[M+H]^+$ calcd for $C_{33}H_{31}O_3F_3PS$ = 595.1678, found = 595.1672; HPLC (Lux® 5 µm Amylose-1 column, hexane/propan-2-ol 95/5, flow rate 0.8 mL/min at 20 °C, detection at 280 nm): t_R = 20.7 min (*S*), t_R = 23.7 min (*R*).

[2'-(Diphenylphosphino)-5,5',6,6',7,7',8,8'-octahydro-[1,1'-binaphthalen]-2-yl]diphenylphosphine oxide (322):

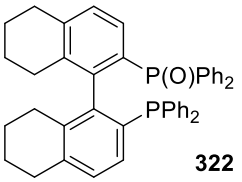

322

Under nitrogen, dry *i*-Pr_2NEt (0.91 mL, 5.2 mmol) was added to a solution of (*S*)-**329** (775 mg, 1.3 mmol), diphenylphosphine oxide (527 mg, 2.6 mmol), $Pd(OAc)_2$ (29 mg, 0.13 mmol), and 1,3-bis(diphenylphosphino)butane (56 mg, 0.13 mmol) in dry DMSO (10 mL). The reaction mixture was stirred at rt for 20 min and then at 110 °C (oil bath temperature) for 23 h. After this time, the reaction mixture was cooled down to rt and water (40 mL) was added. The resulting solution was extracted with DCM (5 x 20 mL). The combined organic layer was dried over anhydrous $MgSO_4$ and concentrated under reduced pressure. The residue was purified by silica gel column chromatography (hexane/EtOAc 4/1) to afford (*S*)-**322** as a white solid (460 mg, 55% yield). Starting from (*R*)-enantiomer (*R*)-**329**, compound (*R*)-**322** was yielded as a white solid (259 mg, 31% yield). Racemization during reaction course caused that desired products (*R*)-**322** and (S)-**322** were not enantiomerically pure (ee varied from 18% to 82%): ^{1}H NMR (400 MHz, $CDCl_3$) δ 7.72 – 7.53 (m, 4H), 7.49 – 7.21 (m, 13H), 7.21 – 7.08 (m, 4H), 7.08 – 6.93 (m, 3H), 2.77 – 2.61 (m, 4H), 1.91 – 1.65 (m, 3H), 1.57 – 1.06 (m, 8H), 0.81 – 0.68 (m, 1H); ^{13}C NMR (101 MHz, $CDCl_3$) δ 146.5 – 125.0 (36C, aromatic carbons, observed complexity due to C−P splitting), 30.3 (s), 29.9 (s), 27.8 (s), 26.9 (s), 23.0 (s), 22.7 (s), 22.4 (s), 22.3 (s); ^{31}P NMR (162 MHz, $CDCl_3$) δ 27.7 (s), −17.1 (s); HRMS (ESI) m/z: $[M+H]^+$ calcd for $C_{44}H_{41}OP_2$= 647.2627, found = 647.2623; HPLC (Lux® 5 µm Amylose-1 column, hexane/propan-2-ol 97/3, flow rate 0.8 mL/min at 20 °C, detection at 280 nm): t_R = 16.2 min (*R*), t_R = 34.5 min (*S*).

Diphenylphosphine oxide (330):[256]

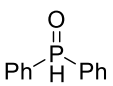
330

Under nitrogen, chlorodiphenylphosphine (4.2 mL, 22.7 mmol) was added to a suspension of K_2CO_3 (626 mg, 45.3 mmol) in acetonitrile (25 mL). The reaction mixture was cooled to 0 °C using an ice bath and degassed distilled water (2.2 mL, 120.1 mmol) was added slowly. The reaction mixture was warmed up to rt and stirred at rt overnight. Then water (25 mL) was added and the resulting solution was extracted with DCM (5 x 20 mL). The combined organic layer was washed with $NaHCO_3$ (sat aq), dried over anhydrous $MgSO_4$, and concentrated under reduced pressure. Residual oil was freeze-dried to afford compound **330** as an off-white solid (3283 mg, 72% yield): ^{1}H NMR (500 MHz, $CDCl_3$) δ 8.07 (d, *J* = 480.7, 1H), 7.72 – 7.67 (m, 4H), 7.59 – 7.48 (m, 6H); ^{13}C NMR (126 MHz, $CDCl_3$) δ 132.5 (d, *J* = 2.9 Hz), 131.4 (d, *J* = 101.5 Hz),

130.7 (d, J = 11.5 Hz), 128.9 (d, J = 12.9 Hz); ^{31}P NMR (202 MHz, $CDCl_3$) δ 21.5 (s). ^{1}H NMR corresponds to the literature.[256]

(*S*)-5,5',6,6',7,7',8,8'-Octahydro-[1,1'-binaphthalene]-2,2'-diol ((*S*)-326):

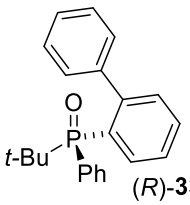

(*R*)-**338**

NaOH (2 M aq, 2.9 mL) was added to a suspension of bistriflate (*S*)-**327** (200 mg, 0.36 mmol) in a mixture of dioxane (2 mL) and methanol (1 mL). The reaction mixture was stirred at rt overnight. Then HCl (2 M aq) was added until a pH of 1 and the resulting mixture was extracted with DCM (5 x 20 mL). The combined organic layer was dried over anhydrous $MgSO_4$ and concentrated under reduced pressure. The residue was purified by silica gel column chromatography (hexane/EtOAc 4/1) to afford (*S*)-**326** as a white solid (60 mg, 57% yield, 99% ee): ^{1}H NMR (500 MHz, $CDCl_3$) δ 7.07 (d, J = 8.3 Hz, 2H), 6.83 (d, J = 8.3 Hz, 2H), 4.55 (br s, 2H), 2.78 – 2.72 (m, 4H), 2.34 – 2.25 (m, 2H), 2.21 – 2.11 (m, 2H), 1.78 – 1.62 (m, 8H); ^{13}C NMR (126 MHz, $CDCl_3$) δ 151.3, 137.1, 131.1, 130.1, 118.8, 112.9, 29.2, 27.1, 23.0, 22.9; HPLC (Lux® 5 µm Amylose-1 column, hexane/propan-2-ol 99/1 until 120 min and then hexane/propan-2-ol 90/10, flow rate 0.8 mL/min at 20 °C, detection at 280 nm): t_R = 46.0 min (*S*), t_R = 126.3 min (*R*). ^{1}H NMR corresponds to the literature.[296]

13.3 Synthesis of axially chiral phosphinoalcohols 323 and 324

(*S*)-2'-(Diphenylphosphino)-5,5',6,6',7,7',8,8'-octahydro-[1,1'-binaphthalene]-2-ol ((*S*)-323):

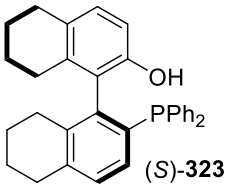

(*S*)-**323**

NaOH (2 M aq, 1.4 mL) was added to a suspension of triflate (*S*)-**329** (200 mg, 0.34 mmol) in a mixture of dioxane (2 mL) and methanol (1 mL). The reaction mixture was subjected to three freeze-pump-thaw cycles (10 minutes each). The reaction mixture was stirred at rt for 24 h and then concentrated under reduced pressure. The residue was purified by silica gel column chromatography (hexane/EtOAc 10/1) to afford (*S*)-**323** as a white solid (105 mg, 68% yield): ^{1}H NMR (400 MHz, $CDCl_3$) δ 7.31 – 7.26 (m, 6H), 7.25 – 7.17 (m, 4H), 7.09 (d, J = 7.9 Hz, 1H), 7.05 – 6.99 (m, 2H), 6.69 (d, J = 8.2 Hz, 1H), 4.05 (s, 1H), 2.86 – 2.77 (m, 2H), 2.72 – 2.65 (m, 2H), 2.33 – 2.13 (m, 2H), 2.01 – 1.85 (m, 2H), 1.80 – 1.52 (m, 6H), 1.52 – 1.38 (m, 1H), 1.37 – 1.22 (m, 1H); ^{13}C NMR (101 MHz, $CDCl_3$) δ 149.9 – 112.5 (24C, aromatic carbons, observed complexity due to C–P splitting), 30.1 (s), 29.2 (s), 27.7 (d, J = 2.5 Hz), 27.1 (d, J = 2.0 Hz), 23.2 (s), 22.9 (s), 22.8 (s), 22.6 (s); ^{31}P NMR (162 MHz, $CDCl_3$) δ −15.1 (s).

Methyl(*S*)-2'-{[(trifluoromethyl)sulfonyl]oxy}-5,5',6,6',7,7',8,8'-octahydro-[1,1'-binaphthalene]-2-carboxylate ((*S*)-331):

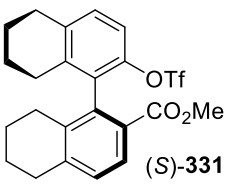

(*S*)-**331**

Compound (*S*)-**327** (1.5 g, 2.69 mmol), $Pd(OAc)_2$ (109 mg, 0.48 mmol), bis(diphenylphosphino)propane (100 mg, 0.24 mmol), and Et_3N (3.7 mL, 26.90 mmol) were dissolved in a mixture of DMSO (75 mL) and MeOH (50 mL) and the reaction mixture was subjected to three freeze-pump-thaw cycles (30 minutes each). After charging the reaction flask with CO, the reaction mixture was stirred at 70 °C (oil bath temperature) for 18 h. After this time, the reaction mixture was cooled down to rt and water (50 mL) was added. The resulting solution was extracted with DCM (5 x 20 mL). The combined organic layer was dried over anhydrous $MgSO_4$ and concentrated under reduced pressure. The residue was purified by silica gel column chromatography (hexane/EtOAc 9/1) to afford (*S*)-**331** and (*S*)-**332**. **((*S*)-331)** was obtained as a white solid (650 mg, 52% yield): ^{1}H NMR (500 MHz, $CDCl_3$) δ 7.83 (d, J = 8.0 Hz, 1H), 7.20 (d, J = 8.1 Hz, 1H), 7.14 (d, J =

8.5 Hz, 1H), 7.09 (d, *J* = 8.5 Hz, 1H), 3.63 (s, 3H), 2.93 – 2.78 (m, 4H), 2.38 – 2.23 (m, 2H), 2.17 – 2.02 (m, 2H), 1.82 – 1.60 (m, 8H); ^{13}C NMR (101 MHz, $CDCl_3$) δ 166.9 (s), 144.1 (s), 142.9 (s), 138.2 (s), 137.3 (s), 136.5 (s), 135.3 (s), 133.2 (s), 129.6 (s), 129.4 (s), 127.8 (s), 127.5 (s), 118.3 (q, *J* = 319.8 Hz) 117.9 (s), 51.9 (s), 30.4 (s), 29.7 (s), 27.7 (s), 27.2 (s), 23.0 (s), 22.8 (s), 22.7 (s), 22.5 (s); ^{19}F NMR (376 MHz, $CDCl_3$) δ −74.9 (s); HRMS (ESI) *m/z*: $[M+H]^+$ calcd for $C_{23}H_{24}O_5F_3S$ = 469.1291, found = 469.1277.

Dimethyl (*S*)-5,5',6,6',7,7',8,8'-octahydro-[1,1'-binaphtha-lene]-2,2'-dicarboxylate ((*S*)-332) as a viscous colourless oil (71 mg, 7% yield): ^{1}H NMR (400 MHz, $CDCl_3$) δ 7.76 (d, *J* = 8.0 Hz, 2H), 7.12 (d, *J* = 8.1 Hz, 2H), 3.57 (s, 6H), 2.93 – 2.77 (m, 4H), 2.23 – 2.09 (m, 2H), 2.06 – 1.92 (m, 2H), 1.80 – 1.57 (m, 8H); ^{13}C NMR (101 MHz, $CDCl_3$) δ 167.4, 141.8, 141.7, 135.2, 128.0, 127.0, 126.3, 51.6, 30.3, 27.3, 23.1, 22.5. ^{1}H NMR corresponds to the literature.[297]

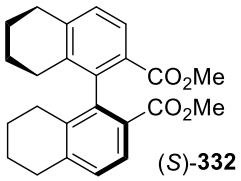

(*S*)-**332**

Methyl (*S*)-2'-(diphenylphosphoryl)-5,5',6,6',7,7',8,8'-octahydro-[1,1'-binaphthalene]-2-carboxylate ((*S*)-333):

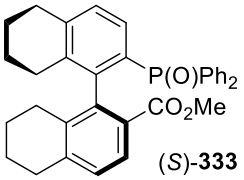

(*S*)-**333**

Under nitrogen, dry *i*-Pr_2NEt (0.27 mL, 1.54 mmol) was added to a solution of (*S*)-**331** (150 mg, 0.32 mmol), diphenylphosphine oxide (130 mg, 0.64 mmol), $Pd(OAc)_2$ (7 mg, 0.03 mmol), and bis(diphenylphosphino)butane (14 mg, 0.03 mmol) in dry DMSO (2.5 mL). The reaction mixture was stirred at 110 °C (oil bath temperature) for 3 days. After this time, the reaction mixture was cooled down to rt and water (10 mL) was added. The resulting solution was extracted with DCM (5 x 20 mL). The combined organic layer was dried over anhydrous $MgSO_4$ and concentrated under reduced pressure. The residue was purified by gradient silica gel column chromatography (hexane to hexane/EtOAc 2/1) to afford the desired product (*S*)-**333** as a white solid (126 mg, 61% yield): ^{1}H NMR (400 MHz, $CDCl_3$) δ 7.62 – 7.51 (m, 3H), 7.48 – 7.40 (m, 3H), 7.39 – 7.32 (m, 3H), 7.28 – 7.22 (m, 2H), 7.22 – 7.13 (m, 1H), 7.10 – 7.04 (m, 1H), 6.97 (d, *J* = 8.1 Hz, 1H), 3.49 (s, 3H), 2.93 – 2.78 (m, 2H), 2.75 – 2.67 (m, 2H), 2.35 – 2.11 (m, 2H), 2.03 – 1.84 (m, 2H), 1.76 – 1.57 (m, 6H), 1.57 – 1.46 (m, 2H); ^{13}C NMR (101 MHz, $CDCl_3$) δ 166.7 (s), 145.5 – 125.5 (24C, aromatic carbons, observed complexity due to C–P splitting), 51.5 (s), 30.4 (s), 30.4 (s), 27.7 (s), 27.2 (s), 23.3 (s), 23.0 (s), 22.7 (s), 22.4 (s); ^{31}P NMR (162 MHz, $CDCl_3$) δ 27.2 (s); HRMS (ESI) *m/z*: $[M+H]^+$calcd for $C_{34}H_{34}O_3P$ = 521.2240, found = 521.2226.

(*S*)-[2'-(Diphenylphosphino)-5,5',6,6',7,7',8,8'-octahydro-[1,1'-binaphthalen]-2-yl]methanol ((*S*)-334):

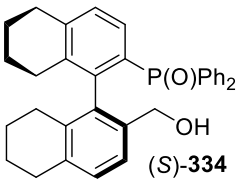

(*S*)-**334**

Under argon, a solution of compound (*S*)-**333** (50 mg, 0.08 mmol) in dry THF (1 mL) was cooled to 0 °C in an ice bath and a solution of $LiAlH_4$ (2.4 M in THF, 32 µL) was added slowly. The reaction mixture was stirred at rt for 20 h and then NaOH (2 M aq, 2 mL) was added. Suspension was filtered through a celite pad using Et_2O (10 mL) as an eluent. The combined organic layer was dried over anhydrous $MgSO_4$ and concentrated under reduced pressure. The residue was purified by gradient silica gel column chromatography (hexane to hexane/EtOAc 4/1) to afford phosphine oxide (*S*)-**334** as a white solid (12 mg, 34% yield): ^{1}H NMR (400 MHz, $CDCl_3$) δ 7.75 – 7.68 (m, 2H), 7.56 – 7.40 (m, 7H), 7.39 – 7.32 (m, 2H), 7.13 – 6.99 (m, 3H), 4.30 (d, *J* = 11.1 Hz, 1H), 4.11 (d, *J* = 11.1 Hz, 1H), 2.85 (t, *J* = 6.2 Hz, 2H), 2.59 (dt, *J* = 16.4, 5.6 Hz, 1H), 2.45 – 2.36 (m, 1H), 2.06 – 1.98 (m, 2H), 1.80 – 1.58 (m, 8H), 1.44 – 1.19 (m, 2H), 0.85 – 0.74 (m, 1H); ^{31}P NMR (162 MHz, $CDCl_3$) δ 29.9 (s).

13.4 Synthesis of the ligand with a chiral centre on the phosphorus atom

***tert*-Butyl(phenyl)phosphine oxide (*rac*-336):** Under argon, dichlorophenylphosphine (**335**, 3.8 mL, 27.9 mmol) was dissolved in dry pentane (56 mL) in a two-necked flask. The resulting solution was subjected to three freeze-pump-thaw cycles (30 minutes each) and cooled to −78 °C (acetone/dry ice bath). Then *tert*-butyl lithium (1.7 M in pentane, 16.4 mL) was added slowly *via* a syringe and the reaction mixture was stirred at −78 °C for 1 h and at rt for 1 h. Then it was cooled to 0 °C in an ice bath and sulfuric acid (2 M aq, 50 mL) was added slowly. The resulting solution was stirred at 0 °C for 1 h and concentrated under reduced pressure. The residue was extracted with DCM (5 x 20 mL). The combined organic layer was dried over anhydrous $MgSO_4$ and concentrated under reduced pressure. The residue was purified by gradient silica gel column chromatography (hexane/EtOAc 5/1 to pure EtOAc) to afford racemic product *rac*-**336** as a white solid (4021 mg, 79% yield): ^{1}H NMR (400 MHz, $CDCl_3$) δ 7.72 – 7.64 (m, 2H), 7.63 – 7.54 (m, 1H), 7.53 – 7.46 (m, 2H), 6.48 (br s, 1H), 1.15 (d, J = 16.6 Hz, 9H); ^{13}C NMR (101 MHz, $CDCl_3$) δ 132.4 (d, J = 2.8 Hz), 130.9 (d, J = 10.0 Hz), 129.3 (s), 128.5 (d, J = 11.8 Hz), 32.0 (d, J = 69.3 Hz), 23.4 (d, J = 2.1 Hz); ^{31}P NMR (162 MHz, $CDCl_3$) δ 47.5 (s); HPLC (Chiralpak® AD-H column, hexane/propan-2-ol 90/10, flow rate 1.0 mL/min at 20 °C, detection at 220 nm): t_R = 10.26 min, t_R = 14.15 min. ^{1}H, ^{13}C and ^{31}P NMR correspond to the literature.[298]

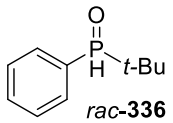

rac-**336**

Kinetic resolution of racemic phosphine oxide *rac*-336:[261] Under argon, a flame-dried round-bottom flask equipped with a reflux condenser was charged with racemic compound *rac*-**336** (1000 mg, 5.5 mmol) and (*R*,*R*)-dibenzoyl tartaric acid (2360 mg, 6.6 mmol). Freshly distilled diisopropyl ether (80 mL) was added. Distillation was done to get rid of BHT, which is used as a stabilizer for diisopropylether and can interfere with the radical mechanism of DKR. The reaction mixture was subjected to three freeze-pump-thaw cycles (30 minutes each). The reaction mixture was heated to 60 °C (oil bath temperature) to dissolve the solid compounds and iodine (20 mg, 0.08 mmol) was added under argon flow. The reaction mixture was stirred at 70 °C (oil bath temperature) for 16 h and then the hot suspension was filtered. The white filter cake was dissolved in a mixture of NaOH (1 M aq, 40 mL) and $CHCl_3$ (40 mL). The layers were separated and the aqueous layer was extracted with $CHCl_3$ (5 x 20 mL). The combined organic layer was dried over anhydrous $MgSO_4$ and concentrated under reduced pressure to afford desired product (*R*)-**336** as a white solid (455 mg, 46% yield, 65% ee). Filtrate obtained by the hot filtration was concentrated under reduced pressure and the residue was dissolved in a mixture of NaOH (1 M aq, 20 mL) and $CHCl_3$ (20 mL). The layers were separated and the aqueous layer was extracted with $CHCl_3$ (5 x 20 mL). The combined organic layer was dried over anhydrous $MgSO_4$ and concentrated under reduced pressure to afford (*S*)-**336** as a white solid (445 mg, 45% yield, −78% ee). Total yield of both enantiomers was 91%. HPLC (Chiralpak® AD-H column, hexane/propan-2-ol 90/10, flow rate 1.0 mL/min at 20 °C, detection at 220 nm): t_R = 10.12 min (*S*), t_R = 14.29 min (*R*).

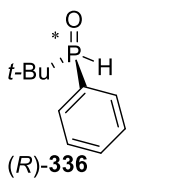

(*R*)-**336**

([1,1'-biphenyl]-2-yl)(*tert*-butyl)(phenyl)phosphine oxide (*rac*-338): Under argon, *i*-Pr_2NEt (3.5 mL, 20.09 mmol) was added to a solution of compound *rac*-**336** (925 mg, 5.07 mmol), $Pd(OAc)_2$ (114 mg, 0.51 mmol), dppb (432 mg, 1.01 mmol), and triflate **337** (1533 mg, 5.07 mmol) in dry DMSO (23 mL). The reaction mixture was stirred at 100 °C (oil bath temperature) for 16 h and then it was cooled down to rt. Water (150 mL) was added and the resulting solution was extracted with DCM (5 x 20 mL). The combined

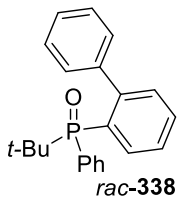

rac-**338**

organic layer was dried over anhydrous $MgSO_4$ and concentrated under reduced pressure. The residue was purified by gradient silica gel column chromatography (hexane to hexane/EtOAc 1/2) to afford desired racemic product *rac*-**336** as a white solid (1050 mg, 62% yield): HPLC (Chiralpak® AD-H column, hexane/propan-2-ol 97/3, flow rate 0.8 mL/min at 20 °C, detection at 220 nm): t_R = 22.3 min, t_R = 28.3 min.

(*R*)-([1,1'-biphenyl]-2-yl)(*tert*-butyl)(phenyl)phosphine oxide ((*R*)-338):

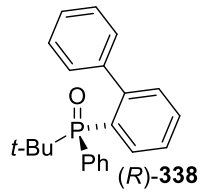

(*R*)-**338**

Under argon, compound (*R*)-**336** (65% ee, 100 mg, 0.55 mmol), $Pd(OAc)_2$ (12.3 mg, 0.055 mmol), ligand (0.11 mmol) and triflate **337** (166 mg, 0.55 mmol) were dissolved in dry DMSO (2.5 mL) and *N*,*N*-diisopropylethylamine (0.38 mL, 2.2 mmol) was added under argon flow. The reaction mixture was stirred at 100 °C (oil bath temperature) for 20 h and it was allowed to cool down to rt. Water (25 mL) was added and the resulting solution was extracted with DCM (5 x 15 mL). The combined organic layer was dried over anhydrous $MgSO_4$ and concentrated under reduced pressure. The residue was purified by gradient silica gel column chromatography (hexane to hexane/EtOAc 1/2) to afford (*R*)-**338** as a white solid.

Using dppb as ligand afforded (*R*)-**338** as a white solid (125 mg, 68% yield, 41% ee). Using Xantphos as a ligand afforded (*R*)-**338** as a white solid (41% yield, 11% ee, yield was determined by ^{1}H NMR using 1,3,5-trimethoxybenzene (0.173 M in $CDCl_3$, 0.7 mL) as an inner standard).

^{1}H NMR (500 MHz, $CDCl_3$) δ. 8.12 (ddd, *J* = 10.9, 7.7, 1.1 Hz, 1H), 7.55 – 7.50 (m, 1H), 7.47 – 7.42 (m, 1H), 7.31 – 7.22 (m, 5H), 7.17 – 7.11 (m, 2H), 7.09 – 7.03 (m, 1H), 7.03 – 6.95 (m, *J* = 3.1 Hz, 3H), 1.64 (br s, 1H), 1.30 (d, *J* = 14.3 Hz, 9H); ^{13}C NMR (126 MHz, $CDCl_3$) δ 148.6 (d, *J* = 6.5 Hz), 140.6 (d, *J* = 3.7 Hz), 133.1 (d, *J* = 9.1 Hz), 132.8 (s), 132.1 (s), 131.6 (d, *J* = 8.8 Hz), 131.1 (s), 131.0 (d, *J* = 2.5 Hz), 130.4 (s), 130.4 (d, *J* = 2.8 Hz), 130.2 (s), 127.4 (d, *J* = 11.3 Hz), 126.6 (s), 125.9 (d, *J* = 11.1 Hz), 34.3 (d, *J* = 70.7 Hz), 26.1 (s); ^{31}P NMR (202 MHz, $CDCl_3$) δ 40.8 (s); HPLC (Chiralpak® AD-H column, hexane/propan-2-ol 97/3, flow rate 0.8 mL/min at 20 °C, detection at 220 nm): t_R = 22.3 min (minor), t_R = 28.2 min (major).

[1,1'-biphenyl]-2-yl trifluoromethanesulfonate (337): Under nitrogen, dry pyridine (1.1 mL, 13.2 mmol) was added to a solution of phenylphenol (1500 mg, 8.8 mmol) in dry DCM (10 mL). The mixture was cooled to 0 °C and triflic anhydride (1.8 mL, 10.6 mmol) was added slowly. The reaction mixture was stirred at 0 °C for 1 h, and at rt overnight. Then HCl (10 wt% aq, 30 mL) was added. The layers were separated and the aqueous layer was extracted with DCM (5 x 20 mL). The combined organic layer was dried over anhydrous $MgSO_4$ and concentrated under reduced pressure. The residue was purified by silica gel column chromatography (hexane/EtOAc 10/1) to afford **337** as a white solid (2404 mg, 90% yield): ^{1}H NMR (500 MHz, $CDCl_3$) δ. 7.52 – 7.38 (m, 9H); ^{13}C NMR (126 MHz, $CDCl_3$) δ 146.8 (s), 135.6 (s), 132.0 (s), 129.4 (s), 129.0 (s), 128.5 (s), 128.5 (s), 128.3 (s), 122.1 (s), 118.37 (q, *J* = 320.5); ^{19}F NMR (471 MHz, $CDCl_3$) δ −74.1 (s). ^{1}H, ^{13}C, and ^{19}F NMR correspond to the literature.[299]

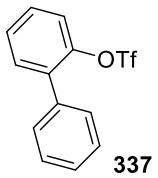

337

([1,1'-biphenyl]-2-yl)(*tert*-butyl)(phenyl)phosphine (*rac*-325): A flame-dried round-bottom flask equipped with a reflux condenser was charged with phosphine oxide *rac*-**338** (250 mg, 0.75 mmol), TMDS (0.33 mL, 1.87 mmol), and $Ti(OiPr)_4$ (0.22 mL, 0.075 mmol), evacuated and backfilled with argon. Dry toluene (1.6 mL) was added and the resulting solution was subjected to three freeze-pump-thaw cycles (10 minutes each). The reaction mixture was

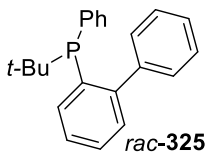

rac-**325**

stirred at 100 °C (oil bath temperature) for 2 days. Then it was concentrated under reduced pressure and the residue was purified by gradient silica gel column chromatography (hexane to hexane/EtOAc 10/1) to afford *rac*-**325** as a white solid (93 mg, 39% yield): ^{1}H NMR (500 MHz, $CDCl_3$) δ 7.71 – 7.66 (m, 1H), 7.35 – 7.05 (m, 13H), 1.03 (d, *J* = 12.5 Hz, 9H); ^{13}C NMR (101 MHz, $CDCl_3$) δ 149.6 (d, *J* = 28.0 Hz), 142.4 (d, *J* = 6.1 Hz), 134.1 (d, *J* = 1.4 Hz), 134.0 (s), 133.9 (s), 130.7 (d, *J* = 4.9 Hz), 130.1 (d, *J* = 4.1 Hz), 128.4 (s), 127.7 (s), 127.7 (s), 127.6 (s), 127.3 (s), 126.7 (s), 126.5 (s), 31.2 (d, *J* = 17.0 Hz), 28.8 (d, *J* = 15.1 Hz); ^{31}P NMR (202 MHz, $CDCl_3$) δ 5.8 (s). ^{1}H and ^{31}P NMR correspond to the literature.[300]

13.5 General procedure to prepare Buchwald-type catalysts

Under nitrogen, Buchwald dimer **343** (123 mg, 0.16 mmol) and phosphine (0.32 mmol) were dissolved in dry DCM (2 mL) and the reaction mixture was stirred at rt for 1 h. The reaction mixture was concentrated under reduced pressure. The residue was trituated with *n*-pentane. Filtration and vacuum drying provided the title compound.[268]

SPhos precatalyst 344 as a brown crystalline compound (254 mg, 99% yield): ^{1}H NMR (400 MHz, CD_3OD) δ 8.14 (t, *J* = 8.4 Hz, 1H), 7.86 – 7.76 (m, 1H), 7.65 – 7.59 (m, 1H), 7.53 – 7.41 (m, 2H), 7.39 – 7.24 (m, 5H), 7.23 – 7.17 (m, 1H), 7.12 – 7.02 (m, 3H), 6.84 (ddd, *J* = 7.7, 3.1, 1.4 Hz, 1H), 3.93 (s, 3H), 3.39 (s, 3H), 2.67 (s, 3H), 2.52 – 2.35 (m, 1H), 2.24 – 2.12 (m, 2H), 2.11 (dd, *J* = 5.9, 2.5 Hz, 3H), 2.01 (s, 4H), 1.91 (dd, *J* = 11.0, 7.1 Hz, 1H), 1.79 (d, *J* = 13.3 Hz, 1H), 1.72 – 1.66 (m, 1H), 1.63 – 1.44 (m, 2H), 1.40 (d, *J* = 13.1 Hz, 1H), 1.38 – 1.33 (m, 2H), 1.28 – 0.92 (m, 4H), 0.92 – 0.71 (m, 2H), 0.08 – 0.05 (m, 1H); ^{31}P NMR (162 MHz, CD_3OD) δ 45.9 (s). ^{1}H and ^{31}P NMR correspond to the literature.[268]

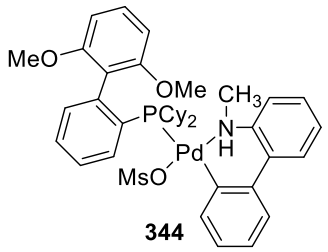

344

XPhos precatalyst 345 as a grey crystalline compound (262 mg, 98% yield): ^{1}H NMR (400 MHz, CD_3OD) δ 7.91 – 7.83 (m, 1H), 7.58 – 7.54 (m, 2H), 7.53 – 7.48 (m, 3H), 7.31 – 7.14 (m, 5H), 7.06 – 7.00 (m, 1H), 6.92 – 6.85 (m, 2H), 3.37 – 3.24 (m, 1H), 2.91 – 2.77 (m, 1H), 2.60 (s, 3H), 2.46 (dd, *J* = 19.9, 11.9 Hz, 1H), 2.33 – 2.24 (m, 1H), 2.23 – 2.13 (m, 1H), 2.09 – 1.97 (m, 4H), 1.94 – 1.84 (m, 2H), 1.83 – 1.65 (m, 6H), 1.46 (dd, *J* = 6.9, 1.8 Hz, 7H), 1.43 – 1.14 (m, 8H), 1.15 – 0.92 (m, 7H), 0.84 – 0.75 (m, 4H), 0.58 (d, *J* = 6.8 Hz, 2H), 0.12 – 0.01 (m, 1H); ^{31}P NMR (162 MHz, CD_3OD) δ 38.2 (s). ^{1}H and ^{31}P NMR correspond to the literature.[268]

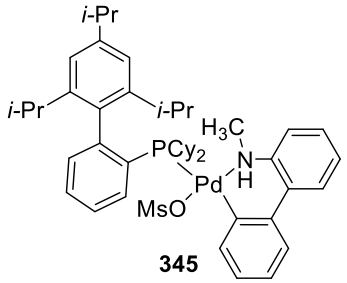

345

(*S*)-(*H*$_8$)-BINAP(O) precatalyst 346: The reaction mixture was subjected to three freeze-pump-thaw cycles (5 minutes each) and subsequently it was stirred at rt for 1 h. White crystalline compound (300 mg, 91% yield): ^{1}H NMR (500 MHz, $CDCl_3$) δ 8.18 – 8.05 (m, 3H), 7.92 – 7.84 (m, 3H), 7.81 – 7.70 (m, 4H), 7.56 (d, *J* = 7.4 Hz, 1H), 7.42 – 7.34 (m, 3H), 7.18 – 7.09 (m, 6H), 7.06 – 6.97 (m, 4H), 6.97 – 6.88 (m, 3H), 6.83 (d, *J* = 8.0 Hz, 1H), 6.55 – 6.48 (m, 1H), 6.49 – 6.40 (m, 1H), 6.03 (t, *J* = 7.2 Hz, 1H), 5.92 (d, *J* = 7.6 Hz, 1H), 4.90 – 4.80 (m, 1H), 2.78 (s, 3H), 2.63 – 2.54 (m, 1H), 2.49 – 2.43 (m, 3H), 2.41 (d, *J* = 6.5 Hz, 2H), 2.13 – 1.90 (m, 4H), 1.74 – 1.64 (m, 1H), 1.51 – 1.18 (m, 4H), 1.11 – 1.00 (m, 1H), 0.99 – 0.86 (m, 1H), 0.80 – 0.70 (m, 1H), −0.20 – (−0.34) (m, 1H); ^{13}C NMR (126 MHz, $CDCl_3$) δ 145.5 – 120.5 (48C, aromatic carbons, observed

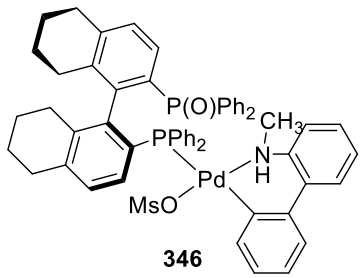

346

complexity due to C−P splitting), 41.4 (s), 39.6 (s), 29.9 (s), 29.4 (s), 27.4 (s), 25.2 (s), 22.0 (s), 21.9 (s), 21.6 (s), 21.4 (s); ^{31}P NMR (162 MHz, $CDCl_3$) δ 40.3 (s), 26.3 (s).

1,4-Bis(diphenylphosphino)butane precatalyst 347 as a brown crystalline compound (251 mg, 97% yield): ^{1}H NMR (500 MHz, $CDCl_3$) δ 7.81 – 7.72 (m, 2H), 7.69 – 7.62 (m, 2H), 7.61 – 7.50 (m, 3H), 7.50 – 7.29 (m, 11H), 7.20 – 7.07 (m, 6H), 6.95 (t, *J* = 7.3 Hz, 1H), 6.63 (t, *J* = 7.4 Hz, 1H), 6.48 (dd, *J* = 13.3, 7.5 Hz, 1H), 6.30 (d, *J* = 7.6 Hz, 1H), 3.86 (br s, 1H), 3.29 – 3.15 (m, 1H), 2.80 (s, 3H), 2.78 – 2.69 (m, 1H), 2.44 – 2.32 (m, 1H), 2.30 – 2.14 (m, 1H), 1.96 (dd, *J* = 5.5, 2.0 Hz, 2H), 1.80 (s, 3H), 1.76 – 1.62 (m, 1H), 1.52 – 1.37 (m, 1H); ^{13}C NMR (126 MHz, $CDCl_3$) δ 141.1 – 121.0 (36C, aromatic carbons, observed complexity due to C–P splitting), 39.8 (br s), 39.6 (br s), 28.3 (m), 25.7 (d, *J* = 18.2), 24.1 (br s), 22.3 (m); ^{31}P NMR (202 MHz, $CDCl_3$) δ 32.9 (d, *J* = 40.3 Hz), 15.0 (d, *J* = 41.3 Hz).

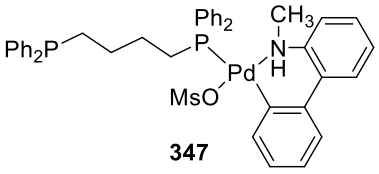

347

13.6 Direct catalytic asymmetric C−H arylations

13.6.1 Typical procedure for the reaction with Pd(dba)$_2$

Chromium complex **319a** (23.2 mg, 0.1 mmol), Ag_2CO_3 (18.0 mg, 0.065 mmol), (*H*$_8$)-BINAP(O) **322** (2.1 mg, 0.0033 mmol), Cy_2CHCO_2H (11.0 mg, 0.050 mmol), K_2CO_3 (28.0 mg, 0.2 mmol), Pd(dba)$_2$ (1.7 mg, 0.0030 mmol), methyl 4-iodobenzoate (**132a**, 52.4 mg, 0.2 mmol) were weighed into a flame-dried 10 mL microwave vial equipped with a magnetic stir bar. Then dry toluene (0.1 mL) and TMP (34 μL, 0.2 mmol) were added under argon flow and the vial was sealed and wrapped with aluminium foil. The reaction was heated at 40 °C for 40 h (stirring rate 200 rpm), then the vial was cooled down to rt. The suspension was filtrated through a short silica pad (2 × 2 cm) using acetone (10 mL) as an eluent and concentrated under reduced pressure to afford **320a** and **321**. Yields were determined from ^{1}H NMR spectra using 1,3,5-trimethoxybenzene as an inner standard (0.143 M in $CDCl_3$, 0.7 mL).

13.6.2 General procedure for the reaction with Buchwald-type catalysts

Chromium complex **319a** (23.2 mg, 0.1 mmol), Ag_2CO_3 (18.0 mg, 0.065 mmol), ligand (0.0055 mmol), Cy_2CHCO_2H (11.0 mg, 0.050 mmol), K_2CO_3 (28.0 mg, 0.2 mmol), Buchwald-type catalyst (0.0050 mmol), methyl 4-iodobenzoate (**132a**, 52.4 mg, 0.2 mmol) were weighed into a flame-dried 10 mL microwave vial equipped with a magnetic stir bar. Then dry toluene (0.1 mL) and TMP (34 μL, 0.2 mmol) were added under argon flow and the vial was sealed and wrapped with aluminium foil. The reaction was heated at 40 °C for 40 h (stirring rate 200 rpm), then the vial was cooled down to rt. The suspension was filtrated through a short silica pad (2 × 2 cm) using acetone (10 mL) as an eluent and concentrated under reduced pressure to afford **320a** and **321**. Yields were determined from ^{1}H NMR spectra using 1,3,5-trimethoxybenzene as an inner standard (0.143 M in $CDCl_3$, 0.7 mL).

(Methyl (*S*)-2'-fluoro-[1,1'-biphenyl]-4-carboxylate)tricarbonylchromium (320a): Silica gel column chromatography (hexane/Et_2O 7/3) afforded a yellow solid **320a** (14.6 mg, 40% yield, 80% ee): ^{1}H NMR (400 MHz, $CDCl_3$) δ 8.09 (d, *J* = 8.3 Hz, 2H), 7.63 (d, *J* = 7.3 Hz, 2H), 5.77 (dd, *J* = 5.5, 5.3 Hz, 1H), 5.60 – 5.55 (m, 1H), 5.45 (dd, *J* = 6.4, 6.3 Hz, 1H), 5.03 – 4.98 (m, 1H), 3.95 (s, 3H); ^{13}C NMR (126 MHz, $CDCl_3$) δ 231.2 (s, 3C), 166.5 (s), 144.6 (d, *J* = 266.8 Hz), 136.8 (s), 130.8 (s), 130.0 (s, 2C), 129.6 (s), 129.6 (s), 97.6 (d, *J* = 13.2 Hz), 94.8 (s), 93.2 (d,

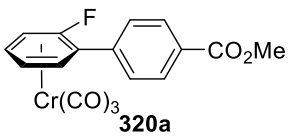

320a

J = 7.5 Hz), 85.9 (s), 78.5 (d, J = 22.0 Hz), 52.5 (s); ^{19}F NMR (471 MHz, $CDCl_3$) δ −137.2 (s); HRMS (ESI) m/z: $[M+K]^+$ calcd for $C_{17}H_{11}O_5CrFK$ = 404.9633, found = 404.9621; HPLC (Chiralpak® IB, hexane/propan-2-ol 97/3, flow rate 0.8 ml/min at 20 °C, detection at 280 nm): t_R = 26.56 min (minor), t_R = 29.48 min (major).

(Dimethyl 2^2-fluoro-[1^1,2^1:2^3,3^1-terphenyl]-1^4,3^4-carboxylate)tricarbonylchromium (321) Bisarylated compound **321** was obtained as a main by-product by silica gel column chromatography (acetone). A yellow solid (6.9 mg, 14% yield): ^{1}H NMR (400 MHz, acetone-d_6) δ 8.13 (d, J = 8.5 Hz, 4H), 7.86 (dd, J = 8.4, 1.6 Hz, 4H), 6.37 – 6.34 (m, 2H), 5.62 – 5.59 (m, 1H), 3.93 (s, 6H); ^{13}C NMR (101 MHz, acetone-d_6) δ 232.6 (d, J = 1.8 Hz), 166.7 (s), 143.8 (d, J = 265.6 Hz), 137.9 (d, J = 2.2 Hz), 131.8 (s), 131.0 (d, J = 2.6 Hz), 130.4 (s), 98.8 (d, J = 14.2 Hz), 97.8 (d, J = 3.7 Hz), 88.2 (s), 52.6 (s).

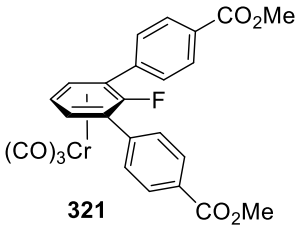

321

14 Publications

Included in the thesis

Gergelitsová, I.; Tauchman, J.; Císařová, I.; Veselý, J. Bifunctional (Thio)urea-Phosphine Organocatalysts Derived from D-Glucose and α-Amino Acids and Their Application to the Enantioselective Morita-Baylis-Hillman Reaction. *Synlett* **2015**, *26*, 2690 – 2696.

Batuecas, M.; Luo, J. **Gergelitsová, I.**; Krämer, K.; Whitaker, D.; Vitorica-Yrezabal, I. J.; Larrosa, I. Catalytic Asymmetric C−H Arylation of (η^6-Arene)Chromium Complexes: Facile Access to Planar-Chiral Phosphines. *ACS Catalysis* **2019**, *9*, 5268 – 5278.

Not included in the thesis

Gergelitsová, I.; Veselý, J. Diastereoselective Addition of Organometallic Reagents to Chiral Carbonyl Compounds. In *Asymmetric Synthesis of Drugs and Natural Products*, Nag. A. (Ed.), Boca Raton: CRC Press, 2018, 29 – 74.

Ceban, V.; Tauchman, J.; Meazza, M.; Gallagher, G.; Light M. E.; **Gergelitsová, I.**; Veselý, J.; Rios, R. Expanding the Scope of Metal-Free Enantioselective Allylic Substitutions: Anthrones. *Sci. Rep.* **2015**, *5*, 1 – 9.

Tobrman, T.; **Jurásková, I.**; Dvořák, D. Negishi Cross-Coupling Reaction as a Simple and Efficient Route to Functionalized Amino and Alkoxy Carbene Complexes of Chromium, Molybdenum, and Tungsten. *Organometallics* **2014**, *33*, 6593 – 6603

Tobrman, T.; **Jurásková, I.**; Váňová, H.; Dvořák, D. Lithiation of Chromium and Tungsten Aminocarbene Complexes: An Easy Approach to Functionalized Aminocarbene Complexes. *Organometallics* **2014**, *33*, 2990 – 2996.

15 References

(1) Langenbeck, W. Fermentproblem Und Organische Katalyse. *Angew. Chem.* **1932**, *45* (5), 97–99.

(2) Tu, Y.; Wang, Z.-X.; Shi, Y. An Efficient Asymmetric Epoxidation Method for *trans*-Olefins Mediated by a Fructose-Derived Ketone. *J. Am. Chem. Soc.* **1996**, *118* (40), 9806–9807.

(3) Denmark, S. E.; Wu, Z.; Crudden, C. M.; Matsuhashi, H. Catalytic Epoxidation of Alkenes with Oxone. 2. Fluoro Ketones. *J. Org. Chem.* **1997**, *62* (24), 8288–8289.

(4) Yang, D.; Yip, Y.-C.; Tang, M.-W.; Wong, M.-K.; Zheng, J.-H.; Cheung, K.-K. A C_2 Symmetric Chiral Ketone for Catalytic Asymmetric Epoxidation of Unfunctionalized Olefins. *J. Am. Chem. Soc.* **1996**, *118* (2), 491–492.

(5) Sigman, M. S.; Jacobsen, E. N. Schiff Base Catalysts for the Asymmetric Strecker Reaction Identified and Optimized from Parallel Synthetic Libraries. *J. Am. Chem. Soc.* **1998**, *120* (19), 4901–4902.

(6) Corey, E. J.; Grogan, M. J. Enantioselective Synthesis of α-Amino Nitriles from N-Benzhydryl Imines and HCN with a Chiral Bicyclic Guanidine as Catalyst. *Org. Lett.* **1999**, *1* (1), 157–160.

(7) Miller, S. J.; Copeland, G. T.; Papaioannou, N.; Horstmann, T. E.; Ruel, E. M. Kinetic Resolution of Alcohols Catalyzed by Tripeptides Containing the *N*-Alkylimidazole Substructure. *J. Am. Chem. Soc.* **1998**, *120* (7), 1629–1630.

(8) List, B.; Lerner, R. A.; Barbas, C. F. Proline-Catalyzed Direct Asymmetric Aldol Reactions. *J. Am. Chem. Soc.* **2000**, *122* (10), 2395–2396.

(9) Ahrendt, K. A.; Borths, C. J.; MacMillan, D. W. C. New Strategies for Organic Catalysis: The First Highly Enantioselective Organocatalytic Diels−Alder Reaction. *J. Am. Chem. Soc.* **2000**, *122* (17), 4243–4244.

(10) Berkessel, A.; Gröger, H. *Asymmetric Organocatalysis: From Biomimetic Concepts to Applications in Asymmetric Synthesis*; Wiley-VCH, Weinheim, Germany, 2005.

(11) List, B. Organocatalysis. *Beilstein J. Org. Chem.* **2012**, *8*, 1358–1359.

(12) Vicario, J. L.; Badia, D.; Carrillo, L.; Reyes, E. *Organocatalytic Enantioselective Conjugate Addition Reactions*; Royal Society of Chemistry, 2010.

(13) Brak, K.; Jacobsen, E. N. Asymmetric Ion-Pairing Catalysis. *Angew. Chem. Int. Ed.* **2013**, *52* (2), 534–561.

(14) Bogliotti, N.; Dalko, P. I. Shape- and Site-Selective Asymmetric Reactions. In *Enantioselective Organocatalysis: Reactions and Experimental Procedures*; Dalko, P. I., Ed.; Wiley-VCH, Weinheim, Germany, 2007, pp 425–449.

(15) Seayad, I.; List, B. Asymmetric Organocatalysis. *Org. Biomol. Chem.* **2005**, *3* (5), 719–724.

(16) *Enantioselective Organocatalysis: Reactions and Experimental Procedures*; Dalko, P. I., Ed.; Wiley-VCH, Weinheim, Germany, 2007.

(17) Palomo, C.; Oiarbide, M.; López, R. Asymmetric Organocatalysis by Chiral Brønsted Bases: Implications and Applications. *Chem. Soc. Rev*. **2009**, *38*, 632–653.

(18) Taylor, M. S.; Jacobsen, E. N. Asymmetric Catalysis by Chiral Hydrogen-Bond Donors. *Angew. Chem. Int. Ed.* **2006**, *45* (10), 1520–1543.

(19) Pihko, P. M. Activation of Carbonyl Compounds by Double Hydrogen Bonding: An

Emerging Tool in Asymmetric Catalysis. *Angew. Chem. Int. Ed.* **2004**, *43* (16), 2062–2064.

(20) Etzenbach-Effers, K.; Berkessel, A. Noncovalent Organocatalysis Based on Hydrogen Bonding: Elucidation of Reaction Paths by Computational Methods. In *Asymmetric Organocatalysis*; List, B., Ed.; Topics in Current Chemistry, vol 291, Springer, Berlin, Heidelberg, 2010.

(21) Zhao, B.; Li, J.; Du, D. Squaramide-Catalyzed Asymmetric Reactions. *Chem. Rec.* **2017**, *17* (10), 994–1018.

(22) Terada, M. Chiral Phosphoric Acids as Versatile Catalysts for Enantioselective Transformations. *Synthesis*. 2010, pp 1929–1982.

(23) Pihko, P. M. *Hydrogen Bonding in Organic Synthesis*; WILEY-VCH: Weinheim, Germany, 2009.

(24) Kotke, M.; Schreiner, P. R. (Thio)Urea Organocatalysts. In *Hydrogen Bonding in Organic Synthesis*; Pihko, P. M., Ed.; Wiley-VCH: Weinheim, Germany; pp 141–351.

(25) Vachal, P.; Jacobsen, E. N.; Enantioselective Catalytic Addition of HCN to Ketoimines. Catalytic Synthesis of Quaternary Amino Acids. *Org. Lett.* **2000**, 2 (6), 867–870.

(26) Vachal, P.; Jacobsen, E. N. Structure-Based Analysis and Optimization of a Highly Enantioselective Catalyst for the Strecker Reaction. *J. Am. Chem. Soc.* **2002**, *124* (34), 10012–10014.

(27) Zuend, S. J.; Jacobsen, E. N. Mechanism of Amido-Thiourea Catalyzed Enantioselective Imine Hydrocyanation: Transition State Stabilization *via* Multiple Non-Covalent Interactions. *J. Am. Chem. Soc.* **2009**, *131* (42), 15358–15374.

(28) Steiner, T. The Hydrogen Bond in the Solid State. *Angew. Chem. Int. Ed.* **2002**, *41* (1), 48–76.

(29) Kotke, M.; Schreiner, P. R. Acid-Free, Organocatalytic Acetalization. *Tetrahedron* **2006**, *62* (2–3), 434–439.

(30) Almaşi, D.; Alonso, D. A.; Gómez-Bengoa, E.; Nájera, C. Chiral 2-Aminobenz-imidazoles as Recoverable Organocatalysts for the Addition of 1,3-Dicarbonyl Compounds to Nitroalkenes. *J. Org. Chem.* **2009**, *74* (16), 6163–6168.

(31) Schuster, T.; Bauch, M.; Dürner, G.; Göbel, M. W. Axially Chiral Amidinium Ions as Inducers of Enantioselectivity in Diels−Alder Reactions. *Org. Lett.* **2000**, *2* (2), 179–181.

(32) Yang, W.; Du, D.-M. Chiral Squaramide-Catalyzed Highly Enantioselective Michael Addition of 2-Hydroxy-1,4-Naphthoquinones to Nitroalkenes. *Adv. Synth. Catal.* **2011**, *353* (8), 1241–1246.

(33) Iwabuchi, Y.; Nakatani, M.; Yokoyama, N.; Hatakeyama, S. Chiral Amine-Catalyzed Asymmetric Baylis−Hillman Reaction: A Reliable Route to Highly Enantiomerically Enriched (α-Methylene-β-Hydroxy)Esters. *J. Am. Chem. Soc.* **1999**, *121* (43), 10219–10220.

(34) Jakab, G.; Tancon, C.; Zhang, Z.; Lippert, K. M.; Schreiner, P. R. (Thio)Urea Organocatalyst Equilibrium Acidities in DMSO. *Org. Lett.* **2012**, *14* (7), 1724–1727.

(35) Schreiner, P. R.; Wittkopp, A. H-Bonding Additives Act Like Lewis Acid Catalysts. *Org. Lett.* **2002**, *4* (2), 217–220.

(36) Bordwell, F. G.; Algrim, D. J.; Harrelson, J. A. The Relative Ease of Removing a

Proton, a Hydrogen Atom, or an Electron from Carboxamides versus Thiocarboxamides. *J. Am. Chem. Soc.* **1988**, *110* (9), 5903–5904.

(37) Connon, S. J. Organocatalysis Mediated by (Thio)Urea Derivatives. *Chem. Eur. J.* **2006**, *12* (21), 5418–5427.

(38) Serdyuk, O. V.; Heckel, C. M.; Tsogoeva, S. B. Bifunctional Primary Amine-Thioureas in Asymmetric Organocatalysis. *Org. Biomol. Chem*. **2013**, *11*, 7051–7071.

(39) Sun, Y.-L.; Wei, Y.; Shi, M. Applications of Chiral Thiourea-Amine/Phosphine Organocatalysts in Catalytic Asymmetric Reactions. *ChemCatChem* **2017**, *9* (5), 718–727.

(40) Okino, T.; Hoashi, Y.; Takemoto, Y. Enantioselective Michael Reaction of Malonates to Nitroolefins Catalyzed by Bifunctional Organocatalysts. *J. Am. Chem. Soc.* **2003**, *125* (42), 12672–12673.

(41) Okino, T.; Hoashi, Y.; Furukawa, T.; Xu, X.; Takemoto, Y. Enantio- and Diastereoselective Michael Reaction of 1,3-Dicarbonyl Compounds to Nitroolefins Catalyzed by a Bifunctional Thiourea. *J. Am. Chem. Soc.* **2005**, *127* (1), 119–125.

(42) Hoashi, Y.; Yabuta, T.; Yuan, P.; Miyabe, H.; Takemoto, Y. Enantioselective Tandem Michael Reaction to Nitroalkene Catalyzed by Bifunctional Thiourea: Total Synthesis of (-)-Epibatidine. *Tetrahedron* **2006**, *62* (2–3), 365–374.

(43) Hoashi, Y.; Yabuta, T.; Takemoto, Y. Bifunctional Thiourea-Catalyzed Enantioselective Double Michael Reaction of γ,δ-Unsaturated β-Ketoester to Nitroalkene: Asymmetric Synthesis of (-)-Epibatidine. *Tetrahedron Lett.* **2004**, *45* (50), 9185–9188.

(44) Li, H.; Wang, J.; Zu, L.; Wang, W. Organocatalytic Asymmetric Conjugate Addition of Thioacetic Acid to β-Nitrostyrenes. *Tetrahedron Lett.* **2006**, *47* (15), 2585–2589.

(45) Liu, T. Y.; Long, J.; Li, B. J.; Jiang, L.; Li, R.; Wu, Y.; Ding, L. S.; Chen, Y. C. Enantioselective Construction of Quaternary Carbon Centre Catalysed by Bifunctional Organocatalyst. *Org. Biomol. Chem.* **2006**, *4* (11), 2097–2099.

(46) Liu, T.-Y.; Li, R.; Chai, Q.; Long, J.; Li, B.-J.; Wu, Y.; Ding, L.-S.; Chen, Y.-C. Enantioselective Michael Addition of α-Substituted Cyanoacetates to Vinyl Ketones Catalyzed by Bifunctional Organocatalysts. *Chem. Eur. J.* **2007**, *13* (1), 319–327.

(47) Inokuma, T.; Hoashi, Y.; Takemoto, Y. Thiourea-Catalyzed Asymmetric Michael Addition of Activated Methylene Compounds to α,β-Unsaturated Imides: Dual Activation of Imide by Intra- and Intermolecular Hydrogen Bonding. *J. Am. Chem. Soc.* **2006**, *128* (29), 9413–9419.

(48) Miyabe, H.; Tuchida, S.; Yamauchi, M.; Takemoto, Y. Reaction of Nitroorganic Compounds Using Thiourea Catalysts Anchored to Polymer Support. *Synthesis (Stuttg).* **2006**, No. 19, 3295–3300.

(49) Zu, L.; Xie, H.; Li, H.; Wang, J.; Jiang, W.; Wang, W. Chiral Amine Thiourea-Promoted Enantioselective Domino Michael-Aldol Reactions between 2-Mercaptobenzaldehydes and Maleimides. *Adv. Synth. Catal.* **2007**, *349* (11–12), 1882–1886.

(50) Yamaoka, Y.; Miyabe, H.; Yasui, Y.; Takemoto, Y. Chiral-Thiourea-Catalyzed Direct Mannich Reaction. *Synthesis.* **2007**, No. 16, 2571–2575.

(51) Wasa, M.; Liu, R. Y.; Roche, S. P.; Jacobsen, E. N. Asymmetric Mannich Synthesis of α-Amino Esters by Anion-Binding Catalysis. *J. Am. Chem. Soc.* **2014**, *136* (37), 12872–12875.

(52) Okino, T.; Nakamura, S.; Furukawa, T.; Takemoto, Y. Enantioselective Aza-Henry Reaction Catalyzed by a Bifunctional Organocatalyst. *Org. Lett.* **2004**, *6* (4), 625–627.

(53) Xu, X.; Furukawa, T.; Okino, T.; Miyabe, H.; Takemoto, Y. Bifunctional-Thiourea-Catalyzed Diastereo- and Enantioselective Aza-Henry Reaction. *Chem. Eur. J.* **2006**, *12* (2), 466–476.

(54) Enders, D.; Gottfried, K.; Raabe, G. Organocatalytic Enantioselective Strecker Synthesis of α-Quaternary α-Trifluoromethyl Amino Acids. *Adv. Synth. Catal.* **2010**, *352* (18), 3147–3152.

(55) Yamaoka, Y.; Miyabe, H.; Takemoto, Y. Catalytic Enantioselective Petasis-Type Reaction of Quinolines Catalyzed by a Newly Designed Thiourea Catalyst. *J. Am. Chem. Soc.* **2007**, *129* (21), 6686–6687.

(56) Dudziński, K.; Pakulska, A. M.; Kwiatkowski, P. An Efficient Organocatalytic Method for Highly Enantioselective Michael Addition of Malonates to Enones Catalyzed by Readily Accessible Primary Amine-Thiourea. *Org. Lett.* **2012**, *14* (16), 4222–4225.

(57) Uehara, H.; Barbas, C. Anti-Selective Asymmetric Michael Reactions of Aldehydes and Nitroolefins Catalyzed by a Primary Amine/Thiourea. *Angew. Chem. Int. Ed.* **2009**, *48* (52), 9848–9852.

(58) Brown, A. R.; Kuo, W.-H.; Jacobsen, E. N. Enantioselective Catalytic α-Alkylation of Aldehydes *via* an S_N1 Pathway. *J. Am. Chem. Soc.* **2010**, *132* (27), 9286–9288.

(59) Yuan, K.; Song, H. L.; Hu, Y.; Fang, J. F.; Wu, X. Y. Enantioselective Intramolecular Morita-Baylis-Hillman Reaction Using Chiral Bifunctional Phosphinothiourea as an Organocatalyst. *Tetrahedron Asymmetry* **2010**, *21* (8), 903–908.

(60) Sohtome, Y.; Tanatani, A.; Hashimoto, Y.; Nagasawa, K. Development of Bis-Thiourea-Type Organocatalyst for Asymmetric Baylis-Hillman Reaction. *Tetrahedron Lett.* **2004**, *45* (29), 5589–5592.

(61) Fuerst, D. E.; Jacobsen, E. N. Thiourea-Catalyzed Enantioselective Cyanosilylation of Ketones. *J. Am. Chem. Soc.* **2005**, *127* (25), 8964–8965.

(62) Zuend, S. J.; Jacobsen, E. N. Cooperative Catalysis by Tertiary Amino-Thioureas: Mechanism and Basis for Enantioselectivity of Ketone Cyanosilylation. *J. Am. Chem. Soc.* **2007**, *129* (51), 15872–15883.

(63) Fang, Y.-Q.; Jacobsen, E. N. Cooperative, Highly Enantioselective Phosphinothiourea Catalysis of Imine−Allene [3 + 2] Cycloadditions. *J. Am. Chem. Soc.* **2008**, *130* (17), 5660–5661.

(64) Yalalov, D. A.; Tsogoeva, S. B.; Shubina, T. E.; Martynova, I. M.; Clark, T. Evidence for an Enol Mechanism in a Highly Enantioselective Mannich-Type Reaction Catalyzed by Primary Amine-Thiourea. *Angew. Chem. Int. Ed.* **2008**, *47* (35), 6624–6628.

(65) Wang, L.; Xu, X.; Huang, J.; Peng, L.; Huang, Q.; Wang, L. Asymmetric Michael Addition of Aromatic Ketones to Nitroolefins Catalyzed by Simple Chiral Bifunctional Primary Amine-Thioureas. *Lett. Org. Chem.* **2010**, *7* (5), 367–372.

(66) Dong, L.; Du, Q.; Lou, C.; Zhang, J.; Lu, R.; Yan, M. Asymmetric Synthesis of Nitrocyclopropanes Catalyzed by Chiral Primary Amines. *Synlett* **2010**, *2010* (02), 266–270.

(67) Chen, X.; Qi, Z.-H.; Zhang, S.-Y.; Kong, L.-P.; Wang, Y.; Wang, X.-W. Enantioselective Construction of Functionalized Thiopyrano-Indole Annulated Heterocycles *via* a Formal Thio [3 + 3]-Cyclization. *Org. Lett.* **2015**, *17* (1), 42–45.

(68) Tian, X.; Jiang, K.; Peng, J.; Du, W.; Chen, Y.-C. Organocatalytic Stereoselective Mannich Reaction of 3-Substituted Oxindoles. *Org. Lett.* **2008**, *10* (16), 3583–3586.

(69) Bastida, D.; Liu, Y.; Tian, X.; Escudero-Adán, E.; Melchiorre, P. Asymmetric Vinylogous Aldol Reaction *via* H-Bond-Directing Dienamine Catalysis. *Org. Lett.* **2013**, *15* (1), 220–223.

(70) Basak, A. K.; Shimada, N.; Bow, W. F.; Vicic, D. A.; Tius, M. A. An Organocatalytic Asymmetric Nazarov Cyclization. *J. Am. Chem. Soc.* **2010**, *132* (24), 8266–8267.

(71) Connon, S. J. Asymmetric Catalysis with Bifunctional Cinchona Alkaloid-Based Urea and Thiourea Organocatalysts. *Chem. Commun*. **2008**, 2499–2510.

(72) Xi, Y.; Shi, X. Cinchonine and Thiourea. *Chem. Commun*. **2013**, *49*, 8583–8585.

(73) Yang, J.; Li, W.; Jin, Z.; Liang, X.; Ye, J. Enantioselective Michael Reaction of α-Alkyl-β-Keto Esters and Enones under Multifunctional Catalysis. *Org. Lett.* **2010**, *12* (22), 5218–5221.

(74) Tan, B.; Candeias, N. R.; Barbas, C. F. Construction of Bispirooxindoles Containing Three Quaternary Stereocentres in a Cascade Using a Single Multifunctional Organocatalyst. *Nat. Chem.* **2011**, *3* (6), 473–477.

(75) Wang, J.; Li, H.; Duan, W.; Zu, L.; Wang, W. Organocatalytic Asymmetric Michael Addition of 2,4-Pentandione to Nitroolefins. *Org. Lett.* **2005**, *7* (21), 4713–4716.

(76) Wang, J.; Li, H.; Yu, X; Zu, L.; Wang, W. Chiral Binaphthyl-Derived Amine-Thiourea Organocatalyst-Promoted Asymmetric Morita-Baylis-Hillman Reaction. Org. Lett. **2005**, *7* (19), 4293–4296.

(77) Hu, F. Le; Wei, Y.; Shi, M. Phosphine-Catalyzed Asymmetric [4+1] Annulation of Activated α,β-Unsaturated Ketones with Morita-Baylis-Hillman Carbonates: Enantioselective Synthesis of Spirooxindoles Containing Two Adjacent Quaternary Stereocenters. *Chem. Commun.* **2014**, *50* (64), 8912–8914.

(78) Herrera, R. P.; Sgarzani, V.; Bernardi, L.; Ricci, A. Catalytic Enantioselective Friedel-Crafts Alkylation of Indoles with Nitroalkenes by Using a Simple Thiourea Organocatalyst. *Angew. Chem. Int. Ed.* **2005**, *44* (40), 6576–6579.

(79) Sibi, M. P.; Itoh, K. Organocatalysis in Conjugate Amine Additions. Synthesis of β-Amino Acid Derivatives. *J. Am. Chem. Soc.* **2007**, *129* (26), 8064–8065.

(80) List, B. The Ying and Yang of Asymmetric Aminocatalysis. *Chemical Commun.* **2006**, 819–824.

(81) Cao, Y. J.; Lai, Y. Y.; Wang, X.; Li, Y. J.; Xiao, W. J. Michael Additions in Water of Ketones to Nitroolefins Catalyzed by Readily Tunable and Bifunctional Pyrrolidine-Thiourea Organocatalysts. *Tetrahedron Lett.* **2007**, *48* (1), 21–24.

(82) Sulzer-Mossé, S.; Alexakis, A. Chiral Amines as Organocatalysts for Asymmetric Conjugate Addition to Nitroolefins and Vinyl Sulfones *via* Enamine Activation. *Chem. Commun*. **2007**, 3123–3135.

(83) Cao, C.-L.; Ye, M.-C.; Sun, X.-L.; Tang, Y. Pyrrolidine−Thiourea as a Bifunctional Organocatalyst: Highly Enantioselective Michael Addition of Cyclohexanone to Nitroolefins. *Org. Lett.* **2006**, *8* (14), 2901–2904.

(84) Miura, T.; Masuda, A.; Ina, M.; Nakashima, K.; Nishida, S.; Tada, N.; Itoh, A. Asymmetric Michael Reactions of α,α-Disubstituted Aldehydes with Maleimides Using a Primary Amine Thiourea Organocatalyst. *Tetrahedron Asymmetry* **2011**, *22* (16–17), 1605–1609.

(85) Muller, P. Glossary of Terms Used in Physical Organic Chemistry: (IUPAC Recommendations 1994). *Pure Appl. Chem.* **1994**, *66* (5), 1077–1184.

(86) Gaunt, M. J.; Johansson, C. C. C. Recent Developments in the Use of Catalytic Asymmetric Ammonium Enolates in Chemical Synthesis. *Chem. Rev*. **2007**, *107* (12), 5596–5605.

(87) France, S.; Guerin, D. J.; Miller, S. J.; Lectka, T. Nucleophilic Chiral Amines as Catalysts in Asymmetric Synthesis. *Chem. Rev.* **2003**, *103* (8), 2985–3012.

(88) Cowen, B. J.; Miller, S. J. Enantioselective Catalysis and Complexity Generation from Allenoates. *Chem. So. Rev*. **2009**, *38*, 3102–3116.

(89) Methot, J. L.; Roush, W. R. Nucleophilic Phosphine Organocatalysis. *Adv. Synth. Catal.* **2004**, *346* (910), 1035–1050.

(90) Ni, H.; Chan, W. L.; Lu, Y. Phosphine-Catalyzed Asymmetric Organic Reactions. *Chem. Rev*. **2018**, *118* (18), 9344–9411.

(91) Guo, H.; Fan, Y. C.; Sun, Z.; Wu, Y.; Kwon, O. Phosphine Organocatalysis. *Chem. Rev*. **2018**, *118* (20), 10049–10293.

(92) Fan, Y. C.; Kwon, O. Advances in Nucleophilic Phosphine Catalysis of Alkenes, Allenes, Alkynes, and MBHADs. *Chem. Commun.* **2013**, *49* (99), 11588–11619.

(93) Xiao, Y.; Sun, Z.; Guo, H.; Kwon, O. Chiral Phosphines in Nucleophilic Organocatalysis. *Beilstein J. Org. Chem*. **2014**, *10*, 2089–2121.

(94) Zhang, H.; Zhou, R. Recent Advances in Phosphine-Promoted (4 + 1) Annulation Reactions. *Eur. J. Org. Chem.* **2020**, 1–11.

(95) Chen, J. R.; Hu, X. Q.; Lu, L. Q.; Xiao, W. J. Formal [4+1] Annulation Reactions in the Synthesis of Carbocyclic and Heterocyclic Systems. *Chem. Rev*. **2015**, *115* (11), 5301–5365.

(96) Kurti, L.; Czako, B. Strategic Applications of Named Reactions in Organic Synthesis, Academic Press, 2005.

(97) Morita, K.; Suzuki, Z.; Hirose, H. A Tertiary Phosphine-Catalyzed Reaction of Acrylic Compounds with Aldehydes. *Bull. Chem. Soc. Jpn.* **1968**, *41* (11), 2815–2815.

(98) Hillman, M.; Baylis, A. (1972) *Reaction of Acrylic Type Compounds with Aldehydes And Certain Ketones* (United States Patent No. US3743669 (A)), U.S. Patent and Trademark Office.

(99) Lima-Junior, C. G.; Vasconcellos, M. L. A. A. Morita-Baylis-Hillman Adducts: Biological Activities and Potentialities to the Discovery of New Cheaper Drugs. *Bioorg. Med. Chem*. **2012**, *20* (13), 3954–3971.

(100) Zhong, N. J.; Wang, Y. Z.; Cheng, L.; Wang, D.; Liu, L. Recent Advances in the Annulation of Morita-Baylis-Hillman Adducts. *Org. Biomol. Chem.* **2018**, *16*, 5214–5227.

(101) Burk, M. J.; Goel, O. P.; Hoekstra, M. S.; Mich, T. F.; Mulhern, T.; Ramsden, J. A. (2005) *Asymmetric Synthesis of Pregabalin* (United States Patent No. US006891059B2), U.S. Patent and Trademark Office.

(102) Pellissier, H. Recent Developments in the Asymmetric Organocatalytic Morita−Baylis−Hillman Reaction. *Tetrahedron*. **2017**, *73* (20), 2831–2861.

(103) Wei, Y.; Shi, M. Recent Advances in Organocatalytic Asymmetric Morita–Baylis–Hillman/Aza-Morita–Baylis–Hillman Reactions. *Chem. Rev.* **2013**, *113* (8), 6659–6690.

(104) Masson, G.; Housseman, C.; Zhu, J. The Enantioselective Morita-Baylis-Hillman Reaction and Its Aza Counterpart. *Angew. Chem. Int. Ed*. **2007**, *46* (25), 4614–4628.

(105) Declerck, V.; Martinez, J.; Lamaty, F. *Aza*-Baylis−Hillman Reaction. *Chem. Rev.* **2009**, *109* (1), 1–48.

(106) Cantillo, D.; Kappe, C. O. A Unified Mechanistic View on the Morita−Baylis−Hillman Reaction: Computational and Experimental Investigations. *J. Org. Chem.* **2010**, *75* (24), 8615–8626.

(107) Amarante, G. W.; Milagre, H. M. S.; Vaz, B. G.; Vilachã Ferreira, B. R.; Eberlin, M. N.; Coelho, F. Dualistic Nature of the Mechanism of the Morita−Baylis−Hillman Reaction Probed by Electrospray Ionization Mass Spectrometry. *J. Org. Chem.* **2009**, *74* (8), 3031–3037.

(108) Aggarwal, V. K.; Fulford, S. Y.; Lloyd-Jones, G. C. Reevaluation of the Mechanism of the Baylis-Hillman Reaction: Implications for Asymmetric Catalysis. *Angew. Chem. Int. Ed.* **2005**, *44* (11), 1706–1708.

(109) Robiette, R.; Aggarwal, V. K.; Harvey, J. N. Mechanism of the Morita−Baylis−Hillman Reaction: A Computational Investigation. *J. Am. Chem. Soc.* **2007**, *129* (50), 15513–15525.

(110) Price, K. E.; Broadwater, S. J.; Jung, H. M.; McQuade, D. T. Baylis−Hillman Mechanism: A New Interpretation in Aprotic Solvents. *Org. Lett.* **2005**, *7* (1), 147–150.

(111) Price, K. E.; Broadwater, S. J.; Walker, B. J.; McQuade, D. T. A New Interpretation of the Baylis−Hillman Mechanism. *J. Org. Chem.* **2005**, *70* (10), 3980–3987.

(112) Buskens, P.; Klankermayer, J.; Leitner, W. Bifunctional Activation and Racemization in the Catalytic Asymmetric Aza-Baylis−Hillman Reaction. *J. Am. Chem. Soc.* **2005**, *127* (48), 16762–16763.

(113) Raheem, I. T.; Jacobsen, E. N. Highly Enantioselective Aza-Baylis-Hillman Reactions Catalyzed by Chiral Thiourea Derivatives. *Adv. Synth. Catal.* **2005**, *347* (11–13), 1701–1708.

(114) Iwabuchi, Y.; Hatakeyama, S. Recent Progress in the Morita-Baylis-Hillman Reactions. *J. Synth. Org. Chem. Japan* **2002**, *60* (1), 2–14.

(115) Nakano, A.; Kawahara, S.; Akamatsu, S.; Morokuma, K.; Nakatani, M.; Iwabuchi, Y.; Takahashi, K.; Ishihara, J.; Hatakeyama, S. β-Isocupreidine-Hexafluoroisopropyl Acrylate Method for Asymmetric Baylis-Hillman Reactions. *Tetrahedron* **2006**, *62* (2–3), 381–389.

(116) Nakamoto, Y.; Urabe, F.; Takahashi, K.; Ishihara, J.; Hatakeyama, S. α-Isocupreine, an Enantiocomplementary Catalyst of β-Isocupreidine. *Chem. Eur. J.* **2013**, *19* (38), 12653–12656.

(117) Iwabuchi, Y.; Furukawa, M.; Esumia, T.; Hatakeyama, S. An Enantio- and Stereocontrolled Synthesis of (−)-Mycestericin E *via* Cinchona Alkaloid-Catalyzed Asymmetric Baylis–Hillman Reaction. *Chem. Commun.* **2001**, 2030–2031.

(118) Iwabuchi, Y.; Sugihara, T.; Esumi, T.; Hatakeyama, S. An Enantio- and Stereocontrolled Route to Epopromycin B *via* Cinchona Alkaloid-Catalyzed Baylis-Hillman Reaction. *Tetrahedron Lett.* **2001**, *42* (44), 7867–7871.

(119) Yoshimura, H.; Takahashi, K.; Ishihara, J.; Hatakeyama, S. Unified Synthesis of Tirandamycins and Streptolydigins. *Chem. Commun.* **2015**, *51* (95), 17004–17007.

(120) Yuan, K.; Song, H. L.; Hu, Y.; Wu, X. Y. Chiral Phosphinothiourea-Catalyzed

Asymmetric Morita-Baylis-Hillman Reactions of Acrylates with Aromatic Aldehydes. *Tetrahedron* **2009**, *65* (39), 8185–8190.

(121) Han, X.; Wang, Y.; Zhong, F.; Lu, Y. Enantioselective Morita-Baylis-Hillman Reaction Promoted by L-Threonine-Derived Phosphine-Thiourea Catalysts. *Org. Biomol. Chem.* **2011**, *9* (19), 6734–6740.

(122) Isenegger, P. G.; Bächle, F.; Pfaltz, A. Asymmetric Morita-Baylis-Hillman Reaction: Catalyst Development and Mechanistic Insights Based on Mass Spectrometric Back-Reaction Screening. *Chem. Eur. J.* **2016**, *22* (49), 17595–17599.

(123) Song, H. L.; Yuan, K.; Wu, X. Y. Chiral Phosphine-Squaramides as Enantioselective Catalysts for the Intramolecular Morita-Baylis-Hillman Reaction. *Chem. Commun.* **2011**, *47* (3), 1012–1014.

(124) Guan, X.-Y.; Wei, Y.; Shi, M. Construction of Chiral Quaternary Carbon through Morita-Baylis-Hillman Reaction: An Enantioselective Approach to 3-Substituted 3-Hydroxyoxindole Derivatives. *Chem. Eur. J.* **2010**, *16* (46), 13617–13621.

(125) Zhong, F.; Chen, G.-Y.; Lu, Y. Enantioselective Morita−Baylis−Hillman Reaction of Isatins with Acrylates: Facile Creation of 3-Hydroxy-2-Oxindoles. *Org. Lett.* **2011**, *13* (1), 82–85.

(126) Liu, Y.-L.; Wang, B.-L.; Cao, J.-J.; Chen, L.; Zhang, Y.-X.; Wang, C.; Zhou, J. Organocatalytic Asymmetric Synthesis of Substituted 3-Hydroxy-2-Oxindoles *via* Morita−Baylis−Hillman Reaction. *J. Am. Chem. Soc.* **2010**, *132* (43), 15176–15178.

(127) Chauhan, P.; Chimni, S. S. Organocatalytic Enantioselective Morita-Baylis-Hillman Reaction of Maleimides with Isatins. *Asian J. Org. Chem.* **2013**, *2* (7), 586–592.

(128) He, Q.; Zhan, G.; Du, W.; Chen, Y.-C. Application of 7-Azaisatins in Enantioselective Morita–Baylis–Hillman Reaction. *Beilstein J. Org. Chem.* **2016**, *12*, 309–313.

(129) Wang, C. C.; Wu, X. Y. Catalytic Asymmetric Synthesis of 3-Hydroxyl-2-Oxindoles *via* Enantioselective Morita-Baylis-Hillman Reaction of Isatins. *Tetrahedron* **2011**, *67* (16), 2974–2978.

(130) Qian, J. Y.; Wang, C. C.; Sha, F.; Wu, X. Y. Chiral Phosphine-Squaramide-Catalyzed Morita-Baylis-Hillman Reaction: Enantioselective Synthesis of 3-Hydroxy-2-Oxindoles. *RSC Adv.* **2012**, *2* (14), 6042–6048.

(131) Dong, Z.; Yan, C.; Gao, Y.; Dong, C.; Qiu, G.; Zhou, H.-B. Tunable Bifunctional Phosphine-Squaramide Promoted Morita-Baylis-Hillman Reaction of *N*-Alkyl Isatins with Acrylates. *Adv. Synth. Catal.* **2015**, *357* (9), 2132–2142.

(132) Zhang, Q.; Yang, L.; Tong, X. 2-(Acetoxymethyl)Buta-2,3-Dienoate, a Versatile 1,4-Biselectrophile for Phosphine-Catalyzed (4 + n) Annulations with 1,n-Bisnucleophiles (N=1,2). *J. Am. Chem. Soc.* **2010**, *132* (8), 2550–2551.

(133) Han, X.; Yao, W.; Wang, T.; Tan, Y. R.; Yan, Z.; Kwiatkowski, J.; Lu, Y. Asymmetric Synthesis of Spiropyrazolones through Phosphine-Catalyzed [4+1] Annulation. *Angew. Chem. Int. Ed.* **2014**, *53* (22), 5643–5647.

(134) Ziegler, D. T.; Riesgo, L.; Ikeda, T.; Fujiwara, Y.; Fu, G. C. Biphenyl-Derived Phosphepines as Chiral Nucleophilic Catalysts: Enantioselective [4+1] Annulations to Form Functionalized Cyclopentenes. *Angew. Chem. Int. Ed.* **2014**, *53* (48), 13183–13187.

(135) Zhang, X. N.; Deng, H. P.; Huang, L.; Wei, Y.; Shi, M. Phosphine-Catalyzed Asymmetric [4+1] Annulation of Morita-Baylis-Hillman Carbonates with Dicyano-2-Methylenebut-3-Enoates. *Chem. Commun.* **2012**, *48* (69), 8664–8666.

(136) Mishra, A.; Mishra, N.; Tiwari, V. K. Carbohydrate-Based Organocatalysts: Recent Developments and Future Perspectives. *Curr. Org. Synth.* **2015**, *13* (2), 176–219.

(137) Phillips, A. M. F. Applications of Carbohydrate-Based Organocatalysts in Enantioselective Synthesis. *Eur. J. Org. Chem.* **2014**, *2014* (33), 7291–7303.

(138) Agarwal, J. Progress in Aminosugar Derived Asymmetric Organocatalysis. *Org. Biomol. Chem.* **2016**, *14* (46), 10747–10762.

(139) Singh, N.; Pandey, J.; Tripathi, R. P. D-Glucosamine, a Natural Aminosugar as Organocatalyst for an Ecofriendly Direct Aldol Reaction of Ketones with Aromatic Aldehydes in Water. *Catal. Commun.* **2008**, *9* (5), 743–746.

(140) Agarwal, J.; Peddinti, R. K. Glucosamine-Based Primary Amines as Organocatalysts for the Asymmetric Aldol Reaction. *J. Org. Chem.* **2011**, *76* (9), 3502–3505.

(141) Li, L.; Fang, Z.; Fang, J.; Zhou, J.; Xiang, Y. D-Fructose-Derived β-Amino Alcohol Catalyzed Direct Asymmetric Aldol Reaction in the Presence of *p*-Nitrophenol. *RSC Adv.* **2013**, *3* (43), 21084–21091.

(142) Tsutsui, A.; Takeda, H.; Kimura, M.; Fujimoto, T.; Machinami, T. Novel Enantiocontrol System with Aminoacyl Derivatives of Glucoside as Enamine-Based Organocatalysts for Aldol Reaction in Aqueous Media. *Tetrahedron Lett.* **2007**, *48* (30), 5213–5217.

(143) Shen, C.; Shen, F.; Zhou, G.; Xia, H.; Chen, X.; Liu, X.; Zhang, P. Novel Carbohydrate-Derived Prolinamide as a Highly Efficient, Recoverable Catalyst for Direct Aldol Reactions in Water. *Catal. Commun.* **2012**, *26*, 6–10.

(144) Wenzel, A. G.; Jacobsen, E. N. Asymmetric Catalytic Mannich Reactions Catalyzed by Urea Derivatives: Enantioselective Synthesis of *β* -Aryl- *β* -Amino Acids. *J. Am. Chem. Soc.* **2002**, *124* (44), 12964–12965.

(145) Becker, C.; Hoben, C.; Kunz, H. Enantioselective Organocatalysis of Strecker and Mannich Reactions Based on Carbohydrates. *Adv. Synth. Catal.* **2007**, *349* (3), 417–424.

(146) Wang, C.; Zhou, Z.; Tang, C. Novel Bifunctional Chiral Thiourea Catalyzed Highly Enantioselective Aza-Henry Reaction. *Org. Lett.* **2008**, *10* (9), 1707–1710.

(147) Ma, H.; Liu, K.; Zhang, F.-G.; Zhu, C.-L.; Nie, J.; Ma, J.-A. Chiral Bifunctional Thiourea-Catalyzed Enantioselective Michael Addition of Ketones to Nitrodienes. *J. Org. Chem.* **2010**, *75* (5), 1402–1409.

(148) Nie, J.; Li, X. J.; Zheng, D. H.; Zhang, F. G.; Cui, S.; Ma, J. A. Chiral Bifunctional Thiourea-Catalyzed Enantioselective Aldol Reaction of Trifluoroacetaldehyde Hemiacetal with Aromatic Ketones. *J. Fluor. Chem.* **2011**, *132* (7), 468–473.

(149) Liu, K.; Cui, H.-F. F.; Nie, J.; Dong, K.-Y. Y.; Li, X.-J. J.; Ma, J.-A. A. Highly Enantioselective Michael Addition of Aromatic Ketones to Nitroolefins Promoted by Chiral Bifunctional Primary Amine-Thiourea Catalysts Based on Saccharides. *Org. Lett.* **2007**, *9* (5), 923–925.

(150) Lu, A.; Hu, K.; Wang, Y.; Song, H.; Zhou, Z.; Fang, J.; Tang, C. Enantioselective Synthesis of *Trans*-Dihydrobenzofurans *via* Primary Amine-Thiourea Organocatalyzed Intramolecular Michael Addition. *J. Org. Chem.* **2012**, *77* (14), 6208–6214.

(151) Gu, Q.; Guo, X. T.; Wu, X. Y. Highly Enantioselective Michael Addition of Acetone to Nitroolefins Catalyzed by Chiral Bifunctional Primary Amine-Thiourea Catalysts with Acetic Acid. *Tetrahedron* **2009**, *65* (27), 5265–5270.

(152) Lu, A.; Gao, P.; Wu, Y.; Wang, Y.; Zhou, Z.; Tang, C. Highly Enantio- and

Diastereoselective Michael Addition of Cyclohexanone to Nitroolefins Catalyzed by a Chiral Glucose-Based Bifunctional Secondary Amine-Thiourea Catalyst. *Org. Biomol. Chem.* **2009**, *7* (15), 3141–3147.

(153) Wang, Y.; Yang, H.; Yu, J.; Miao, Z.; Chen, R. Highly Enantioselective Biginelli Reaction Promoted by Chiral Bifunctional Primary Amine-Thiourea Catalysts: Asymmetric Synthesis of Dihydropyrimidines. *Adv. Synth. Catal.* **2009**, *351* (18), 3057–3062.

(154) Kong, S.; Fan, W.; Wu, G.; Miao, Z. Enantioselective Synthesis of Tertiary α-Hydroxy Phosphonates Catalyzed by Carbohydrate/Cinchona Alkaloid Thiourea Organocatalysts. *Angew. Chem. Int. Ed.* **2012**, *51* (35), 8864–8867.

(155) Yuan, H.-N.; Li, S.; Nie, J.; Zheng, Y.; Ma, J.-A. Highly Enantioselective Decarboxylative Mannich Reaction of Malonic Acid Half Oxyesters with Cyclic Trifluoromethyl Ketimines: Synthesis of β-Amino Esters and Anti-HIV Drug DPC 083. *Chem. Eur. J.* **2013**, *19* (47), 15856–15860.

(156) Pu, X.; Li, P.; Peng, F.; Li, X.; Zhang, H.; Shao, Z. Asymmetric Conjugate Addition of Acetylacetone to Nitroolefins with Chiral Organocatalysts Derived from Both α-Amino -Acids and Carbohydrates. *Eur. J. Org. Chem.* **2009**, *2009* (27), 4622–4626.

(157) Pu, X. W.; Peng, F. Z.; Zhang, H. Bin; Shao, Z. H. Doubly Stereocontrolled Asymmetric Conjugate Addition of Acetylacetone to Nitroolefins Catalyzed by Bifunctional Tertiary Amine-Thiourea Catalysts Derived from Both Acyclic α-Amino Acids and Carbohydrates. *Tetrahedron* **2010**, *66* (21), 3655–3661.

(158) Puglisi, A.; Benaglia, M.; Raimondi, L.; Lay, L.; Poletti, L. Novel Carbohydrate-Based Bifunctional Organocatalysts for Nucleophilic Addition to Nitroolefins and Imines. *Org. Biomol. Chem.* **2011**, *9* (9), 3295–3302.

(159) Yang, W.; Sha, F.; Zhang, X.; Yuan, K.; Wu, X. Enantioselective Morita-Baylis-Hillman Reaction Organocatalyzed by Glucose-Based Phosphinothiourea. *Chinese J. Chem.* **2012**, *30* (11), 2652–2656.

(160) Hussain, I.; Singh, T. Synthesis of Biaryls through Aromatic C-H Bond Activation: A Review of Recent Developments. *Adv. Synth. Catal.* **2014**, *356* (8), 1661–1696.

(161) *Metal-Catalyzed Cross-Coupling Reactians;* de Meijere, A., Bräse, S, Oestreich, M., Eds.; Wiley-VCH: Weinheim, Germany, 2004.

(162) Dasgupta, R.; Maltl, B. R. Thermal Dehydrocondensation of Benzene to Diphenyl in a Nonisothermal Flow Reactor. *Ind. Eng. Chem. Process Des. Dev.* **1986**, *25* (2), 381–386.

(163) Constable, D. J. C.; Dunn, P. J.; Hayler, J. D.; Humphrey, G. R.; Leazer, J. L.; Linderman, R. J.; Lorenz, K.; Manley, J.; Pearlman, B. A.; Wells, A.; Zaks, A.; Zhang, T. Y. Key Green Chemistry Research Areas - A Perspective from Pharmaceutical Manufacturers. *Green Chem.* **2007**, *9* (5), 411–420.

(164) Alberico, D.; Scott, M. E.; Lautens, M. Aryl-Aryl Bond Formation by Transition-Metal-Catalyzed Direct Arylation. *Chem. Rev.* **2007**, *107*, 174–238.

(165) Seregin, I. V.; Gevorgyan, V. Direct Transition Metal-Catalyzed Functionalization of Heteroaromatic Compounds. *Chem. Soc. Rev.* **2007**, *36* (7), 1173–1193.

(166) McGlacken, G. P.; Bateman, L. M. Recent Advances in Aryl-Aryl Bond Formation by Direct Arylation. *Chem. Soc. Rev*. **2009**, *38*, 2447–2464.

(167) Ackermann, L.; Vicente, R.; Kapdi, A. R. Transition-Metal-Catalyzed Direct Arylation of (Hetero)Arenes by C-H Bond Cleavage. *Angew. Chem. Int. Ed.* **2009**, *48* (52), 9792–

9826.

(168) Wencel-Delord, J.; Dröge, T.; Liu, F.; Glorius, F. Towards Mild Metal-Catalyzed C-H Bond Activation. *Chem. Soc. Rev*. **2011**, *40*, 4740–4761.

(169) Yamaguchi, J.; Itami, K. Biaryl Synthesis through Metal-Catalyzed C-H Arylation. In *Metal-Catalyzed Cross-Coupling Reactians and More;* de Meijere, A., Bräse, S, Oestreich, M., Eds.; Wiley-VCH: Weinheim, Germany, 2013, pp 1315–1387.

(170) Campeau, L. C.; Parisien, M.; Jean, A.; Fagnou, K. Catalytic Direct Arylation with Aryl Chlorides, Bromides, and Iodides: Intramolecular Studies Leading to New Intermolecular Reactions. *J. Am. Chem. Soc.* **2006**, *128* (2), 581–590.

(171) Kuhl, N.; Hopkinson, M. N.; Wencel-Delord, J.; Glorius, F. Beyond Directing Groups: Transition-Metal-Catalyzed C-H Activation of Simple Arenes. *Angew. Chem. Int. Ed*. **2012**, *51* (41), 10236–10254.

(172) Lafrance, M.; Fagnou, K. Palladium-Catalyzed Benzene Arylation: Incorporation of Catalytic Pivalic Acid as a Proton Shuttle and a Key Element in Catalyst Design. *J. Am. Chem. Soc.* **2006**, *128* (51), 16496–16497.

(173) Ricci, P.; Krämer, K.; Cambeiro, X. C.; Larrosa, I. Arene–Metal π-Complexation as a Traceless Reactivity Enhancer for C–H Arylation. *J. Am. Chem. Soc.* **2013**, *135* (36), 13258–13261.

(174) Ricci, P.; Krämer, K.; Larrosa, I. Tuning Reactivity and Site Selectivity of Simple Arenes in C-H Activation: Ortho-Arylation of Anisoles *via* Arene-Metal π-Complexation. *J. Am. Chem. Soc.* **2014**, *136* (52), 18082–18086.

(175) Zhang, S.; Shi, L.; Ding, Y. Theoretical Analysis of the Mechanism of Palladium(II) Acetate-Catalyzed Oxidative Heck Coupling of Electron-Deficient Arenes with Alkenes: Effects of the Pyridine-Type Ancillary Ligand and Origins of the *meta*-Regioselectivity. *J. Am. Chem. Soc.* **2011**, *133* (50), 20218–20229.

(176) Lapointe, D.; Fagnou, K. Overview of the Mechanistic Work on the Concerted Metallation–Deprotonation Pathway. *Chem. Lett.* **2010**, *39* (11), 1118–1126.

(177) Boutadla, Y.; Davies, D. L.; Macgregor, S. A.; Poblador-Bahamonde, A. I. Mechanisms of C–H Bond Activation: Rich Synergy between Computation and Experiment. *J. Chem. Soc., Dalton Trans*. **2009**, 5820–5831.

(178) Newton, C. G.; Wang, S. G.; Oliveira, C. C.; Cramer, N. Catalytic Enantioselective Transformations Involving C-H Bond Cleavage by Transition-Metal Complexes. *Chem. Rev.* **2017**, *117* (13), 8908–8976.

(179) Wencel-Delord, J.; Colobert, F. Asymmetric C(Sp^2)-H Activation. *Chem. Eur. J.* **2013**, *19* (42), 14010–14017.

(180) Davies, H. M. L.; Manning, J. R. Catalytic C-H Functionalization by Metal Carbenoid and Nitrenoid Insertion. *Nature*. **2008**, *451*, 417–424.

(181) Shi, B.-F.; Maugel, N.; Zhang, Y.-H.; Yu, J.-Q. Pd^{II}-Catalyzed Enantioselective Activation of C(Sp^2)-H and C(Sp^3)-H Bonds Using Monoprotected Amino Acids as Chiral Ligands. *Angew. Chem. Int. Ed.* **2008**, *47* (26), 4882–4886.

(182) Cheng, G.-J.; Chen, P.; Sun, T.-Y.; Zhang, X.; Yu, J.-Q.; Wu, Y.-D. A Combined IM-MS/DFT Study on [Pd(MPAA)]-Catalyzed Enantioselective C-H Activation: Relay of Chirality through a Rigid Framework. *Chem. Eur. J.* **2015**, *21* (31), 11180–11188.

(183) Shi, B. F.; Zhang, Y. H.; Lam, J. K.; Wang, D. H.; Yu, J. Q. Pd(II)-Catalyzed Enantioselective C-H Olefination of Diphenylacetic Acids. *J. Am. Chem. Soc.* **2010**, *132* (2), 460–461.

(184) Laforteza, B. N.; Chan, K. S. L.; Yu, J.-Q. Enantioselective *Ortho*-C-H Cross-Coupling of Diarylmethylamines with Organoborons. *Angew. Chem. Int. Ed.* **2015**, *54* (38), 11143–11146.

(185) Dai, L. X.; Hou, X. L. *Chiral Ferrocenes in Asymmetric Catalysis: Synthesis and Applications*; Dai, L.-X., Hou, X.-L., Eds.; Wiley-VCH: Weinheim, Germany, 2010.

(186) Gao, D. W.; Shi, Y. C.; Gu, Q.; Zhao, Z. Le; You, S. L. Enantioselective Synthesis of Planar Chiral Ferrocenes *via* Palladium-Catalyzed Direct Coupling with Arylboronic Acids. *J. Am. Chem. Soc.* **2013**, *135* (1), 86–89.

(187) Pi, C.; Li, Y.; Cui, X.; Zhang, H.; Han, Y.; Wu, Y. Redox of Ferrocene Controlled Asymmetric Dehydrogenative Heck Reaction *via* Palladium-Catalyzed Dual C-H Bond Activation. *Chem. Sci.* **2013**, *4* (6), 2675–2679.

(188) Shi, Y.-C.; Yang, R.-F.; Gao, D.-W.; You, S.-L. Enantioselective Synthesis of Planar Chiral Ferrocenes *via* Palladium-Catalyzed Annulation with Diarylethynes. *Beilstein J. Org. Chem.* **2013**, *9* (1), 1891–1896.

(189) Gao, D. W.; Gu, Q.; You, S. L. An Enantioselective Oxidative C-H/C-H Cross-Coupling Reaction: Highly Efficient Method to Prepare Planar Chiral Ferrocenes. *J. Am. Chem. Soc.* **2016**, *138* (8), 2544–2547.

(190) Albicker, M.; Cramer, N. Enantioselective Palladium-Catalyzed Direct Arylations at Ambient Temperature: Access to Indanes with Quaternary Stereocenters. *Angew. Chem. Int. Ed.* **2009**, *48* (48), 9139–9142.

(191) Cheng, X. F.; Li, Y.; Su, Y. M.; Yin, F.; Wang, J. Y.; Sheng, J.; Vora, H. U.; Wang, X. S.; Yu, J. Q. Pd(II)-Catalyzed Enantioselective C-H Activation/C-O Bond Formation: Synthesis of Chiral Benzofuranones. *J. Am. Chem. Soc.* **2013**, *135* (4), 1236–1239.

(192) Pi, C.; Cui, X.; Liu, X.; Guo, M.; Zhang, H.; Wu, Y. Synthesis of Ferrocene Derivatives with Planar Chirality *via* Palladium-Catalyzed Enantioselective C-H Bond Activation. *Org. Lett.* **2014**, *16* (19), 5164–5167.

(193) Uemura, M.; Miyake, R.; Nishimura, H.; Matsumoto, Y.; Hayashi, T. New Chiral Phosphine Ligands Containing (η^6-Arene)chromium and Catalytic Asymmetric Cross-Coupling Reactions. *Tetrahedron: Asymmetry* **1992**, *3* (2), 213–216.

(194) Ogasawara, M.; Tseng, Y. Y.; Arae, S.; Morita, T.; Nakaya, T.; Wu, W. Y.; Takahashi, T.; Kamikawa, K. Phosphine-Olefin Ligands Based on a Planar-Chiral (π-Arene)Chromium Scaffold: Design, Synthesis, and Application in Asymmetric Catalysis. *J. Am. Chem. Soc.* **2014**, *136* (26), 9377–9384.

(195) Hayashi, Y.; Sakai, H.; Kaneta, N.; Uemura, M. New Chiral Chelating Phosphine Complexes Containing Tricarbonyl(η^6-Arene) Chromium for Highly Enantioselective Allylic Alkylation. *J. Organomet. Chem.* **1995**, *503* (1), 143–148.

(196) Nelson, S. G.; Hilfiker, M. A. Asymmetric Synthesis of Monodentate Phosphine Ligands Based on Chiral η^6-Cr[Arene] Templates. *Org. Lett.* **1999**, *1* (9), 1379–1382.

(197) Han, J. W.; Jang, H. Y.; Chung, Y. K. Synthesis and Use in Palladium-Catalyzed Asymmetric Allylic Alkylation of New Planar Chiral Chromium Complexes of 1,2-Disubstituted Arenes Having Pyridine and Aryl Phosphine Groups. *Tetrahedron Asymmetry* **1999**, *10* (15), 2853–2861.

(198) Vasen, D.; Salzer, A.; Gerhards, F.; Gais, H. J.; Stürmer, R.; Bieler, N. H.; Togni, A. Optically Active Transition-Metal Complexes. 10.[1] Bifunctional Arene-Chromium-Tricarbonyl Complexes Derived from (*R*)-Phenylethanamine: Easily Accessible Planar-Chiral Diphosphines and Their Application in Enantioselective Hydrogenation,

Hydroamination, and Allylic Sulfonation. *Organometallics* **2000**, *19* (4), 539–546.

(199) Uemura, M.; Miyake, R.; Nakayama, K.; Shiro, M.; Hayashi, Y. Chiral (η^6-Arene)chromium Complexes in Organic Synthesis: Stereoselective Synthesis of Chiral (Arene)chromium Complexes Possessing Amine and Hydroxy Groups and Their Application to Asymmetric Reactions. *J. Org. Chem.* **1993**, *58* (5), 1238–1244.

(200) Ogasawara, M.; Wu, W. Y.; Arae, S.; Watanabe, S.; Morita, T.; Takahashi, T.; Kamikawa, K. Kinetic Resolution of Planar-Chiral (η^6-Arene)chromium Complexes by Molybdenum-Catalyzed Asymmetric Ring-Closing Metathesis. *Angew. Chem. Int. Ed.* **2012**, *51* (12), 2951–2955.

(201) Englert, U.; Haerter, R.; Vasen, D.; Salzer, A.; Eggeling, E. B.; Vogt, D. Optically Active Transition-Metal Complexes. 9.[1] A General Stereoselective Route to α-Chiral (*R*)-Tricarbonyl(η^6-Ethylbenzene)chromium Complexes. Novel Organometallic Phosphine Catalysts for the Asymmetric Hydrovinylation Reaction. *Organometallics* **1999**, *18* (21), 4390–4398.

(202) Son, S. U.; Jang, H. Y.; Lee, I. S.; Chung, Y. K. Synthesis of Planar Chiral (1,2-Disubstituted Arene)chromium Tricarbonyl Compounds and Their Application in Asymmetric Hydroboration. *Organometallics* **1998**, *17* (15), 3236–3239.

(203) Weber, I.; Jones, G. B. Bidentate Planar Chiral η^6-Arene Tricarbonyl Chromium(0) Complexes: Ligands for Catalytic Asymmetric Alkene Hydrosilylation. *Tetrahedron Lett.* **2001**, *42* (40), 6983–6986.

(204) Jones, G. B.; Heaton, S. B.; Chapman, B. J.; Guzel, M. On the Origins of Enantioselectivity in Oxazaborolidine Mediated Carbonyl Reductions. *Tetrahedron Asymmetry* **1997**, *8* (21), 3625–3636.

(205) Pasquier, C.; Naili, S.; Pelinski, L.; Brocard, J.; Mortreux, A.; Agbossou, F. Synthesis and Application in Enantioselective Hydrogenation of New Free and Chromium Complexed Aminophosphine-Phosphinite Ligands. *Tetrahedron Asymmetry* **1998**, *9* (2), 193–196.

(206) Uemura, M.; Nishimura, H.; Hayashi, T. Catalytic Asymmetric Induction of Planar Chirality by Palladium-Catalyzed Asymmetric Cross-Coupling of a Meso (Arene)Chromium Complex. *Tetrahedron Lett.* **1993**, *34* (1), 107–110.

(207) Kamikawa, K.; Harada, K.; Uemura, M. Catalytic Asymmetric Induction of Planar Chirality: Palladium Catalyzed Intramolecular Mizoroki-Heck Reaction of Prochiral (Arene)Chromium Complexes. *Tetrahedron Asymmetry* **2005**, *16* (8), 1419–1423.

(208) Kündig, E. P.; Chaudhuri, P. D.; House, D.; Bernardinelli, G. Catalytic Enantioselective Hydrogenolysis of [$Cr(CO)_3$(5,8-Dibromonaphthalene)]. *Angew. Chem. Int. Ed.* **2006**, *45* (7), 1092–1095.

(209) Mercier, A.; Urbaneja, X.; Yeo, W. C. C.; Chaudhuri, P. D. D.; Cumming, G. R. R.; House, D.; Bernardinelli, G.; Kündig, E. P. P. Asymmetric Catalytic Hydrogenolysis of Aryl-Halide Bonds in Fused Arene Chromium and Ruthenium Complexes. *Chem. Eur. J.* **2010**, *16* (21), 6285–6299.

(210) Gotov, B.; Schmalz, H. G. A Catalytic-Enantioselective Entry to Planar Chiral π-Complexes: Enantioselective Methoxycarbonylation of 1,2-Dichlorobenzene-$Cr(CO)_3$. *Org. Lett.* **2001**, *3* (11), 1753–1756.

(211) Böttcher, A.; Schmalz, H. G. Catalytic-Enantioselective Methoxycarbonylation of 1,3-Dichloroarenetricarbonyl-Chromium(0) Complexes: A Desymmetrization Approach to Planar Chirality. *Synlett* **2003**, *2003* (11), 1595–1598.

(212) Ogasawara, M.; Wu, W.-Y.; Arae, S.; Watanabe, S.; Morita, T.; Takahashi, T.; Kamikawa, K. Kinetic Resolution of Planar-Chiral (η^6-Arene)Chromium Complexes by Molybdenum-Catalyzed Asymmetric Ring-Closing Metathesis. *Angew. Chem. Int. Ed.* **2012**, *51* (12), 2951–2955.

(213) Murai, M.; Uenishi, J.; Uemura, M. Gold(I)-Catalyzed Asymmetric Synthesis of Planar Chiral Arene Chromium Complexes. *Org. Lett.* **2010**, *12* (21), 4788–4791.

(214) Murai, M.; Sota, Y.; Onohara, Y.; Uenishi, J.; Uemura, M. Gold(I)-Catalyzed Asymmetric Induction of Planar Chirality by Intramolecular Nucleophilic Addition to Chromium-Complexed Alkynylarenes: Asymmetric Synthesis of Planar Chiral (1*H*-Isochromene and 1,2-Dihydroisoquinoline)Chromium Complexes. *J. Org. Chem.* **2013**, *78* (21), 10986–10995.

(215) Praly, J. P.; Lemieux, R. U. Influence of Solvent on the Magnitude of the Anomeric Effect. *Can. J. Chem.* **1987**, *65* (1), 213–223.

(216) Moberg, C. The Role of Symmetry in Asymmetric Catalysis. *Isr. J. Chem.* **2012**, *52* (7), 653–662.

(217) Yuan, K.; Zhang, L.; Song, H. L.; Hu, Y.; Wu, X. Y. Chiral Phosphinothiourea Organocatalyst in the Enantioselective Morita-Baylis-Hillman Reactions of Aromatic Aldehydes with Methyl Vinyl Ketone. *Tetrahedron Lett.* **2008**, *49* (43), 6262–6264.

(218) Bergmann, M.; Zervas, L. Synthesen Mit Glucosamin. *Ber. Dtsch. Chem. Ges.* **1931**, *64* (5), 975–980.

(219) Billing, J. F.; Nilsson, U. J. Cyclic Peptides Containing a δ-Sugar Amino Acid - Synthesis and Evaluation as Artificial Receptors. *Tetrahedron* **2005**, *61* (4), 863–874.

(220) Benessere, V.; De Roma, A.; Del Litto, R.; Lega, M.; Ruffo, F. Naplephos through the Looking-Glass: Chiral Bis(Phosphanylamides) Based on β-1,2-D-Glucodiamine and Their Application in Enantioselective Allylic Substitutions. *Eur. J. Org. Chem.* **2011**, *2011* (29), 5779–5782.

(221) Juaristi, E.; Cuevas, G. Recent Studies of the Anomeric Effect. *Tetrahedron* **1992**, *48* (24), 5019–5087.

(222) Liberek, B.; Melcer, A.; Osuch, A.; Wakieć, R.; Milewski, S.; Wiśniewski, A. *N*-Alkyl Derivatives of 2-Amino-2-Deoxy-D-Glucose. *Carbohydr. Res.* **2005**, *340* (11), 1876–1884.

(223) Su, Y.; Xie, J.; Wang, Y.; Hu, X.; Lin, X. Synthesis and Antitumor Activity of New Shikonin Glycosides. *Eur. J. Med. Chem.* **2010**, *45* (7), 2713–2718.

(224) Kühne, M.; Györgydeak, Z.; Lindhorst, T. K. A Simple Method for the Preparation of Glycosyl Isothiocyanates. *Synthesis.* **2006**, No. 6, 949–951.

(225) Pacsu, E. Umlagerung Der β-Glykoside Und β-Acetylzucker in Ihre α-Form. *Ber. Dtsch. Chem. Ges.* **1928**, *61* (1), 137–144.

(226) Ellervik, U.; Jansson, K.; Magnusson, G. Gas Chromatographic Investigation of the Boron Trifluoride Etherate-Induced Formation and Anomerization of Glucopyranosides. *J. Carbohydr. Chem.* **1998**, *17* (4–5), 777–784.

(227) Šardzík, R.; Noble, G. T.; Weissenborn, M. J.; Martin, A.; Webb, S. J.; Flitsch, S. L. Preparation of Aminoethyl Glycosides for Glycoconjugation. *Beilstein J. Org. Chem.* **2010**, *6*, 699–703.

(228) Lindhorst, T. K.; Kieburg, C. Solvent-Free Preparation of Glycosyl Isothiocyanates. *Synthesis.* **1995**, No. 10, 1228–1230.

(229) Kuijpers, B. H. M.; Groothuys, S.; Soede, A. C.; Laverman, P.; Boerman, O. C.; van Delft, F. L.; Rutjes, F. P. J. T. Preparation and Evaluation of Glycosylated Arginine–Glycine–Aspartate (RGD) Derivatives for Integrin Targeting. *Bioconjug. Chem.* **2007**, *18* (6), 1847–1854.

(230) Tsuji, M.; Yamazaki, H. (2000) *Process for the Preparation of Pentaacetyl-beta-D-Glucopyranose* (European Patent No. EP1041080A1), European Patent Office.

(231) Praly, J. P.; Senni, D.; Faure, R.; Descotes, G. Synthesis and Structure of Bromo Glycosyl Imines Readily Obtained from Protected Glycosyl Azides. *Tetrahedron* **1995**, *51* (6), 1697–1708.

(232) Ichikawa, Y.; Nishiyama, T.; Isobe, M. Stereospecific Synthesis of the α- and β-D-Glucopyranosyl Ureas. *J. Org. Chem.* **2001**, *66* (12), 4200–4205.

(233) McKennon, M. J.; Meyers, A. I.; Drauz, K.; Schwarm, M. A Convenient Reduction of Amino Acids and their Derivatives. *J. Org. Chem*. **1993**, *58* (13), 3568–3571.

(234) Dickman, D. A.; Meyers, A. I.; Smith, G. A.; Gawley, R. E. Reduction of α-Amino Aacids: L-Valinol. *Org. Synth.* **1985**, *63*, 136.

(235) Kawamura, K.; Fukuzawa, H.; Hayashi, M. Novel *N,N,P* -Tridentate Ligands for the Highly Enantioselective Copper-Catalyzed 1,4-Addition of Dialkylzincs to Enones. *Org. Lett.* **2008**, *10* (16), 3509–3512.

(236) Saitoh, A.; Uda, T.; Morimoto, T. A New Class of C2-Symmetric Diphosphine Ligands Derived from Valine: Remarkably Diverse Behavior in Catalytic Asymmetric Transformations. *Tetrahedron Asymmetry* **1999**, *10* (23), 4501–4511.

(237) Berkowitz, D. B.; Bernd Schweizer, W. A New Retro-Aza-Ene Reaction: Formal Reductive Amination of an α-Keto Acid to an α-Amino Acid. *Tetrahedron* **1992**, *48* (9), 1715–1728.

(238) Douat-Casassus, C.; Pulka, K.; Claudon, P.; Guichard, G. Microwave-Enhanced Solid-Phase Synthesis of *N*, *N'*-Linked Aliphatic Oligoureas and Related Hybrids. *Org. Lett.* **2012**, *14* (12), 3130–3133.

(239) Wessig, P.; Schwarz, J. A Convenient One-Pot Conversion of *N*-Boc-*β*-Aminoalcohols into *N*-Boc-Aziridines. *Synlett* **1997**, *1997* (8), 893–894.

(240) Anderson, J. C.; Cubbon, R. J.; Harling, J. D. Investigation of the Importance of Nitrogen Substituents in a N-P Chiral Ligand for Enantioselective Allylic Alkylation. *Tetrahedron Asymmetry* **2001**, *12* (6), 923–935.

(241) van Steenis, D. J. V. C.; Marcelli, T.; Lutz, M.; Spek, A. L.; van Maarseveen, J. H.; Hiemstra, H. Construction of Adjacent Quaternary and Tertiary Stereocenters *via* an Organocatalytic Allylic Alkylation of Morita–Baylis–Hillman Carbonates. *Adv. Synth. Catal.* **2007**, *349* (3), 281–286.

(242) Drewes, S. E.; Emslie, N. D.; Field, J. S.; Khan, A. A.; Ramesar, N. Synthesis, Resolution and Assignment of Absolute Configuration of 2-(α-Hydroxy)Aryl Acrylate Esters. *Tetrahedron: Asymmetry* **1992**, *3* (2), 255–260.

(243) Číhalová, S.; Dziedzic, P.; Córdova, A.; Veselý, J. Asymmetric Aza-Morita-Baylis-Hillman-Type Reactions: The Highly Enantioselective Reaction between Unmodified α,β-Unsaturated Aldehydes and *N*-Acylimines by Organo-Co-Catalysis. *Adv. Synth. Catal.* **2011**, *353* (7), 1096–1108.

(244) Zhong, F.; Wang, Y.; Han, X.; Huang, K.-W.; Lu, Y. L-Threonine-Derived Novel Bifunctional Phosphine−Sulfonamide Catalyst-Promoted Enantioselective Aza-Morita−Baylis−Hillman Reaction. *Org. Lett.* **2011**, *13* (6), 1310–1313.

(245) Rout, L.; Harned, A. Allene Carboxylates as Dipolarophiles in Rh-Catalyzed Carbonyl Ylide Cycloadditions. *Chem. Eur. J.* **2009**, *15* (47), 12926–12928.

(246) Hue, B. T. B.; Dijkink, J.; Kuiper, S.; Van Schaik, S.; Van Maarseveen, J. H.; Hiemstra, H. Synthesis of the Tricyclic Core of Solanoeclepin A through Intramolecular [2+2] Photocycloaddition of an Allene Butenolide. *Eur. J. Org. Chem.* **2006**, *2006* (1), 127–137.

(247) Tang, S. Y.; Yu, H. Z.; You, W. L.; Guo, Q. X. Mechanistic Study of Palladium-Catalyzed Oxidative C-H/C-H Coupling of Polyfluoroarenes with Simple Arenes. *Chinese J. Chem. Phys.* **2013**, *26* (4), 415–423.

(248) Yang, Y. F.; Cheng, G. J.; Liu, P.; Leow, D.; Sun, T. Y.; Chen, P.; Zhang, X.; Yu, J. Q.; Wu, Y. D.; Houk, K. N. Palladium-Catalyzed Meta-Selective C-H Bond Activation with a Nitrile-Containing Template: Computational Study on Mechanism and Origins of Selectivity. *J. Am. Chem. Soc.* **2014**, *136* (1), 344–355.

(249) Anand, M.; Sunoj, R. B.; Schaefer, H. F. Non-Innocent Additives in a Palladium(II)-Catalyzed C-H Bond Activation Reaction: Insights into Multimetallic Active Catalysts. *J. Am. Chem. Soc.* **2014**, *136* (15), 5535–5538.

(250) He, C. Y.; Min, Q. Q.; Zhang, X. Palladium-Catalyzed Aerobic Dehydrogenative Cross-Coupling of Polyfluoroarenes with Thiophenes: Facile Access to Polyfluoroarene-Thiophene Structure. *Organometallics* **2012**, *31* (4), 1335–1340.

(251) Whitaker, D.; Burés, J.; Larrosa, I. Ag(I)-Catalyzed C-H Activation: The Role of the Ag(I) Salt in Pd/Ag-Mediated C-H Arylation of Electron-Deficient Arenes. *J. Am. Chem. Soc.* **2016**, *138* (27), 8384–8387.

(252) Mahaffy, C. A. L. The Synthesis and Characterization of Tricarbonylchromium Complexes of Substituted Anilines and Fluorobenzenes. *J. Organomet. Chem.* **1984**, *262* (1), 33–37.

(253) Zhang, X.; Sayo, N. (1997) *Method of preparing optically active diphosphine ligands* (European Patent No. EP0839819A1), European Patent Office.

(254) Gladiali, S.; Pulacchini, S.; Fabbri, D.; Manassero, M.; Sansoni, M. 2-Diphenylphosphino-2'-Diphenylphosphinyl-1,1'-Binaphthalene (BINAPO), an Axially Chiral Heterobidentate Ligand for Enantioselective Catalysis. *Tetrahedron Asymmetry* **1998**, *9* (3), 391–395.

(255) Uozumi, Y.; Tanahashi, A.; Lee, S. Y.; Hayashi, T. Synthesis of Optically Active 2-(Diarylphosphino)-1,1'-Binaphthyls, Efficient Chiral Monodentate Phosphine Ligands. *J. Org. Chem*. **1993**, *58* (7), 1945–1948.

(256) Storch, G.; Siebert, M.; Rominger, F.; Trapp, O. 5,5'-Diamino-BIPHEP Ligands Bearing Small Selector Units for Non-Covalent Binding of Chiral Analytes in Solution. *Chem. Commun.* **2015**, *51* (86), 15665–15668.

(257) Kurz, L.; Lee, G.; Morgans, D.; Waldyke, M. J.; Ward, T. Stereospecific Functionalization of (R)-(-)-1,1′-Bi-2-Naphthol Triflate. *Tetrahedron Lett.* **1990**, *31* (44), 6321–6324.

(258) Li, Q.; Wan, P.; Wang, S.; Zhuang, Y.; Li, L.; Zhou, Y.; He, Y.; Cao, R.; Qiu, L.; Zhou, Z. Synthesis of a Class of New Phosphine-Oxazoline Ligands and Their Applications in Palladium-Catalyzed Asymmetric Addition of Arylboronic Acids to Isatins. *Appl. Catal. A Gen.* **2013**, *458*, 201–206.

(259) Kanth, J. V. B.; Periasamy, M. Selective Reduction of Carboxylic Acids into Alcohols using $NaBH_4$ and I_2. *J. Org. Chem.* **1991**, *56* (20), 5964–5965.

(260) Uozumi, Y.; Suzuki, N.; Ogiwara, A.; Hayashi, T. Preparation of Optically Active Binaphthylmonophosphines (MOP's) Containing Various Functional Groups. *Tetrahedron* **1994**, *50* (15), 4293–4302.

(261) Kortmann, F. A.; Chang, M. C.; Otten, E.; Couzijn, E. P. A.; Lutz, M.; Minnaard, A. J. Consecutive Dynamic Resolutions of Phosphine Oxides. *Chem. Sci.* **2014**, *5* (4), 1322–1327.

(262) Shimizu, H.; Manabe, K. Negishi Coupling Strategy of a Repetitive Two-Step Method for Oligoarene Synthesis. *Tetrahedron Lett.* **2006**, *47* (33), 5927–5931.

(263) Ma, Y. N.; Zhang, H. Y.; Yang, S. D. Pd(II)-Catalyzed P(O)R^1R^2-Directed Asymmetric C-H Activation and Dynamic Kinetic Resolution for the Synthesis of Chiral Biaryl Phosphates. *Org. Lett.* **2015**, *17* (8), 2034–2037.

(264) Bloomfield, A. J.; Herzon, S. B. Room Temperature, Palladium-Mediated P-Arylation of Secondary Phosphine Oxides. *Org. Lett.* **2012**, *14* (17), 4370–4373.

(265) Berthod, M.; Favre-Réguillon, A.; Mohamad, J.; Mignani, G.; Docherty, G.; Lemaire, M. A Catalytic Method for the Reduction of Secondary and Tertiary Phosphine Oxides. *Synlett* **2007**, *2007* (10), 1545–1548.

(266) Li, Y.; Das, S.; Zhou, S.; Junge, K.; Beller, M. General and Selective Copper-Catalyzed Reduction of Tertiary and Secondary Phosphine Oxides: Convenient Synthesis of Phosphines. *J. Am. Chem. Soc.* **2012**, *134* (23), 9727–9732.

(267) Amatore, C.; Broeker, G.; Jutand, A.; Khalil, F. Identification of the Effective Palladium(0) Catalytic Species Generated in Situ from Mixtures of Pd(dba)2 and Bidentate Phosphine Ligands. Determination of Their Rates and Mechanism in Oxidative Addition. *J. Am. Chem. Soc.* **1997**, *119* (22), 5176–5185.

(268) Bruno, N. C.; Niljianskul, N.; Buchwald, S. L. *N*-Substituted 2-Aminobiphenylpalladium Methanesulfonate Precatalysts and Their Use in C-C and C-N Cross-Couplings. *J. Org. Chem.* **2014**, *79* (9), 4161–4166.

(269) Bruno, N. C.; Tudge, M. T.; Buchwald, S. L. Design and Preparation of New Palladium Precatalysts for C-C and C-N Cross-Coupling Reactions. *Chem. Sci.* **2013**, *4* (3), 916–920.

(270) Ávalos, M.; Babiano, R.; Cintas, P.; Hursthouse, M. B.; Jiménez, J. L.; Light, M. E.; Palacios, J. C.; Pérez, E. M. S. Synthesis of Sugar Isocyanates and Their Application to the Formation of Ureido-Linked Disaccharides. *Eur. J. Org. Chem.* **2006**, *2006* (3), 657–671.

(271) Tao, C. Z.; Zhang, Z. T.; Wu, J. W.; Li, R. H.; Cao, Z. L. Synthesis of Unnatural *N*-Glycosyl α-Amino Acids *via* Petasis Reaction. *Chinese Chem. Lett.* **2014**, *25* (4), 532–534.

(272) Haydl, A. M.; Breit, B. Atom-Economical Dimerization Strategy by the Rhodium-Catalyzed Addition of Carboxylic Acids to Allenes: Protecting-Group-Free Synthesis of Clavosolide A and Late-Stage Modification. *Angew. Chem. Int. Ed.* **2015**, *54* (51), 15530–15534.

(273) Bulman Page, P. C.; Chan, Y.; Liddle, J.; Elsegood, M. R. J. Carbohydrate-Derived Iminium Salt Organocatalysts for the Asymmetric Epoxidation of Alkenes. *Tetrahedron* **2014**, *70* (40), 7283–7305.

(274) Rajput, J.; Hotha, S.; Vangala, M. $AuBr_3$-Catalyzed Azidation of per-*O*-Acetylated and per-*O*-Benzoylated Sugars. *Beilstein J. Org. Chem.* **2018**, *14* (1), 682–687.

(275) Tiwari, P.; Misra, A. K. An Efficient Stereoselective Dihydroxylation of Glycals Using

a Bimetallic System, $RuCl_3/CeCl_3/NaIO_4$. *J. Org. Chem.* **2006**, *71* (7), 2911–2913.

(276) Neto, V.; Granet, R.; Krausz, P. Novel Class of Non-Ionic Monocatenary and Bolaform Alkylglycoside Surfactants. Synthesis by Microwave-Assisted Glycosylation and Olefin Cross-Metathesis or by 'Click-Chemistry': Physicochemical Studies. *Tetrahedron* **2010**, *66* (25), 4633–4646.

(277) Fürstner, A.; Praly, J.-P. Von Glycosylaziden über *N*-Bromglycosylimine zu Aldononitrilen. *Angew. Chem.* **1994**, *106* (7), 779–781.

(278) Ratcliffe, A. J.; Fraser-Reid, B. Generation of α-D-Glucopyranosylacetonitrilium Ions. Concerning the Reverse Anomeric Effect. *J. Chem. Soc. Perkin Trans. 1* **1990**, No. 3, 747–750.

(279) Esteves, A. P.; Rodrigues, L. M.; Silva, M. E.; Gupta, S.; Oliveira-Campos, A. M. F.; Machalicky, O.; Mendonça, A. J. Synthesis and Characterization of Novel Fluorescent N-Glycoconjugates. *Tetrahedron* **2005**, *61* (36), 8625–8632.

(280) Camarasa, M. J.; Fernández-Resa, P.; García-López, M. T.; De Las Heras, F. G.; Méndez-Castrillón, P. P.; San Felix, A. A New Procedure for the Synthesis of Glycosyl Isothiocyanates. *Synthesis.* **1984**, *1984* (06), 509–510.

(281) Areti, S.; Khedkar, J. K.; Chilukula, R.; Rao, C. P. Thiourea Linked Peracetylated Glucopyranosyl-Anthraquinone Conjugate as Reversible ON-OFF Receptor for Fluoride in Acetonitrile. *Tetrahedron Lett.* **2013**, *54* (41), 5629–5634.

(282) Tsai, Y. F.; Shih, C. H.; Su, Y. T.; Yao, C. H.; Lian, J. F.; Liao, C. C.; Hsia, C. W.; Shui, H. A.; Rani, R. The Total Synthesis of a Ganglioside Hp-S1 Analogue Possessing Neuritogenic Activity by Chemoselective Activation Glycosylation. *Org. Biomol. Chem.* **2012**, *10* (5), 931–934.

(283) Belokon, Y. N.; Chusov, D.; Borkin, D. A.; Yashkina, L. V.; Bolotov, P.; Skrupskaya, T.; North, M. Chiral Ti(IV) Complexes of Hexadentate Schiff Bases as Precatalysts for Aldehyde Allylation: Unusual Additive Effect of Trimethylsilyl Chloride. *Tetrahedron Asymmetry* **2008**, *19* (4), 459–466.

(284) Pezzetta, C.; Bonifazi, D.; Davidson, R. W. M. Enantioselective Synthesis of *N*-Benzylic Heterocycles: A Nickel and Photoredox Dual Catalysis Approach. *Org. Lett.* **2019**, *21* (22), 8957–8961.

(285) Mroczkiewicz, M.; Winkler, K.; Nowis, D.; Placha, G.; Golab, J.; Ostaszewski, R. Studies of the Synthesis of All Stereoisomers of MG-132 Proteasome Inhibitors in the Tumor Targeting Approach. *J. Med. Chem.* **2010**, *53* (4), 1509–1518.

(286) Jenssen, K.; Sewald, K.; Sewald, N. Synthesis of Marimastat and a Marimastat Conjugate for Affinity Chromatography and Surface Plasmon Resonance Studies. *Bioconjug. Chem.* **2004**, *15* (3), 594–600.

(287) Steves, J. E.; Stahl, S. S. Copper(I)/ABNO-Catalyzed Aerobic Alcohol Oxidation: Alleviating Steric and Electronic Constraints of Cu/TEMPO Catalyst Systems. *J. Am. Chem. Soc.* **2013**, *135* (42), 15742–15745.

(288) Ferreira, B. R. V.; Pirovani, R. V.; Souza-Filho, L. G.; Coelho, F. Nájera Oxime-Derived Palladacycles Catalyze Intermolecular Heck Reaction with Morita-Baylis-Hillman Adducts. An Improved and Highly Efficient Synthesis of α-Benzyl-β-Ketoesters. *Tetrahedron* **2009**, *65* (36), 7712–7717.

(289) Pereira, S. I.; Adrio, J.; Silva, A. M. S.; Carretero, J. C. Ferrocenylphosphines as New Catalysts for Baylis-Hillman Reactions. *J. Org. Chem.* **2005**, *70* (24), 10175–10177.

(290) Nakano, A.; Ushiyama, M.; Iwabuchi, Y.; Hatakeyama, S. Synthesis of an

Enantiocomplementary Catalyst of β-Isocupreidine (β-ICD) from Quinine. *Adv. Synth. Catal.* **2005**, *347* (14), 1790–1796.

(291) Zhou, B.; Li, L.; Liu, X.; Tan, T. De; Liu, J.; Ye, L. W. Yttrium-Catalyzed Tandem Intermolecular Hydroalkoxylation/Claisen Rearrangement. *J. Org. Chem.* **2017**, *82* (19), 10149–10157.

(292) Jacobsen, E.; Chavda, M. K.; Zikpi, K. M.; Waggoner, S. L.; Passini, D. J.; Wolfe, J. A.; Larson, R.; Beckley, C.; Hamaker, C. G.; Hitchcock, S. R. A Mixed Anhydride Approach to the Preparation of Sulfinate Esters and Allylic Sulfones: Trimethylacetic *p*-Toluenesulfinic Anhydride. *Tetrahedron Lett.* **2017**, *58* (31), 3073–3077.

(293) Jeong, Y.; Ryu, J. S. Synthesis of 1,3-Dialkyl-1,2,3-Triazolium Ionic Liquids and Their Applications to the Baylis-Hillman Reaction. *J. Org. Chem.* **2010**, *75* (12), 4183–4191.

(294) Victor, N. J.; Gana, J.; Muraleedharan, K. M. *N*-Methylpyrrolidone Hydroperoxide/Cs_2CO_3 as an Excellent Reagent System for the Hydroxy-Directed Diastereoselective Epoxidation of Electron-Deficient Olefins. *Chem. Eur. J.* **2015**, *21* (42), 14742–14747.

(295) Sheldrick, G. M. A Short History of SHELX. *Acta Crystallogr., Sect. A: Found. Crystallogr*. **2008**, *A64*, 112–122.

(296) Lu, S.; Poh, S. B.; Zhao, Y. Kinetic Resolution of 1,1′-Biaryl-2,2′-Diols and Amino Alcohols through NHC-Catalyzed Atroposelective Acylation. *Angew. Chem. Int. Ed.* **2014**, *53* (41), 11041–11045.

(297) Unni, A. K.; Takenaka, N.; Yamamoto, H.; Rawal, V. H. Axially Chiral Biaryl Diols Catalyze Highly Enantioselective Hetero-Diels-Alder Reactions through Hydrogen Bonding. *J. Am. Chem. Soc.* **2005**, *127* (5), 1336–1337.

(298) Busacca, C. A.; Lorenz, J. C.; Grinberg, N.; Haddad, N.; Hrapchak, M.; Latli, B.; Lee, H.; Sabila, P.; Saha, A.; Sarvestani, M.; Shen, S.; Varsolona, R.; Wei, X.; Senanayake, C. H. A Superior Method for the Reduction of Secondary Phosphine Oxides. *Org. Lett.* **2005**, *7* (19), 4277–4280.

(299) Montgomery, T. P.; Grandner, J. M.; Houk, K. N.; Grubbs, R. H. Synthesis and Evaluation of Sterically Demanding Ruthenium Dithiolate Catalysts for Stereoretentive Olefin Metathesis. *Organometallics* **2017**, *36* (20), 3940–3953.

(300) Stambuli, J. P.; Stauffer, S. R.; Shaughnessy, K. H.; Hartwig, J. F. Screening of Homogeneous Catalysts by Fluorescence Resonance Energy Transfer. Identification of Catalysts for Room-Temperature Heck Reactions. *J. Am. Chem. Soc*. **2001**, *123* (11), 2677–2678.